A MACHINE VISION AND SENSING SYSTEM FOR BRAID DEFECT

DETECTION, DIAGNOSIS AND PREVENTION

DURING MANUFACTURE

Except where reference is made to the work of others, the work described in thesis is my own or was done in collaboration with my advisory committee. This thesis does not include proprietary or classified information.

_____

David John Branscomb

Certificate of Approval:

| | |
|---|---|
| _____ | _____ |
| Royall M. Broughton<br>Professor<br>Polymer and Fiber Engineering | David G. Beale, Chair<br>Professor<br>Mechanical Engineering |
| _____ | _____ |
| Dan M. Marghitu<br>Professor<br>Mechanical Engineering | Peter Schwartz<br>Professor<br>Polymer and Fiber Engineering |

_____

George T. Flowers
Interim Dean
Graduate School

# A MACHINE VISION AND SENSING SYSTEM FOR BRAID DEFECT DETECTION, DIAGNOSIS AND PREVENTION DURING MANUFACTURE

David John Branscomb

A Thesis

Submitted to

the Graduate Faculty of

Auburn University

in Partial Fulfillment of the

Requirements for the

Degree of

Master of Science

Auburn, Alabama
December 17, 2007

A MACHINE VISION AND SENSING SYSTEM FOR BRAID DEFECT

DETECTION, DIAGNOSIS AND PREVENTION

DURING MANUFACTURE

David John Branscomb

Permission is granted to Auburn University to make copies of this thesis at its discretion, upon the request of individuals or institutions and at their expense.

The author reserves all publication rights.

_____

Signature of Author

_____

Date of Graduation

# VITA

David John Branscomb, son of Lewis A. and Marie (Gallagher) Branscomb was born August 10, 1979, in Baton Rouge, Louisiana. He graduated from Sheffield High School in 1998. He attended Auburn University and graduated with Bachelor of Mechanical Engineering in December 2004.

THESIS ABSTRACT

A MACHINE VISION AND SENSING SYSTEM FOR BRAID DEFECT DETECTION, DIAGNOSIS AND PREVENTION DURING MANUFACTURE

David John Branscomb

Master of Science, December 17, 2007
B.M.E., Auburn University, 2004

211 Typed Pages

Directed by David G. Beale

The mechanical properties of braids are often quite convenient for achieving the high performance levels expected of composite materials. A favorable attribute of a braided structure is the ability for the design engineer to tailor reinforcing fiber position and orientation in such a way to achieve a desired geometry. Braiding is of particular interest to the modern manufacturer as new methodologies are required to meet the increasing performance demands of engineered materials technology. In this presentation, a computer controlled machine is designed, constructed, utilizing PC based motion control and machine vision technology to control the take-up process. The computer controlled system presented is capable of observing braid formation,

monitoring braiding machine performance, and finally provide diagnostic measures to recognize and ultimately prevent the manifestation of common mechanical faults. Both visual and mechanical approaches to fault diagnostics are developed. Experiments are carried out in order to characterize the nature of the braiding dynamics and establish the optimum machine operating conditions as a baseline for comparison. The dynamics occurring at the braid formation point undergo three distinct regimes as the braid reaches steady state. It is observed that depending on the initial conditions, transients and migration toward the equilibrium point occur as the braid point reaches steady state. Extensive tests were performed in order to investigate the effects of common mechanical faults (high tension yarns) during

the braiding process; particularly problems related to the proper function of yarn package tensioning mechanisms are investigated. The results of these experiments indicate the dominating influence that high tension yarns have on braid point formation. Knowledge of braid point dynamics is particularly useful if improving response time and reducing product waste is desired. Understanding the nature of braiding and common problems encountered during the braiding process provides a useful foundation necessary for developing control methods to mitigate the adverse effects of braiding faults.

# ACKNOWLEDGEMENTS

The author would like to thank Dr. David Beale for his ideas and encouragement. Jeff Thompson gave tremendously in his efforts and expertise with the braiding machine operation. Dr. Royall Broughton assisted greatly by his many conversations and guidance. Dr. Peter Schwartz supported this project by providing floor space for the experiment. Tom Allen provided useful information regarding servo tuning and expertise. Chris Montgomery of Auburn Fusion Research Lab provided useful programming information. Joe Bryant assisted tremendously with some of the experiments and made helpful contributions. Jeff Landau, owner of Automation Support Group donated a gearhead and provided practical information regarding motion control practice. Sakthivael Kandaswaamy provided CNC expertise. David and Tracy Clark provided technical expertise of welding vintage cast iron parts to stainless steel. Lewis and Marie Branscomb, my wonderful parents, have been a constant source of encouragement and strong ally in times of struggle. My super sisters Mary and Elizabeth edited the thesis. James Alston Branscomb provided excellent editing suggestions. Dr. Steve Bigbee has encouraged me to stay the course and provided countless hours of free counsel. Dr. Joe Bonometti and Kirk Sorenson with NASA provided necessary support. Thanks to God for His love and faithfulness during the difficult times (Psalm 56:11). The research work described in this thesis was supported by a grant from National Aeronautics and Space Administration (NASA).

Style manual or journal used Textile Research Journal (TRJ)

Computer software used Microsoft Word 2003

TABLE OF CONTENTS

LIST OF FIGURES ..... xii
1. INTRODUCTION ..... 1
1.1 Overview of braiding ..... 1
1.2 Braiding Machinery ..... 5
1.3 Literature Review ..... 6
1.4 Scope of Research ..... 7
2. NASA HORIZONTAL BRAIDING MACHINE ..... 10
2.1 Overview ..... 10
2.2 General philosophy of take-up (conventional approach) ..... 12
2.3 NASA horizontal braiding machine: safe installation procedure ..... 17
2.3.1 Selecting a location for braiding machine ..... 17
2.3.2 Braider installation plan ..... 18
2.3.3 Addressing electrical concerns ..... 19
2.4 NASA take-up system: safe installation procedure ..... 21
2.4.1 General installation safety rules: ..... 21
2.4.2 Safety equipment: ..... 21
2.4.3 Procedure for installation: ..... 22
2.4.4 Procedure for initial startup: ..... 22
2.5 Safe operating procedure: NASA horizontal braider ..... 22
2.5.1 Safety features: ..... 23
2.5.2 Operator responsibility ..... 23
2.5.3 General operational safety rules: ..... 23
2.6 Braiding head selection ..... 25
2.7 Braiding machine power up procedure ..... 27
2.7.1 Braiding machine operation: jogging the braiding machine ..... 28
2.7.2 Braiding machine operation: starting a braid ..... 30
2.8 Need for take-up system ..... 33
2.8.1 NASA take-up description ..... 33
2.8.2 Function of a capstan ..... 34
2.9 Take-up machine operation guidelines ..... 35
2.9.1 Take-up machine power up and operation ..... 36
2.9.2 Take-up machine functional requirements ..... 38
2.9.3 Power off take-up machine ..... 40
2.10 Braiding machine maintenance ..... 42
2.10.1 Lubrication information ..... 42
2.10.2 After-use maintenance ..... 43

2.10.3 Cleaning machine surfaces ..... 43
2.11 Example horizontal composite braiding system ..... 45
2.12 Spool Calculations ..... 48
2.13 Conclusion ..... 48
2.14 Useful Information ..... 49
A.1 2BX Springs for Short Pawl Lifts ..... 50
A.2 2BX Springs for Long Pawl Lifts ..... 50
A.3 2BX Tension Springs ..... 50
3. EXPERIMENTAL SETUP OF COMPUTER CONTROLLED TAKE-UP SYSTEM 51
3.1 Overview ..... 51
3.2 Experimental Braiding Machine Description ..... 54
3.3 Braiding Machine track Plate Geometry ..... 55
3.4 Initial electrical requirements ..... 56
3.5 Initial mechanical requirements ..... 58
3.6 Construction of the take-up machine ..... 58
3.7 Capstan axis assembly ..... 59
3.8 CNC Programs ..... 63
3.9 Motion control ..... 66
3.10 Servo Motor Control ..... 71
3.10.1 Torque Reference Inputs ..... 71
3.10.2 Servo Motors ..... 72
3.11 Gearheads ..... 75
3.12 Quadrature Encoders ..... 75
3.13 Braiding Machine Encoder Installation ..... 76
3.14 Characterizing the braiding machine parameters ..... 77
3.15 LabVIEW Motion Control Programs ..... 77
3.16 Machine Vision ..... 78
3.16.1 USB Image Acquisition System Setup ..... 79
3.16.2 Camera Reference Frames ..... 81
3.17 LabVIEW Vision Programs ..... 84
3.18 Camera synchronization verification ..... 88
3.19 Conclusion ..... 90
4. EXPERIMENTAL RESULTS AND DEFAULT CHARACTERIZATION ..... 91
4.1 Introduction ..... 91
4.2 Scope of experiments ..... 93
4.3 Quasi-static testing of braiding machine ..... 94
4.4 Quantifying effective braiding machine spring constant ..... 95
4.5 Braid point dynamics ..... 96
4.6 Steady state braid point motion ..... 101
4.7 Braiding with optimal machine conditions ..... 102
4.8 Effects of take-up speed on braid angle ..... 104
4.9 Braid angle settling time ..... 108
4.10 Limitations of experimental setup ..... 112
4.11 Effects of one locked package ..... 113

4.12 Effect of two diametrically opposed locked packages (same track) on the braid point motion ..... 117
4.13 Effect of two locked packages from opposite tracks on the braid point motion. 122
4.14 The effects of mechanical faults on motion data ..... 129
4.15 Effect of yarn breakage on motion data ..... 131
4.16 Yarn breakage capture ..... 133
4.17 Conclusion ..... 134
5. FAULT DETECTION IN BRAIDING UTILIZING INEXPENSIVE USB MACHINE VISION ..... 136
5.1 Introduction ..... 136
5.2 Results of tension on braided structures ..... 136
5.3 Characteristics of a balanced braid point formation ..... 138
5.4 Comparing the effects of Faulty Package(s) ..... 140
5.5 Investigation of Aberrant Tension: Diametrically opposed locked packages ..... 144
5.6 Transition from slack to taut conditions: Final Analysis ..... 147
5.7 Effects of increasing yarn tension on braiding machine motor speed ..... 153
5.8 Visual Diagnostic Measure ..... 154
5.9 Conclusion ..... 155
6. CONCLUSION ..... 156
6.1 Introduction ..... 156
6.2 Inexpensive PC based components ..... 157
6.3 Improved manufacturing performance ..... 157
6.4 Minimize waste ..... 158
6.5 Ability to produce desired braid angle ..... 158
6.6 Fault Detection and Performance Monitoring ..... 158
6.7 Ability to electronically control tension (precise method) ..... 159
6.8 Speed Variability ..... 159
6.9 Ideal platform for research ..... 159
6.10 Experimental Realizations ..... 160
REFERENCES ..... 161
APPENDIX: TEST DATA ..... 164

## LIST OF FIGURES

Figure 2.1 Tether research facility including braiding machine and take-up ..... 13

Figure 2.2 Initial braids constructed of Kevlar® and carbon without take-up system ..... 14

Figure 2.3 Gantry structure front side view ..... 15

Figure 2.4 Gantry structure rear side view ..... 16

Figure 2.5 Braiding machine displacement ..... 17

Figure 2.6 Dimensions (inches) of PRL lab area 105 used to determine machine location ..... 18

Figure 2.7 Electrical grounding ..... 20

Figure 2.8 Limit switch controlling braid head operation ..... 26

Figure 2.9 Braiding machine air line connect for air bearings ..... 26

Figure 2.10 High pressure air line ..... 27

Figure 2.11 Braiding machine power lock ..... 28

Figure 2.12 Braiding machine main power quick disconnect ..... 29

Figure 2.13 Braiding machine main power switch ..... 29

Figure 2.14 Braiding machine control panel ..... 30

Figure 2.15 Proper capstan wrapping configuration ..... 32

Figure 2.16 High voltage electronics control box ..... 32

Figure 2.17 NASA take-up system ..... 34

Figure 2.18 Capstan Assembly ..... 35

Figure 2.19 Take-up machine main power breaker and power cord ..... 37

Figure 2.20 Take-up machine main power switch ..... 37

Figure 2.21 Take-up machine power switch and emergency stop, Red Lion speed controller ..... 38
Figure 2.22 Proper capstan separator pulley wrap ..... 39
Figure 2.23 Dancer pulley and proximity switch ..... 39
Figure 2.24 Uhing traversing mechanism and mechanical stops ..... 40
Figure 2.25 circular braid formed on NASA braiding machine using take-up machine .. 41
Figure 2.26 braiding machine control panel ..... 41
Figure 2.27 A2BX-26C Carrier [14] ..... 44
Figure 2.28 Base group front view [14] ..... 45
Figure 2.29 Base group rear view [14] ..... 47
Figure 2.30 Spool dimension calculations ..... 48
Figure 3.1 CAD model of take-up machine ..... 53
Figure 3.2 Braiding Machine and Take-up Machine ..... 54
Figure 3.3 Track Plate Paths of Braiding Machine ..... 56
Figure 3.4 Required 240 single phase drop out electrical outlet ..... 57
Figure 3.5 Required 240 single phase drop out electrical outlet ..... 57
Figure 3.6 Capstan Assembly ..... 60
Figure 3.7 Parametric model used to determine capstan properties ..... 61
Figure 3.8 Calculated capstan properties ..... 62
Figure 3.9 CAD model of the capstan driveshaft ..... 62
Figure 3.10 CNC tool paths Servo Side ..... 64
Figure 3.11 CNC Tool paths (1) gearhead side ..... 64
Figure 3.12 CNC tool paths (2) gearhead side ..... 65

Figure 3.13 CNC tool paths (1) for servo motor mount ..... 65
Figure 3.14 CNC tool paths (2) for servo motor mount ..... 65
Figure 3.15 CNC tool paths (3) for servo motor mount ..... 66
Figure 3.16 Motion control flow chart..... 67
Figure 3.17 Take-up machine motion control components ..... 68
Figure 3.18 UMI-7764 ..... 69
Figure 3.19 Motion control hardware wiring: power supplies, UMI 7764, breakout board ..... 70
Figure 3.20 Torque control wiring [21] ..... 72
Figure 3.21 Torque/Input voltage proportionality [21]..... 72
Figure 3.22 BMC 12H Typical Power/Motor Wiring [22]..... 74
Figure 3.23 Encoder installed, mounting bracket, shaft extension ..... 76
Figure 3.24 LabVIEW motion control program ..... 78
Figure 3.25 Lighting environment ..... 80
Figure 3.26 Side view camera..... 80
Figure 3.27 Rear view camera ..... 81
Figure 3.28 Rear View: Establishing ZX Coordinate System (Camera 2 ..... 82
Figure 3.29 Side View camera position..... 82
Figure 3.30 Side View: Establishing ZY Coordinate System (camera 1) ..... 83
Figure 3.31 Rear View camera position ..... 83
Figure 3.32 XYZ machine vision based coordinate system ..... 84
Figure 3.33 LabVIEW vision program ..... 85
Figure 3.34 LabVIEW VI used to determine YZ braid point position ..... 86

Figure 3.35 LabVIEW VI used to determine XZ braid point position ..... 87
Figure 3.36 LabVIEW VI used to determine braid angle ..... 88
Figure 3.37 Movement of the braid point in Z (Rear View) ..... 89
Figure 3.38 Movement of the braid point in Z (Side View) ..... 90
Figure 4.1 Bi-directional effective spring constant ..... 95
Figure 4.2 Braid point moved from center ..... 97
Figure 4.3 Radial transient of first regime (time versus displacement) ..... 98
Figure 4.4 Y direction transient of first regime (frames versus displacement) ..... 99
Figure 4.5 Oscillations and braid point migration toward equilibrium point (second regime) ..... 100
Figure 4.6 Steady state braid point motion (regime 3) ..... 101
Figure 4.7 Circular displacement of optimal braid ..... 102
Figure 4.8 Radial variation of an optimal braid ..... 103
Figure 4.9 Average capstan motor speeds for braid angle test ..... 105
Figure 4.10 Braid angle versus braiding machine revolution ..... 106
Figure 4.11 Braiding machine speed (RPM) for a balanced braid. ..... 107
Figure 4.12 Increasing braid angle versus braiding machine revolution (1 rpm) ..... 108
Figure 4.13 Braid point migration and stabilization distance in pixels (2.5 rpm) ..... 110
Figure 4.14 Braid point migration and stabilization (3 rpm) ..... 111
Figure 4.15 Braid cone angle as a function of capstan motor speed ..... 112
Figure 4.16 Initial position of locked package ..... 114
Figure 4.17 Braid point displacement with 1 locked package (First revolution) ..... 115
Figure 4.18 Braid point displacement with 1 locked package (Second revolution) ..... 116

Figure 4.19 Radial variation of a locked package braid ..... 117
Figure 4.20 Initial position of diametrically opposed locked packages..... 118
Figure 4.21 Braid point motion with 2 diametrically opposed locked packages (First revolution)..... 119
Figure 4.22 Combined braid point motion with 2 diametrically opposed locked packages ..... 120
Figure 4.23 Braid point motion while 2 yarns are slack (1 Rev). ..... 121
Figure 4.24 Radial variation of 2 locked packed braid based on Figures 4.18-23 ..... 122
Figure 4.25 Illustrates the initial, opposite, and crossing points of the locked packages 123
Figure 4.26 Braid point motion with two locked packages on opposite tracks (first revolution ..... 124
Figure 4.27 Braid point motion with two opposite track locked packages (second revolution)..... 125
Figure 4.28 Braid point motion with two opposite track locked packages (third revolution)..... 126
Figure 4.29 Braid point motion with two orthogonally locked packages (.62 revolutions) ..... 127
Figure 4.30 Combined braid point motion with 2 locked packages on opposite tracks (3.62 revolutions)..... 128
Figure 4.31 Effects of faults on braiding machine speed..... 129
Figure 4.32 braiding machine speed spikes from increasing yarn tension ..... 131
Figure 4.33 Capstan speed spikes from increasing yarn tension. ..... 133
Figure 4.34 Rear view before, during, and after yarn breakage ..... 133

Figure 4.35 Side view before, during, and after yarn breakage ..... 133
Figure 5.1 Braid with a high tension yarn resulting from a stiff spring..... 136
Figure 5.2 Braid with a high tension resulting from a locked package ..... 137
Figure 5.3 Fault resulting from a locked package..... 137
Figure 5.4 Braid with two high tension yarns resulting from 2 locked packages..... 137
Figure 5.5 Braid resulting from yarns beyond the jammed state ..... 137
Figure 5.6 Upstream twisting observed after braid is formed beyond jammed state ..... 138
Figure 5.7 Braid with balanced yarn tension ..... 138
Figure 5.9 Comparison of balanced braid and braid with 1 faulty package for 1 braiding machine revolution..... 141
Figure 5.10 Increasing radius of braid point movement as tension in yarn increases .... 142
Figure 5.11 Comparison of braid point motion between 1 and 2 locked packages ..... 143
Figure 5.12 Comparison of balanced braid and braid with 2 faulty yarn packages..... 143
Figure 5.13 Initial Position of diametrically opposed locked Packages ..... 145
Figure 5.14 Effects of slack and taut yarns on braid point position ..... 145
Figure 5.15 Initial Interpretation of braid point formation for Taut and Slack conditions ..... 146
Figure 5.16 Braid point motion of 14 balanced yarns ..... 148
Figure 5.17 Braid point motion while 2 yarns are in high tension ..... 149
Figure 5.18 Braid Point distinct regions corresponding to high and low yarn tension... 150
Figure 5.19 Transition from taut (high) to slack (low) yarn tensions ..... 151
Figure 5.20 Radial Variation of braid point when diametrically opposed yarns are taut and slack..... 152

Figure 5.21 braiding machine motor speed as yarn breaks..... 153

Figure 5.22 capstan motor speed as yarn breaks..... 154

# 1. INTRODUCTION

Braiding is of particular interest to the modern manufacturer because new methodologies are required to meet the increasing performance demands of engineered materials technology. Sophisticated automated technology is presently utilized by industry and researchers. New applications will be realized as available automation technologies are transferring to the realm of braiding manufacture. Precision, quality, and overall efficiency are some of the key advantages offered by automation technology such as servo motion control, machine vision, and other personal computer (PC) based software and hardware deployable solutions.

## 1.1 Overview of braiding

The history of braiding is quite rich. Braiding began as an art form practiced by ancient people. Plaiting of human hair first employed braiding for purposes of personal adornment, and has been argued to be as old as human civilization [1]. Originally a hand process, braiding has evolved into an industrial construction with the advent of the modern braiding machine. Although its fundamental operation has prevailed mostly unchanged, the modern braiding machine has undergone improvements of material construction as well as utilizing sophisticated computerized controls and electric actuation. The first braiding machine emerged in the 18th century, patented by Thomas Walford, and later improved by Johann Bockmühl and others [2].

Braiding is a basic textile construction originating in ancient history. The first evidence of braided structures is over 4000 years old [2]. Originally, braiding was used to make natural fibers more useful. Braids have been used to harness the strength and utility of fibers in a simple construction. Chosen for its structural integrity, flexibility, and versatility in product use, braiding has been used for intricate articles of clothing for battle and royalty [1]. Braided materials are inherently damage tolerant. Garments were constructed in part using braids and were a sign of wealth and power [1].

A braid is a textile structure produced by the interlacing of 3 or more strands, referred to in some literature as oblique interlacing [1]. Braids are typically small fabrics, by other textile standards, due to the machinery required to produce large structures. There are several typical types of braids: circular (tubular) and flat. Circular braids are typically available in three structures: Diamond, Regular, and Hercules, where the structure is dictated by the machine setup [3]. A circular braid is constructed by interlacing fibrous yarns to form a circular fabric that can be used as a freestanding material or as a structural reinforcement in composites.

Braided products are designed to exploit the inherent flexibility of textile materials [2]. The onset of Computer Aided Manufacturing (CAM) techniques has allowed the manufacture of complicated, even three dimensional (3D) braided structures to be realized using specialized braiding machines. The interlocking of continuous yarns in a structure provides a load distribution mechanism. Braids operate on the same principle of the Chinese finger trick i.e. as the braid is pulled in tension, the diameter reduces. This inherent conformability of braids offers a simple and efficient alternative for the manufacture of complex shapes.

Braiding is versatile and the manufacturing methodology of choice for many unique applications. Virtually any industry can benefit from braided products if it does not already. A space tether is a long cable that provides a connection between shuttle, satellites, or virtually any other orbiting mass; and when deployed its electro-mechanical properties such as added angular momentum and electrical conduction can be used to produce propulsion [4]. Space tether design is considered from the point of view of longevity and robustness against collisions with debris and micrometeoroids, making a braided structure is ideal [5]. Tethers are typically tubular braids and the simplest type. Space programs utilize high strength synthetic fiber braids to construct tethers with varied purposes from mooring to electric power generation and transmission. A space tether may incorporate fiber optic cable for data transmission and metal wire for electrical conduction in its design.

Medical applications include surgical stints, custom fit prosthetics, and many other devices useful for promoting human health and life. Industrial applications of braiding are seen in hydraulic systems where braiding reinforces high pressure hoses. Pressure vessels may employ braiding as reinforcement against bursting. Braids are often employed as insulation for electrical cables, and are useful as a wicking agent in candles, lamps, or even de-soldering. Among many other applications, braiding rivals traditional axial load-bearing members such as cable and rope applications. Techniques for splicing braids to make specific configurations commonly used in rigging and marine industries extend braids already utility.

Braiding has many useful applications in engineered materials and particularly composite materials. Composites can be produced by over-braiding, or braiding around a

mandrel, and the result is a structure with dramatically varying cross sections [7]. The construction of composites requiring pre-forms of complicated shapes is facilitated by utilizing the excellent conformability of braided structures [2]. Subsequently, the functional versatility of braiding offers a low cost manufacturing solution to complex composite pre-forms. [4]

The Mechanical properties of braids are often quite convenient for achieving desired effects in engineering materials. Braids offer many properties that make it ideal for reinforcement of structures. Braids can also be used as reinforcement of an existing product. Yarns can be introduced to the braid by stationary guides that allow reinforcement parallel to the braid along the braid axis. Adding axial or longitudinal yarns to the braid increases the stiffness of the braid. The woven or interlaced nature of braids provides excellent resistance to damage, and further increases the feasibility of braid in space tether applications. As a reinforcing or protective-cover the inherent flexible nature of braid is utilized in applications involving pipes, cable, and hoses [4].

A favorable attribute of a braided structure is the ability for the design engineer to tailor reinforcing fiber position and orientation in such a way to achieve a desired result [4]. The interwoven nature of braid is the source of much benefit to the engineered structural material providing resistance to shear loads, delaminating, and fatigue [5].

Although industrial braiding is a versatile technique applicable to a myriad of applications, it has some definite limitations. The size of a braid is limited by the size of the manufacturing equipment involved. In other words, the physical dimensions of a braiding machine are much larger than that of the product. In other words, braid dimensions are limited by machine size due to the geometric requirements of the yarn-

braid formation. Many applications involving a large braid diameter require an extremely large braiding machine, termed “megabraider” by Atkins and Pierce [8].

As mentioned before one notable characteristic of braiding and the braiding machinery requirements is that to make a relatively small fabric, a large amount of machinery is required [9]. Also, the shape or structural geometry of a braid is related to both the machine used to manufacture and the various parameters associated with its take-up or spooling. As yarn tension in the braid increases by slowing the take-up machine such that the braid diameter fully decreases, the braid is said to be in a jammed state. Braids have two fundamental classes: conventional and formed. Conventional braids are formed in space according to the braid reaching equilibrium with the take-up machine.

Finally, braiding is a process of historical significance although it is proving to be an exciting process for developing new material technologies. Utilized in high tech applications of composites, medicine, and even space, braiding is a well established technology. The feasibility of future processes is investigated to offer reliability and reproducibility.

### 1.2 Braiding Machinery

Industrial braiding is often accomplished by horn gears revolving sets spindles carrying yarn bobbins in serpentine like paths about a track plate. The motion of yarns on one track is clockwise and the other is counter clockwise causing the yarns to interlace. The track plate consists of two separate paths: each path 180 degrees out of phase from the other. One path motion is clockwise, while the other path is counter clockwise; at the point where the paths converge, the yarns interact as one yarn travels

over and the other yarn under. The over-under interaction causes an interlacing of the two yarns and is the chief mechanism responsible for the formation of the braided structure. The tension of yarns is controlled by springs.

Yarn is wound on bobbins to store the necessary material for a desired length of braid. Carriers are mechanical devices responsible for transporting the bobbins along the track plate.

The purpose of a take-up machine is to enable continuous and usable braid by placing it on a spool. Parameters of the braid can be achieved by controlling the take-up of the braid. The take-up machine is useful to produce consistent braid by maintaining a constant speed relationship with respect to the braiding machine. Once a significant amount of braid is produced, putting the material on a spool is necessary. The take-up machine controls the braid speed, the lay of the material on the spool, and the tension of the braid.

### 1.3 Literature Review

The traditional maypole style braiding machine has endured greatly, undergoing only minor modifications of functional enhancement. The literature regarding braids and the associated aspects of manufacturing is less publicized than other textile processes. Although braiding may stand in contrast to other textile constructions in terms of information availability, it compares well with others as its quality and construction parameters are closely related to the material properties as well as the manufacturing details. Modeling of braiding is difficult due to the myriad of factors that can affect the process. Brunnschweiler first made a geometric analysis of braids as well as the tensile property of braids [10]. A mathematical analysis describing the circular braiding process

where the relationship between machine parameters and resulting braid geometry is presented by Du and Popper [11]. Du and Popper provided geometric equations for cover factor and other kinematic relationships useful for braid calculations. Pastore and Ko utilized Du and Popper's kinematic relations to develop a computer integrated manufacturing process useful for composite pre-forms [12]. Ko, Pastore, and Pearce wrote an industrial handbook that discussed in detail, materials, formation, structural geometry, and engineering analysis of braids [13].

**1.4 Scope of Research**

Obtain expertise required to implement a successful tether manufacturing facility for NASA per grant stipulations, including installation, maintenance, provision safe operation procedures, and specification of an appropriate take-up machine. Research appropriate areas in order to design and construct a functional take-up machine, utilizing PC based motion control of the take-up process, implement PC based machine vision technology to observe braid formation parameters, monitor braiding machine performance, and finally provide ad hoc diagnostic measures to recognize and ultimately prevent the manifestation of common mechanical faults. Develop ability to control the position of the fabric formation (braid point). Improving braid manufacturing process is of particular engineering and economic interest especially in areas where quality, precision, efficiency, and safety pertain. Extending the capabilities of the existing infrastructure by leveraging the power of PC based technology to meet the increasing needs of engineered materials. The paradigm of industrial manufacturing is changing with the tremendous technological advancements available to end users via PC infrastructure. Typically, industrial based solutions are quite expensive, given their

robust architectures. Industrial automation solutions, particularly in the areas of motion control and machine vision are specialized and costly. However, by using PC based architectures such as LabVIEW that can be prototyped quickly and are limited only by the ability of the programmer the automation of braiding is accomplished.
The ability to leverage the awesome power of PC based deployable technologies in an inexpensive manner is presented in this thesis.

Chapter 1 is useful to provide a brief introduction to braiding, including historical background, overview of braiding, applications of braiding, and discuss some relevant literature. Chapter 2 is written to serve two primary purposes: to outline the work done for NASA at Marshall Space Flight Center and to provide an operation manual for the tether manufacturing lab. Chapter 3 describes many of the design and manufacturing details as well as a general description of the experimental setup of a new PC based servo motion, machine vision prototype machine. Chapter 3 will be useful to anyone wishing to duplicate or continue braiding, motion control, or machine vision research. Chapter 4 describes the results of the static, dynamic, and the mechanical fault related braiding machine experiments performed during the course of this thesis research. Chapter 5 utilizes experimental data to provide a posteriori diagnostic tools useful for improving braiding quality by the detection of flaws. The results of various tension induced flaws are also presented.

Recognizing the characteristics tension induced flaws is valuable as a preventative measure as well as providing the basis of an improved computer control system. Areas of operator safety and material waste can be improved with a vision detection system. The conventional shut down mechanism can be improved by incorporating vision into a

feedback look to stop the machine before yarns break by recognizing the characteristics that high tension yarns have on braid point formation. What is believed to be a new application of machine vision to braiding technology is developed. By utilizing PC based motion control, machine vision, and servo technology the braiding process can be improved simply by using more sophisticated technology. Utilizing closed loop control minimizes variation and promotes consistency. Employing servo technology to control tension provides a more effective solution to traditional dancer mechanism solutions. The dynamic characterization serves a basis for defining future control problems.

# 2. NASA HORIZONTAL BRAIDING MACHINE

## 2.1 Overview

A dual head horizontal composite braiding machine was installed in the NASA Propulsion Research Laboratory (PRL). The machine had previously been in operation with Missile Sustainment, Function, Propulsion and Structures Directorate with the U.S. Army Aviation and Missile Research in the Development and Engineering Center and was transferred to NASA for the purposes of establishing a tether research facility. There were several engineering challenges, including determining optimal position for intended functions such as composite tube manufacture and tether manufacture, access feasibility, power considerations, take-up machine position, development and design. The intent of this project was to modify the braiding machine such that it could be used dually for tether manufacture as well as with composites. The braiding machine contains two braid heads, each contains 144 carriers. The braiding machine can shift operation from one braiding head to another for various purposes along stainless steel plates via air bearings.

The braiding machine had been disassembled for transportation, and was subsequently in pieces. A full inventory was taken, including relevant measurements and pictures to determine the status of the machine, as it had been out of use for some time prior to this project. As a result of this inventory, it was determined that the bearings were in need of replacement. The manufacturer serial number was obtained and replacements were ordered and installed by NASA technicians. After a careful study of

the parts inventory and dimensions of the parts, a Computer-Aided Design (CAD) model of braiding machine footprint and the PRL (Lab Area 105) was constructed for the purposes of determining feasibility of different machine locations and the implications they would have on tether manufacturing, access to available power, preventing obstruction to the adjoining offices, and any other foreseeable safety considerations. An installation plan was developed in order to successfully assemble, wire, and prepare the braiding machine for tether manufacture available to NASA for research and development. Upon completion of the installation, the machine was serviced to prepare for consistent operation including cleaning, and lubricating. Figure 2.1 shows the braiding machine after completion of the installation plan.

A multitude of variation exists in the braiding machine industry, thus a custom made take-up machine was specified, designed, and constructed in conjunction with Steeger USA, an industrial braiding-solutions company, to allow the braided structures to be put on a spool. Calculations regarding the spool size and required pulling force were made in order to ensure proper sizing of the take-up machine. The electrical requirements of the braiding machine are: 460 Volts, Alternating Current (AC) transmitted along 3 phases. This is a potentially lethal amount of power and precautions should be taken to prevent electrical shock.

The braiding machine frame was grounded to the stainless plates which sit on the concrete floor of the lab. Schematics were made of electrical limit switches necessary to enable concurrent operation of both braid heads. Once the braiding machine was made fully operable, several braids were made as shown in Figure 2.2.

## 2.2 General philosophy of take-up (conventional approach)

The philosophy behind the modern take-up machine involves two electric motor types, namely constant speed and constant torque. The constant speed motor typically controls the capstan which is set to follow the braiding machine speed according to a given ratio which dictates the angle of take-up, unless a former ring is employed to force yarn convergence. Depending on the capstan design, the braid is wrapped around the capstan or the capstan in conjunction with a series of pulleys, and relies on friction between the braid and the capstan surface to prevent the braid from slipping. This friction based connection of the capstan provides an appropriate interface for constant take-up. The braiding machine orchestrates the movement of the yarns while the take-up machine provides the force required to un-spool the bobbins and ultimately this mechanical collaboration causes the yarns to interlace and produce a braid. The newly formed braid must be wound on a spool in order to be used later. Winding or spooling the braid involves both a turning and simultaneous traversing motion to control how the material is placed on the spool; the tension and the pitch are controlled by this take-up process. The braiding machine as installed is capable of shifting operation from one braiding head to another for various purposes. The shifting motion is accomplished along stainless steel plates via air bearings.

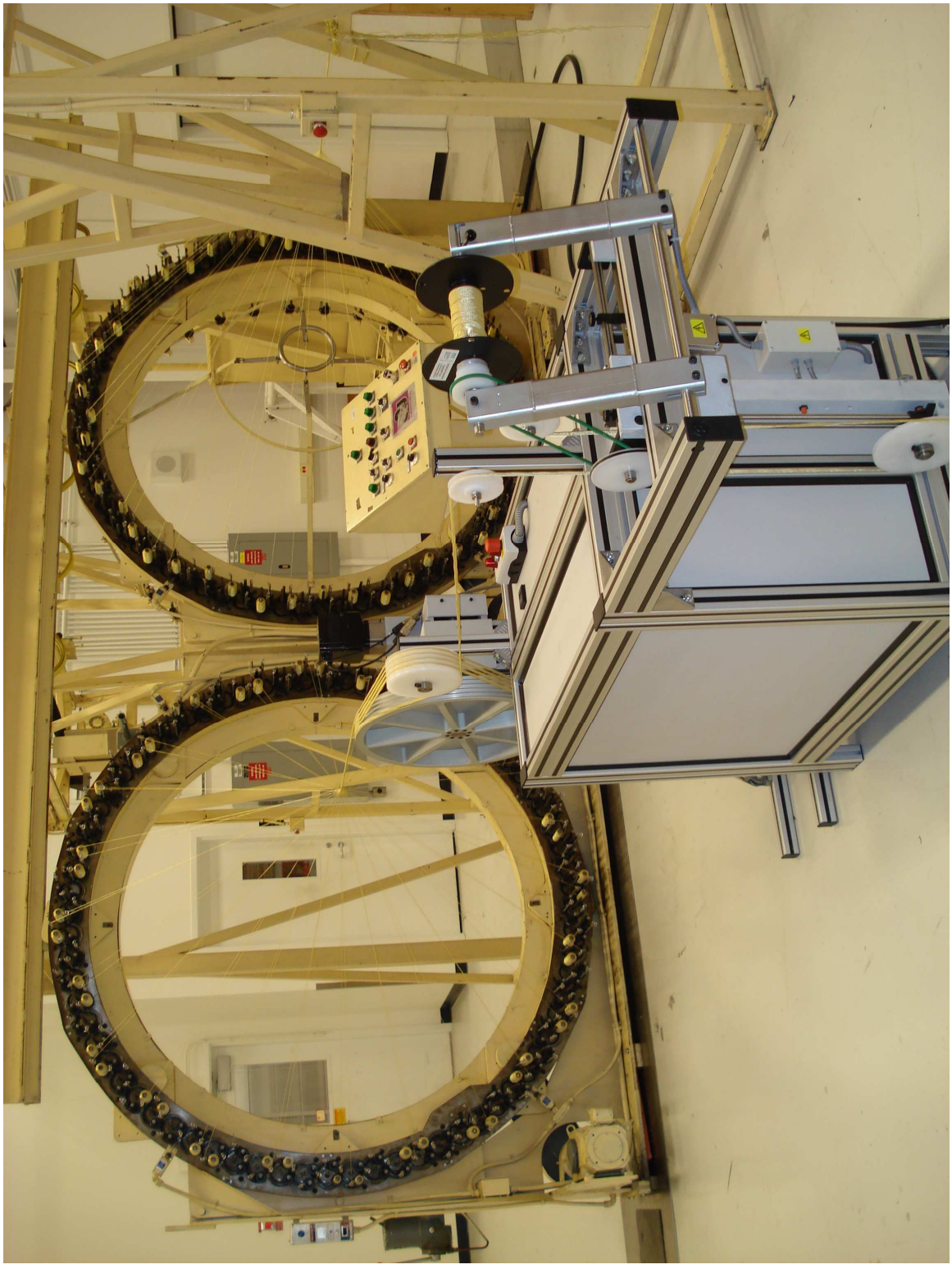

**Figure 2.1 Tether research facility including braiding machine and take-up**

**Figure 2.2 Initial braids constructed of Kevlar® and carbon without take-up system**

Figure 2.2 shows an example of the initial braided structures made upon complete installation. Notice that without the aid of a take-up machine the resulting braid will have many imperfections due to inability to consistently take-up the braided product.

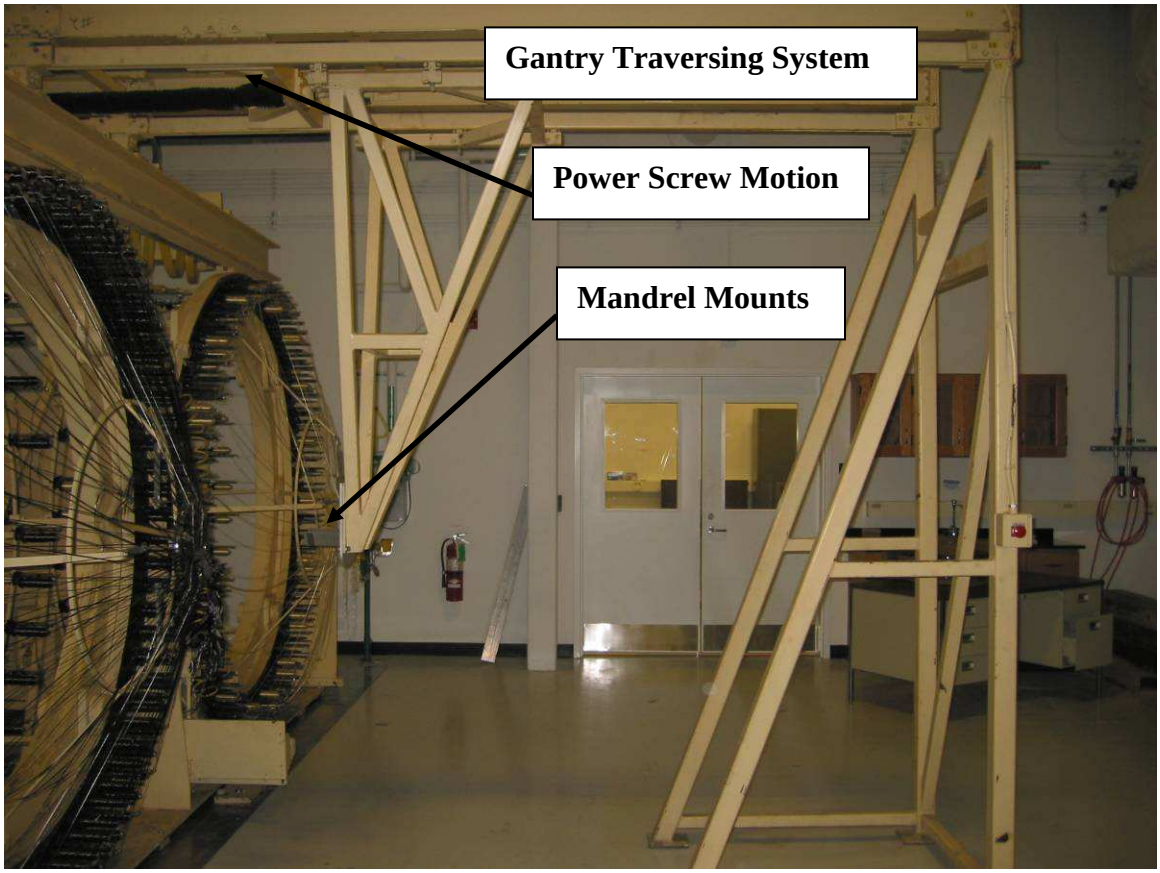


**Figure 2.3 Gantry structure front side view**

The gantry system shown along the top portion of Figure 2.3 is essentially a power screw driven mechanism that moves with respect to the braiding plane, allowing for over-braiding of a given mandrel. The purpose of the gantry is to support and move mandrels through the braid point, a necessary control of formation and manufacture of braid over composites. Figure 2.4 shows the motor responsible for powering the gantry system.

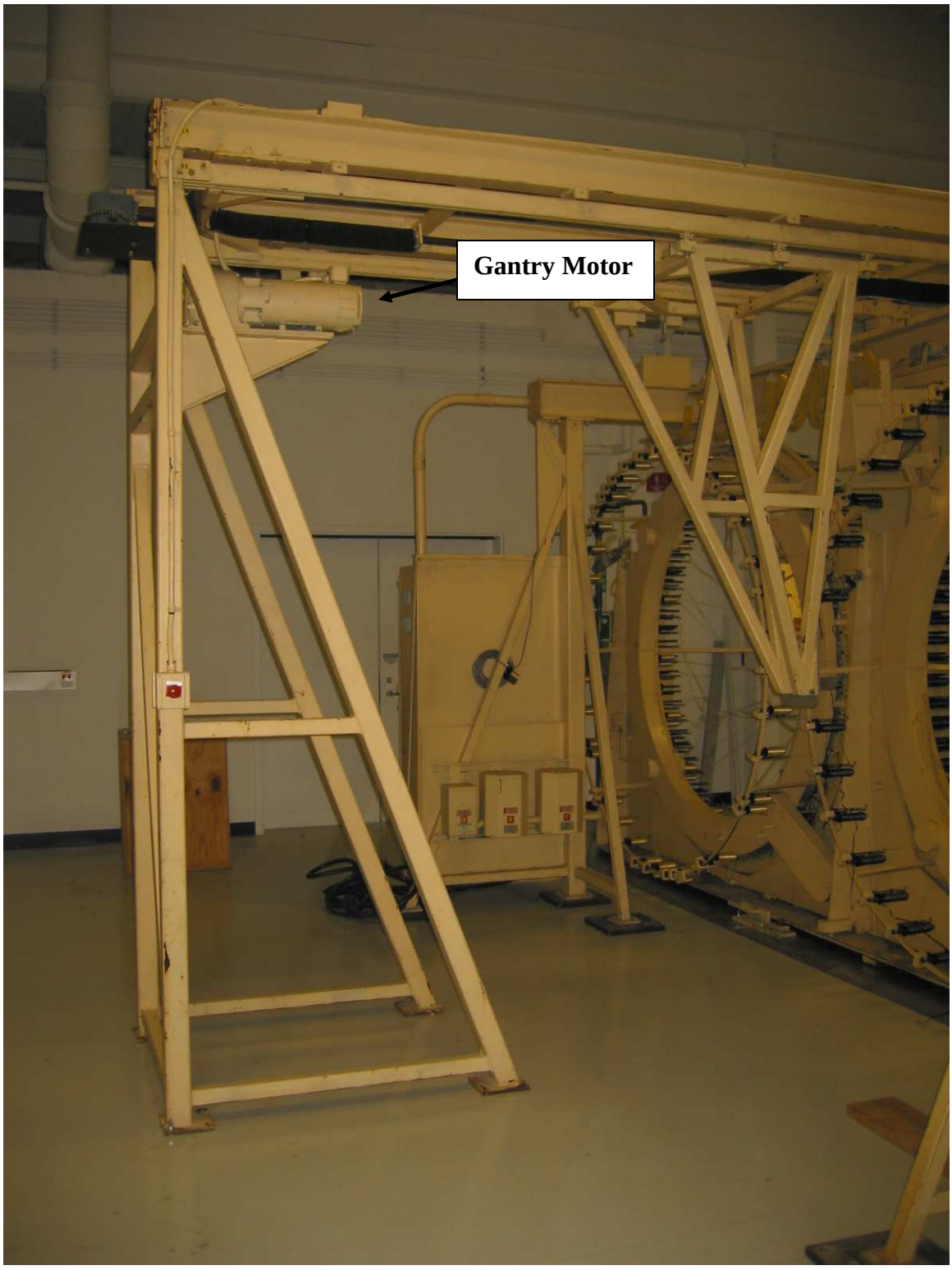


**Figure 2.4 Gantry structure rear side view**

### 2.3 NASA horizontal braiding machine: safe installation procedure

The following sections discuss the steps required to ensure that the installation of the braiding machine would result in a safe plan of action that promotes the safety of those involved both in the installation and future use of the machine.

#### 2.3.1 Selecting a location for braiding machine

The braiding machine must be positioned such that easy access and safety are maintained during all times of operation, service, and maintenance. Due to the size of the braiding machine footprint and considering meeting the various requirements such as air, electrical power, and floor level, an appropriate location was determined to insure proper functionality while maintaining access to the adjacent laboratories and offices (Fig. 2.5 and 2.6). A barrier is set up around the perimeter of the machine to offer a further measure of safety and prevent unauthorized personnel from entering a potential danger zone.

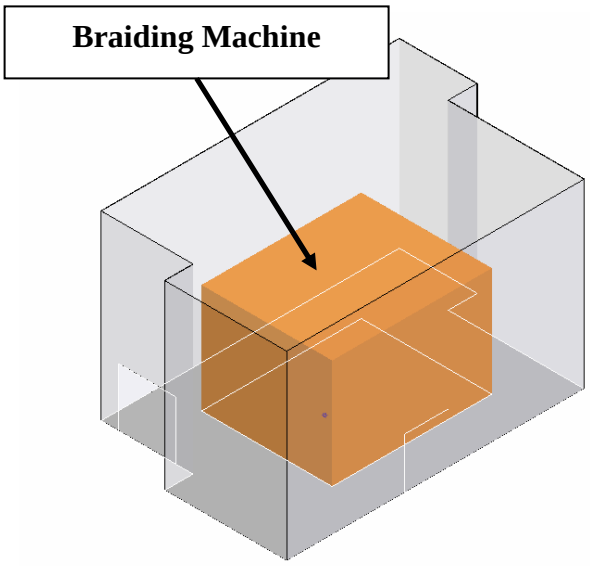


**Figure 2.5 Braiding machine displacement**

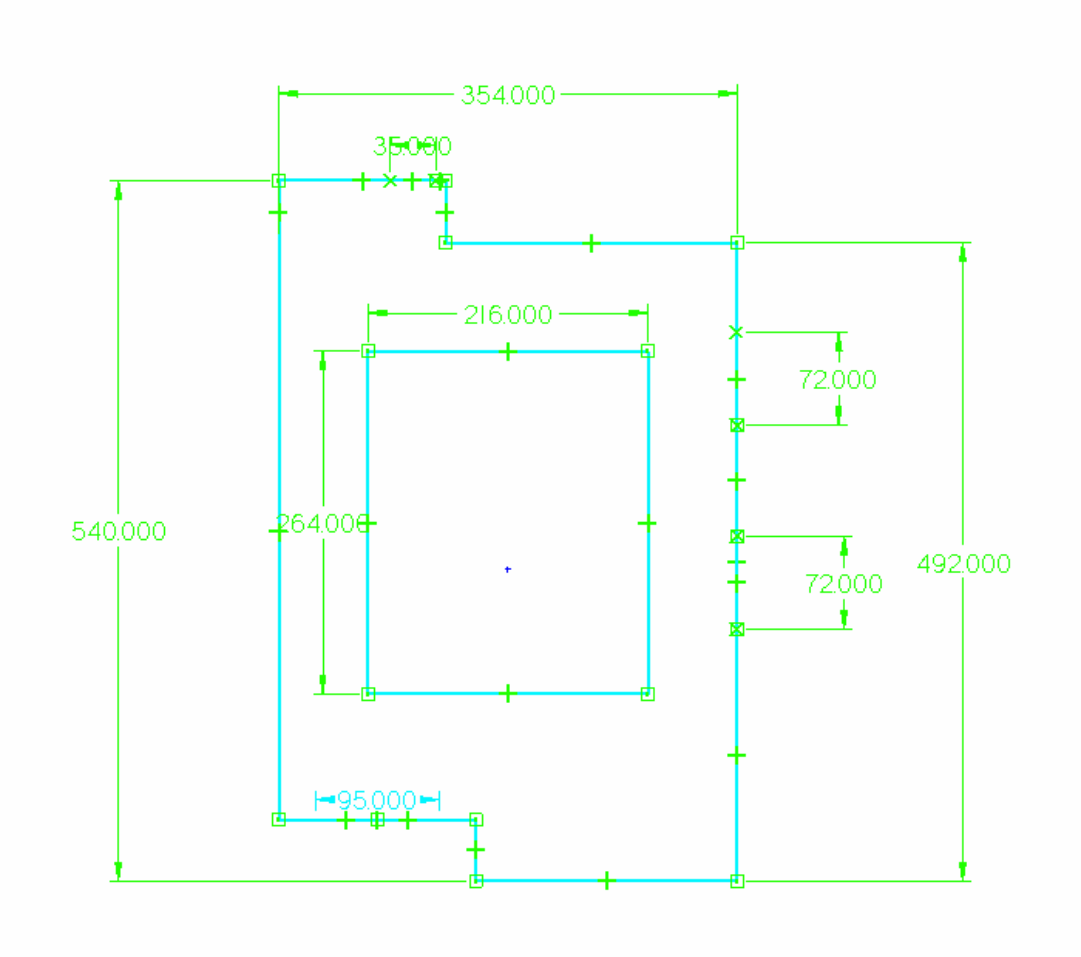


**Figure 2.6 Dimensions (inches) of PRL lab area 105 used to determine machine location**

### 2.3.2 Braider installation plan

Below are listed the steps taken to install the braider successfully.

1. Complete Assembly: position braid head frame onto track using forklift, position plates to left and right frame, position frame to the far right, (wait on bolting to floor – spacer plates on side frames, front and rear frame, braid head stops). Check for alignment using string, line level, and torpedo level. Check free movement of traverse. Check, if

possible, for free movement of braiding gear train. Check for proper clearances with walls (maximum traverse extension, check the existing bolt hole locations for stops of the braid head movement). Purchase replacement bolts and anchors. Check for stability of all structural pieces.

2. Electrical Hookup – reattach wires. Review electrical regulations. Review prior electrical hookup photograph (Army facility). Replace/repair damaged conduit.

3. Obtain Electrical System Approval before power up.

4. Machine Startup – Test motors through Console for 5 minutes – test traverse and braiding speeds (IF MOTOR DOES NOT MOVE, STOP TEST). Check motor direction. Measure and compare to console selected speeds. Test air bearings.

5. Maintenance- remove back panel. Cleanup/lubricate per Wardwell recommendations. Check feed lines and central lubrication unit.

6. 10 Minute Run – braid on mandrel.

7. Anchor Machine to Floor

8. Design/select/test as necessary creel/puller/take-up options.

### 2.3.3 Addressing electrical concerns

On the recommendation of Henry Cobb, a licensed professional engineer and staff member of the Auburn University Department of Electrical Engineering, grounding leads were installed between the stainless steel plates and the frame to insure that the stainless plates remain at ground potential.

Mr. Cobb checked the electrical grounding of the machine and noted that during certain procedures that involve use of the air bearing, it would be possible for the

stainless steel track plates to become electrically isolated from the frame. He recommended that the plates have a grounding lead to the frame in order to *insure that the track plates remain at ground potential.* He mentioned that NASA personnel had expressed a need to increase the range of machine motion, which would require the relocation of certain limit switches. NASA personnel indicated that the issues of track plate grounding and limit switch relocation would be addressed immediately.

During his visit to MSFC, Mr. Cobb assisted in bringing the braiding machine up to the original design operation. He also made the following recommendations for safety:

1. Install and/or verify proper operation of emergency stop switches;
2. Insure that key lock mechanisms are in place;
3. Install appropriate caution signs on the machine. [15]

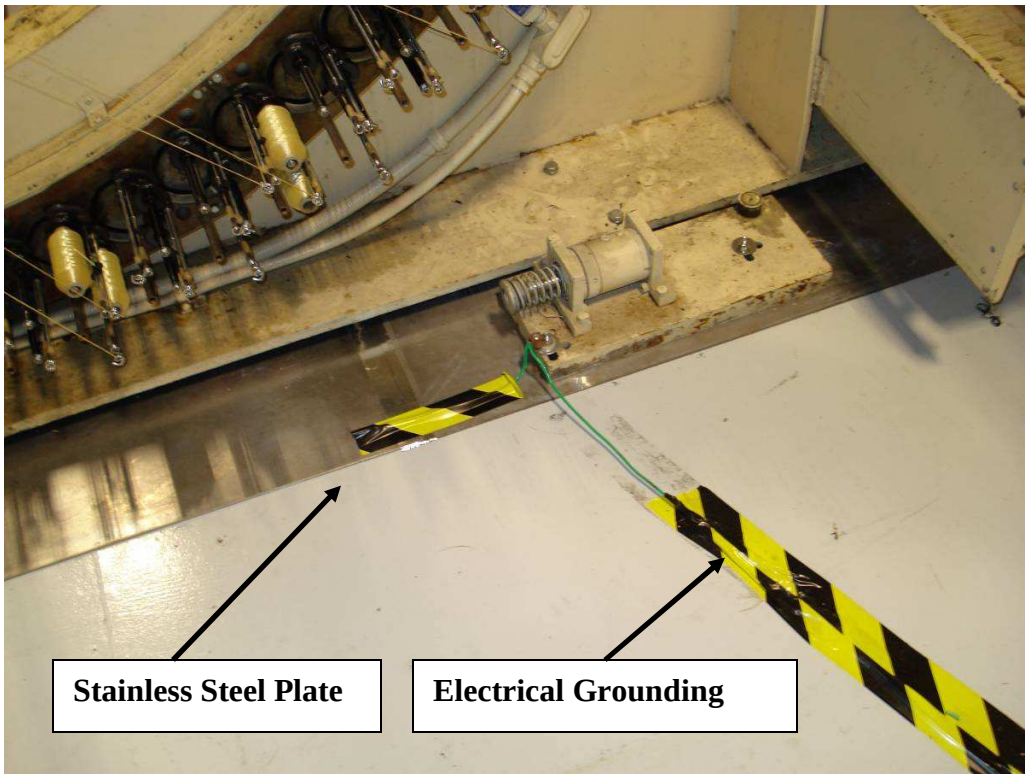


**Figure 2.7 Electrical grounding**

### 2.4 NASA take-up system: safe installation procedure

Once the installation requirements have been identified, the purpose of the following work is to establish safe installation procedures in order to install the NASA take-up system, which will work in conjunction with the NASA braider. The installation of the take-up system will be addressed in detail in subsequent section. The take-up system is delivered in 2 pieces: the capstan frame and take-up frame. Each frame assembly weighs approximately 400 lb. These will need to be removed from the box, positioned, connected together, and secured.

#### 2.4.1 General installation safety rules:

1. Abide by all NASA safety regulations
2. Always assume that the machine might fall when moved and stay clear of the fall path.
3. Select sufficient strength equipment for moving braider and associated parts.
4. Never jeopardize personal safety by reaching or crawling under the raised machine.
5. Make sure machine is properly grounded.
6. After all electrical connections have been made check rotation of the Capstan and spool.

#### 2.4.2 Safety equipment:

At any time during the installation or operation of the braiding and take-up machine adhere to the following safety equipment:

1. Close toe shoes at minimum, steel toe boots are recommended.

2. Safety glasses.
3. Ear Protection
4. Long hair containment

### 2.4.3 Procedure for installation:

1. Disassemble box walls (Phillips head screwdriver).
2. Position both frames with forklift and remove pallet.
3. Shim to level.
4. Bolt together frame using included hardware.
5. Connect Power.

### 2.4.4 Procedure for initial startup:

1. Turn main power on.
2. Set speed on controller.
3. Start take-up system.
4. Verify proper operation.

## 2.5 Safe operating procedure: NASA horizontal braider

The purpose of this document is to identify the common hazards associated with operation of the NASA Wardwell braiding machine, and establish safe practice to maintain efficiency and the safety of the operator. Warning signs must be observed and obeyed at all times. Any unusual observations or potentially hazardous conditions should be reported immediately to appropriate personnel. If the operator is at any time uncomfortable with the machine, it should be shut down without delay.

Wardwell braiding machines are constructed with the maximum operator safety in mind; however the operator should be intimately familiar with the standard operations and conditions described in this document. Using the machine under proper operating conditions according to the outlined safety guidelines promotes the mutual safety of the operator and any others in the vicinity. Safe operation means being aware of the dangers that exceeding machine limitations impose, while also having familiarity with the safety mechanisms. [14]

### 2.5.1 Safety features:

The Wardwell Horizontal braider is equipped with several safety features. The operator should understand the intent of these features. Switches are positioned around the braid path to stop motion in the event yarn breakage occurs or if a bobbin runs out of material. The gantry paths have limit switches to prevent the machine from over traveling. Several emergency stop switches are positioned around the machine frame.

### 2.5.2 Operator responsibility

It is the operator's responsibility to understand the potential hazards inherent to operation of the braiding machine and operate the machine safely within those confines. The operator should be constantly aware of unexpected sounds or vibrations and be prepared to quickly shut down the machine at any moment.

### 2.5.3 General operational safety rules:

1. Abide by all NASA safety regulations.
2. Run braider at designed braid head speed.

3. Keep electrical control boxes closed during operation.
4. Check that all safety guards are in place.
5. Do not wear clothing conducive to being caught or pulled by moving components.
6. Ensure that all bobbins are securely fastened.

**2.5.4 Potential hazards**:

1. Leaving objects on or around the machine
2. Moving parts and pinch points.
3. Clothing or hair entanglement.
4. Fiber thrown by rotating mechanisms.

**2.5.6 Safety equipment**: (to be worn during operation)

1. Close toe shoes or steel toe boots
2. Safety glasses
3. Ear Protection
4. Long hair containment
5. Appropriate particle dust mask

**2.5.7 Prior-to-operation safety checks**:

1. Familiarize yourself with the operation features.
2. Know the control panel functions; especially the location of emergency stops.
3. Ensure that the area around the machine is free from any tripping hazard or debris around the stainless steel track plates.
4. Before applying power to the braider observe any “common sense” safety issues.

### 2.5.8 Operational safety checks:

1. Ensure the work area remains free of people and debris.
2. Do not leave the machine running unattended.
3. Avoid contact with moving parts.
4. Do not leave anything on top of the control panel.
5. Ensure correct settings are selected.
6. Fully engage bobbin locks on carrier spindles

## 2.6 Braiding head selection

The Wardwell Horizontal composites braiding machine has two braiding heads. Each head consists of 144 yarn Carriers. The left braid head is outfitted to manufacture tether and the right braid head is suited for braid over mandrel composite architecture. A directional limit switch must be moved from the left to the right side in order to control the appropriate braid head packages (Figure 2.16). The braiding machine is equipped with air bearings that when inflated form a seal with the stainless steel plates; increasing the pressure allows the compressed air to lift the braiding machine. A high pressure air line must be connected between the braiding machine (Figure 2.17) and the building supply air (on the right side of the room, see Figure 2.18), and pressurized slowly to 30 pounds per square inch (PSI). Once the air bearings are pressurized the machine can be pushed to the desired braid head position. Disconnect the hose before braiding.

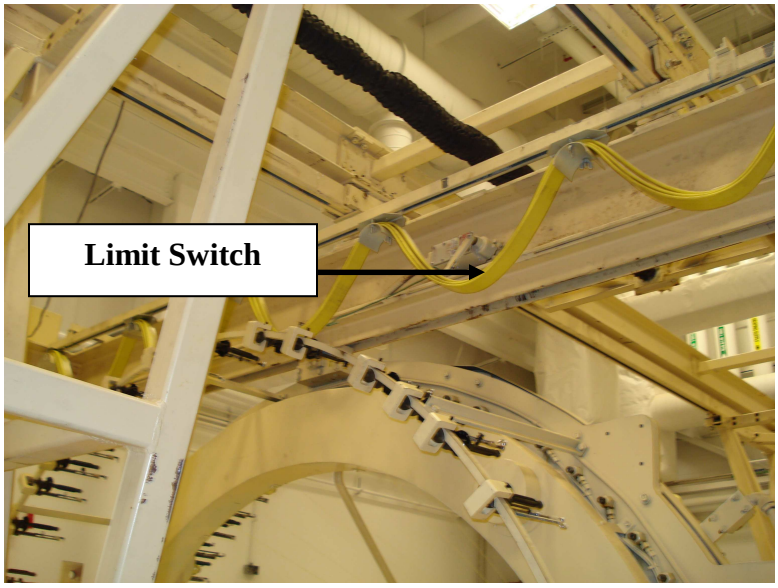


**Figure 2.8 Limit switch controlling braid head operation**

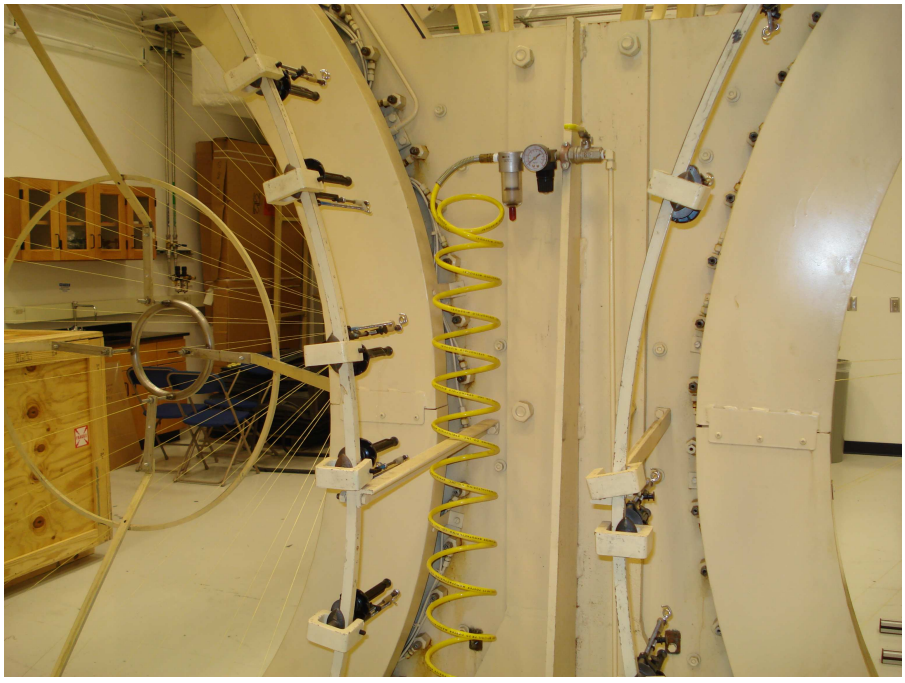

**Figure 2.9 Braiding machine air line connect for air bearings**

**Figure 2.10 High pressure air line**

**2.7 Braiding machine power up procedure:**

1. Remove the yellow lock on the main power cord (shown in Figure 2.8).
2. Plug in the power cord to main breaker (shown in Figure 2.9).
3. Push disconnect lever up (shown in Figure 2.9).
4. Turn electrical cabinet lever to “ON” position (Figure 2.10).
5. Turn the Jog/Run button to the run position (Figure 2.11)
6. Main traverse can be set to either FWD or REV (Figure 2.11).
7. Traverse Ratio must be set to zero to prohibit activation of the gantry traversing system (2.11).
8. Turn the Auto/Man switch to the Man position (Figure 2.11). Note: During the move and installation process, the wiring of this switch is incorrect.
9. Stop Motion must be set to the “IN” position (Figure 2.11).

10. Feed Braider must be selected (Figure 2.11)
11. Master speed must be selected and synchronized with the take-up machine speed controls
12. If the braiding machine is stopped using the E-Stop must be pressed, the E-Stop must be reset in order to resume operation.

### 2.7.1 Braiding machine operation: jogging the braiding machine

Jogging the machine is useful to position the packages or to determine the initial settings for the braiding machine as well as the take-up machine.

1. Feed Braider “ON” position (Figure 2.11)
2. Jog Mode (Figure 2.11)
3. Press Start (Figure 2.11)

**Figure 2.11 Braiding machine power lock**

**Figure 2.12 Braiding machine main power quick disconnect**

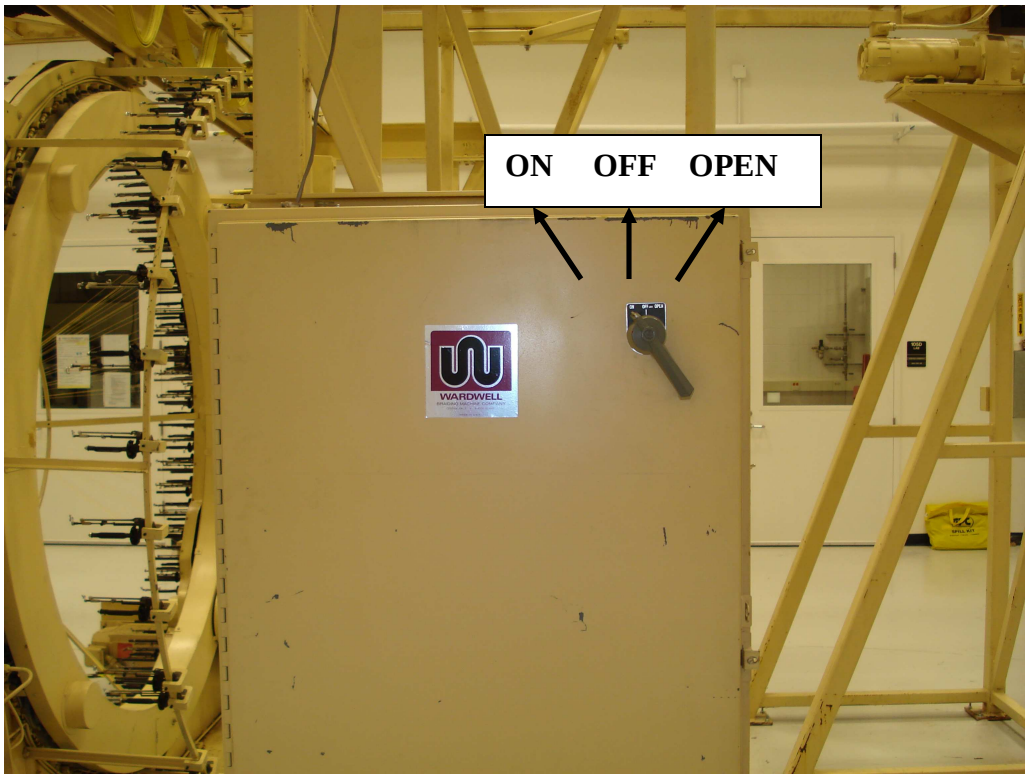


**Figure 2.13 Braiding machine main power switch**

The braiding machine electrical operation is controlled inside this panel.

**Figure 2.14 Braiding machine control panel**

### 2.7.2 Braiding machine operation: starting a braid

The steps listed below are necessary only during the initial process of determining the package configuration. Once the packages have been loaded, two people are required; one to hold the yarns under tension and one person to operate the braiding machine controls. The following steps will be useful to start the braiding process. The section (Take-up Machine Operation Guidelines) regarding the operation of the take-up machine provides specific explanations and should be observed.

1. Choose bobbins with enough material to produce the desired braid length.

2. Place bobbins on appropriate carriers.
3. Pull yarn such that the bobbin begins to rotate clockwise while material is paid off (released). This should be a smooth motion.
4. Pull all the yarns to the center of the ring and maintain tension, preventing the yarns from slacking. The braid head can be turned on to initiate the formation of a braided structure. This operation requires two people.
5. Turn on the take-up machine and set the speed appropriately.
6. Braid a sufficient amount of time to begin wrapping around the capstan.
7. Wrap partially around the capstan and the accompanying pulleys, continuing until all the grooves and pulleys are connected (see figure 2.12).
8. Continue braiding until enough material can be fed under the dancer pulley and affixed to the spool.

The electronic transformers, motor drives, relays, and various safety fuse connections are found inside the main electronics control box, shown in Figure 2.13. The door must remain closed during operation.

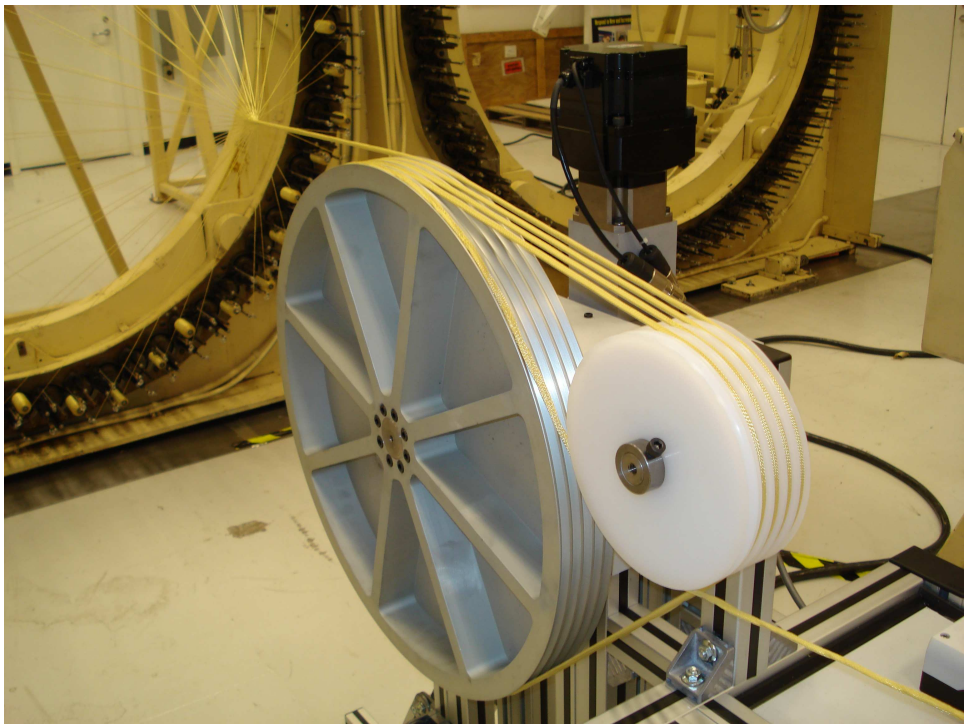

**Figure 2.15 Proper capstan wrapping configuration**

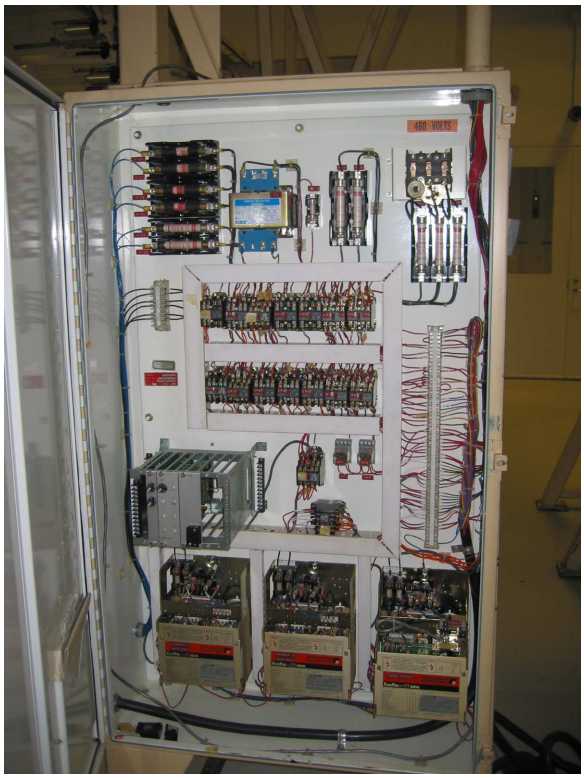

**Figure 2.16 High voltage electronics control box.**

## 2.8 Need for take-up system

A composite braiding machine can be used equally well for “traditional braiding” i.e. space tether manufacture. However, instead of a traversing-gantry-mandrel system, as is the case here, an independent take-up system must be employed. Utilizing a take-up system allows the yarn to be held under tension as the packages rotate thus forming a braid of length limited only by the amount of material available and not mandrel or gantry path length.

### 2.8.1 NASA take-up description

The NASA system consists of electrical controls, Yaskawa AC servo motor, Apex gearhead, transmission system, separator pulleys, dancer pulley tensioning system, Uhing Drive traversing unit, constant torque motor, and spool seen in Figure 2.14. The take-up speed is controlled by a Red Lion open loop voltage controller, which maintains an input voltage level that the servo amplifier/drive then converts to motor velocity and thus controls the take-up speed.

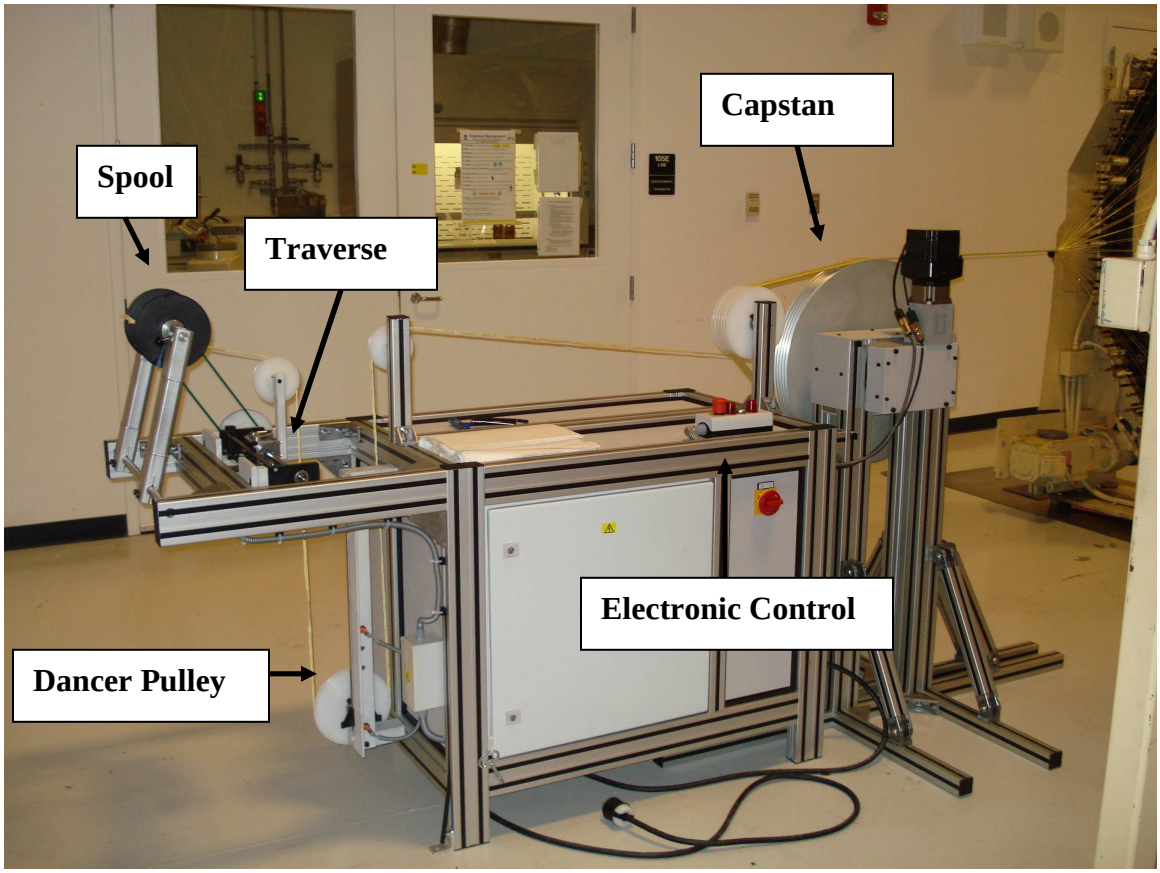


**Figure 2.17 NASA take-up system**

### 2.8.2 Function of a capstan

According to braided rope manufacturers, "A capstan is a rotating cylinder used in winding of rope or cable" [16]. The purpose of the capstan is dual in nature: wrapping fabric around its perimeter provides holding friction, while rotating torque provides the pulling force to un-spool the yarns. The NASA capstan assembly includes a servo actuated axis, transmission system, separator pulleys that work in conjunction with the capstan pulley as seen in Figure 2.18.

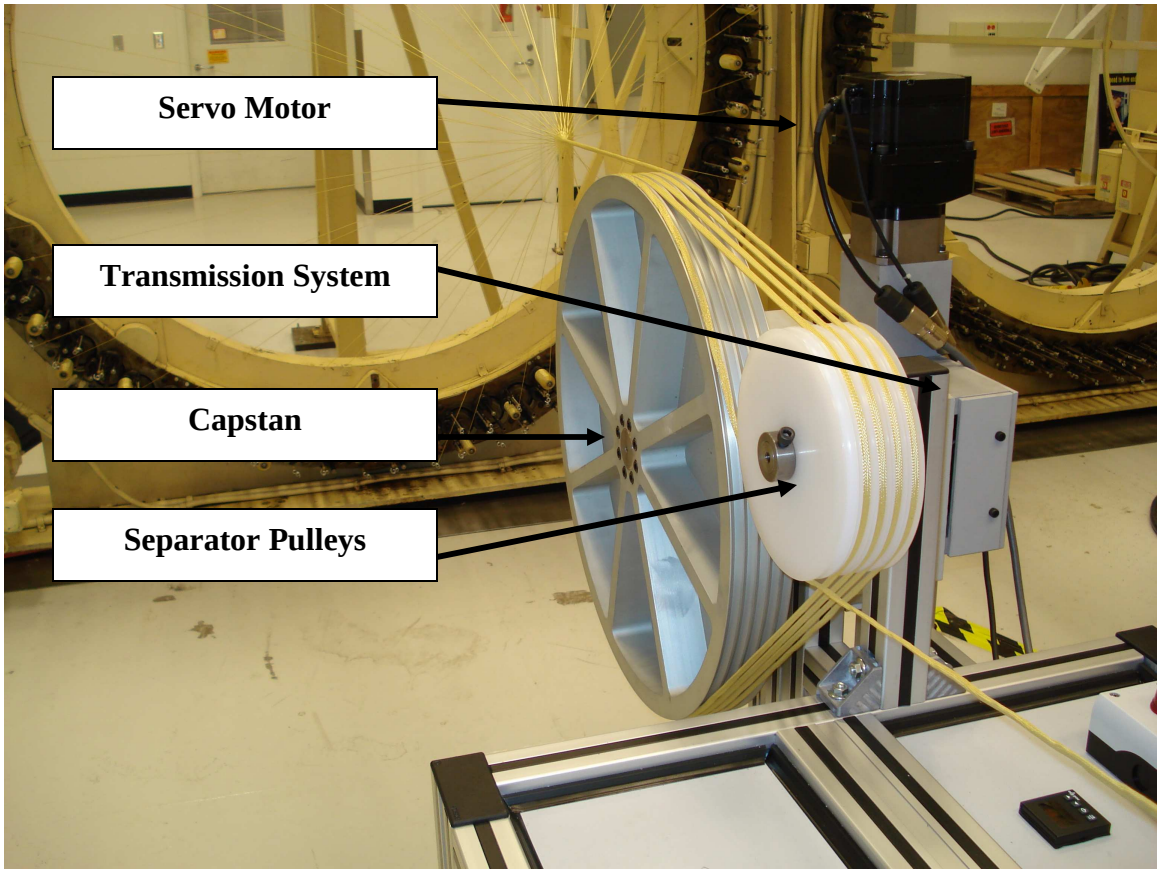


**Figure 2.18 Capstan Assembly**

### 2.9 Take-up machine operation guidelines

The following guidelines will ensure proper function of the take-up machine.

1. Once on, the capstan will begin to turn. Set the speed by adjusting the Red Lion voltage controller up or down buttons
2. Wrap the braid partly around each pulley keeping the braid in the groove.
3. Guide braid over next pulley.
4. Guide braid under dancer mechanism (next pulley toward the spool.)
5. Guide braid over traversing mechanism (next pulley toward the spool).
6. Tape the braid to spool
7. Adjust take-up speed to match braiding speed.

### 2.9.1 Take-up machine power up and operation

1. Plug in power cord to breaker (Figure 2.12)
2. Push disconnect lever upward to enable breaker power (Figure 2.12).
3. Turn red power switch to vertical position (Figure 2.13). A red light (right) illuminates, for 1 second, to indicate power, then turns off.
4. Pull up emergency stop (Figure 2.14).
5. Press green button to start take-up machine. The red light on the left will indicate Capstan motion. The Capstan should now be in motion, with the speed indicated by red 7 segment LED's on the Red Lion speed controller (Figure 2.14).
    a. A jog mode can be entered by depressing the E-Stop and holding the green on button to jog the axis. The red light on left will indicate capstan motion (Figure 2.14).
    b. If the red light on right is illuminated neither jog mode nor run mode are permitted and the main power switch position must be reset to return to normal operation mode (Figure 2.14).
6. Red Lion Capstan Speed Controller: Adjust up and down arrows to set Capstan speed indicated by a voltage reading on the display (Figure 2.14).

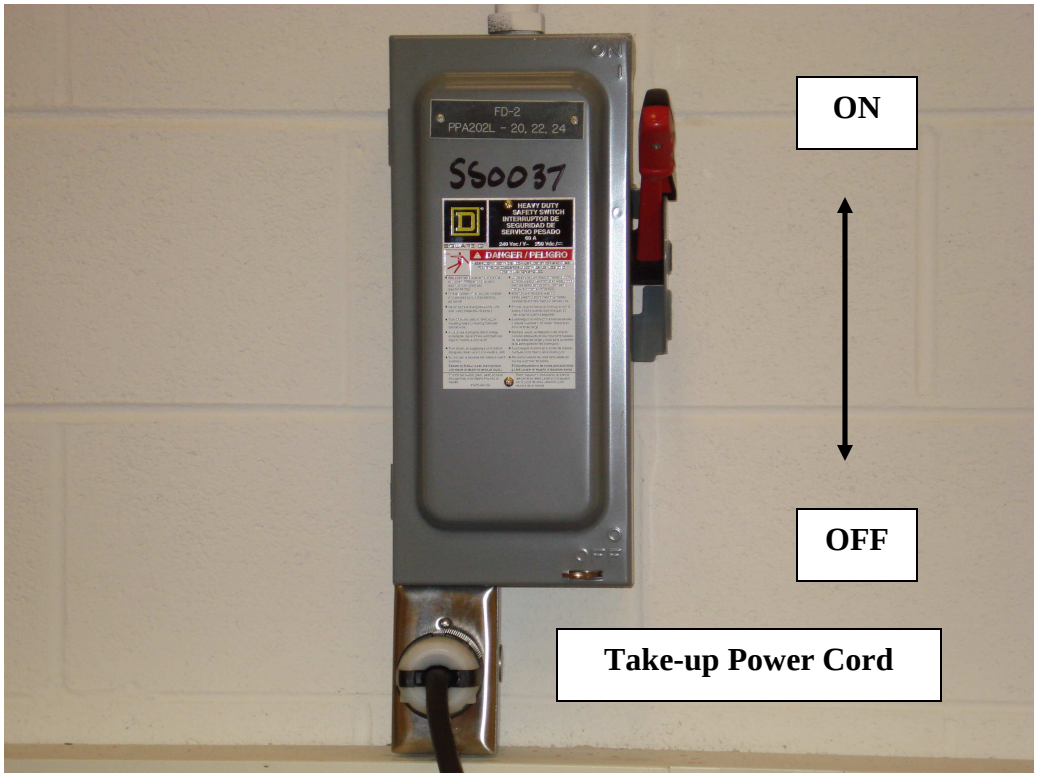


**Figure 2.19 Take-up machine main power breaker and power cord**

**Figure 2.20 Take-up machine main power switch**

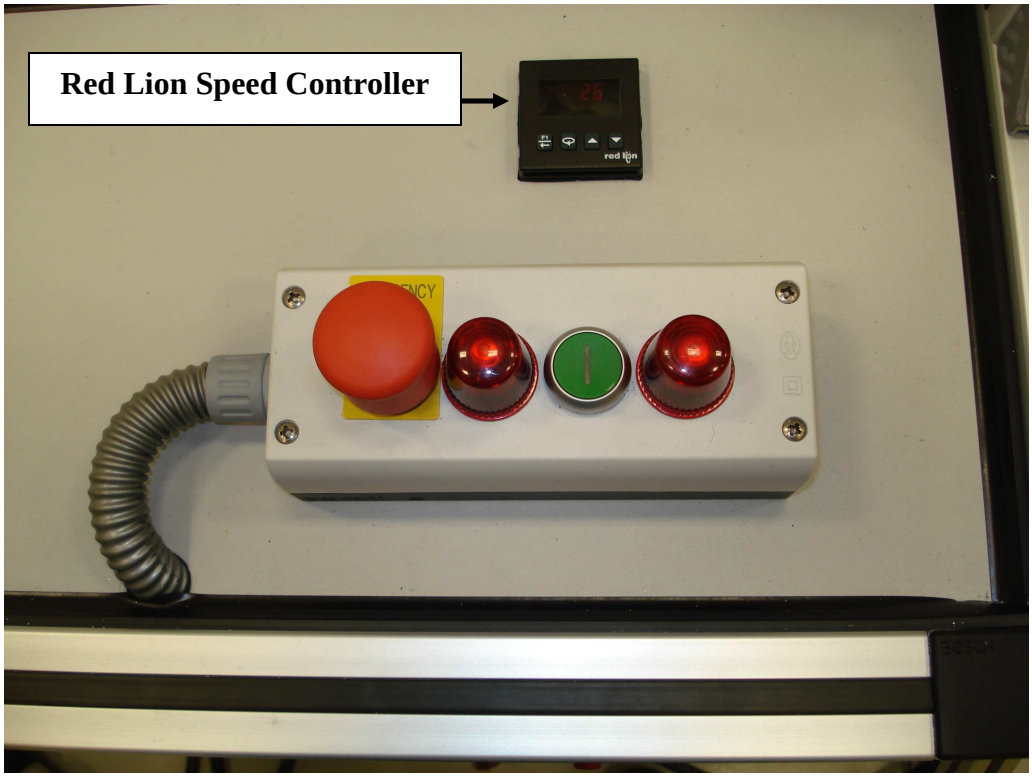


**Figure 2.21 Take-up machine power switch and emergency stop, Red Lion speed controller**

### 2.9.2 Take-up machine functional requirements

1. The take-up machine is powered on by 240 Volt, 3 phase Alternating Current.
2. Wrap braid around Capstan grooves and separator pulleys. See Figure 2.18 for example.
3. Wrap braid under dancer pulley (Figure 2.18). Note the proximity switches that function to control the start/stop action of the motor responsible for operating the take-up and traversing mechanism.
4. A Uhing Drive traversing mechanism allows adjustment of nature of the braid placement on the spool i.e. the wind angle or pitch (Figure 2.24).

5. Adjust the mechanical limit stops on the aforementioned Uhing device according to the spool size (Figure 2.24).

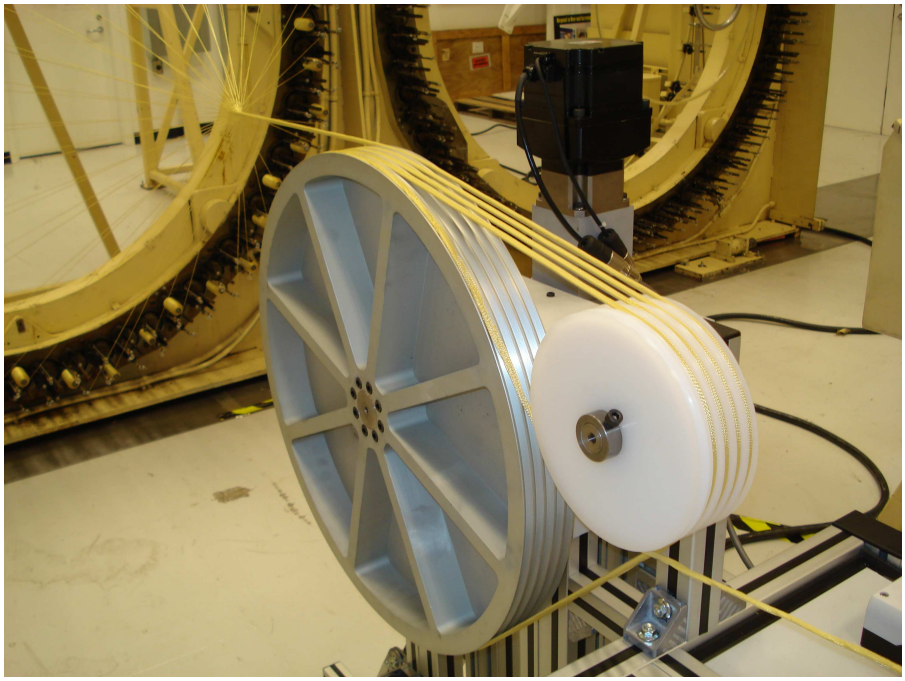

**Figure 2.22 Proper capstan separator pulley wrap**

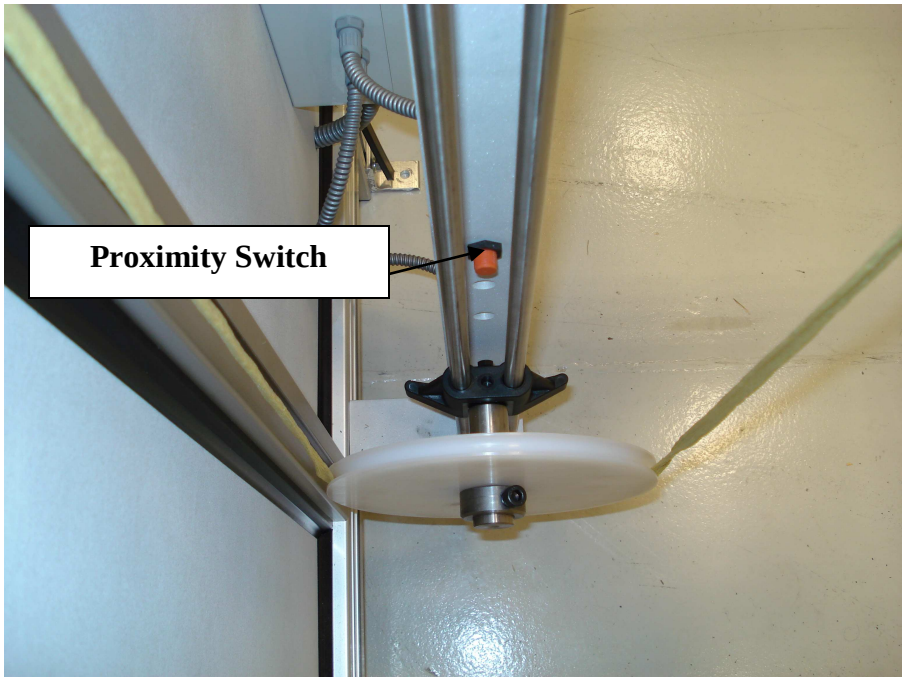


**Figure 2.23 Dancer pulley and proximity switch**

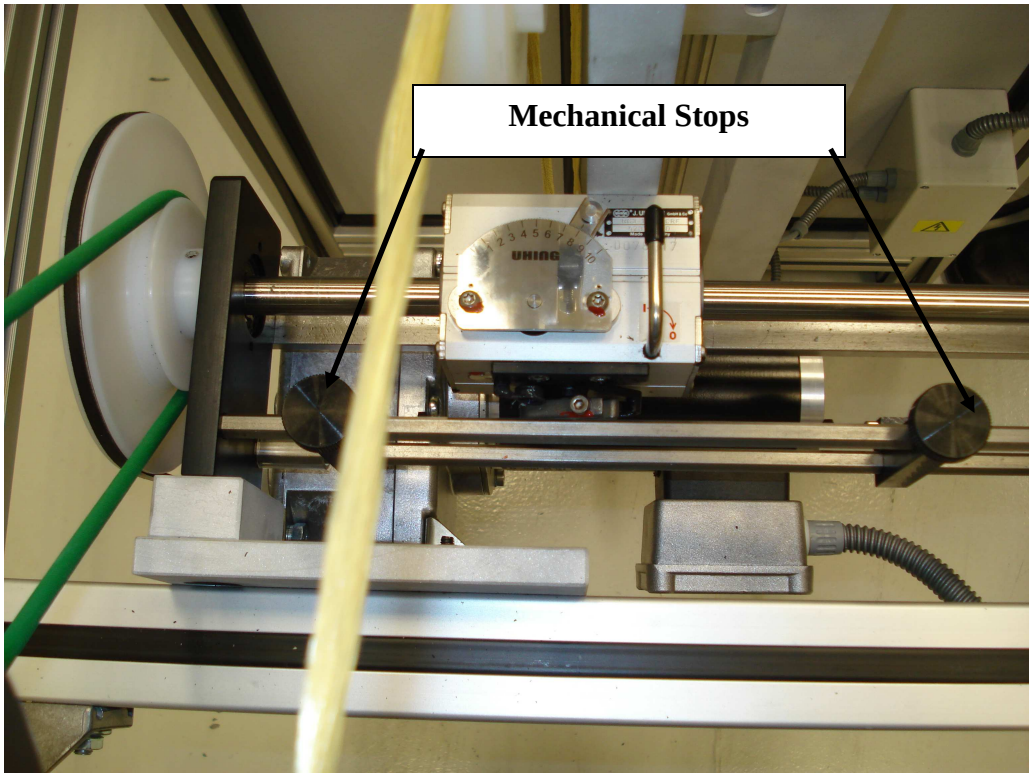


**Figure 2.24 Uhing traversing mechanism and mechanical stops**

### 2.9.3 Power off take-up machine

1. Depress E-Stop (Figure 2.21).
2. Turn red switch to horizontal (off) position (Figure 2.20).
3. Pull disconnect lever on wall breaker.
4. Unplug extension cord and store under take-up machine.

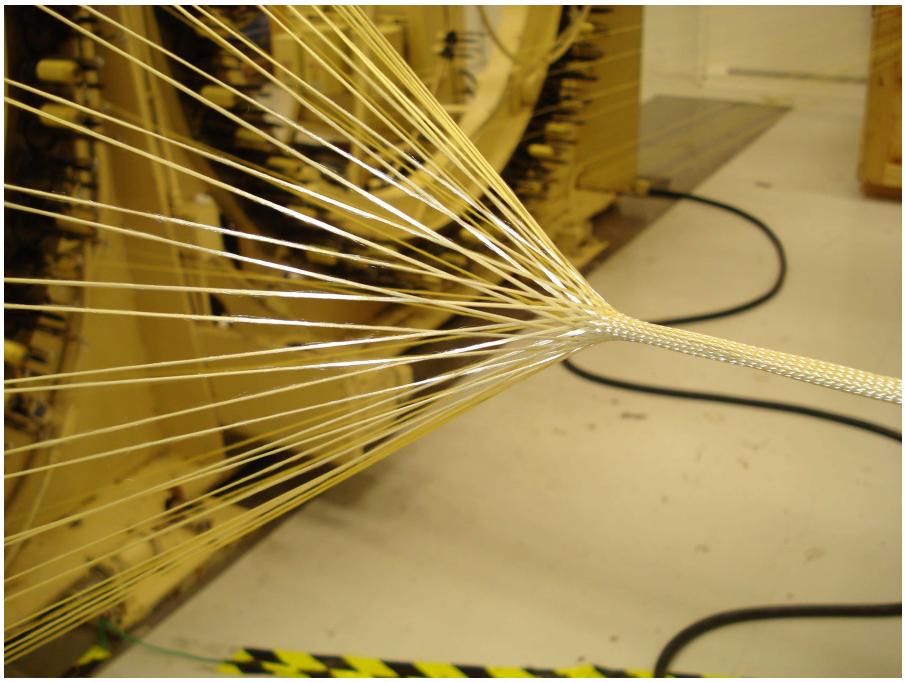

**Figure 2.25 circular braid formed on NASA braiding machine using take-up machine**

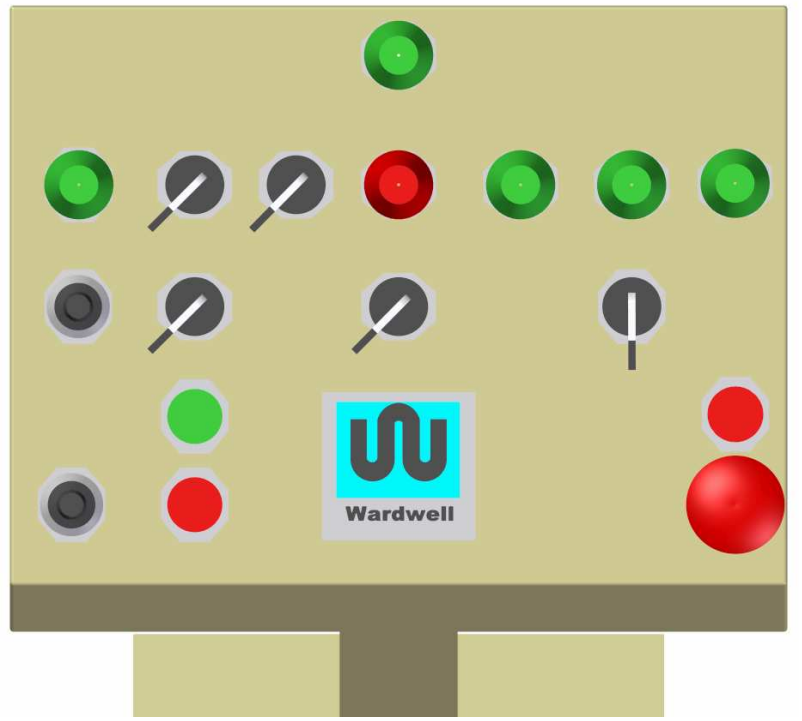


**Figure 2.26 braiding machine control panel**

### 2.10 Braiding machine maintenance

Maintaining the machine properly is an important task. In order to promote safe, consistent operation and longevity of machine performance, a regular maintenance regimen should be observed.

**All Maintenance, Service, or Repairs MUST be done with the POWER OFF!**

**General Maintenance Safety**

1. Disconnect all power before attempting any maintenance procedures.

#### 2.10.1 Lubrication information

Lubricate the carrier path on the top plate by applying a few drops of oil every 90 degrees such that the carriers will evenly distribute the oil. Use Non-Fluid Oil (Mobilplex # EP-23) for proper lubrication. If this is not possible, an equivalent containing the properties of Table 1 may be used.

| | |
|---|---|
| Apparent Viscosity @ 77 deg. F | 350 cps |
| Texture | Smooth thixotrope |
| **Base Oil:** | |
| Viscosity @ 100 deg F (SUS) | 310 |
| Viscosity @ 212 deg F (SUS) | 48 |

Table 2.1 Lubricant properties [14]

Fill pump reservoir of hand pump lubrication system with a # 2 general purpose white lithium grease and lubricate the bushings (see Table 2.4 #35). [14]

1. Daily oiling of carrier path (Every 8 hours of operation).
2. Periodic Lubrication
    a. Horn-gear bushings lubricated by hand pump lubrication system.

### 2.10.2 After-use maintenance

1. Properly power down machine.
2. Leave machine work area safe:  clean and free of debris.

### 2.10.3 Cleaning machine surfaces

Clean operating surfaces produce an optimum quality braiding environment and minimize wear.  Under normal operating conditions the braiding head should be cleaned every 8 hours of operation.  Remove excess fibers that may accumulate on the spindles and track.

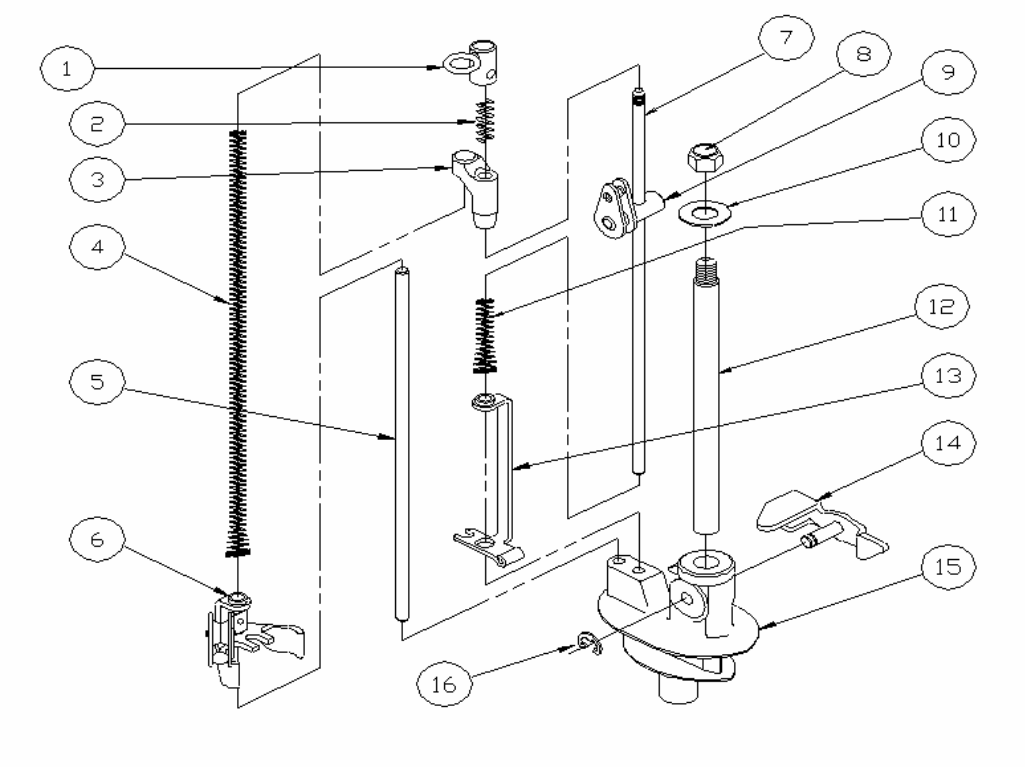


**Figure 2.27 A2BX-26C Carrier [14]**

| Item No: | Part No: | Description: | Qty: |
|---|---|---|---|
| 1 | 006045 | Ceramic Guide Assembly | 1 |
| 2 | 2BX-26 | Connecting Link Shift Spring | 1 |
| 3 | 2BX-25 | Connecting Link | 1 |
| 4 | - | See Spring Chart | 1 |
| 5 | 2BX-24 | Tension Rod | 1 |
| 6 | 006043 | Braider Stop Assembly | 1 |
| 7 | 2BX-27 | Center Rod 7-1/4lg | 1 |
| 8 | 2BX-18 | Elastic Stop Nut | 1 |
| 9 | 006044 | Center Sheave Wheel Assembly | 1 |
| 10 | 2BX-17 | Spacer Washer | 1 |
| 11 | - | See Spring Chart | 1 |
| 12 | 2BX-15 | Spindle w/Threads | 1 |
| 13 | 2BX-21 | Pawl Lift- Short | 1 |
| 14 | 2BX-19 | Pawl | 1 |
| 15 | 2BX09 | Carrier Base .601 | 1 |
| 16 | 2BX-20 | Retaining Ring | |

**Table 2.2 A2BX-26C Carrier part description [14]**

## 2.11 Example horizontal composite braiding system

The NASA braider, according to Wardwell engineers, is a custom machine designed specifically for the Army. Subsequently no other official documentation exists. [Verbal Communication with Manufacturer] However, Auburn University has a similar traversing horizontal composite braiding machine and its documentation will be referenced to provide examples. Wardwell horizontal composite style braiding machines operate on essentially the same principles and the following should provide pertinent information for properly identifying the location of parts requiring maintenance and in the event service from the manufacturer is required.

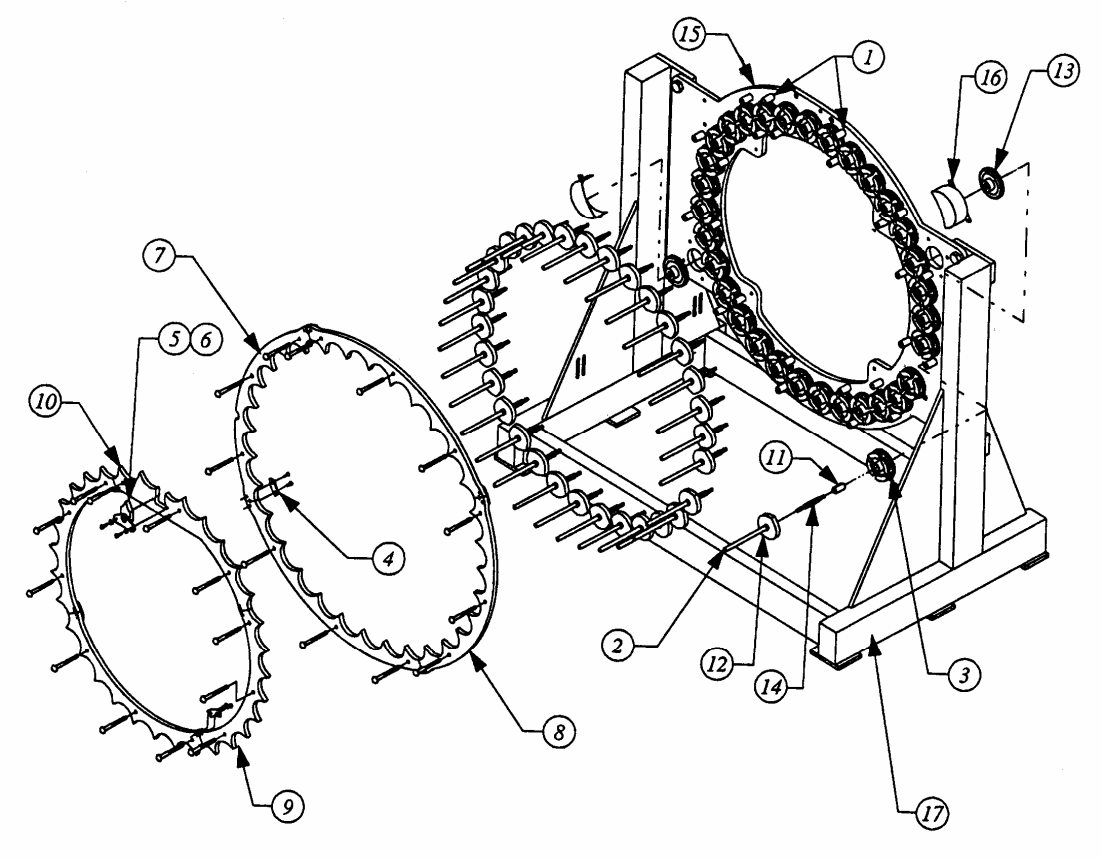


**Figure 2.28 Base group front view [14]**

| Number | Description |
|---|---|
| 1 | Horn Gear Bushing |
| 2 | Tubular Warp Guide |
| 3 | #2-4 Horn Gear-C.I.-Low Hub |
| 4 | Fish Plate |
| 5 | Thick Button |
| 6 | Button Strap |
| 7 | Rim Section |
| 8 | Rim Section |
| 9 | Star Section |
| 10 | Star Section with Button |
| 11 | Horn Gear Bushing |
| 12 | Quoit |
| 13 | Drive Gear |
| 14 | Warp Stud |
| 15 | Bottom Plate |
| 16 | Drive Gear Guard |
| 17 | Braider Frame |

**Table 2.3 [14]**

| Number | Description | Number | Description |
|---|---|---|---|
| 1 | Bearing | 18 | Housing |
| 2 | Bearing | 19 | Retaining Cover |
| 3 | Bushing | 20 | Shaft |
| 4 | Torque Limiter | 21 | Chain Tensioner |
| 5 | Collar | 22 | Drive Shaft |
| 6 | Thrust Washer | 23 | Spacer |
| 7 | Snap Ring | 24 | Adjusting Plate |
| 8 | Bushing | 25 | Mounting Plate |
| 9 | Taper Bushing | 26 | Sprocket -48 Tooth |
| 10 | Bushing | 27 | Idler Sprocket – 26 Tooth |
| 11 | Reducer | 28 | Idler Shaft |
| 12 | Sprocket- 40 Tooth | 29 | Tensioner Shaft |
| 13 | Adjustment Hub | 30 | Sprocket – 26 Tooth |
| 14 | Sprocket -48 Tooth | 31 | Bronze Bushing |
| 15 | 2 H.P. Motor | 32 | Drive Sprocket – 35 Tooth |
| 16 | Warp Stud Nut for Grease | 33 | Main Chain Drive Guard |
| 17 | Carboloy Ring Nut | 34 | Main Drive Guard |
| | | 35 | Lube System with Hand Pump |

**Table 2.4 [14]**

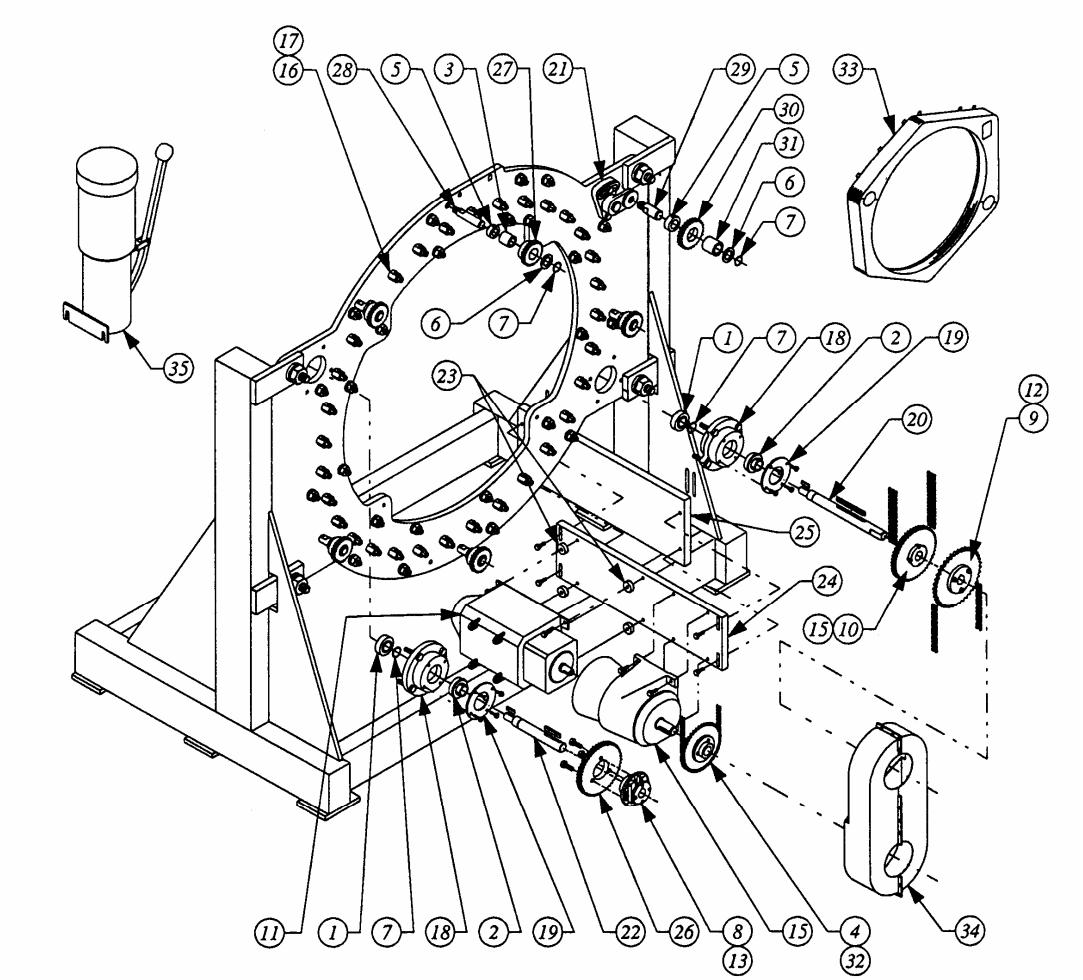


**Figure 2.29 Base group rear view [14]**

## 2.12 Spool Calculations

Calculations were made to determine the spool size required to hold a 10000 foot tether according to the following equation [17]:

$$\textbf{Factor} = (H + B) \times (H) \times (T) \times (0.262)$$

$$\textbf{Length of Cable} = \textbf{Reel Factor} / (\textbf{Cable Diameter})^2$$

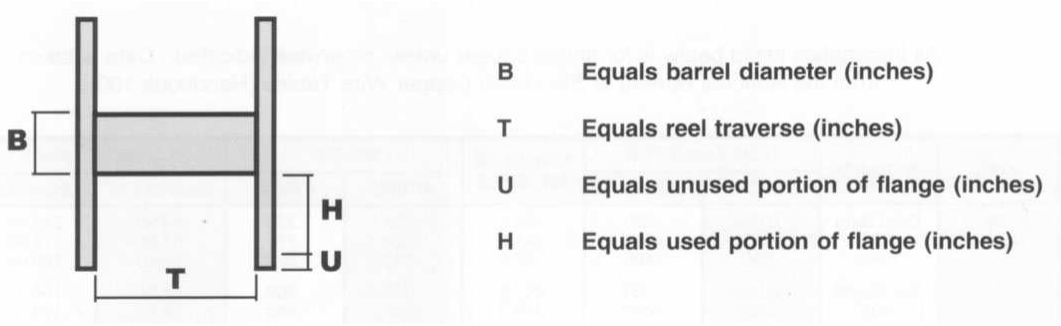


**Figure 2.30 Spool dimension calculations**

In addition to the spool capacity determination, the maximum pull force required to un-spool material for braiding was calculated. Knowing the requirements of the braiding machine and the desired tether length, practically define the take-up machine parameters. This information was used in conjunction with the manufacturer to design the machine and ensure that take-up machine is appropriately sized.

## 2.13 Conclusion

This chapter describes the practical aspects of fulfilling the responsibility to help establish a tether research facility as part of the AU-NASA contract (specific). Several MSFC (abbreviation intros) site visits were made to determine the practical aspects necessary for establishing a tether research facility. The development of a safe installation plan was made to include specific steps to ensure safety and proper set up of the machine. The plan required outlining the necessary aspects of assembly, replacing of

faulty components, cleaning and lubricating the NASA braiding machine. The take-up machine follows the conventional approach of programmed machine control and is more of an open loop system. Collaboration with the take-up machine manufacturer to determine the relevant parameters was done to ensure the take-up machine is sized appropriately. A safe installation procedure was also developed as guidelines to facilitate the take-up machine assembly. Presently the NASA take-up machine follows a conventional approach, in terms of tension and motor control technology. This conventional approach can be easily adapted to a more precise closed loop strategy by the addition of a desktop computer, PCI motion control card, and a control program.

**2.14 Useful Information**

The following spring charts are useful when determining which springs to use when setting the tension of the release mechanisms. Some useful pictures are included at the end.

## A.1 2BX Springs for Short Pawl Lifts

| Part No. | Size | Color |
|---|---|---|
| 2BX-32 | .010" X 1-1/2" | Red |
| 2BX-33 | .011" X 1-1/2" | Green |
| 2BX-34 | .012" X 1-1/2" | Orange |
| 2BX-35 | .014" X 1-1/2" | Natural |
| 2BX-36 | .016" X 1-1/2" | Black |
| 2BX-37 | .018" X 1-1/2" | Blue |
| 2BX-128 | .022" X 1-1/2" | Natural |

## A.2 2BX Springs for Long Pawl Lifts

| Part No. | Size | Color |
|---|---|---|
| 1BX-18 | .009" X 1-1/8" | Natural |
| 2BX-38 | .010" X 1-1/8" | Red |
| 2BX-39 | .011" X 1-1/8" | Green |
| 2BX-40 | .012" X 1-1/8" | Orange |
| 2BX-41 | .014" X 1-1/8" | Natural |
| 2BX-42 | .016" X 1-1/8" | Black |
| 2BX-43 | .018" X 1-1/8" | Blue |

## A.3 2BX Tension Springs

| Part No. | Size | Color | Tension in Ounces |
|---|---|---|---|
| 2BX-68 | .009" X 6-3/8" | Natural | 5/8 |
| 1BX-27 | .010" X 5-1/2" | Red | 3/4 |
| 2BX-70 | .010" X 6-3/8" | Red | 1 |
| 2BX-71 | .011" X 6-3/8" | Green | 1-1/2 |
| 2BX-72 | .012" X 6-3/8" | Orange | 2 |
| 2BX-73 | .014" X 6-3/8" | Natural | 3 |
| 2BX-74 | .016" X 6-3/8" | Black | 6 |
| 2BX-75 | .018" X 6-3/8" | Blue | 10 |
| 2BX-76 | .020" X 6-3/8" | Gray | 16 |
| 2BX-77 | .022" X 6-3/8" | Pink | 21 |

# 3. EXPERIMENTAL SETUP OF COMPUTER CONTROLLED TAKE-UP SYSTEM

## 3.1 Overview

An industrial braiding machine consists of an electric motor that powers horn gears, imparting motion to yarn carriers, referred to in this thesis as packages, that weave over and under along the sinuous path of a track plate. This over-under yarn interaction causes the yarns to interlace and form a braid. The braiding machine is obviously the most important aspect of braiding and without it the process could not be accomplished. Obviously, the braiding machine and the proper operation of its components are paramount; however, only adjustments of speed and spring tension can be made with regard to its fundamental operation. However, industrial braiding is a product of two operations: braiding and take-up. Thus the resulting fabric formation is a function of both. Given the limited adjustments on the braiding machine itself, an adjustable take-up machine is designed and manufactured, as described herein. This unique arrangement of PC based technology incorporates motion control and machine vision to control and analyze the geometry of the braid in order to understand the effects of mechanical faults.

This chapter outlines the necessary steps taken to design and build a computer controlled multi-servo axis take-up machine. Many obstacles were encountered and many actions were required to accomplish the goal of producing a functioning computer controlled take-up system; including electrical and mechanical operations such as

delivering appropriate power and modifying equipment to produce the environment conducive to accomplishing the research objective of improving the braiding process. A machine was designed and manufactured to allow computer controlled actuation. The machine consists of many parts both new and old and some heavily modified. The result of these efforts is a functioning and inexpensive approach to servo motion control and machine vision.

A 3D CAD rendering depicts the take-up machine (Figure 3.1). Three computer controlled servo axes are utilized by the take-up machine are as follows: capstan, variable pitch traverse, and spool. These components are mounted to an adjustable height table to accommodate various braiding machines. Two computers are utilized during this experiment: a desktop computer to handle the motion control, camera, and data acquisition and a laptop computer allows image acquisition from a second camera. Presently LabVIEW can only acquire from 1 USB webcam at a time, thus necessitating a second computer. The primary computer responsible for most of the experiment is a Dell Optiplex GX620 including an Intel Pentium D 3GHz processor with 2 GB RAM.

All servo axes can be electronically coordinated via electronic gearing. By coordinating the braiding machine encoder with the capstan allows for the braiding machine and capstan to maintain a constant relationship. Maintaining a constant relationship between these two axes is how conventional machines operate. The traverse axes controls the pitch or spacing of between the braid when laying it on a spool. The spool axis is unique in that as more material is constantly accumulated, the diameter ever increases which requires an ever decreasing of speed to maintain a constant spooling rate. Operating the spool axis independently, that is independent of the other axes parameters,

is useful for maintaining tension between the capstan and the spool. The spool axis can be torque controlled by using armature current signal feedback from the servo amplifier.

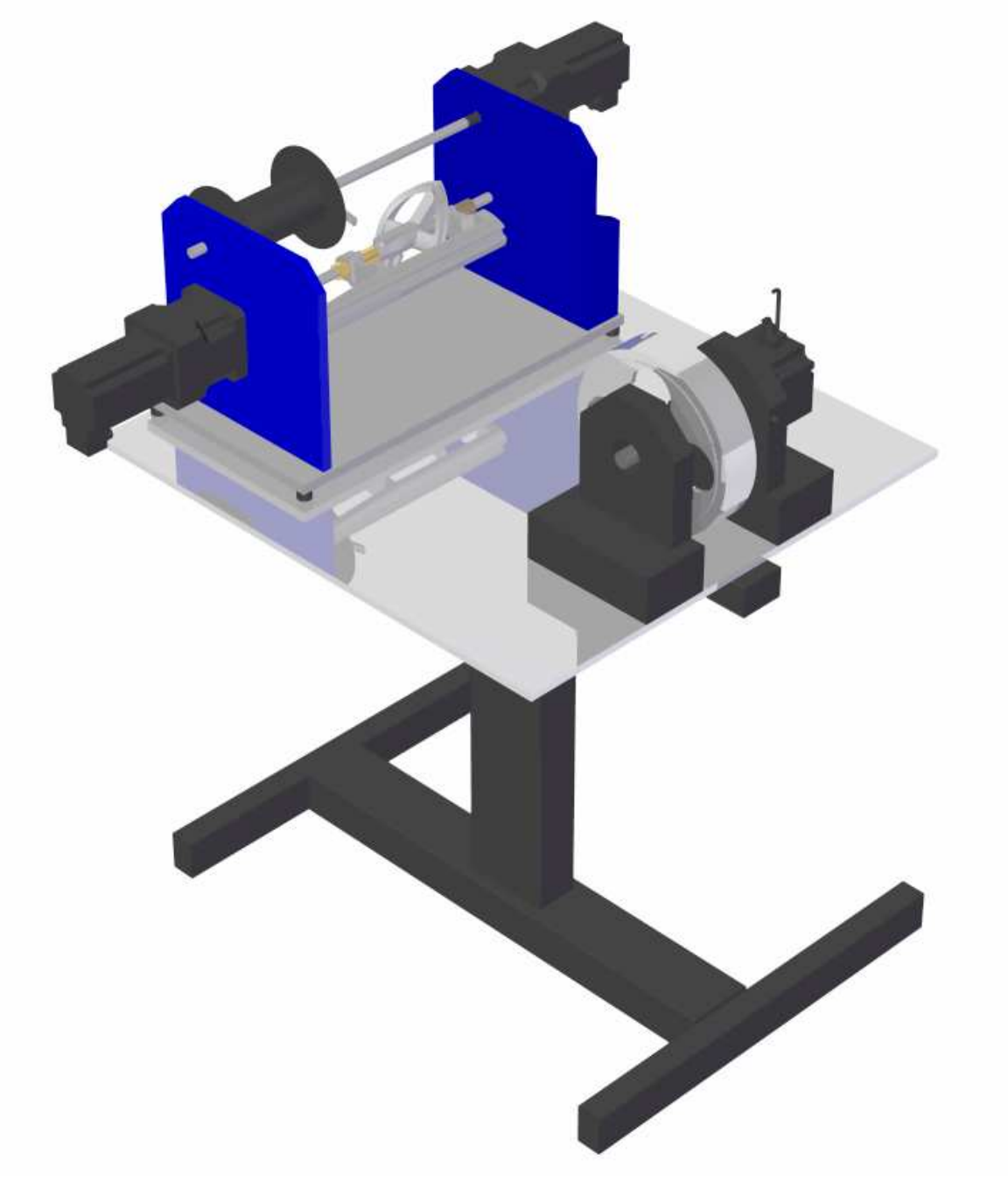

**Figure 3.1 CAD model of take-up machine**

A CAD rendering of the take-up assembly is shown in Figure 3.1.The use of computer software is a major part of the design process and enables practical problems such as interferences to be accounted for prior to final design. Producing a fully dimensioned, accurate 3D models allow evaluating the feasibility of integrating existing parts in a given structure to be done quickly and with good results. This method is used extensively as many of the parts were scavenged from surplus textile equipment.

### 3.2 Experimental Braiding Machine Description

A Wardwell Horizontal 32 carrier braiding machine is used during duration of the thesis experiments, shown in Figure 3.2. It is powered by a speed controlled DC motor which is manually adjusted. Stationary yarn carriers can be mounted from behind the machine to allow for the inclusion of axial yarns resulting in the construction of a tri-axial braided structure.

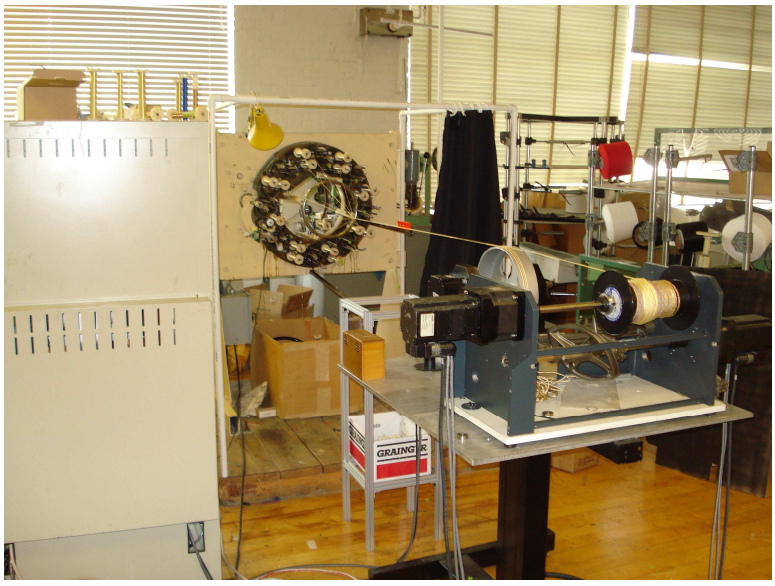

**Figure 3.2 Braiding Machine and Take-up Machine**

### 3.3 Braiding Machine track Plate Geometry

The geometry of the braid is directly related to the machinery responsible for its formation [24]. The serpentine nature of the track plates is depicted in Figure 3.3, and takes a periodic form according to equations (1) and (2) where the x and y values follow a geometric series. The negative signs are adjusted to plot corresponding values in appropriate quadrants:

$$X = \left[\frac{15}{8}\cos(2\pi t) + \frac{16.5}{2}\right]\cos(-\frac{\pi}{4}t) \qquad (1)$$

$$Y = \left[\frac{15}{8}\cos(2\pi t) + \frac{16.5}{2}\right]\sin(-\frac{\pi}{4}t) \qquad (2)$$

The yarn packages or carriers travel on two separate paths (orange and blue in Figure 3.3); together each path contributes to the yarns interlacing over and under and thus producing a tubular braid [24]. The track paths are sinusoidal, each consisting of eight peaks and valleys. The shape of Figure 3.3 is important in understanding the motion of the braid formation point when tension induced faults occurs, described in Chapter 4 and 5. As the package approaches the peak, the yarn is pulled from the greatest radial distance from the center (braid point). Conversely, when the package approaches the valley the yarn is closest to the center.

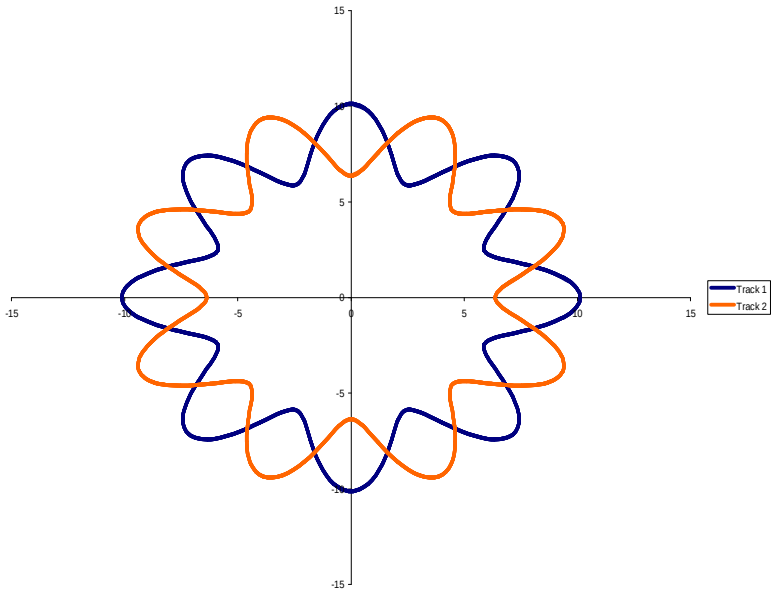


**Figure 3.3 Track Plate Paths of Braiding Machine**

### 3.4 Initial electrical requirements

The Yaskawa Sigma II servo motor requires 240 volt, single phase Alternating Current (AC), power. However, this power requirement was not initially available in the Polymer and Fiber Composites Laboratory. Drop out box outlets were installed and two legs of the single phase existing power were connected in series to produce the appropriate power for the servo motor drive (shown in Figures 3.4, 3.5).

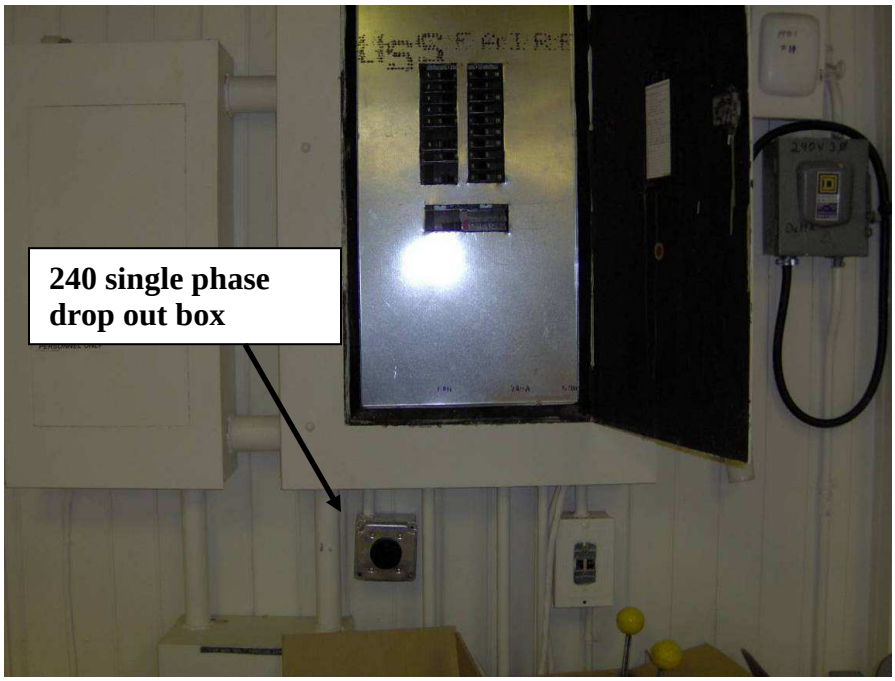


**Figure 3.4 Required 240 single phase drop out electrical outlet**

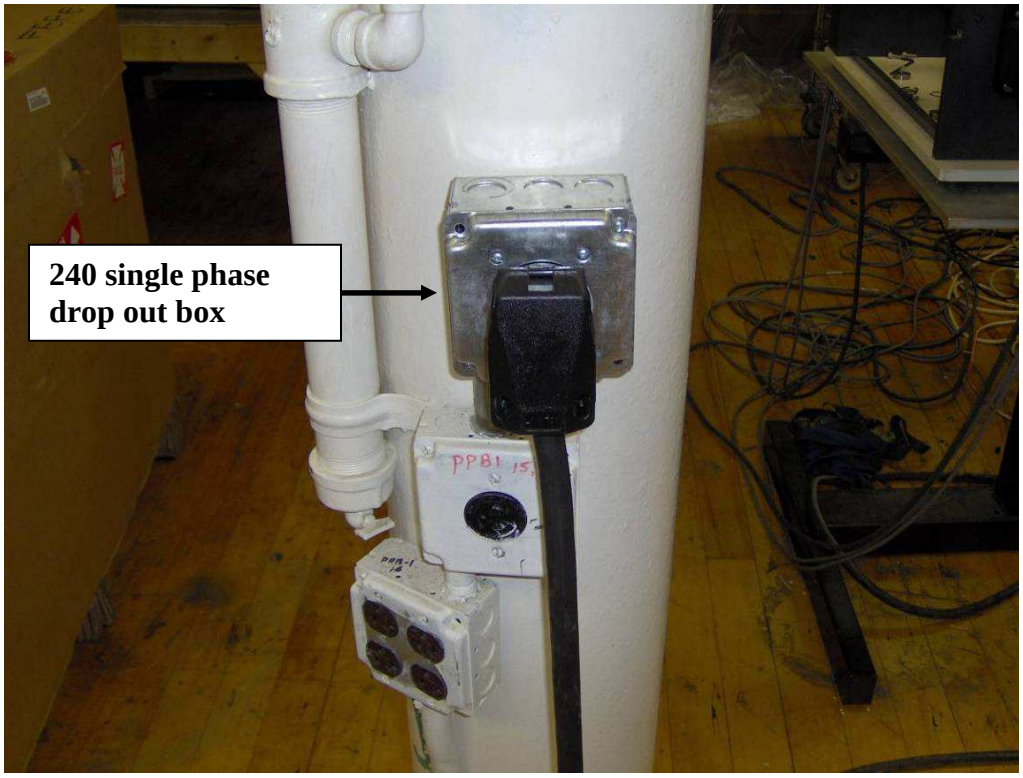


**Figure 3.5 Required 240 single phase drop out electrical outlet**

### 3.5 Initial mechanical requirements

The 32 carrier Wardwell Horizontal braiding machine initially had a mechanically geared capstan coupled to the braiding machine motor via the main input shaft. The capstan was used in conjunction with a plastic former ring to force braid point convergence before being wrapped around the capstan. However, this arrangement is fixed in nature and interfered with the objectives of this research and was subsequently removed.

### 3.6 Construction of the take-up machine

The machine as constructed consists of several scavenged parts from obsolete textile machines including an elliptical cam (patented circa 1890's) that converts rotary to linear motion to lay the braid on the spool. The measuring wheel from a yarn counter serves as the capstan. Most of the other parts came from the scrap bins of the machine shop and various other places on campus, including an adjustable height table, so the take-up system can be used in various configurations. Fortunately, the AU Design and Manufacturing Lab (DML) has advanced machining capabilities and 3D models of the available parts and scrap materials were created and quickly modified to fit, and then sent directly to be Computer Numerically Controlled (CNC) machined.

The construction of the take-up machine utilized several facilities on campus. The DML provided material as well as the Computer Aided Manufacturing (CAM) software and the CNC machine to satisfy the precision required by rigid shaft connections. The alignment of shaft, couplings, and bearings is crucial when employing rigid couplings. Polymer and Fiber Engineering has a light duty machine shop which the milling machine and lathe were used in the manufacture of the braiding machine encoder

mounting bracket and shaft extension. Auburn University Physics department instrument shop provided manufacturing expertise for some critical parts as well as an arbor press to seat the oil impregnated shaft bushings. The Auburn University Fusion Laboratory provided access to a Faro Coordinate Measuring Machine (CMM) that was used to produce a CAD model of the traversing elliptical cam.

A computer aided design approach was taken in the design of the take-up machine design and manufacturing process was greatly enhanced by utilizing a design first, build last methodology. Especially since many of the parts were scavenged from obsolete textile machinery, and modified heavily from their original design intent. A CAD prototype approach proved invaluable as available material often limits design considerations but allows for the feasibility of available components to be assessed in various configurations.

### 3.7 Capstan axis assembly

The capstan is an important part of the take-up machine. Its surface provides holding friction and prevents the braid from slipping so that it can be paid off at a given speed from the braiding machine. The capstan is the first servo axis, shown in Figure 3.6.

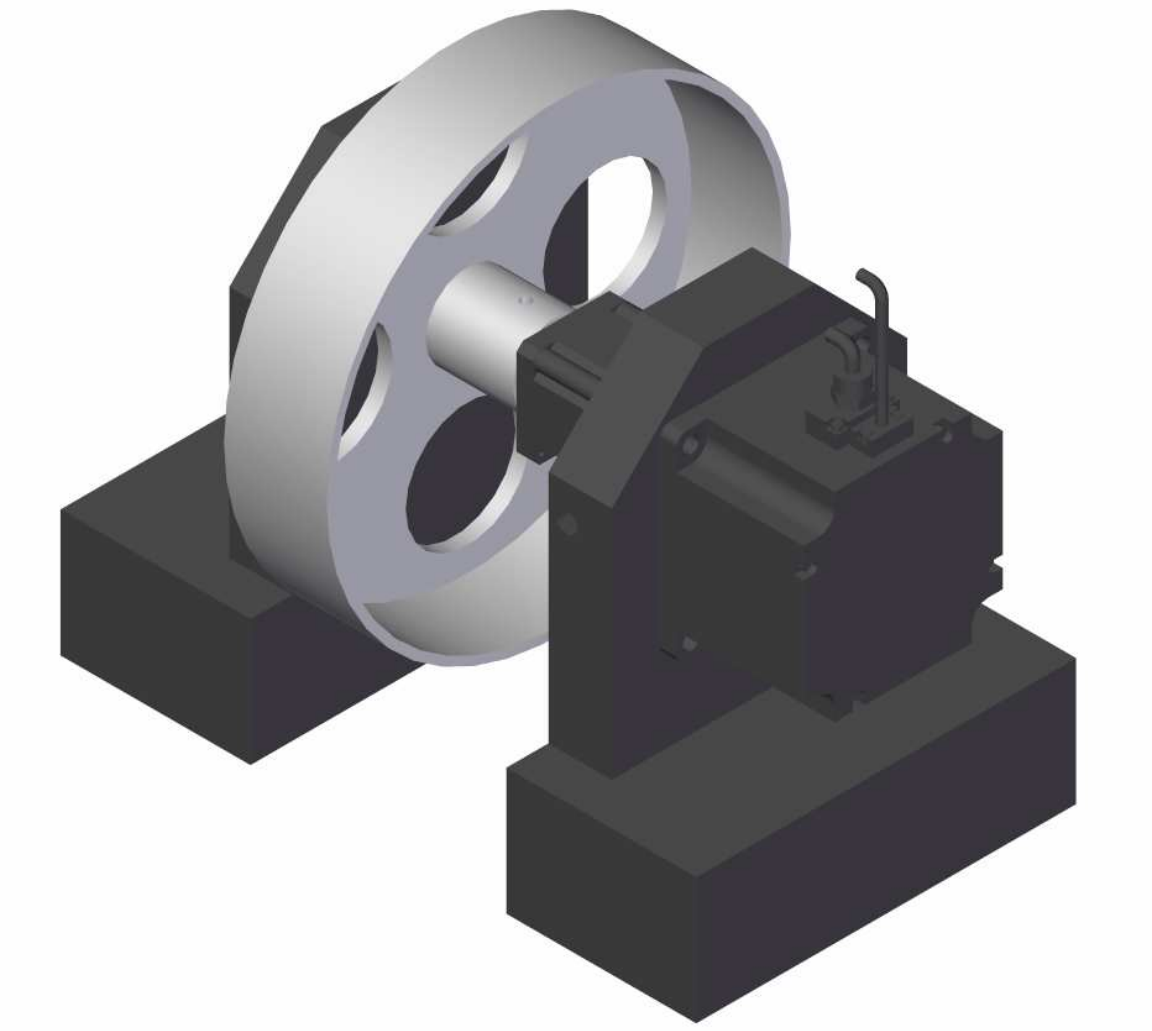

**Figure 3.6 Capstan Assembly**

A yarn counter was disassembled and the counting wheel is utilized as the capstan for the take-up machine. A CAD model was made to help predict the reflected inertia at the Yaskawa servo (Figure 3.7).

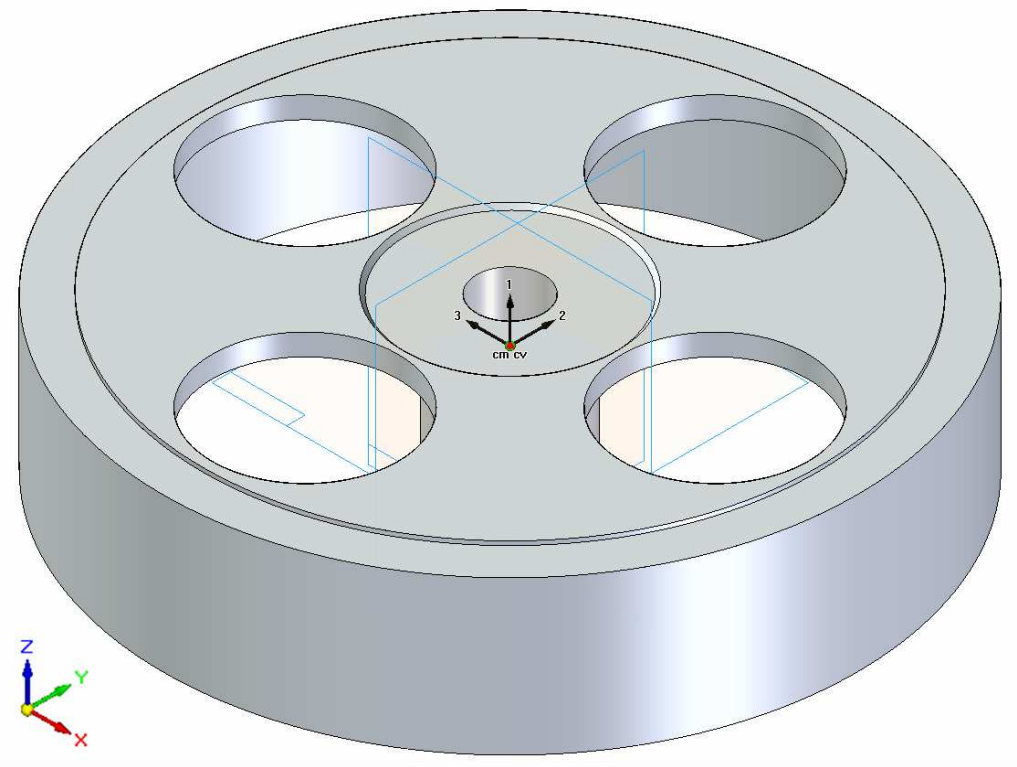


**Figure 3.7 Parametric model used to determine capstan properties**

Good agreement exists between the predicted properties from the CAD models and those measured with lab equipment. Solid Edge software calculates the mass and moment of inertia. The predicted mass was within 1% of the actual mass measured on a 6 digit precision digital balance. The ability to easily apply material properties to the inherent geometric nature of CAD based calculations provides an excellent tool for determining with accuracy otherwise tedious calculations, but vital parameters such as mass, volume, and inertia are easily obtained. Figure 3.8 is an example of some of the mechanical properties generated in the CAD software.

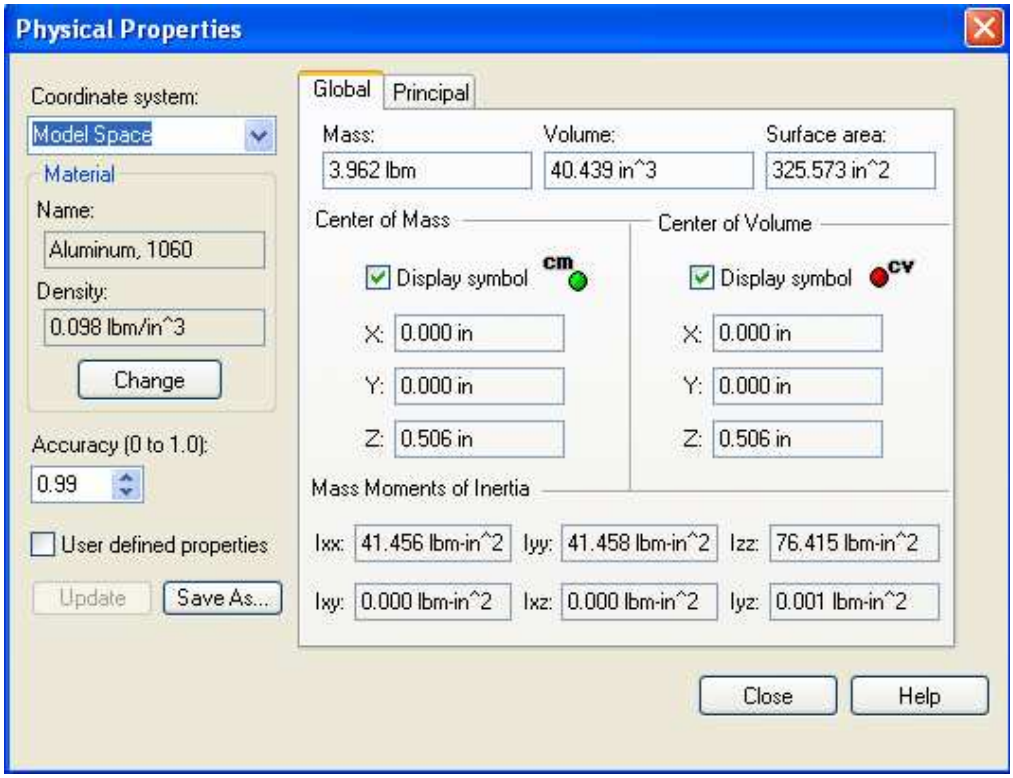


**Figure 3.8 Calculated capstan properties**

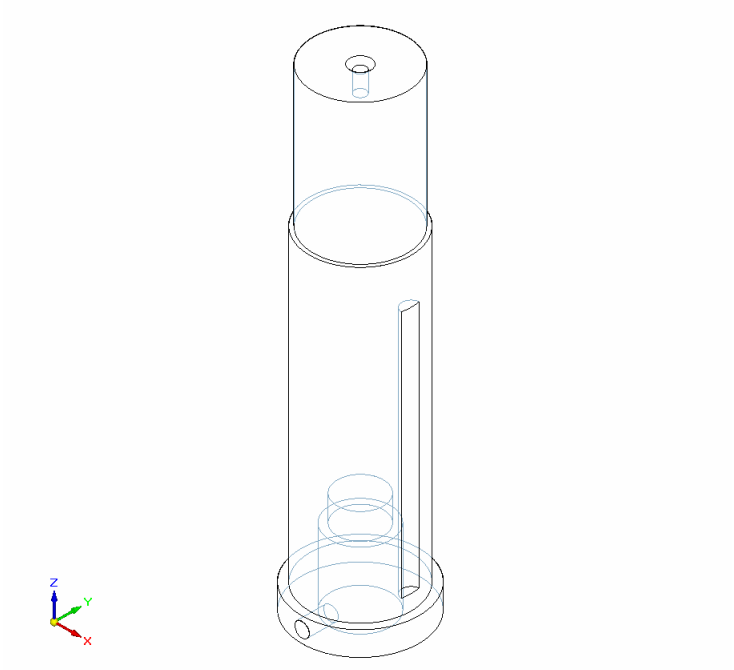


**Figure 3.9 CAD model of the capstan driveshaft**

A CAD drawing of the Capstan driveshaft in Figure 3.9 shows a stepped shaft which proved necessary to accommodate differences in the available bearings and the capstan inner diameter. The drive shaft was manufactured using a lathe. It was a fairly complex piece to manufacture including operations of turning, drilling, boring, and keyway cutting. Design considerations included a rigid connection of the drive shaft, achieved by a compression set screw, to the gearhead output shaft; and a reduced diameter to accommodate the bearing surface.

### 3.8 CNC Programs

Mastercam X, a PC based CAM software, was used to generate the tool paths and visually examine the machining processes before sending them to the CNC milling [20]. The CNC machine is a Cincinnati Arrow 750, which employs an Acramatic A2100 controller. Mastercam X produces tool path files which are sent to a post-processor and used to generate g-code specific to the Cincinnati Arrow 750, providing line by line instructions for the CNC machine tool actions (See Figures 3.10-14). The accuracy of the Cincinnati Arrow 750 is 0.0001" [19].

The take-up machine is comprised of two separate portions: the capstan assembly and the spooling mechanism, both of which utilized CNC and other machine tool technology manufacturing techniques. The spooling mechanism and the capstan assembly required several machining operations, some performed on manual machine tools and others on CNC machinery. The CAD models produced using Solid Edge V19 were imported into Mastercam X where the appropriate tool paths and code were generated.

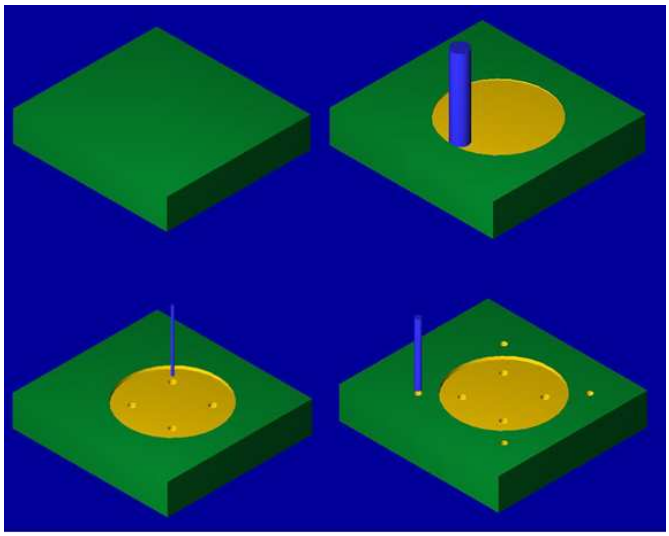

**Figure 3.10 CNC tool paths Servo Side**

CNC machining provides good accuracy and is generally much quicker than manual methods for complex parts. The CNC process is accomplished using servo motors and a motion controller to provide command signals required to machine a desired part. Due to the strict requirements of precision required for servo axes and the tacit difficulties of establishing axial alignment between large parallel plates, CNC operations are preferable. Utilizing a precision based manufacturing approach allowed the use of less expensive; although less forgiving to misalignment, rigid shaft couplings.

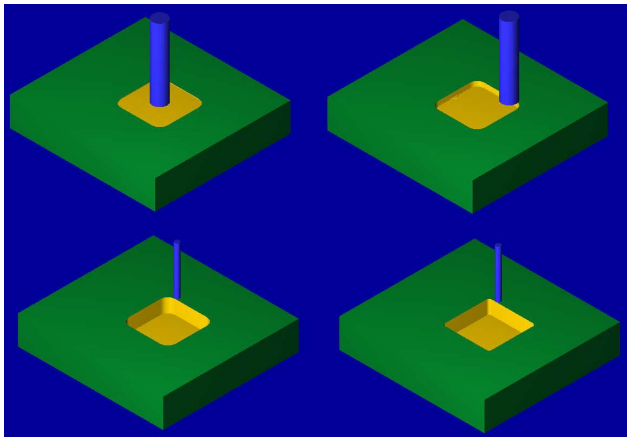

**Figure 3.11 CNC Tool paths (1) gearhead side**

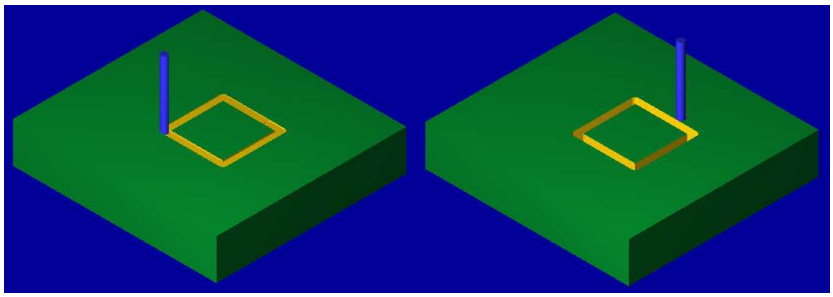

**Figure 3.12 CNC tool paths (2) gearhead side**

Figure 3.12 shows how the gearhead pocket had to be enlarged slightly to account for some minor interference.

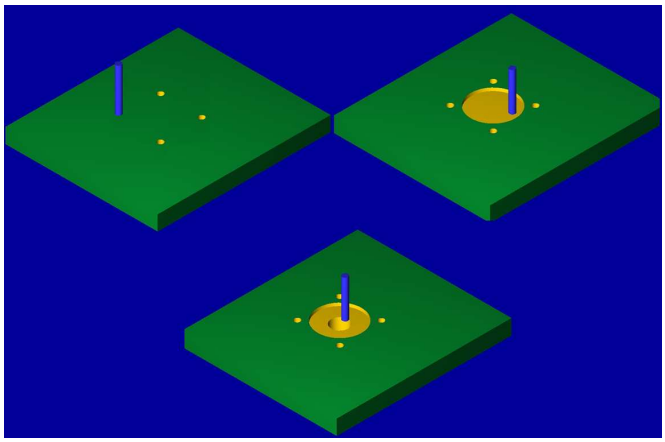

**Figure 3.13 CNC tool paths (1) for servo motor mount**

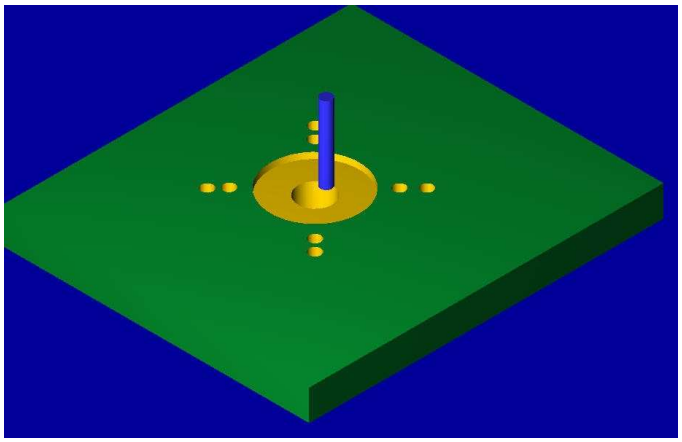

**Figure 3.14 CNC tool paths (2) for servo motor mount**

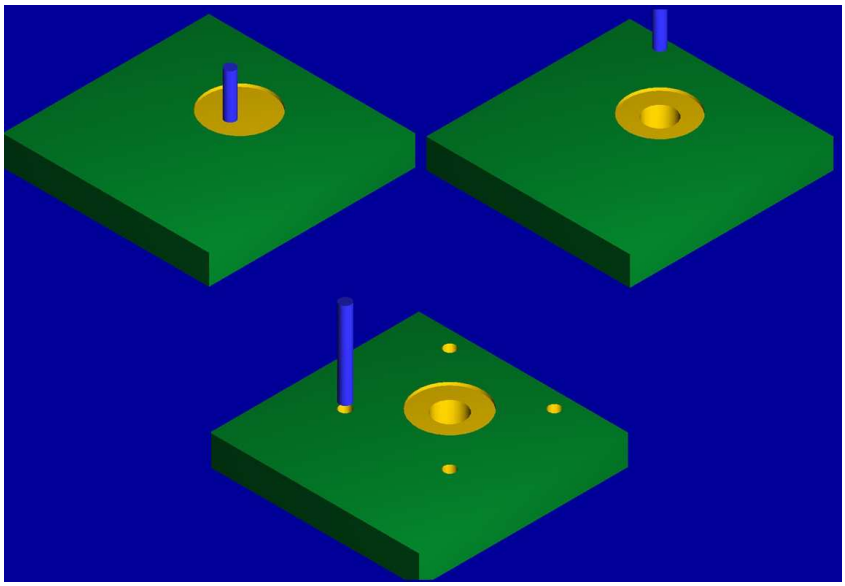

**Figure 3.15 CNC tool paths (3) for servo motor mount**

### 3.9 Motion control

Motion control involves precise control of position in a given direction and can be linear or rotary motion. In the case of this research all axes are rotational in nature; however, the traverse gives reciprocating linear movement; although its control is rotational. The motion controller calculates trajectories, torque, and closes the position/position derived loops (PID) via the encoder. If the motor position moves from the commanded position (desired) a correcting torque will be produced as the motion controller senses a position error. The servo amplifier (drive) outputs a current proportional to an input signal-voltage received from the motion controller. The amplifier closes the current loop via associated electronic hardware.

The motion controller used throughout the course of this thesis research is a National Instruments (NI) PCI 7344; it is a four axis motion controller that uses high performance motion controller architecture including an onboard CPU with an embedded real-time operating system. This motion controller can control up to four servo motors

whose drives are configured in a torque operation mode. A Universal Motion Interface (UMI) 7764 is used as a signal breakout board for accessing the 7344 Inputs/Outputs (I/O).

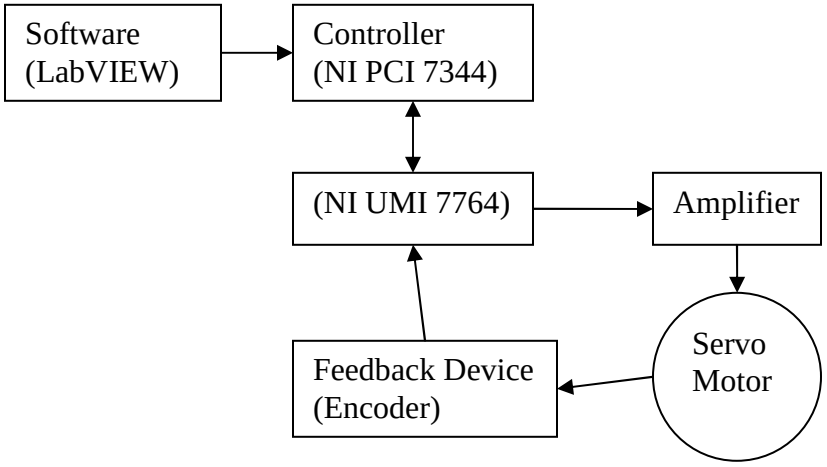


**Figure 3.16 Motion control flow chart**

Figure 3.16 is a schematic representation for PC based motion control. The 7344 is a combination servo and stepper motor controller for PCI bus computers. The 7344 can provide fully programmable motion control for up to four independent or coordinated axes of motion. The fourth axis is dedicated to a shaft mounted encoder that measures the braiding machine drive shaft position, from which braiding speed is derived.

The NI 7344 sends a +- 10 V (configurable) signal that the motor drive (amplifier) converts to an appropriate current or torque to send the servo motor. The 7344 has a Proportional Integral Derivative (PID) update rate of 62 μs per axis. This device has four general purpose analog outputs that are used for monitoring and feedback. A servo axis operates in closed-loop mode, using quadrature encoders or analog inputs to provide position feedback. [18]

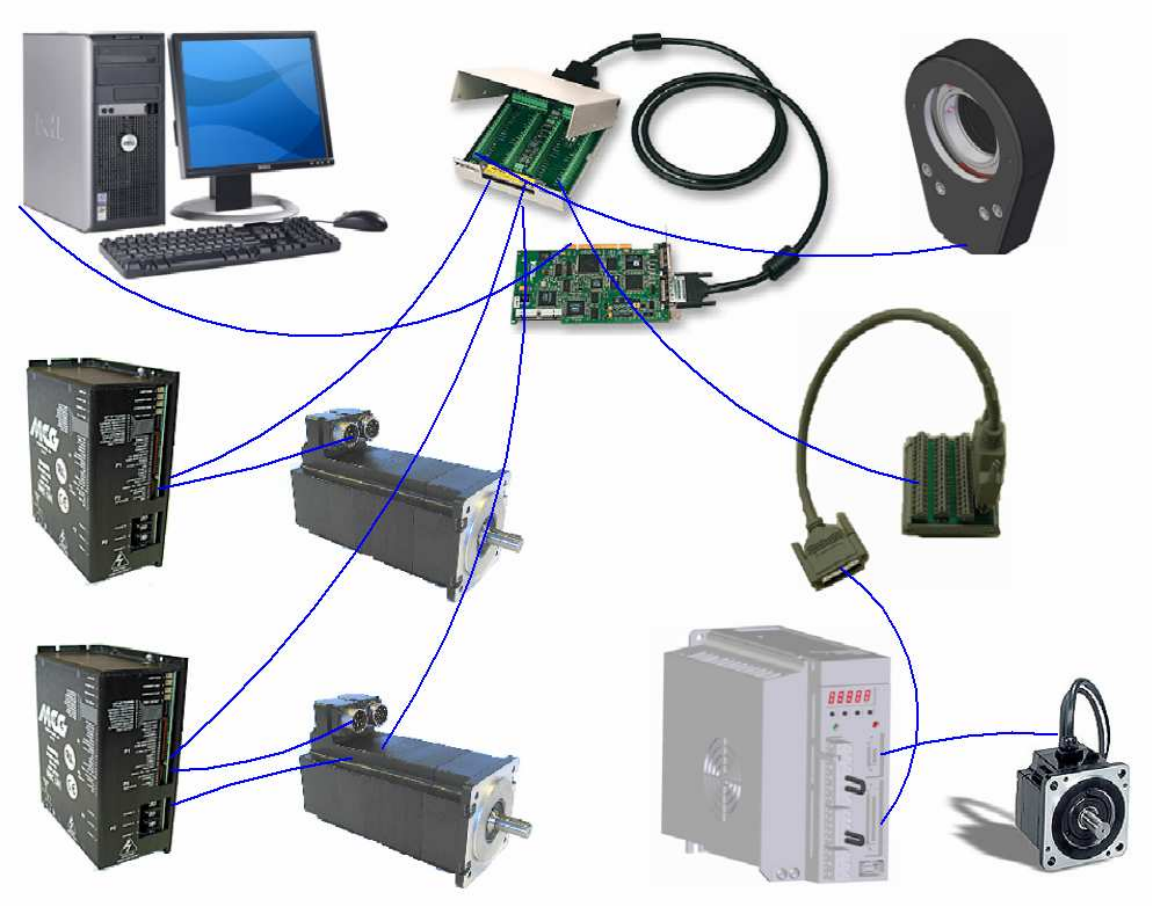

**Figure 3.17 Take-up machine motion control components**

Figure 3.17 is a visual representation of the motion control hardware including some actual components and their connectivity.

The NI UMI-7764 is used to provide connectivity between servo drives and the 7734 motion controller. All the inputs of the control system come through the UMI 7764 via screw terminals such as encoder and motor current monitor signals.

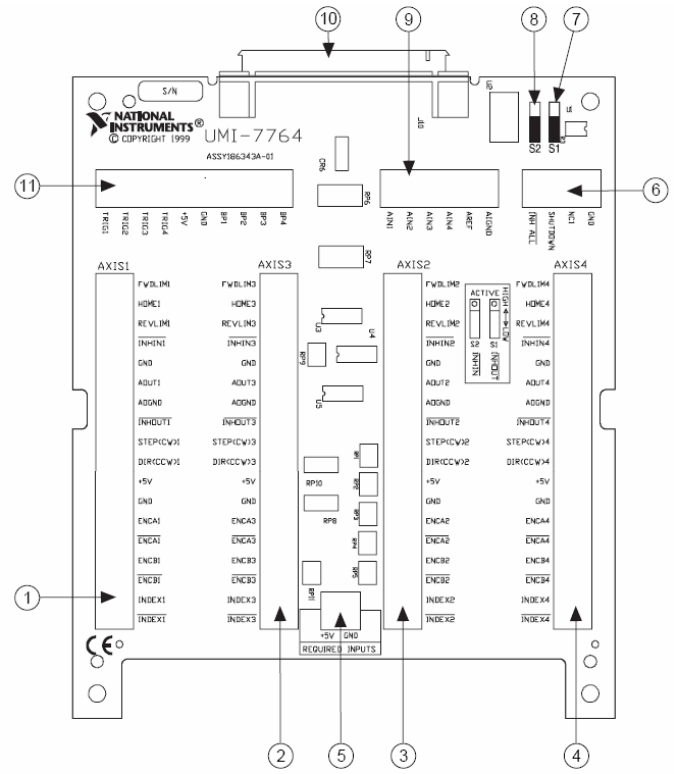


**Figure 3.18 UMI-7764**

Figure 3.18 is a representation of the signal breakouts on the UMI-7764.

| | |
|---|---|
| 1 | Axis 1 I/O Terminal Block |
| 2 | Axis 3 I/O Terminal Block |
| 3 | Axis 2 I/O Terminal Block |
| 4 | Axis 4 I/O Terminal Block |
| 5 | Power Input Terminal Block |
| 6 | Shutdown/Inhibit All Terminal Block |
| 7 | Inhibit Output Polarity Switch (S1) |
| 8 | Inhibit Input Polarity Switch (S1) |
| 9 | Analog Input Terminal Block |
| 10 | 68-Pin Motion I/O Terminal |
| 11 | Breakpoint/Trigger Terminal Block |

**Table 3.1 UMI-7764**

Table 3.1 describes the individual UMI 7764 breakout connections.

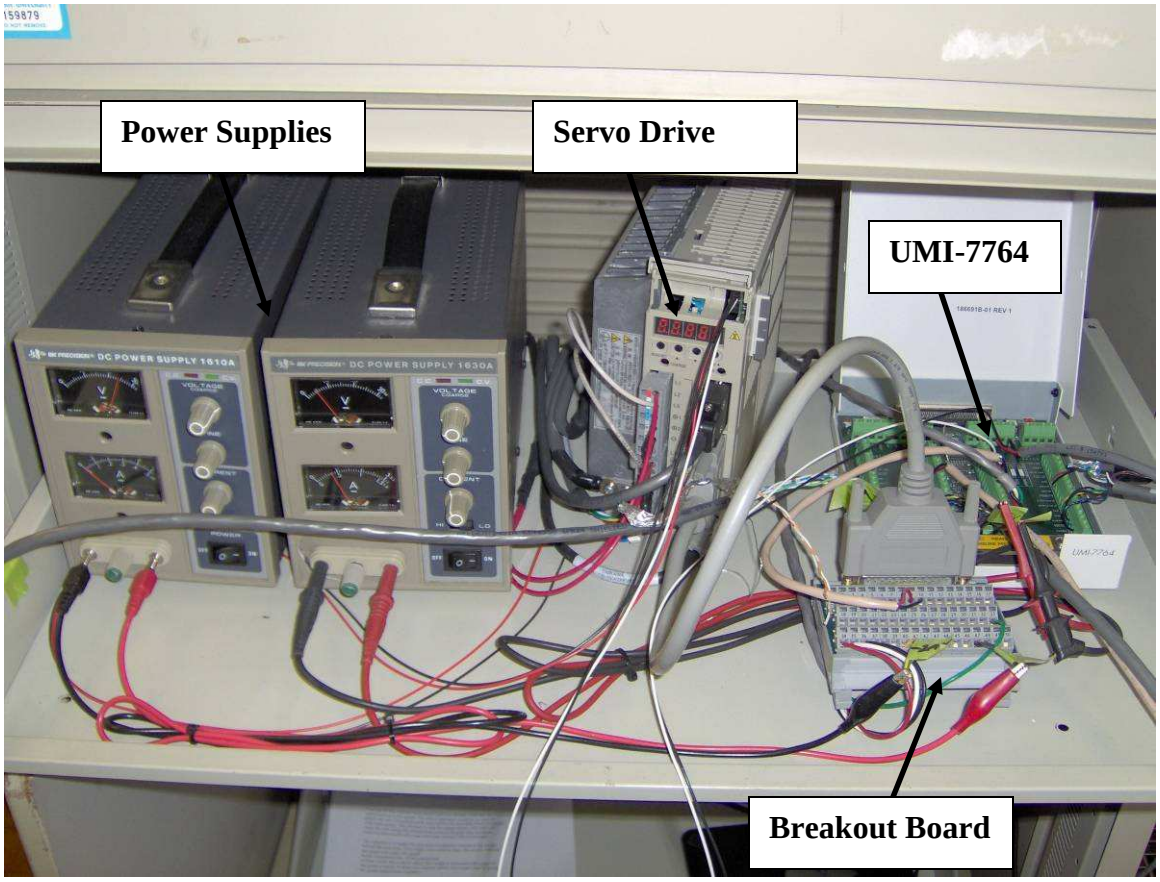


**Figure 3.19 Motion control hardware wiring: power supplies, UMI 7764, breakout board**

Figure 3.19 shows the peripheral power and signal wires for motion control. All electrical connections are made with shielded, twisted pair 22 American Wire Gage (AWG) cables for improved signal transmission and noise immunity.

### 3.10 Servo Motor Control

Servo control can be accomplished by a variety of methodologies differing primarily in their primary means of feedback. Servo control methods include velocity, force, and torque control. The differences are often in the way the amplifiers are configured. Torque mode is the primary method of servo control used in this thesis research. When a servo drive is configured for torque (current) mode, the drive produces an output current that is proportional to the analog input command signal. In the case of brushless DC motors, torque is directly proportional to the motor current by the following relation $T = ki$, where T is torque, k is the constant of proportionality and i is the armature current. In order to achieve the appropriate operation mode, the drives must be carefully configured and so various parameters must be set. In order for the National Instruments hardware to work properly, torque control mode must be configured in the servo amplifier.

#### 3.10.1 Torque Reference Inputs

As an example of how torque control is configured the servo amplifier, some of the methods used to control the Yaskawa servo are presented. Figure 3.20 shows how servo motor torque is controlled by the proportionality of the input voltage between T-REF and SG. A torque reference signal is sent from the 7344 to the servo amplifier in order to control motor torque [21].

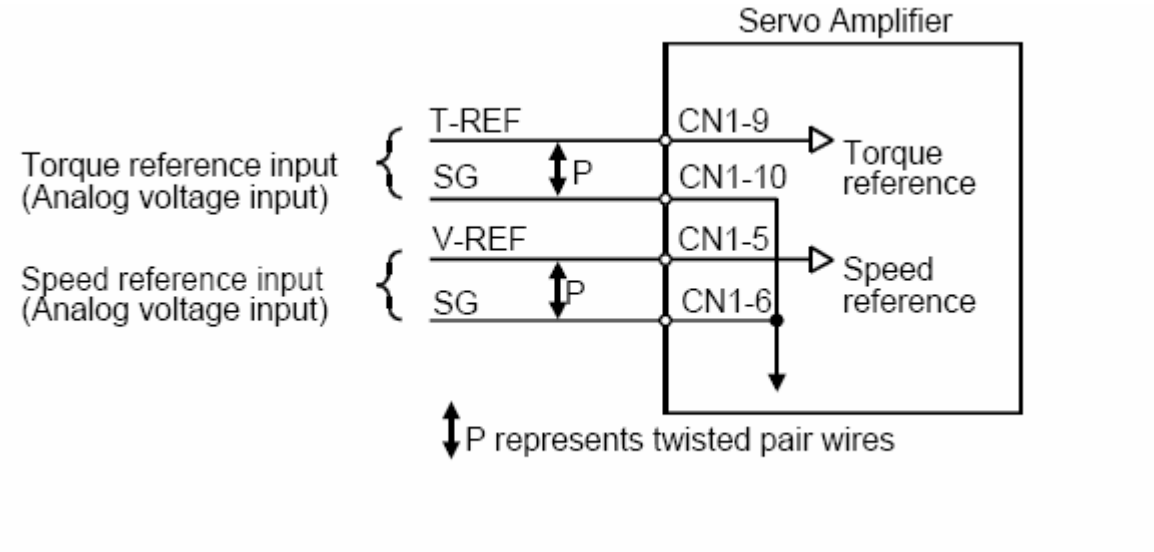


**Figure 3.20 Torque control wiring [21]**

Figure 3.20 is an example of how the amplifier is wired for torque control.

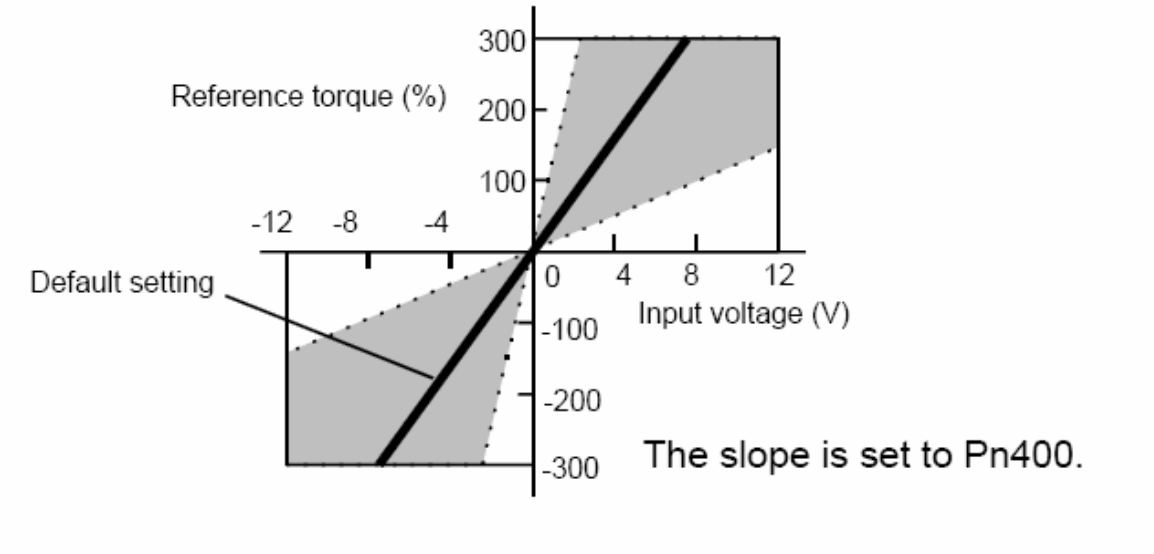


**Figure 3.21 Torque/Input voltage proportionality [21]**

Figure 3.21 shows the relationship between torque and input voltage.

### 3.10.2 Servo Motors

The capstan axis is a Yaskawa servo and the traversing mechanism and spool axes are Motion Control Group (MCG). The Yaskawa servo system required a 3m Power Cable,

3m Encoder Cable, I/O Breakout board kit to connect the motor to the amplifier. The inputs/outputs (I/O) are available through several ports. The CN5 cable is used to measure the voltage from analog input (AI2; white and black wires) that corresponds to the motor current. A serial programming cable along with Sigma Win+ software is used to configure the drive. 24 VDC source (Figure 3.19) is required on CN 1-47 to enable servo control.

The traversing mechanism and spool axes are driven by MCG BMC 12H Pulse Width Modulation (PWM) brushless servo amplifier designed to drive brushless type DC servo motors at a high switching frequency. Operating efficiencies for this amplifier approach 99%. The amplifier features an analog interface and 15 turn potentiometers to adjust various gains and limits. The potentiometers have one inactive turn indicating end of travel; and are approximately linear between ends. The analog interface of the servo amplifier is used to control motor torque. The general specifications of the servo motor are presented in Table 3.2. [22]

| | |
|---|---|
| Supply Voltage | 70-270 VAC |
| Peak output current (2 sec) | 25 Amp |
| Maximum continuous Current | 12.5 Amp |
| Power Dissipation @ continuous current | 55 Watts |
| Shunt Turn ON | 390 VDC |

Table 3.2 MCG Brushless motor properties [22]

The BMC 12H servo amplifier can be configured into 5 different operating modes via a DIP switch, for the purposes of this research Torque (current) mode is chosen. The actual current in the motor is proportional to the voltage measured across P1-8 current monitor and P1-2 signal ground. The signal is scaled 2 Amperes/Volt when SW3 is off.

Table 3.3 lists the potentiometer settings that must be set to configure amplifier to current mode.

| SW1 | SW2 | SW3 | SW4 | SW5 | SW6 | SW7 | SW8 | SW9 | SW10 | ENC | TACH |
|---|---|---|---|---|---|---|---|---|---|---|---|
| OFF | OFF | ON | ON | OFF | OFF | ON | ON | ON | ON | NC | NC |

**Table 3.3 DIP switch settings [22]**

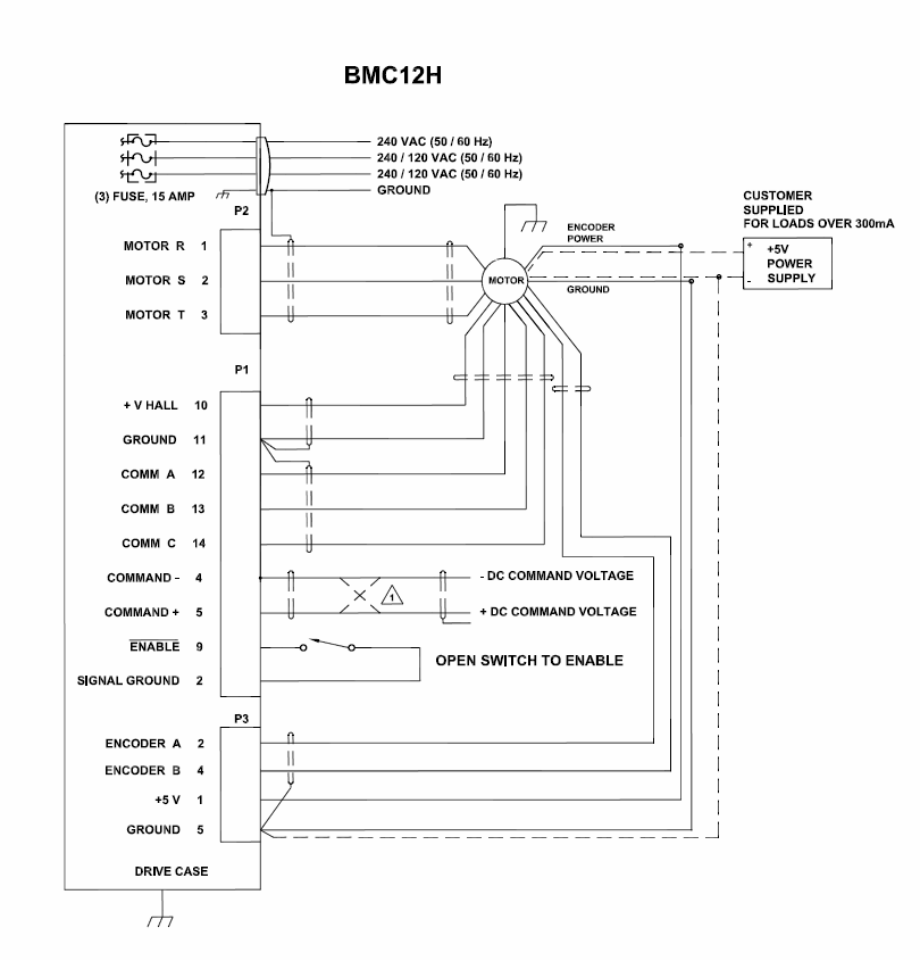


**Figure 3.22 BMC 12H Typical Power/Motor Wiring [22]**

The BMC 12H encoder requires 5VDC, has a maximum 5 kHz frequency response, and 1000 lines per revolution or 4000 pulses per revolution quadrature output.

### 3.11 Gearheads

Due to the inherently slow nature of braiding, the take-up process must operate very slowly even by servo motion standards, making the use of gearheads a convenient solution. Using a gearhead offers several advantages over direct drive. Utilizing a gearhead increases the speed required of the motor by an amount directly proportional to the gear ratio. Increasing the servo speed by an amount proportional to the gearhead ratio allows the motor to operate in a higher speed range where control is easier. The resolution of a servo move is limited by the resolution of the motor encoder. Gearheads improve torque transmission as well as servo resolution by increasing the number of encoder counts per degree of actual motion. Gearheads are also useful to reduce the reflected inertia to the motor by the square of the gear ratio. That is, if the mismatch between the load and the servo rotor is 25:1 employing a 5:1 gearhead will reduce the mismatch by the square of the ratio and the resulting mismatch reflected to the motor will be 5:1 (within the recommendations of many servo manufacturers). Danaher Motion NEMA TRUE size 60 mm gearhead is used on the capstan axis (15:1 Ratio). Bayside Stealth inline gearhead, PXI-42-005, is used on the traverse and spool axes; where the 42 and 005 refer to NEMA 42 size and 5:1 gear ratio.

### 3.12 Quadrature Encoders

An encoder is an electromechanical device that converts motion to an electronic signal that can be used to determine position and direction. Encoder devices are often based on optical transmission where a light source, an interfering quadrature track, and a photo detector are used to determine position and velocity. Quadrature encoders are popular among motion control applications and typically serve as the primary feedback

device for servo axes. Quadrature encoders have two channels A and B and each channel has a complement A' and B', depending on the relative phase between A and B, the direction can be determined. Often, a third channel is used, referred to as index, and provides a signal once every complete revolution. For example, the encoders used in this research under clockwise rotation output a signal where A leads B. Quadrature output signals includes two main channels: A and B along with their complements A' and B'.

### 3.13 Braiding Machine Encoder Installation

An aluminum mounting plate and steel shaft extension were designed and manufactured to allow an optical encoder to measure the braiding machine driveshaft position. The shaft position also corresponds to the yarn packages rotation.

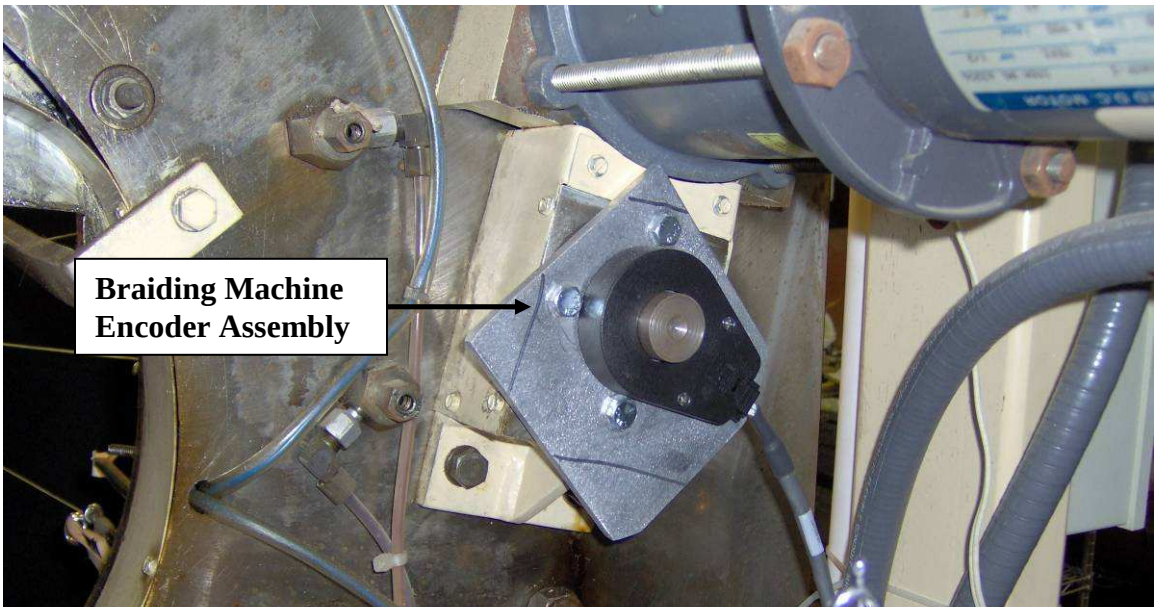


**Figure 3.23 Encoder installed, mounting bracket, shaft extension**

Figure 3.23 shows the mounting bracket and shaft extension that were required in order to instrument the braiding machine with and encoder. The signal wire is connected

to the UMI-7764, and 5 VDC is supplied. The encoder used is a US Digital E6D-2048-1000 HEDS with 2048 Counts per Revolution (CPR) or 8192 Pulses per Revolution (PPR). The encoder also provides an accurate measure of the braiding machine motor speed. The motor speed is observed to vary somewhat as the packages rotate during braiding.

### 3.14 Characterizing the braiding machine parameters

The capstan gear ratio is calculated by measuring the number of encoder counts per capstan revolution. 81920 counts were recorded as an indexed yarn package completed one revolution; thus a 10:1 ratio is determined to exist between the package and the input drive shaft. Furthermore, 227.56 pulses represent 1 degree of package motion. Mechanically geared capstans generally require replacing gears to alter the take-up speed. The ratio originally designed for this machine was determined by measuring the encoder pulses per capstan revolution; and was calculated to be 381.235:1. Thus the packages must make 38.1235 revolutions for every capstan revolution.

### 3.15 LabVIEW Motion Control Programs

Controlling the servo motors is facilitated by LabVIEW programs. Many different programs have been used during the course of this research. The motion control programs are written using LabVIEW. Figure 3.24 includes an example of the motion control code.

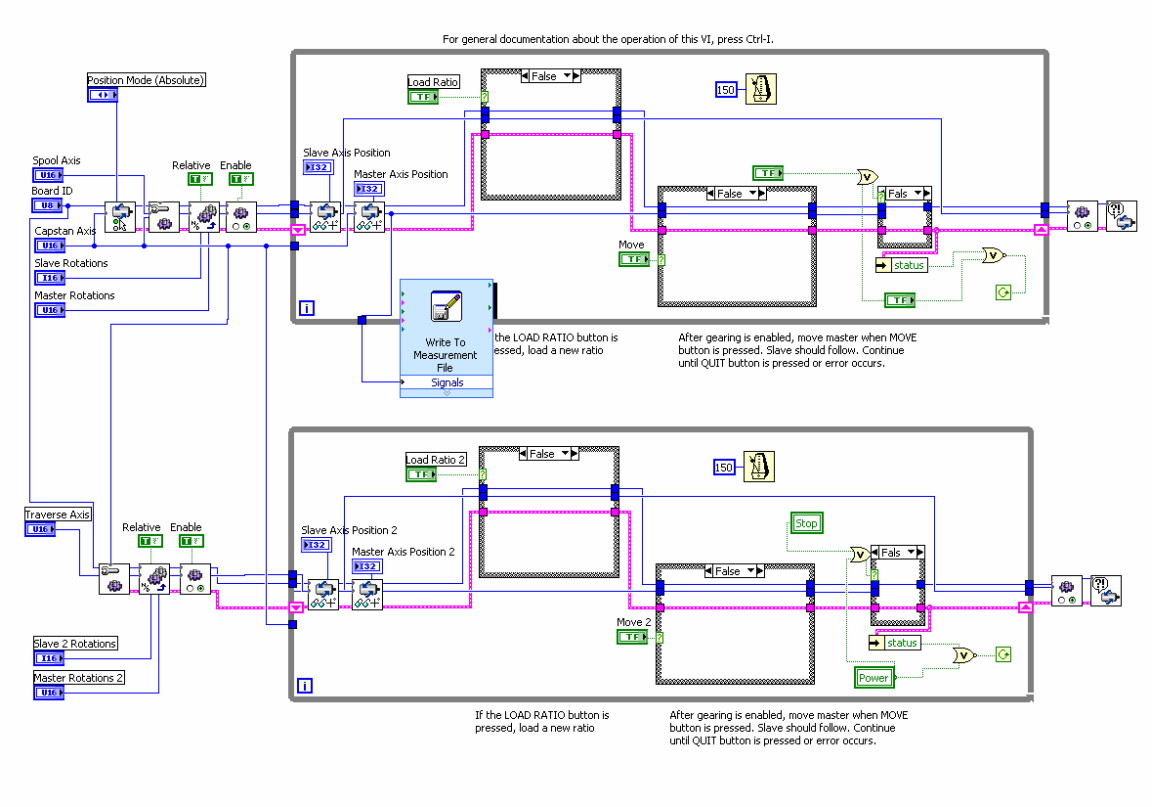


**Figure 3.24 LabVIEW motion control program**

Figure 3.24 shows some of the code used for motion control during this research.

### 3.16 Machine Vision

Machine vision involves utilizing image acquisition and analysis for the purposes of carrying out automation processes. Incorporating cameras into machine design to perform specific tasks is useful in many applications. Industrial cameras are very expensive and require an image acquisition device to acquire and store the image data. Fortunately, PC technology offers an inexpensive alternative to traditional industrial image acquisition. In place of an image acquisition device, the Universal Serial Bus (USB) is used to acquire and store images. LabVIEW has a USB interface which allows for inexpensive "web cameras" to be used in lieu of industrial cameras. Once a connection is established with the camera, programs are used to manipulate images in

such a way to accomplish particular objectives of this thesis such as observing braid motion and calculating braid formation geometry. An image can be triggered according to encoder position or software command. The image can be stored and processed to yield information of interest. The information provided by the images serves as the basis for analysis or can be incorporated into the control loop.

Machine vision provides an excellent non invasive technique for observing braid point motion as well as a means to measure braid formation angle. Utilizing two cameras in tandem allows for a 3 dimensional reference frame to be established. Each camera essentially provides a two dimensional matrix composed of 640X480 pixels. The side view camera observes the braid formation from the side where Z direction is the vertical and Y is horizontal or axial direction. The Rear view Camera observes the rear view of the braid and provides Z and X directions, where Z is vertical and X is horizontal. The acquired images can be calibrated by a pixel space to real space transformation. A fiducial reference marker, or object of known dimension, is used to determine the number of pixels corresponding to a given unit.

### 3.16.1 USB Image Acquisition System Setup

Proper lighting is important for improving the image quality and useful for providing consistent light. The yellow light in Figure 3.26 is used to help provide consistent lighting conditions. A dark background is used to provide contrast. A plastic pipe frame was constructed to hold the background curtain which helps maintain the lighting environment. Two USB web cameras are mounted orthogonally for the purpose of establishing a XYZ reference frame.

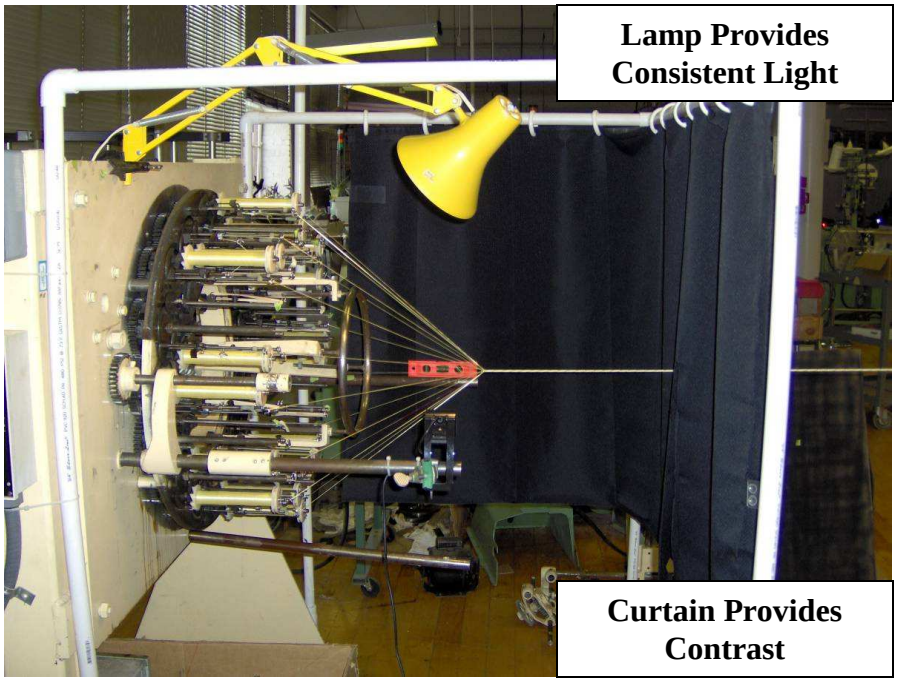


**Figure 3.25 Lighting environment**

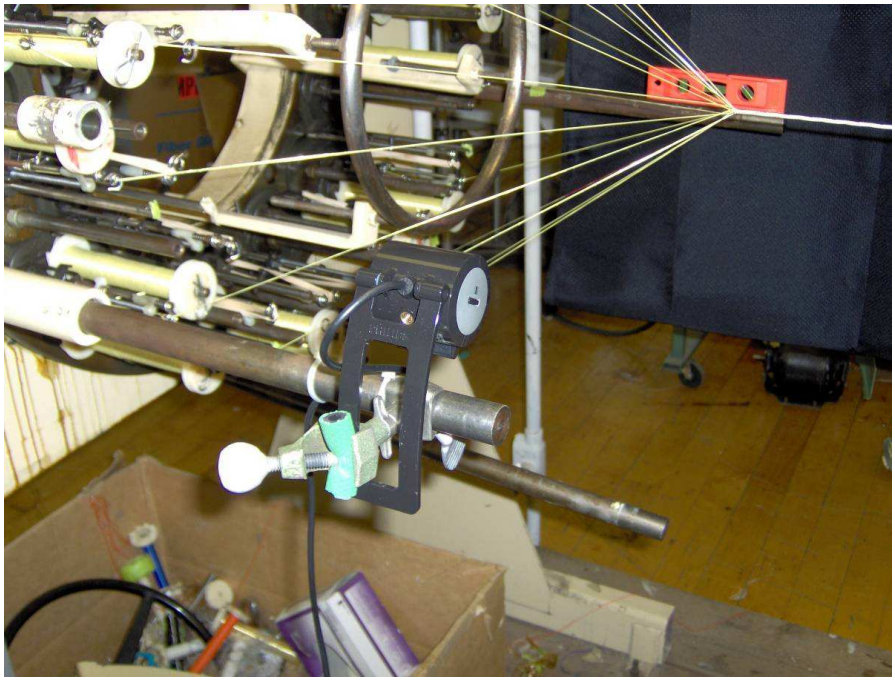

**Figure 3.26 Side view camera**

The rear view Camera of Figure 3.26 observes the rear view of the braid and provides Z and X directions, where Z is vertical and X is horizontal.

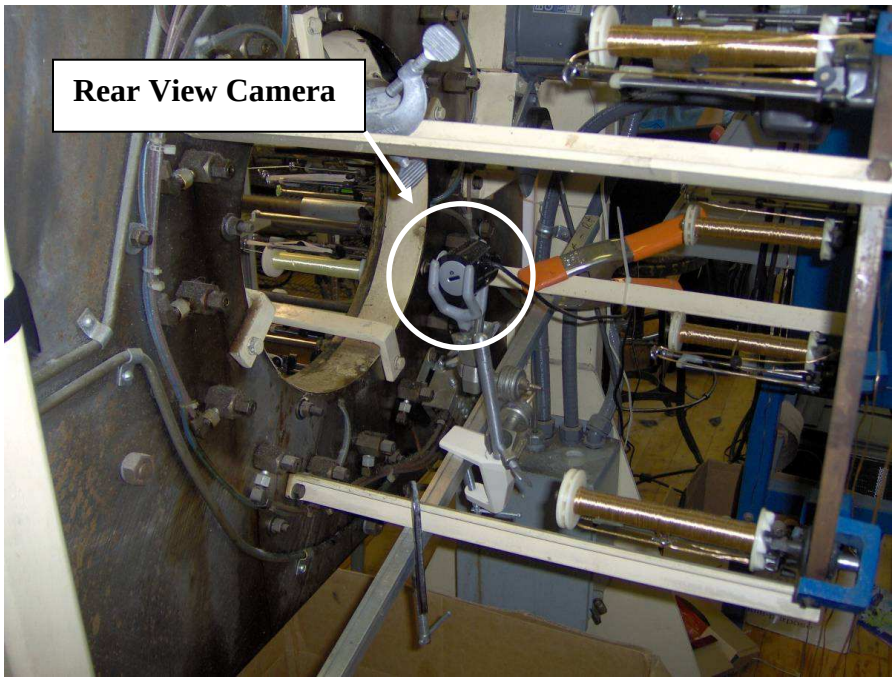


**Figure 3.27 Rear view camera**

Figure 3.27 shows the rear view camera.

### 3.16.2 Camera Reference Frames

Two Universal Serial Bus (USB) cameras were installed on the braiding machine. They are positioned orthogonally in order to establish a XYZ coordinate system. Figure 3.28 shows the Y and Z axes as obtained by the side view camera. Figure 3.29 shows the side view camera position. Figure 3.30 shows the X and Z axes as obtained bye the rear view camera. Figure 3.31 shows the rear view camera position.

**Figure 3.28 Rear View: Establishing ZX Coordinate System (Camera 2)**

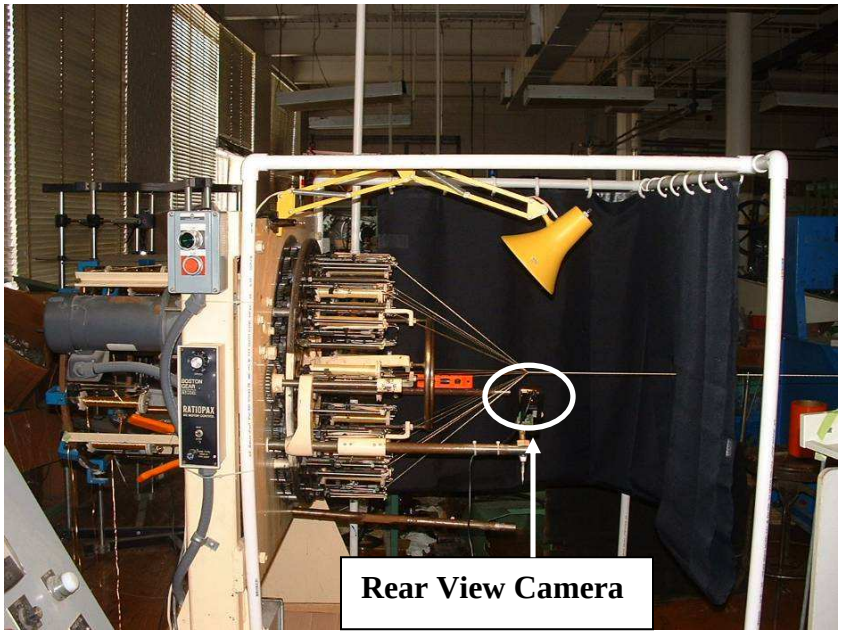


**Figure 3.29 Side View camera position**

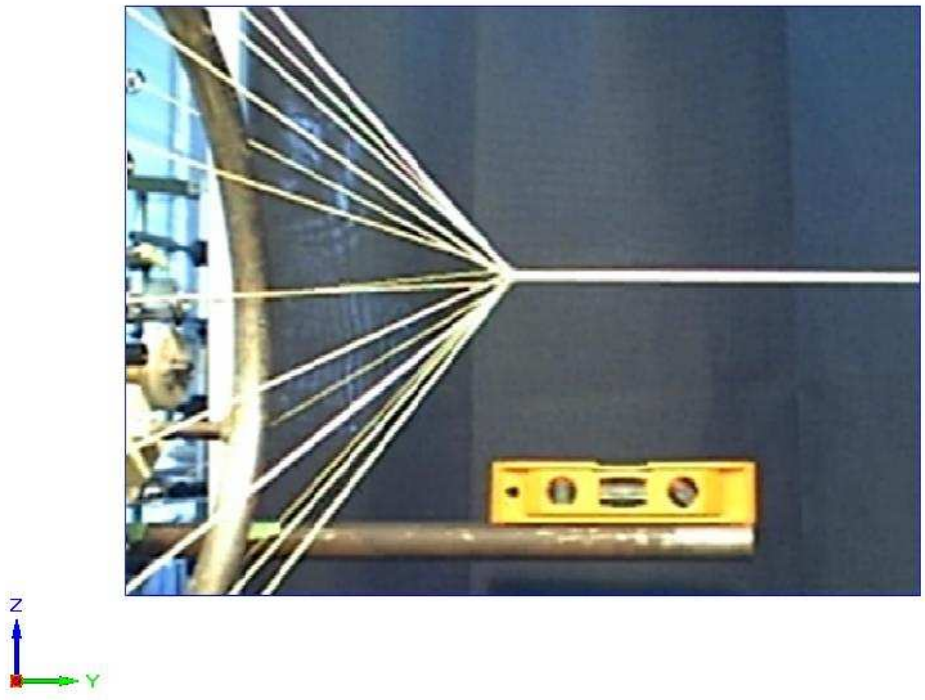


**Figure 3.30 Side View: Establishing ZY Coordinate System (camera 1)**

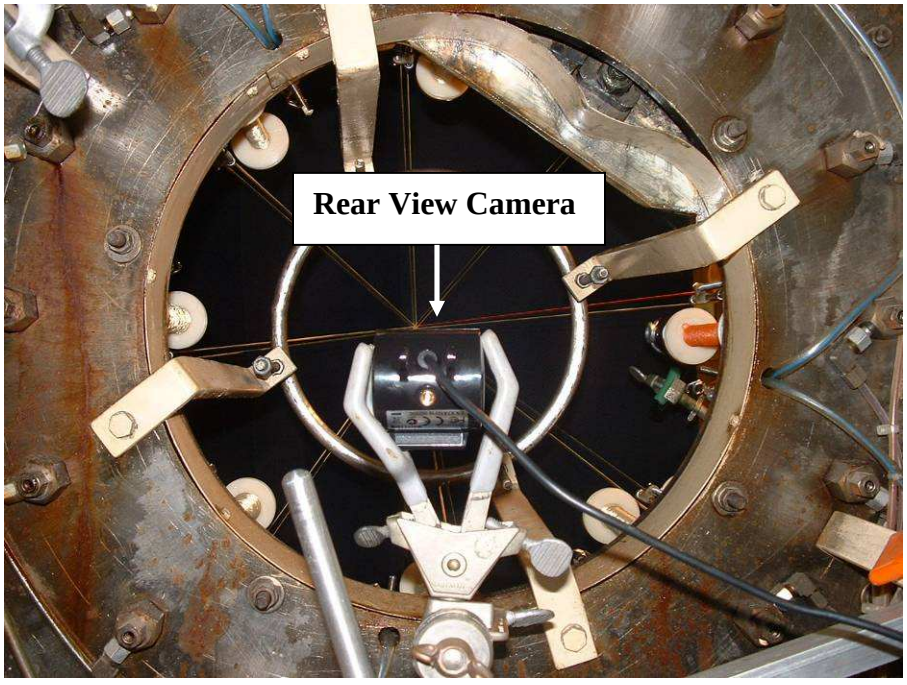


**Figure 3.31 Rear View camera position**

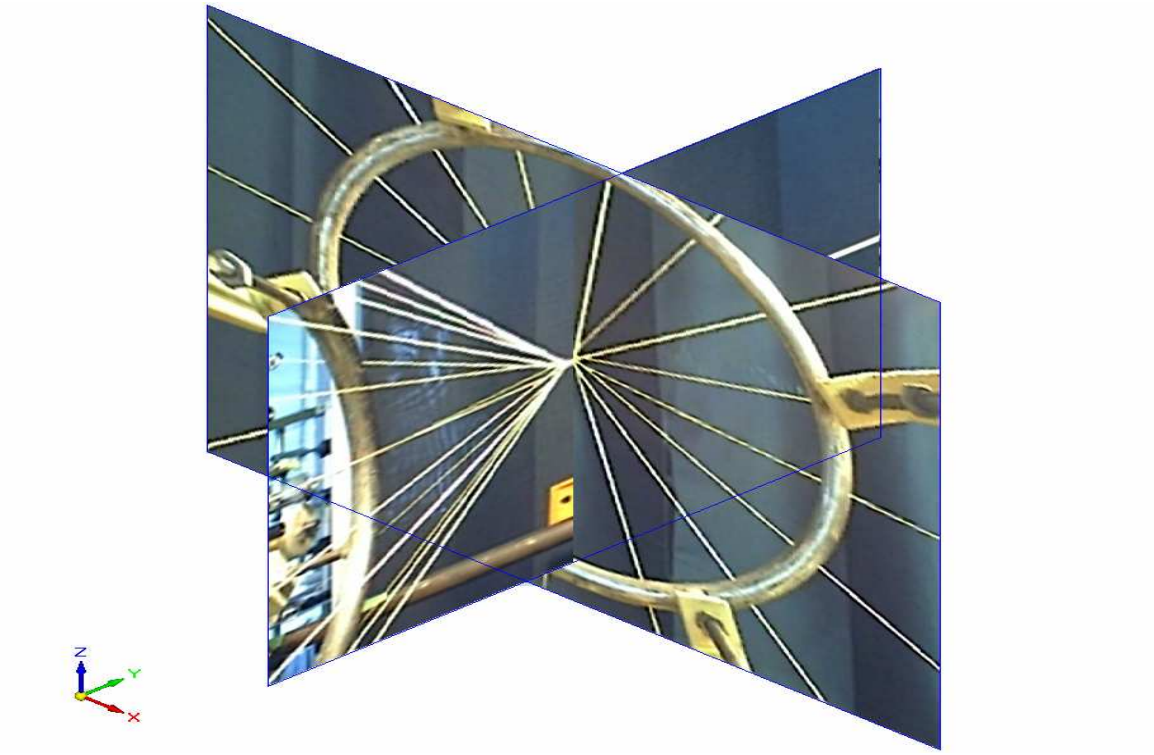


**Figure 3.32 XYZ machine vision based coordinate system**

Figure 3.32 gives an isometric view of the reference system made by combining the images Figures 3.28 and 30 orthogonally.

### 3.17 LabVIEW Vision Programs

Controlling the cameras is facilitated by LabVIEW programs. Many different programs have been used during the course of this research. The motion control programs are written using LabVIEW. Figure 3.33 includes an example of the machine vision code. The acquired images are manually loaded into a LabVIEW Virtual Instrument (VI) i.e. computer program and using common machine vision algorithms, the images are manipulated to return information of braid point position and yarn formation angle. Figures 3.34-36 are screenshots of the machine vision user interface.

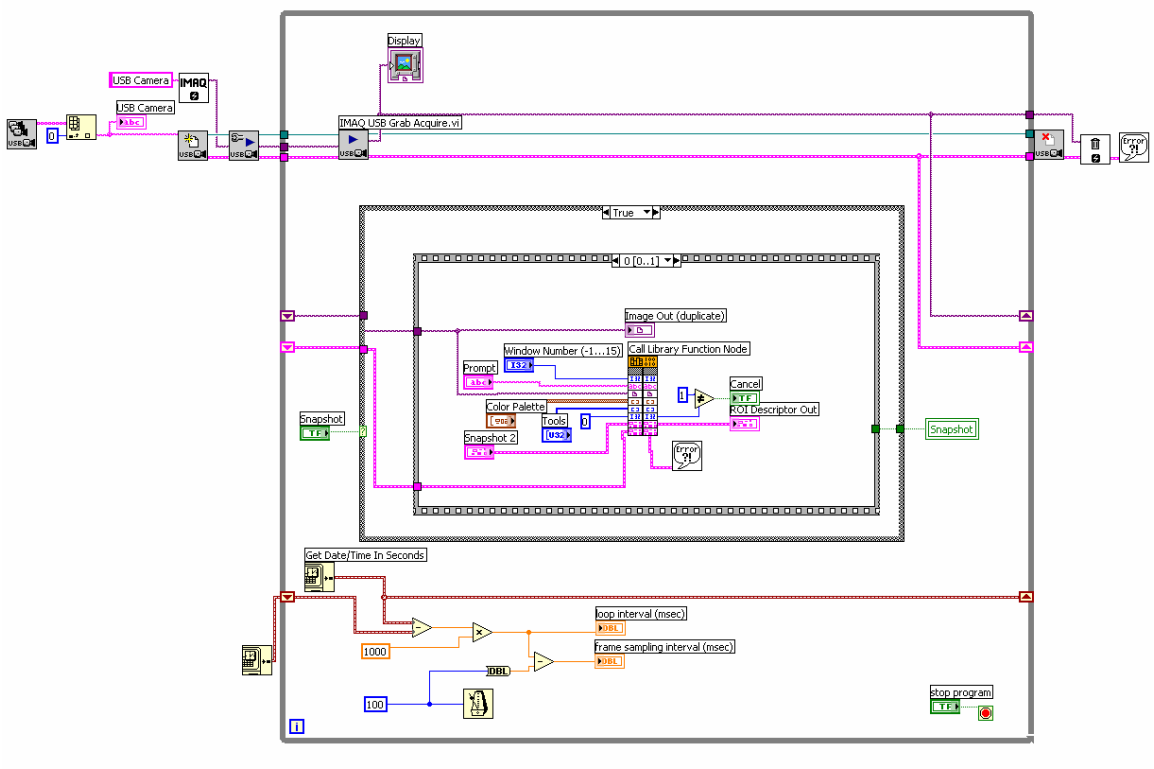


**Figure 3.33 LabVIEW vision program**

Figure 3.33 is an image of the LabVIEW block diagram responsible for initializing the USB camera and acquiring images.

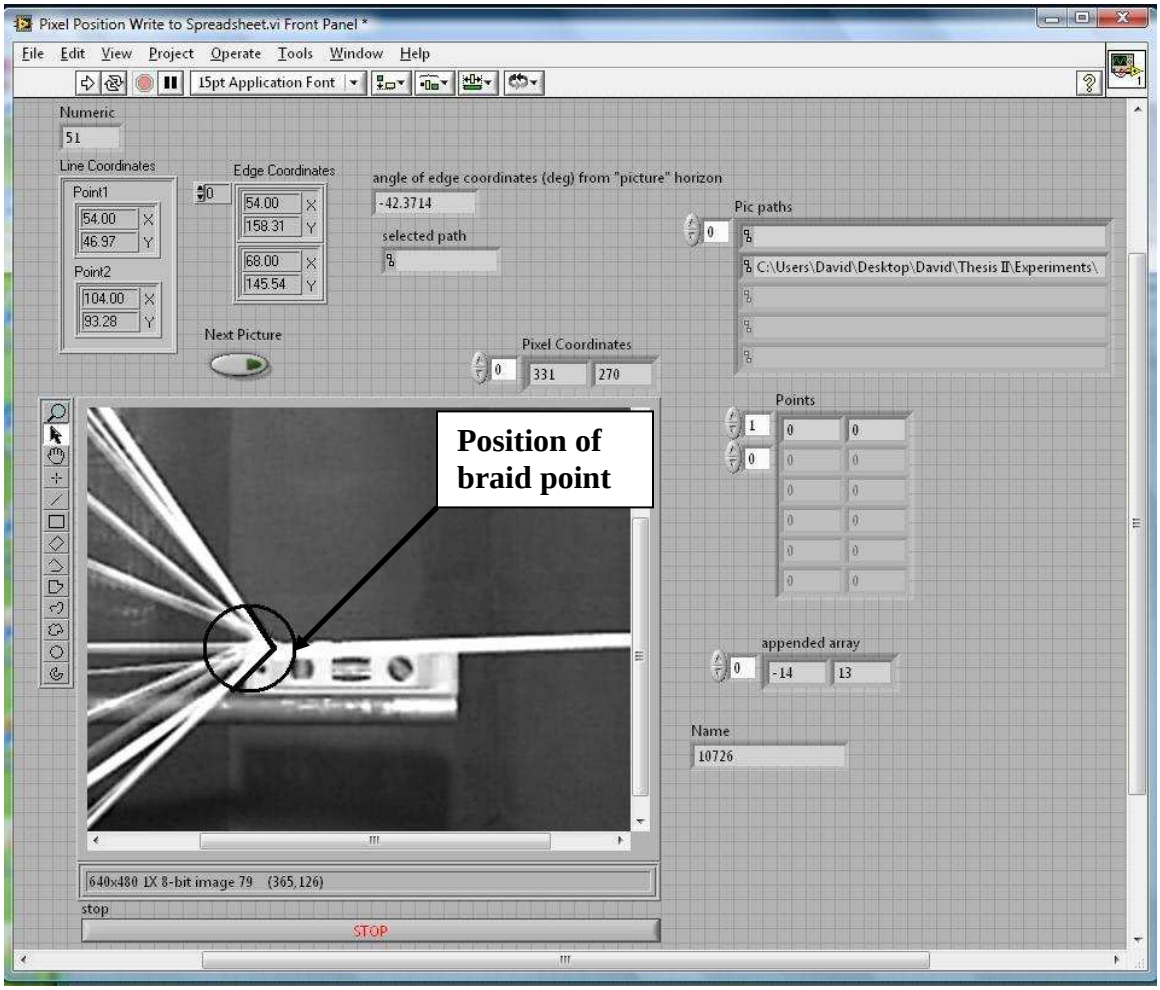


**Figure 3.34 LabVIEW VI used to determine YZ braid point position**

Figure 3.34 is a screenshot of a program that is used to determine the braid point position. The braid point is selected and the pixel values are stored in a spreadsheet.

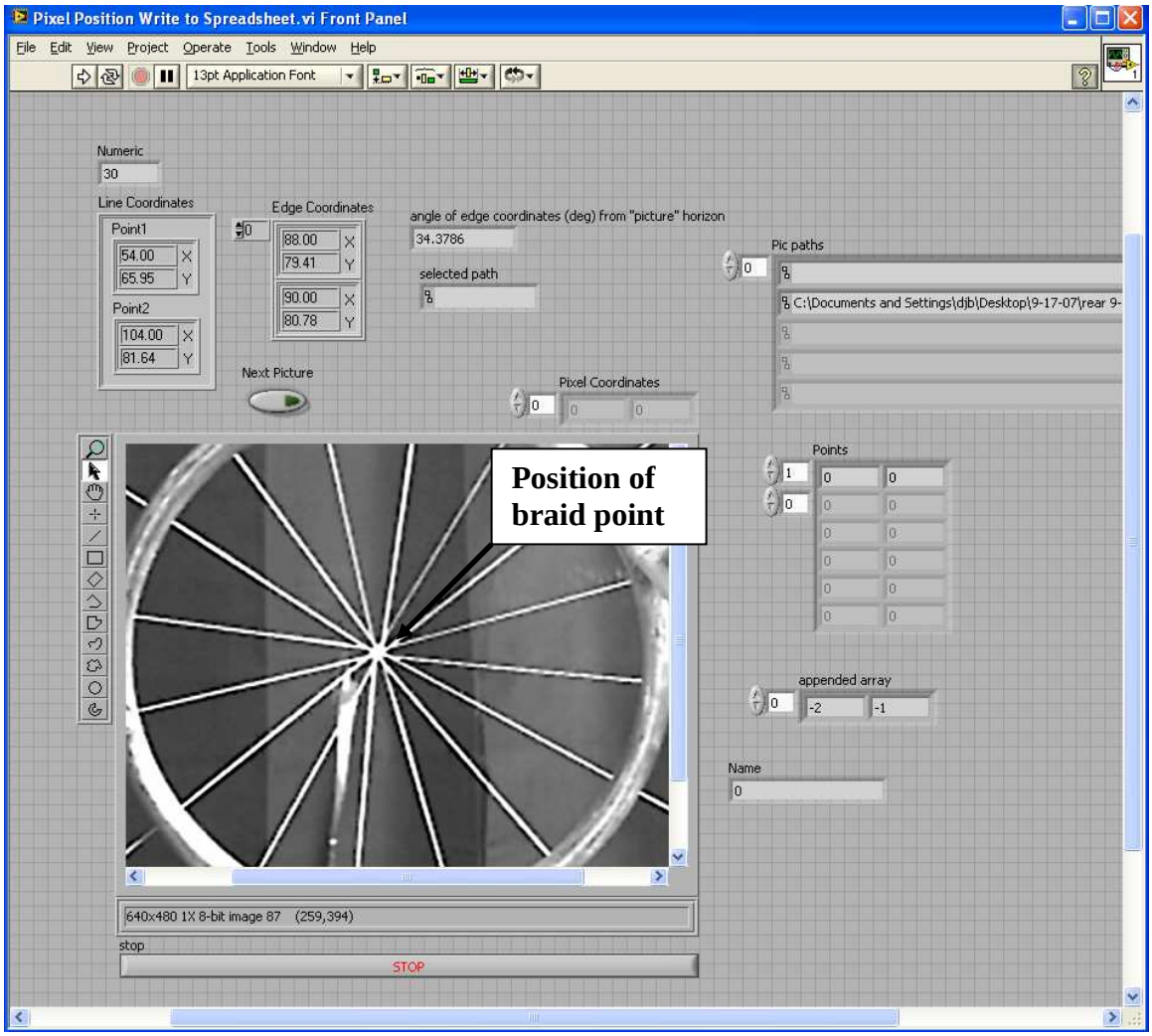


**Figure 3.35 LabVIEW VI used to determine XZ braid point position**

Figure 3.35 is a screenshot of a program that is used to determine the braid point position. The braid point is selected and the pixel values are stored in a spreadsheet.

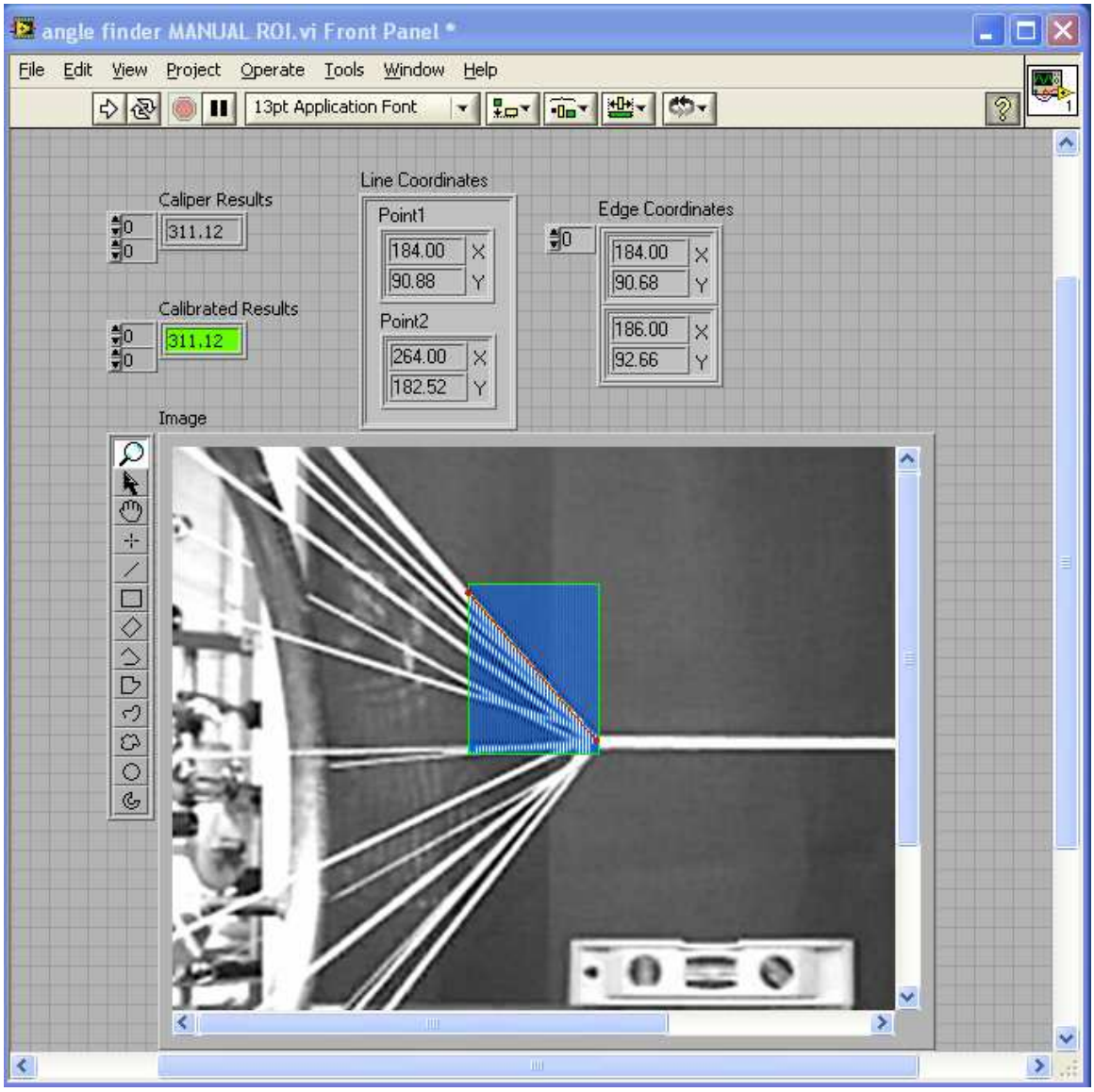


**Figure 3.36 LabVIEW VI used to determine braid angle**

Figure 3.36 is a screenshot of a program that is used to determine the braid point formation angle.

### 3.18 Camera synchronization verification

Unfortunately LabVIEW does not presently permit two simultaneous USB image acquisitions. It is important to have synchronized images for understanding the spatial orientation of the braid at a given moment. Knowing that each image acquired from one

camera corresponds to the other camera is important. An experiment is performed to determine whether the cameras are properly synchronized. The cameras were initialized manually and the graphs, show good agreement to conclude that images from one camera correspond to the other.

Figures 3.37 and 38 represent the first successful experiment of synchronizing 2 cameras. The cameras are manually synchronized to acquire a selected number of sequential images. The capstan is initiated, followed by the braiding machine. The images evaluated are those which capture the first observed braid point movement until the end of the sequence. The XY pixel data corresponding to the braid point is logged and plotted.

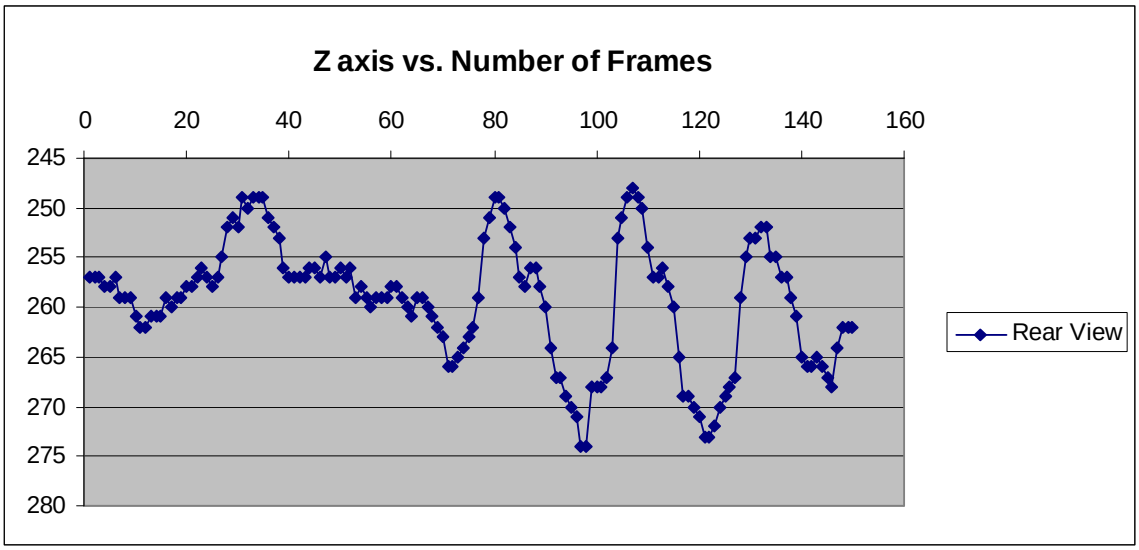


**Figure 3.37 Movement of the braid point in Z (Rear View)**

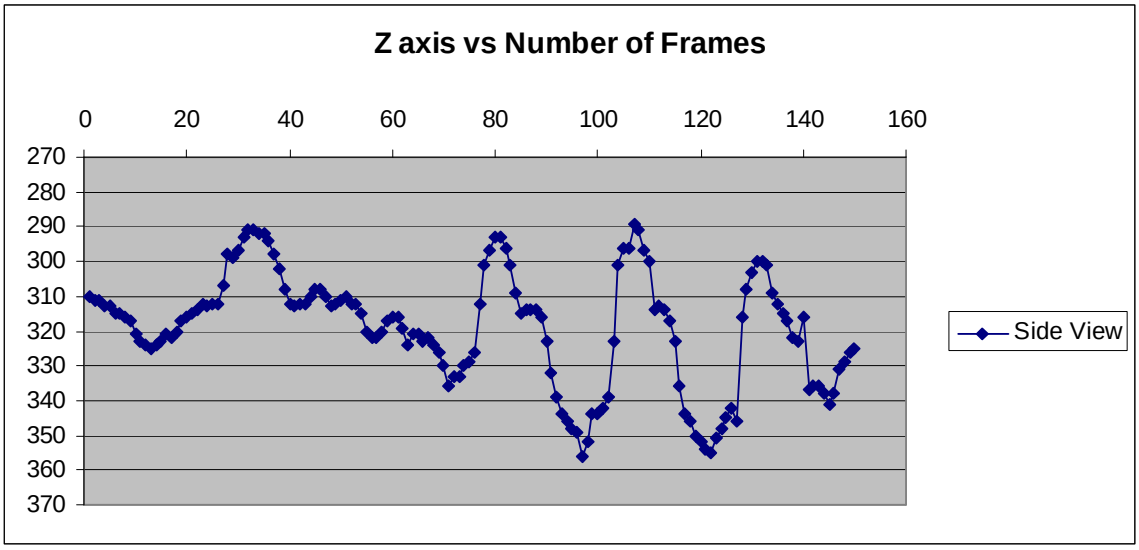


**Figure 3.38 Movement of the braid point in Z (Side View)**

As expected, the plot shape of Figure 3.38 matches Figure 3.37. The matching plot shapes indicate the success of the 2 camera system synchronization. It is important to note that the scale of these images is relative and when the images are calibrated, they show the same scale. The cameras are calibrated by including a fiducial or reference marker of known dimension in the image and simply counting the number of pixels required to represent the fiducial. In this way, a scale factor for each camera is ascertained by counting the number of pixels per inch.

### 3.19 Conclusion

The design and construction of the take-up machine and vision system presented in this chapter was an excellent exercise in PC based servo motion control, computer aided design, machine tool technology both manual and computer controlled, machine vision, and resourcefulness. The take-up machine system is an excellent platform for future research with its data acquisition, motion, and vision capabilities. The vision described is believed to be a new application of machine vision for braiding.

# 4. EXPERIMENTAL RESULTS AND DEFAULT CHARACTERIZATION

## 4.1 Introduction

The purpose of this chapter is to describe the results from a series of experiments that measure braid point motion and to characterize the behavior of common faults during the process of industrial braiding. The objectives of this work are to 1) observe the dynamics involved in braid point formation, 2) categorize the common braiding faults that can occur during industrial braiding, 3) observe the characteristics of optimum machine operating conditions to produce quality braid, and 4) to understand the factors involved by precise experimental measures. The primary experimental method is a vision based measure of braid point position. Vision based measures utilize images acquired with a camera that are manipulated in software to yield desired information.

The experimental setup is the same as that presented in Chapter 3. An external, shaft mounted optical encoder is used to measure braiding machine position and calculate motion parameters. A four axis motion controller provides the trajectory signals to the servo amplifiers so that desired motor speeds may be achieved. LabVIEW code controls the servo motion controller and provides the interface for image acquisition as well. Servo motors are capable of precisely actuating motion, in the case of this experiment a Yaskawa AC servo motor controls the speed of the capstan and MCG DC servo motors control the speed of the traverse and spool axes.

Extensive tests were performed to investigate the effects of common mechanical faults during the braiding process, particularly problems related to the proper function of yarn package tensioning mechanisms. The nature of the experimental methods contained herein is two fold: first data obtained from indirect, visual methods and second corresponding data is obtained from direct mechanical measurement. Some experiments, such as the angle as a function of speed rely on the combination of methodologies, visual and mechanical, to make meaningful measurements. One experiment involved testing the force required to release yarn by pulling the braid with the capstan and measuring the tension at given displacements (section 4.4). A second experiment (section 4.8) involves determining the relationship between braid angle and take-up speed. A third experiment required ensuring that the necessary parameters conducive to proper braiding machine operation are met so that an optimal braid may be produced to serve as the baseline for comparison. Finally, experiments involving the effect of high-tension yarns, whether induced by increasing spring tension force (Appendix) to release the yarn or by locking the package(s) (sections 4.11-13) so that the release of yarn is not permitted are performed. Experiments pertaining to the graphs obtained from encoder data (on both the braider and capstan) show high yarn tension causes increased variation in motor speed and large spikes in speed, increasing up until the point where yarn breakage occurs.

Braiding is inherently a slow fabric-forming process; it is observed that a significant number of braiding machine revolutions is required until the braid angle reaches a steady state depending on initial position. Braid angle experimental measures (as a function of take-up speed) demonstrate that the number of machine revolutions required to reach the final braid point is significant. Knowledge of this phenomenon is

particularly useful if improving response time and reducing product waste is desired. Overcoming this limitation by implementing suitable control methodologies will certainly improve industrial braiding technology. High tension yarns play a significant role in the braid point motion and formation. High tension yarns during the braiding process are observed experimentally to have a dramatic effect on the braid point motion and motor speed.

**4.2 Scope of experiments**

In an attempt to properly understand the characteristics of braided fabric formation a series of experiments are devised to capture important aspects involved in the braiding process. The nature of these experiments is organized as follows: quasi-static testing, dynamic testing, and testing of the effects tension induced mechanical faults have on the braid formation. Quasi-static testing involves a series of steps where the capstan is slowly moved in very small increments. The quasi-static test is carried out by turning off the braider and followed by slowly pulling all interlaced yarns in the braid and measuring the force required to un-spool the material and subsequently determining the effective spring constant of the package mechanisms. Dynamic testing involve the experiments where the braiding machine and capstan are in motion resulting in motion of the braid point. Dynamic tests indicate the presence of initial transients of the braid point position, as it seeks a steady state position, followed by the steady state sinusoidal behavior. An interesting indicator of the braid point dynamics is observed in the results of an experiment (section 4.9) designed to measure settled braid point angle as a function of take-up and braiding speed. Braiding is inherently slow to form fabric; thus it is observed that a significant amount braiding machine revolutions are required until the braid angle

settles. It is later discovered that there is some variation over long time periods in the steady state conditions (e.g. occurring as slight braid point migration trends are observed). Finally, mechanical faults are introduced to discover the relationship between aberrant tension yarns and the resulting braid formation. Increase production, look for faults,

### 4.3 Quasi-static testing of braiding machine

A static test was performed to determine the nature of force required by the capstan up and to the point of un-spooling of yarn. A digital fish scale was put inline with the braid. The experiment initially acted on a slack braid and the braid is slowly pulled in increments of 2000 encoder pulses (approximately .56 inches), tension is measured, and an image acquired. The LabVIEW code monitors the capstan torque which is converted to tension as another verification measure. Encoder counts on the servo axis are calibrated to a corresponding capstan wrapping length. From this conversion it is possible to determine the displacement in more intuitive units i.e. inches of braided material for a given force; and thus determine the spring constant of the mechanisms involved in braid formation. The sections dealing with quasi-static experiments seek to quantify the effective spring force of the braid tension mechanism used during the focus of the thesis research.

## 4.4 Quantifying effective braiding machine spring constant

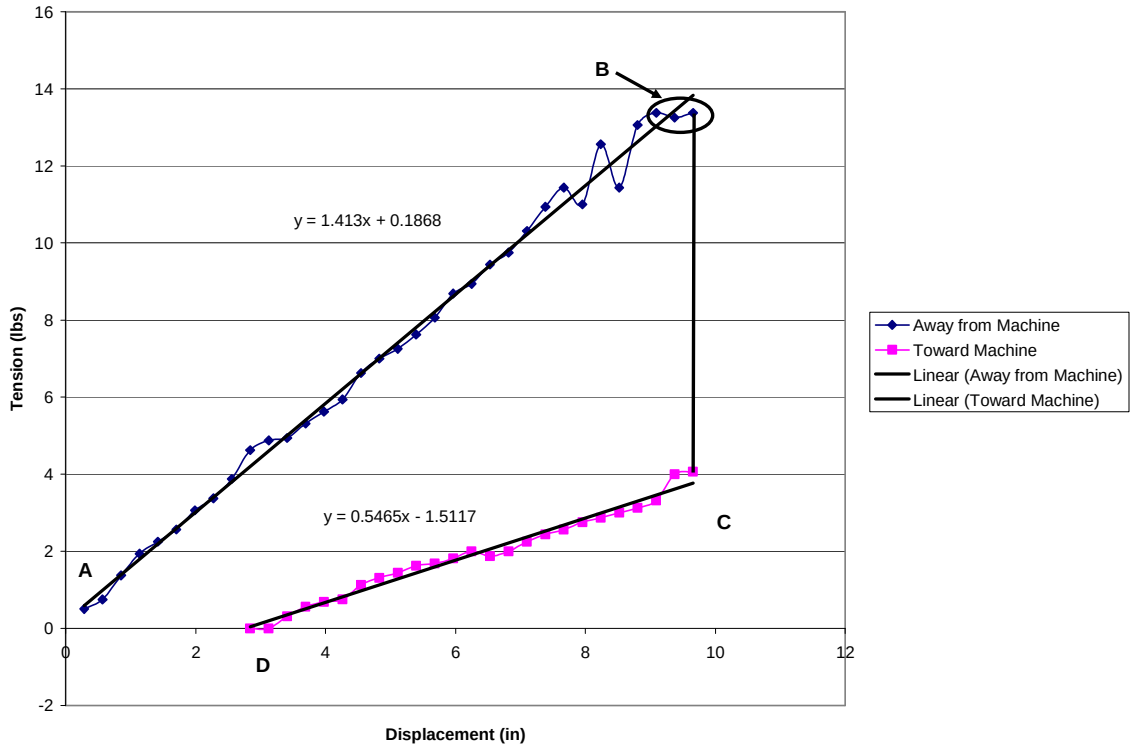


**Figure 4.1 Bi-directional effective spring constant**

Figure 4.1 is a plot of the bi-directional nature of the effective spring constant observed in the tensioning mechanism. Point A corresponds to a braid point position where the package springs are uncompressed. The braid point is then pulled away from the braiding machine until the packages begin to release yarn (point B). At this point, Point C in Figure 4.1, the resulting tension in the braid is allowed to pull backward against the capstan, following the same incremental path used to get there. Point C shows an immediate drop in tension (around eight pounds) when the braid is allowed to pull against the capstan beginning for approximately the same position. Point D is the final position of the braid point where zero tension exists; it does not return at the initial position due to the un-spooling of yarn.

### 4.5 Braid point dynamics

The results presented in this section demonstrate the dynamics of braid point motion. In Figure 3.37 it is shown an example of how the braid point moves in the z direction as it approaches steady state (oscillating motion). The height of the sinusoids is related to the tension imbalance from the packages.

The dynamic nature of braiding is categorized by three regimes. The first regime consists of an initially changing braid point position that occurs rapidly followed by an oscillation transient. The second regime is characterized as a slowly changing (migratory) and oscillating transient. The third regime is characterized as a steady state oscillating equilibrium, where the pull from each package is nearly the same and the resulting braid is balanced. The transient motion is expected in all 3 directions of braid point motion depending on the initial position. Typically, an initial transient occurs in the take-up direction as the yarns are pulled, until the tension necessary for loading the package springs is reached. After this initial Y displacement transient, occurring up until the point where the ratcheting mechanisms begin to work, the resulting steady state behavior is sinusoidal in nature as will be seen in Figure 4.6.

The braid point position is the result of the braiding machine speed and take-up speed reaching equilibrium. After the initial transient, the braid oscillates and continues to migrate toward the equilibrium point where it resides so long as all machine and package tensioning system parameters remain constant. The oscillating phenomenon associated with braid point position movement is due in part to the collective nature that the constituent yarns play in the interlacing process. While some yarns are being un-spooled and experiencing an abrupt change in tension, albeit slight, others are increasing

tension as the spring mechanism compresses. (This particular phenomenon is observed while running the capstan with the braiding machine stationary. The braid point moves up and down as it travels toward the capstan, demonstrating the effects of tension from the other member yarns while new material is un-spooled.) After the initial transient there is an oscillation in tension in the braid resulting from packages loading and those un-spooling under the constant force of the capstan. Another contributor to continuously changing yarn tension is a result of the increasing torque necessary to turn the bobbin as the yarn coil position moves from one bobbin flange to the other thus affecting the torque [8].

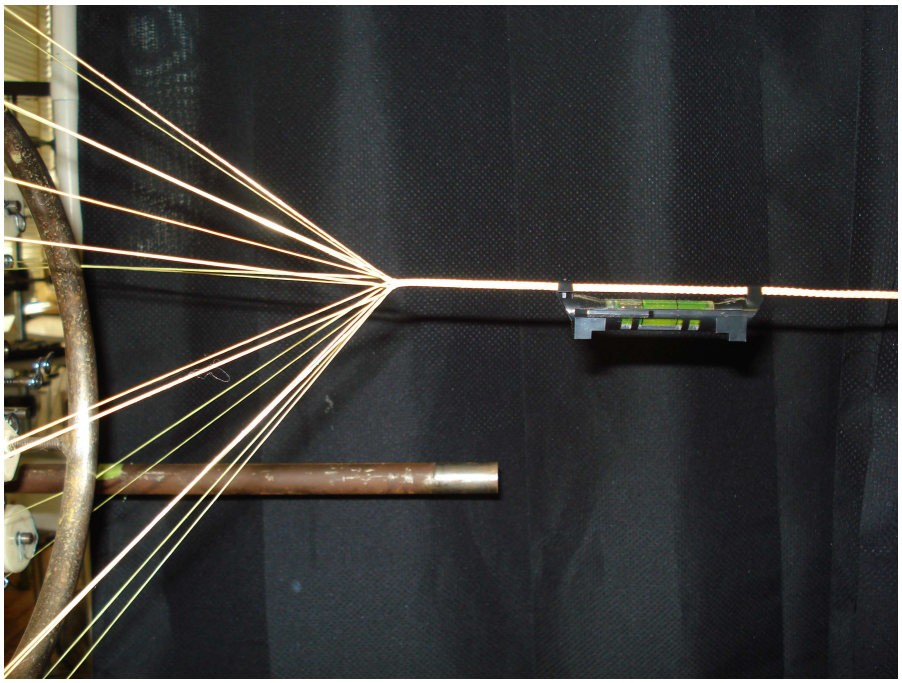

**Figure 4.2 Braid point moved from center**

Figure 4.2 shows an example of the braid point moved radially from braiding machine central axis. The white line is horizontal and useful for comparison. How far radially the braid point is from center affects the tension balance as some springs must compress in order to supply the additional yarn required to allow the braid point to move

radially. As an example, the braid point is physically moved upward (causing the formed braid to deviate from level position as seen in Figure 4.2) then as the interlacing process occurs; the braid will quickly be pulled back to the center thus causing a transition to the steady state position.

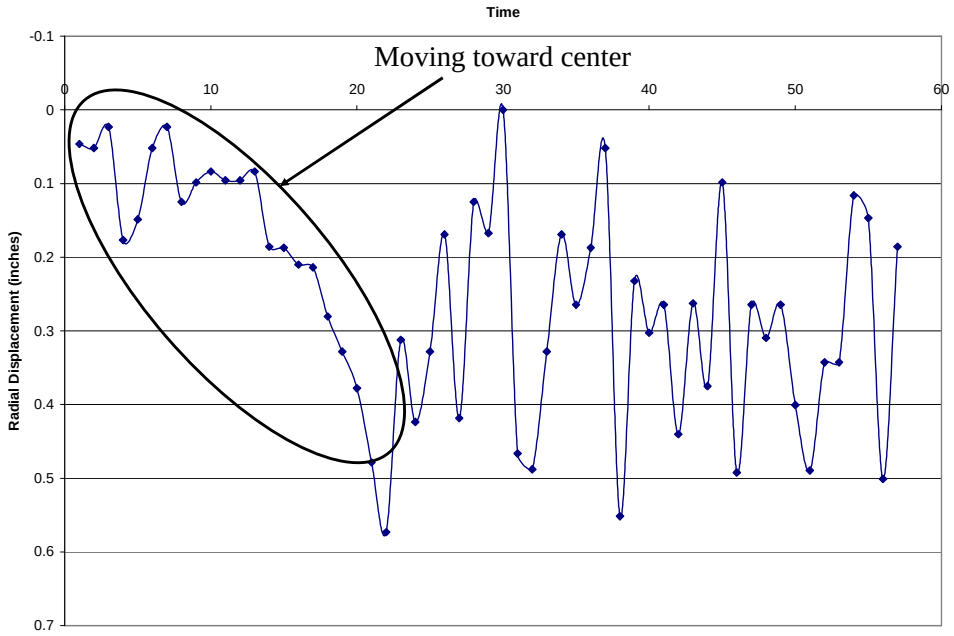


**Figure 4.3 Radial transient of first regime (time versus displacement)**

Figure 4.3 is plot of the initial radial displacement versus time. When the braid point lies outside the central axis of the braiding machine a tension imbalance exists causing an initial transient motion of a braid point toward the center. The first regime consists of an initially changing braid point position that occurs rapidly followed by an oscillation transient.

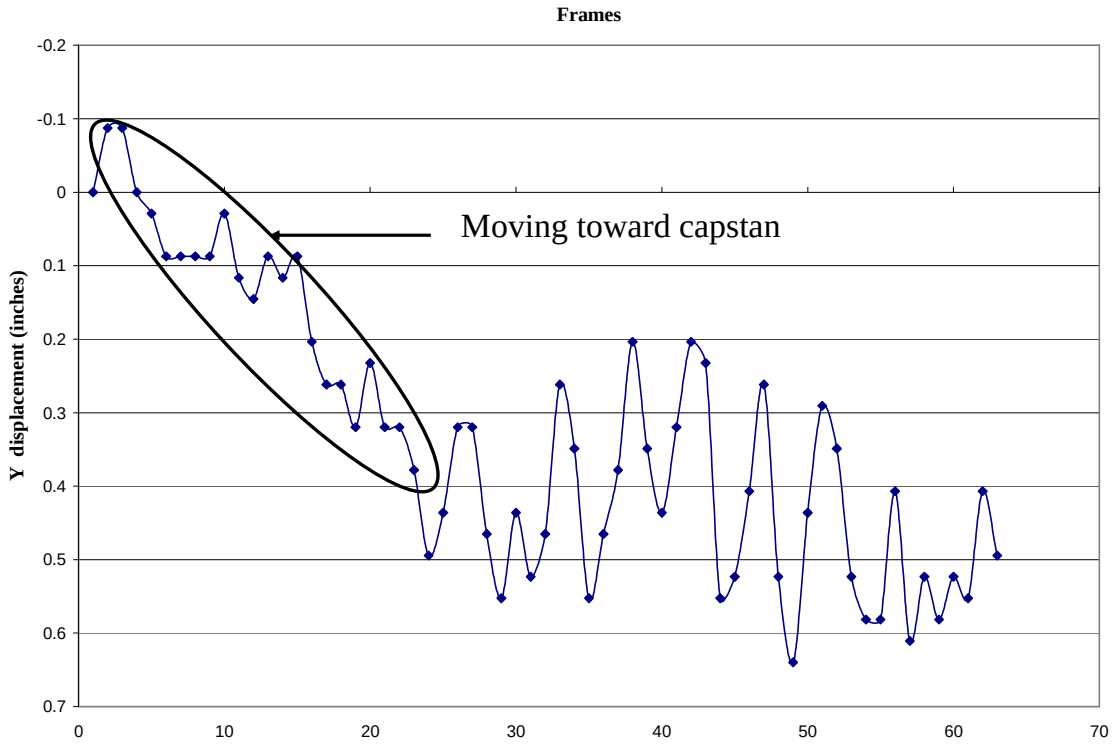


**Figure 4.4 Y direction transient of first regime (frames versus displacement)**

Similar to the radial direction transient, an initial transient is observed in Figure 4.3 and in another experiment as the braid point moves toward the capstan in the y direction. The data from Figure 4.4 corresponds to 1/10 of a braiding machine revolution. The y axis is given as displacement along the axial or take-up direction and the x direction is given in number of sequential frames. Figure 4.4 shows the braid point moving toward the capstan as the slack is taken up in the braid and the tension mechanism springs are being compressed. Figure 4.4 is a plot of the braid point in the first regime.

The extent of the initial transient depends on tension in the yarns at start up. The startup transient can also be observed in the x, y, and z directions as a result of the initial position of the braid point at startup. A transient in the radial direction is determined

with the x and z reference frame data. In the y (axial or take-up) direction, the startup transient is attributed to the braid point moving toward the capstan as slack is relieved in the yarns. The transient behavior observed in the radial (x and z) direction is related to the initial position of the braid point.

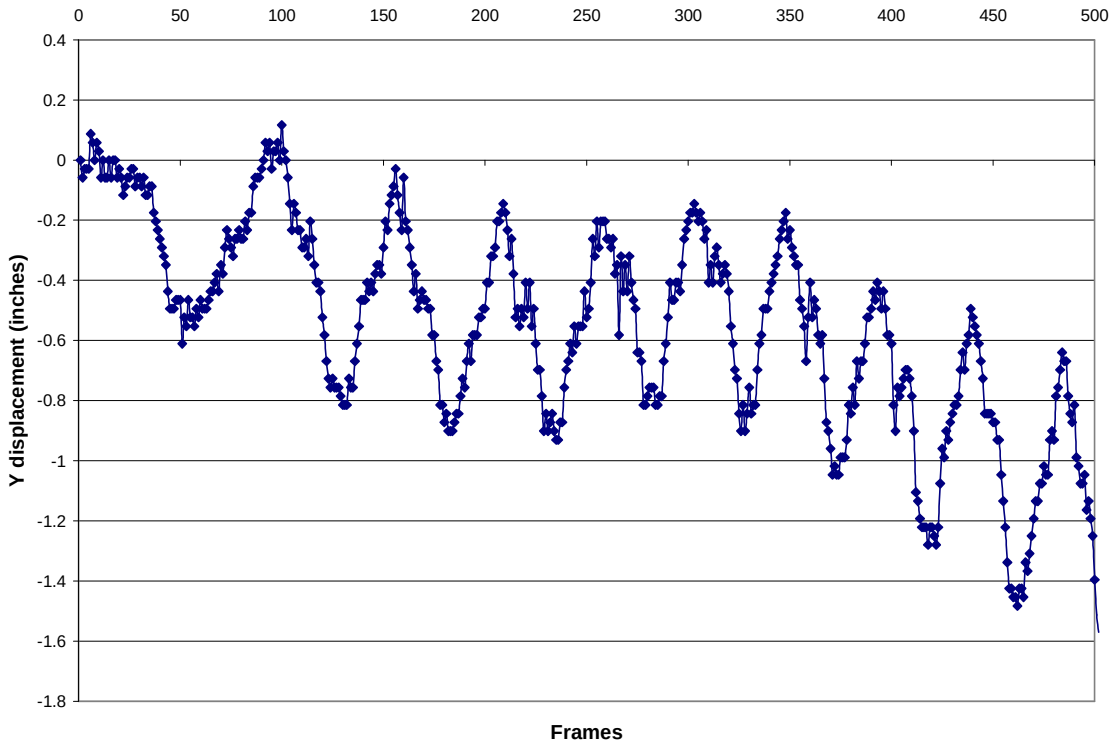


**Figure 4.5 Oscillations and braid point migration toward equilibrium point (second regime)**

Figure 4.5 demonstrates the braid point migrating toward the braiding machine while finding its own position [8]. Another aspect of the dynamics encountered in braiding occurs after the initial transient as the braid point migrates toward its equilibrium. This phenomenon is discussed in the previous section. Figure 4.5 shows the

braid point oscillating similar to the behavior encountered in steady state, but with some migration toward the equilibrium point along the y direction.

If adequate tension between the yarns and the braid exists, the startup transient is not observed. After the transient effects of loading the package mechanism have subsided, the resulting steady state behavior is a sinusoidal oscillation. Although seeming steady state, some migration may in fact occur, as pointed out in the previous section, until the braid point is indeed balanced between the braiding machine and capstan.

### 4.6 Steady state braid point motion

The braid point motion may pass through the first and second regimes until finally reaching the steady state oscillations of regime 3.

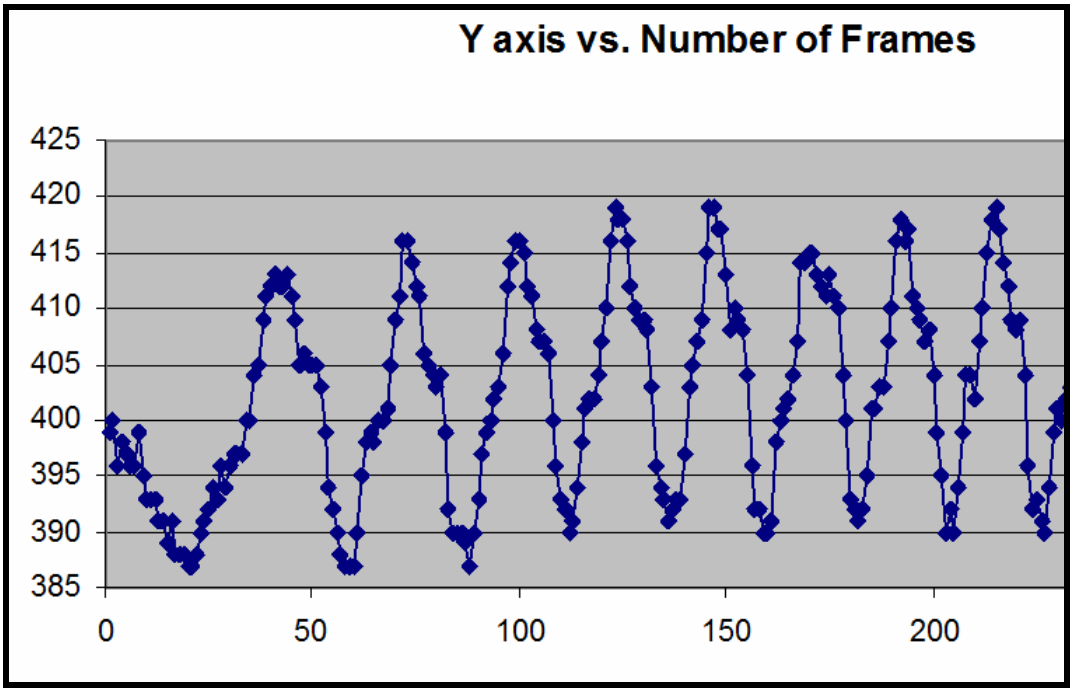


**Figure 4.6 Steady state braid point motion (regime 3)**

Figure 4.6 is a plot of the braid point motion in the Y direction with respect to time. The x axis is given in sequential camera frames and the y axis is given in pixels.

Figure 4.6 is captures the 3 transient regimes although they may be difficult to distinguish. Regime 3 begins after frame 100 and continues as steady state oscillations. The experiments presented in this section capture the initial braid point behavior and indicate evidence of a brief transient, followed by a migration toward steady state oscillations.

### 4.7 Braiding with optimal machine conditions

In order to establish a basis for comparison, a braid is formed using sixteen well lubricated packages, same amount of material per bobbin (1420 denier Kevlar®) and the same size springs. Clean, well lubricated packages with the same material are factors most easily controlled by the braiding machine operator.

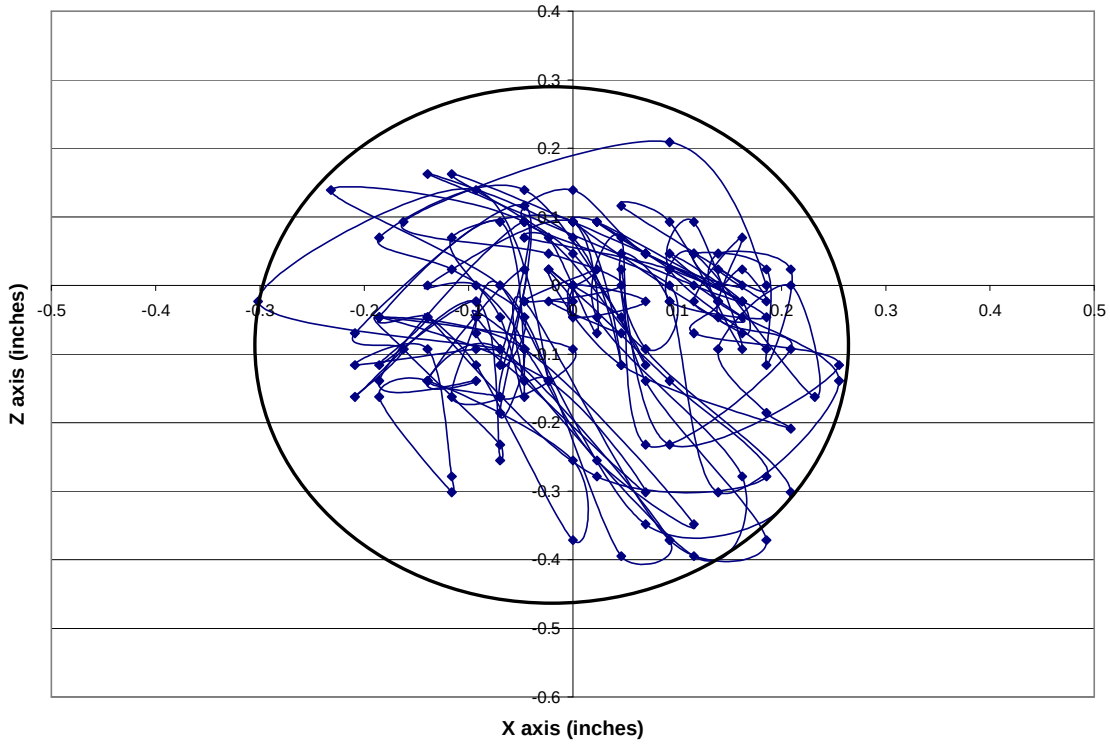


**Figure 4.7 Circular displacement of optimal braid**

Figure 4.7 is a plot of the motion of an optimal braid point for 3.86 braiding machine revolutions. Test data was acquired for Figure 4.7 after the braid point had reached the steady state oscillating equilibrium of regime 3. Images are acquired with a camera frame rate of 30 frames per second. Figure 4.13 shows the balanced braid point motion stays within a circle. The values are shifted centered about the origin and indicate that an optimal, balanced braid undergoes small (less than ~0.5 inch) radial variations.

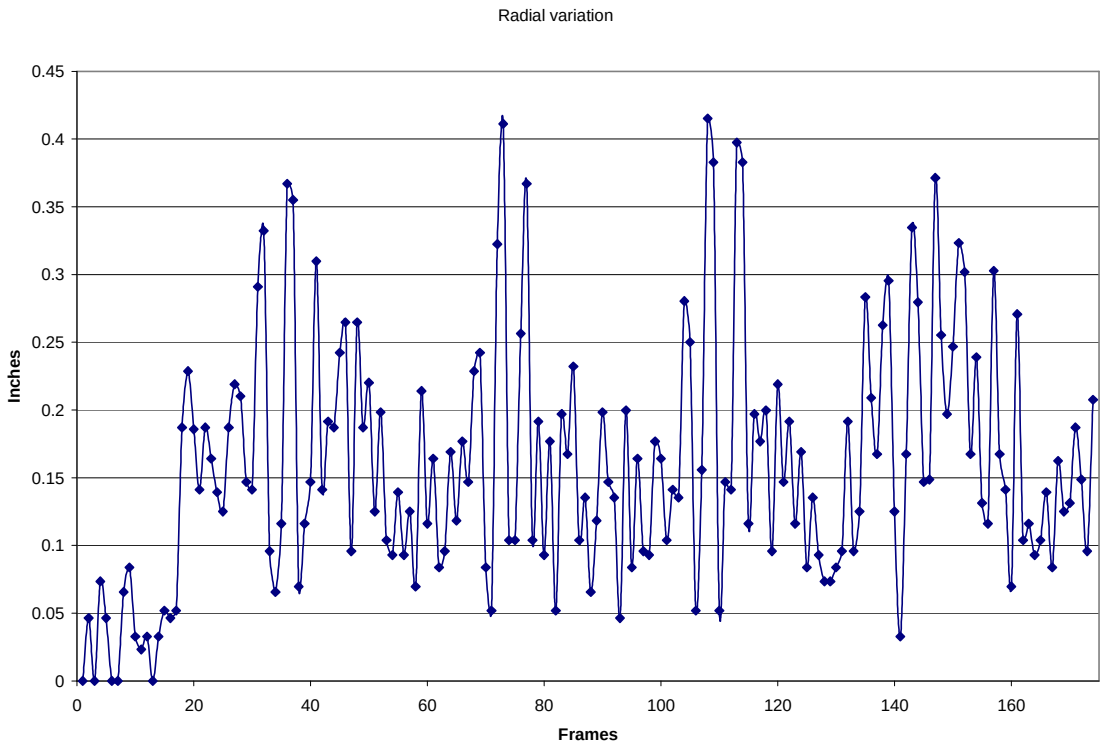


**Figure 4.8 Radial variation of an optimal braid**

Figure 4.8 is a plot of the radial variation of the braid point using the same data from Figure 4.7. It is Figure 4.8 plotted showing its variation in time. The data in Figure 4.8 is configured using the distance formula and comparing the distance of each braid point position to the initial position. It is conjectured that this data is akin to noise,

because it is very small and does not appear to have a discernable trend and is a result of individual packages randomly releasing yarn during the braiding process.

As previously established, the braid point formation occurs somewhere between the bobbins and the take-up machine. The formation point tends to be along the central axis of the track plates or typically the center of the machine. The track plate forms an overall circular path. Therefore, the interlacing facilitated by the carriers in balanced braid architectures causes the braid point to undergo circular displacements as seen in Figure 4.7.

**4.8 Effects of take-up speed on braid angle**

An experiment is performed and discussed in this section that aims to acquire data regarding the angle of the yarn, as a function of take-up speed. In this experiment, images are acquired for a given take-up speed. When a particular yarn reaches an indexed position, occurring once every complete braid revolution, an image is acquired. The springs for each package are the same and therefore the yarn tension is balanced. The yarn package is moved to the top most position (or can be any position of interest) and the braiding machine encoder position is initialized to zero. Initializing the encoder to zero with the yarn package in a desired position is useful in measuring the angle of braid point formation, by allowing desired images to be acquired according to any increment or position.

In the case of this experiment, the software acquired an image approximately every 81920 encoder counts corresponding to one complete braiding machine revolution. By using the encoder as a trigger, the resulting image acquisition insures that the same yarn is captured in the same position. The braid angle is measured using a USB web

camera in conjunction with LabVIEW programs designed to process the image appropriately (section 3.17). The data is recorded and the results are plotted. A shaft mounted encoder attached on the braiding machine triggers the camera to acquire an image (section 3.13).

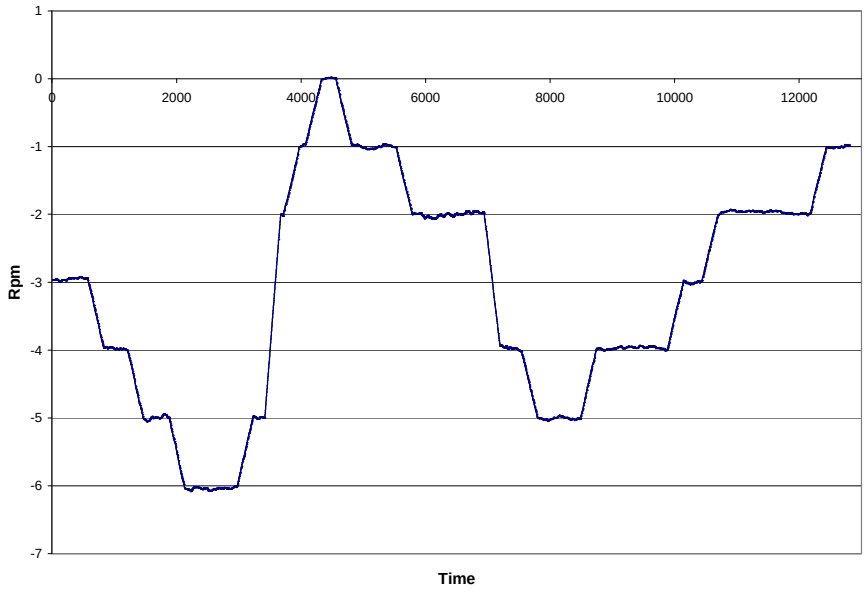


**Figure 4.9 Average capstan motor speeds for braid angle test**

Figure 4.9 is a plot of the average capstan speed increments during the angle test. The braid point was in the second regime (discussed in section 4.5) and did not reach a steady state condition (third regime). The capstan speed is set in increments of 1 rpm from 3 to 6 and then 6 to 0, 0 to 5, and 5 back to 1 rpm. The x-axis in Figure 4.9 corresponds to the data acquisition time interval during the experiment and is given in time increments of 0.047 seconds. Interestingly, there is a lag in the braid angle and take-up speed.

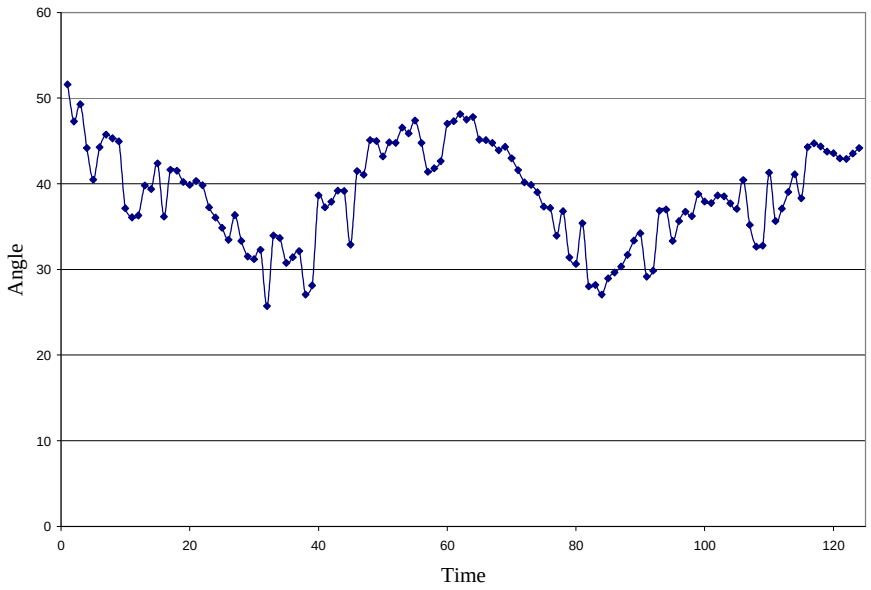


**Figure 4.10 Braid angle versus braiding machine revolution**

Figure 4.10 demonstrates how increasing the take-up speed (see Figure 4.9) decreased the angle formed by the yarns at the braid point for a given braiding machine speed (see Figure 4.4). The x-axis in Figure 4.10 corresponds to the image acquisition time interval during the experiment and is given in time increments of 0.033 seconds. The y axis is the braid point angle given in degrees. Figures 4.9-10 illustrate the direct relationship between take-up motor speed and braid angle while in the second dynamic regime.

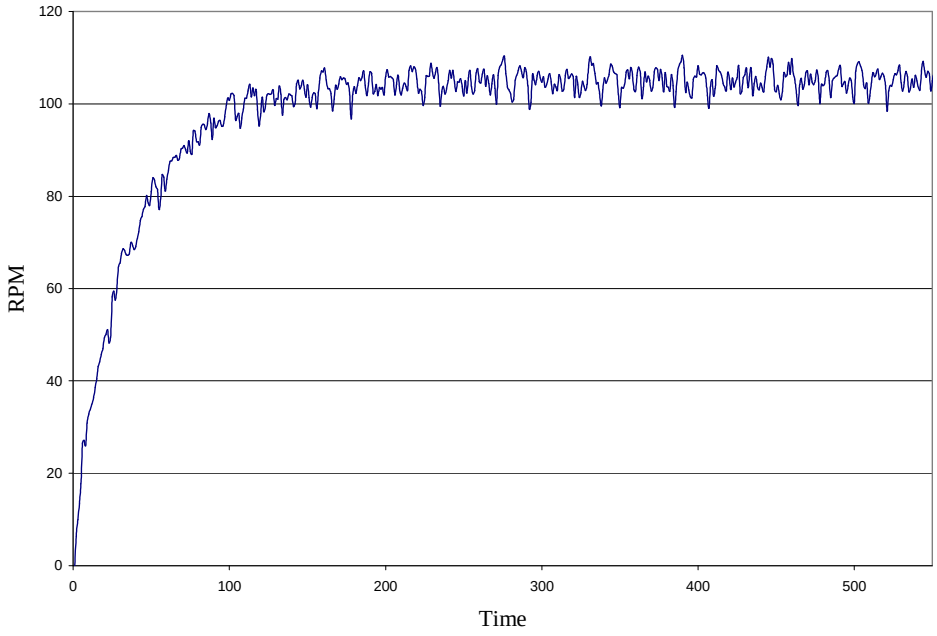


**Figure 4.11 Braiding machine speed (RPM) for a balanced braid.**

Figure 4.11 is a plot of the braiding machine speed during this test. The y axis is the braiding machine speed given in revolutions per minute (RPM). The x-axis in Figure 4.11 corresponds to the data acquisition time interval during the experiment and is given in time increments of 0.047 seconds. It should be noted that for this experiment the braiding speed is fixed and the braid point angle is a function of the capstan and braiding machine motor speed ratio.

### 4.9 Braid angle settling time

The following section demonstrates that the braid point motion migrates toward or away from the braiding machine depending on its initial position with respect to its final equilibrium steady state position (for a given take-up speed).

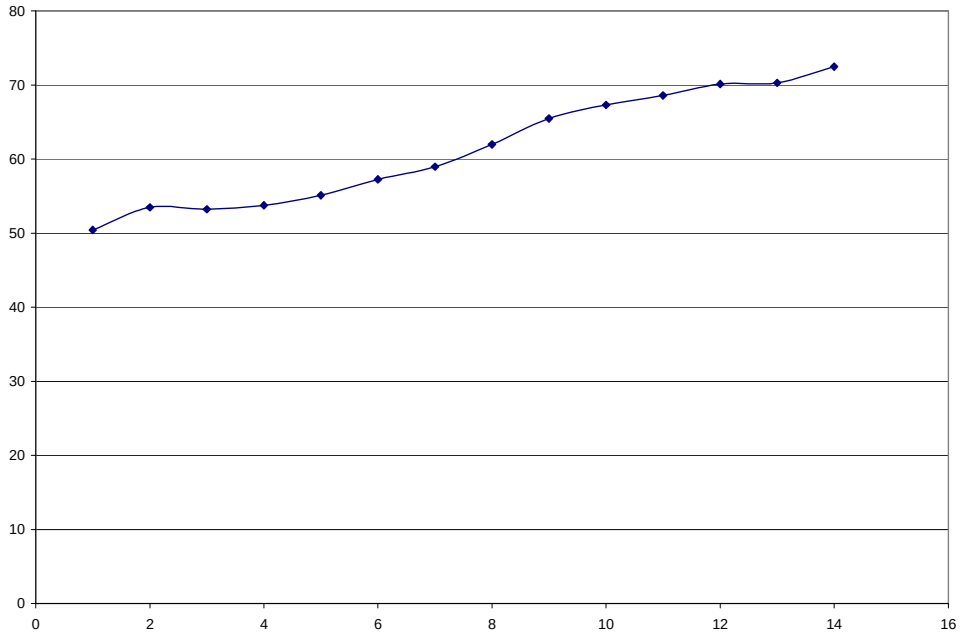


**Figure 4.12 Increasing braid angle versus braiding machine revolution (1 rpm)**

Figure 4.12 shows the increasing angle for a capstan speed of 1 rpm. The x axis is the number of braiding machine revolutions. The y axis is the braid point angle. It is observed that for a constant take-up speed, the braid point continues to migrate until finally reaching its final position. It is determined that the previous experiments do not result in a steady state braid point position. In order to capture the full extent of braid dynamics including the braid position transitioning into steady state, more acquisition time is required.

In light of the observations that the braid point requires significant amount of time to settle from previous experimental results from Figures 4.12, it was determined that

additional data is required to make more conclusive results regarding braid angle migration and settling. The objective of the new experiment described in this section is to understand the number of braiding machine revolutions (or time) required to reach a constant braid angle.

The experiment involves repeating the experiments of determining braiding angle as a function of take-up speed; much like Figures 4.9 and 4.10 except the braid point is allowed to reach the steady state oscillations of the third regime. It is finally realized from Figure 4.12, that the braid angle settling for the given speeds may require as many as 70-80 complete braid revolutions to stabilize, depending strongly on its initial location with respect to the final location.

The capstan take-up speed sequence employed for this experiment is as follows: 1 rpm (Appendix Figure A.4), 1.5 rpm (Appendix Figure A.5), 2.5 rpm (Appendix Figure A.10), 3.5 rpm (Appendix Figure A.10), 3 rpm (Appendix Figure A.10), and finally returned to 2.5 rpm (Appendix Figure A.10). The braid reaches a jammed (or slightly greater) state at 1 rpm (because of the interference with the steel braid ring). At 1.5 rpm as well as 1rpm, the steel braid ring interferes with the braid yarns and is out of the range of the cameras FOV. 2.5 rpm is observed for 9 or so revolutions; however, in an attempt to move the braid point to a more convenient position, the capstan motor speed is increased to 3.5 rpm. Although, 3.5 rpm brings the braid beyond the FOV, 3 rpm stabilizes within the camera FOV. Finally, 2.5 rpm is revisited and the drift from 3 rpm steady state position is observed.

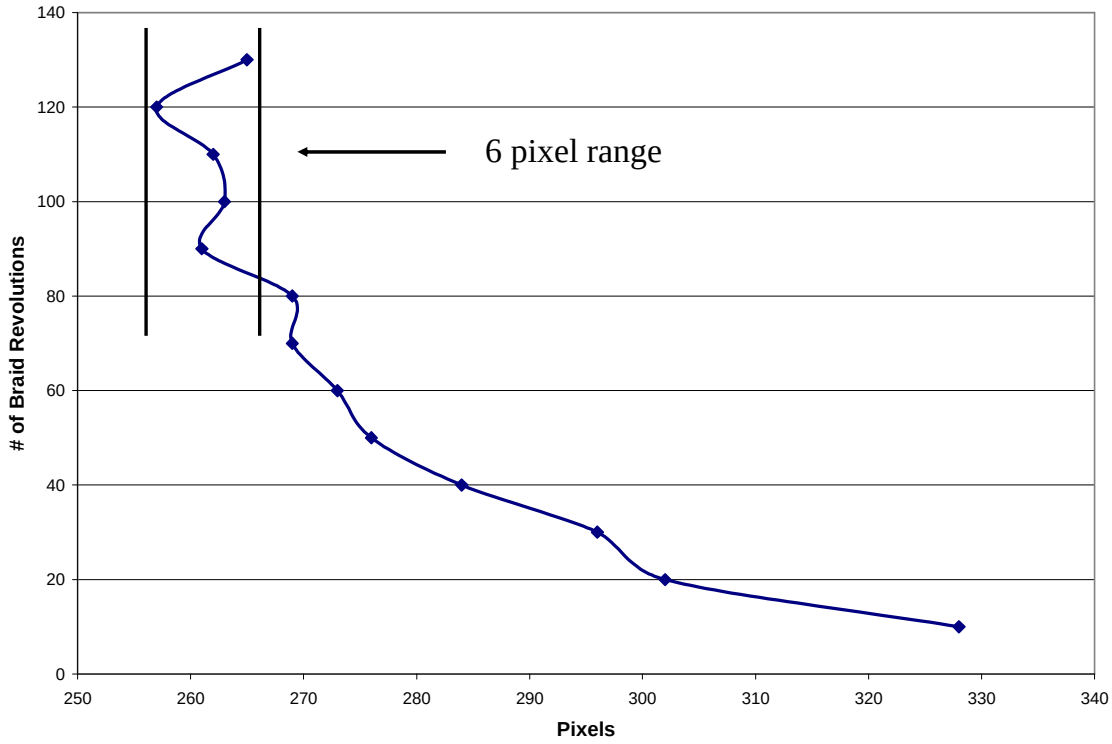


**Figure 4.13 Braid point migration and stabilization distance in pixels (2.5 rpm)**

Figure 4.13 shows the braid point migration to final position for a capstan motor speed of 2.5 rpm. The x axis is given in pixels and the y axis is the number of braiding machine revolutions. In Figure 4.13 the braid point begins to stabilize around 80 revolutions in the Y direction. The braid point moves from the right to the left toward the braiding machine. Although some oscillation is observed (6 pixels), the capstan and braiding machine have essentially reached equilibrium. The side view camera from which the data in Figure 4.13 corresponds has a calibration factor of 43.08 pixels per inch.

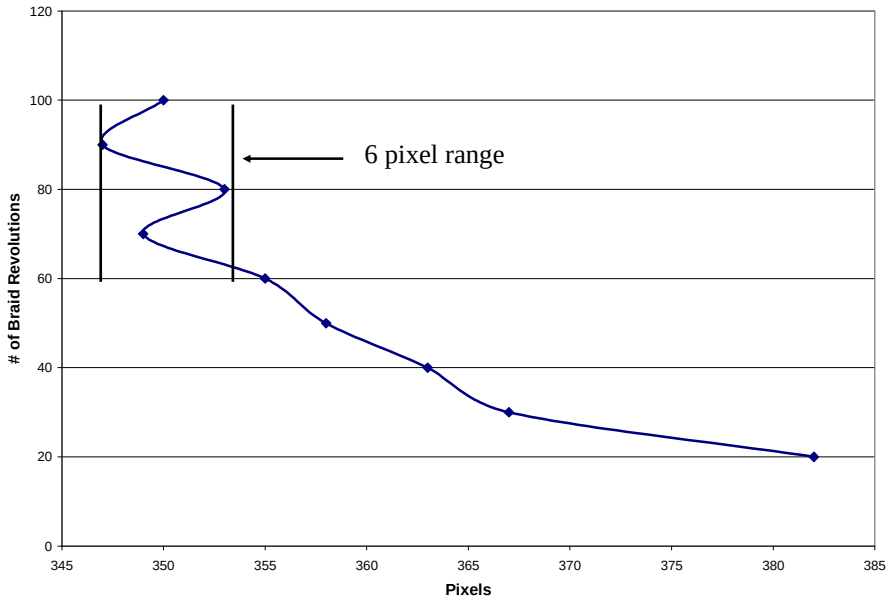


**Figure 4.14 Braid point migration and stabilization (3 rpm)**

Figure 4.14 shows the braid point migration to final position for a capstan motor speed of 3 rpm. The x axis is given in pixels and the y axis is the number of braiding machine revolutions. In Figure 4.14, the braid point begins to stabilize around 60 revolutions in the Y direction. The braid point moves from the right to the left toward the braiding machine. The side view camera, from which the data in Figure 4.14 corresponds, has a calibration factor of 43.08 pixels per inch.

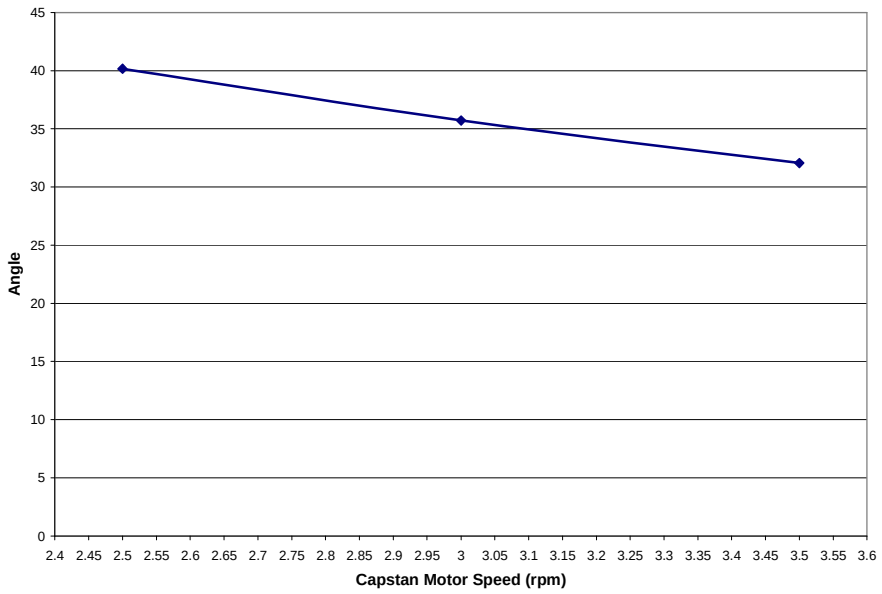


**Figure 4.15 Braid cone angle as a function of capstan motor speed**

Figure 4.15 shows the relationship between stabilized angle and capstan motor speed for a given braiding machine speed (Figure 4.11). The y axis is the braid point angle, given in degrees and the x axis is the capstan motor speed given in rpm. The braid point position is allowed to stabilize and the angle corresponding to the steady state position is plotted. This plot is particularly useful if the angle of braid point formation is desired. The angle of braid point formation can be achieved by setting the capstan motor speed accordingly.

### 4.10 Limitations of experimental setup

The ability of the experimental system to determine the angle of yarn at the point of fabric formation is affected by several factors; however the primary factor is the limitations imposed by the camera field of view (FOV). For the given experimental setup, the range of take-up speeds causing the braid point to reside within the camera

FOV is somewhat limited. The attainable range of braid point positions occur between 2.5 and 3.5 capstan motor rpm.

An interesting indication of the dynamics involved with braid point formation is observed in the results of the previous experiments of sections 4.12-4.14. If the current braid point is significantly far from the equilibrium position then as many as 80 (Figure 4.13) braiding machine revolutions may be required for the braid point to reach actual steady state i.e. no drift. If factors such as motor speed that affect the braid point dynamics, as investigated in this chapter remain constant, then the braid point will reach a steady state where after the quality of the braid will be highest. In order to promote high quality manufacture of braid, it is important that motor speed and tension remain constant when the braid point has reached equilibrium. The experiments of braid angle and take-up speed provide further evidence of the nature of the braid point transient behavior and the notion that braiding is an inherently slow process is reinforced.

**4.11 Effects of one locked package**

The bottom most package is locked, in such a way as to cause a faulty release mechanism. The effect of a locked package is that the amount of material available to the braid from the spool is fixed. As the capstan pulls the braid, the properly functioning packages release yarn and this material contributes to the braid formation.

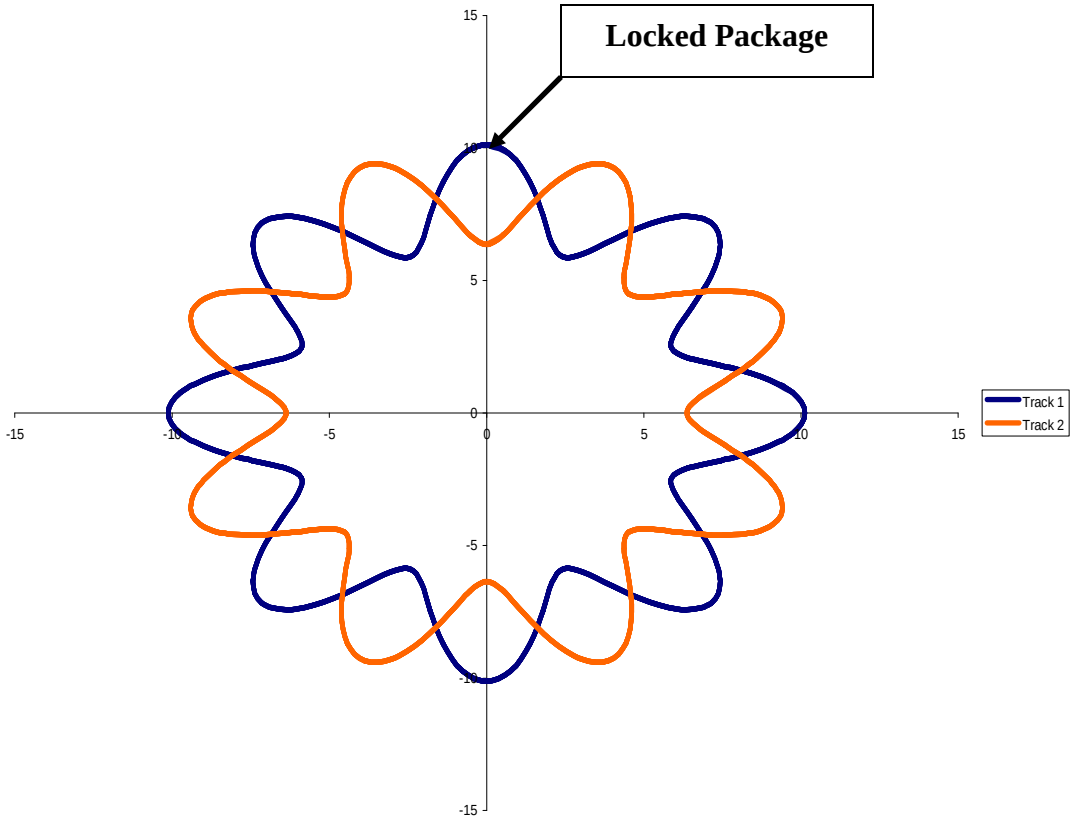


**Figure 4.16 Initial position of locked package**

Figure 4.16 is a plot of the braid point motion for the first braiding machine revolution, showing where initial position of the package that is locked (goes clockwise).

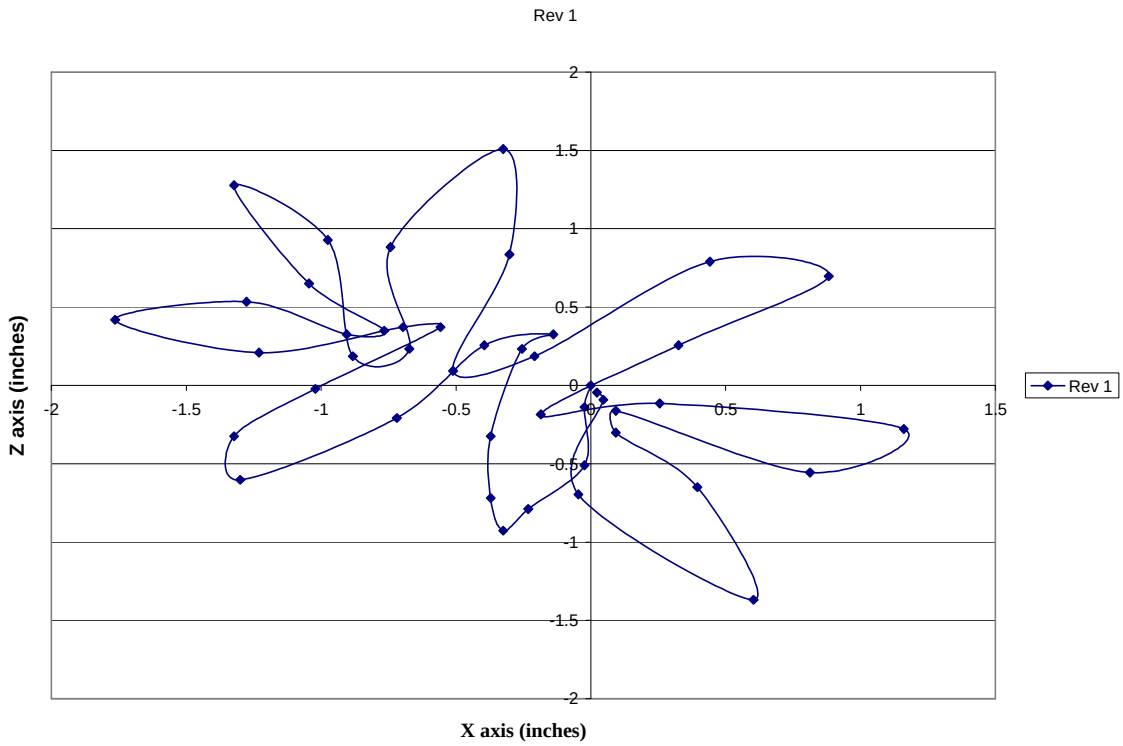


**Figure 4.17 Braid point displacement with 1 locked package (First revolution)**

Figure 4.17 is made by plotting the x-z values of the braid point for the first braiding machine revolution. The axes, x and z, are the radial displacement of the braid point given in inches. Figure 4.17 shows the dominant effect of a high tension yarn on the braid point formation. The path of the braid point corresponds to the shape of the track plate paths (Figure 4.16), as the braid point follows the carrier with the high tension as it travels around the track plate path.

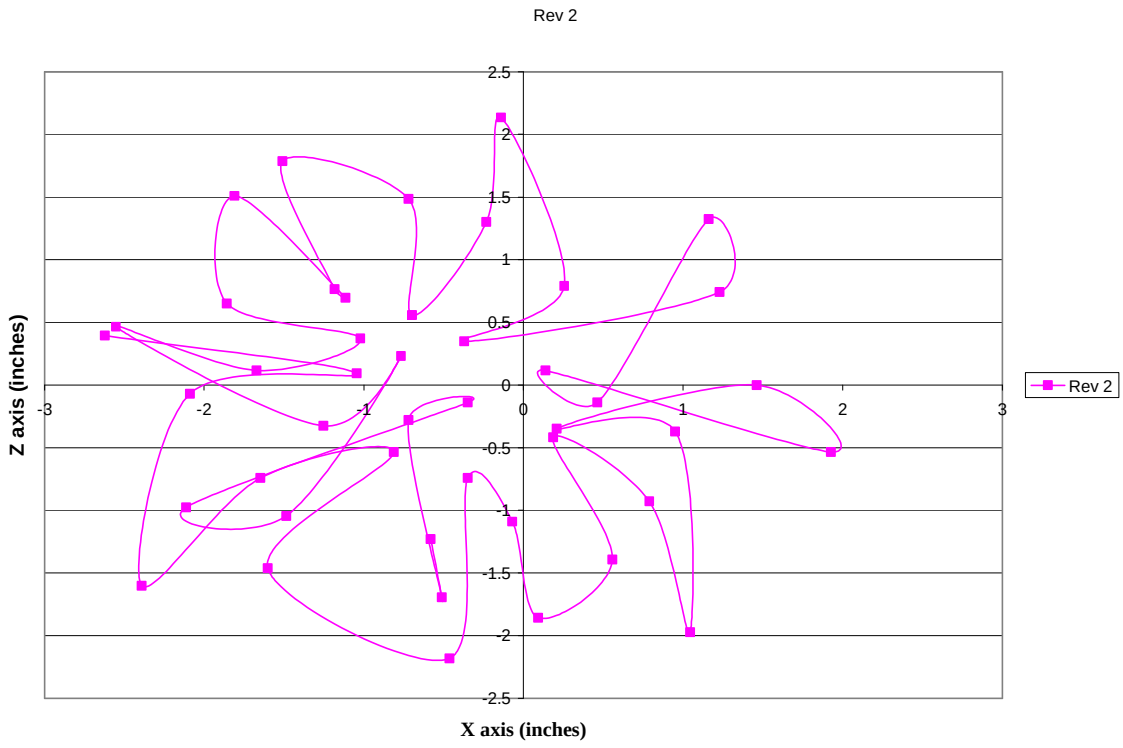


**Figure 4.18 Braid point displacement with 1 locked package (Second revolution)**

Figure 4.18 is a plot of the braid point motion for the second revolution when one package is locked. The axes, x and z, are the radial displacement of the braid point given in inches. Figure 4.18 is a continuation of the locked package experiment. Similar to Figure 4.17, Figure 4.18 shows the dominant effect of a high tension yarn on the braid point formation. The path of the braid point corresponds to the shape of the track plate paths, as the braid point follows the carrier with the high tension as it travels around the track plate path. The radial variation of Figure 4.17 from has now increased from that observed in Figure 4.18.

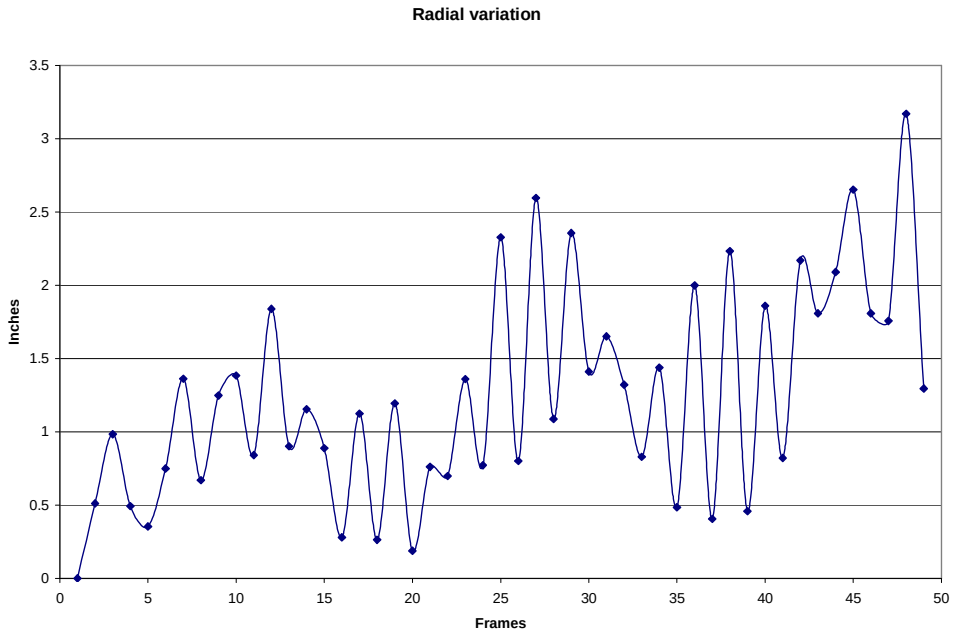


**Figure 4.19 Radial variation of a locked package braid**

Figure 4.19 is a plot of the distance formula applied to the x-z position of the braid point. The data in Figure 4.19 is configured using the distance formula by comparing the distance of each braid point position to the initial position. The x-axis in Figure 4.19 corresponds to the image acquisition time interval during the experiment and is given as the sequential frames which translate in time increments to 0.033 seconds per frame. The average distance from the starting braid point for one locked package is 1.24 inches. The effect of one locked package also causes a twisting of the braided material as the high tension yarn twists the braid as it proceeds around the track plate.

**4.12 Effect of two diametrically opposed locked packages (same track) on the braid point motion**

This experiment involved locking two diametrically opposed yarn packages on the same track path to study further the effects of various faulty package behavior. The yarn packages locked in this experiment are seen in Figure 4.22.

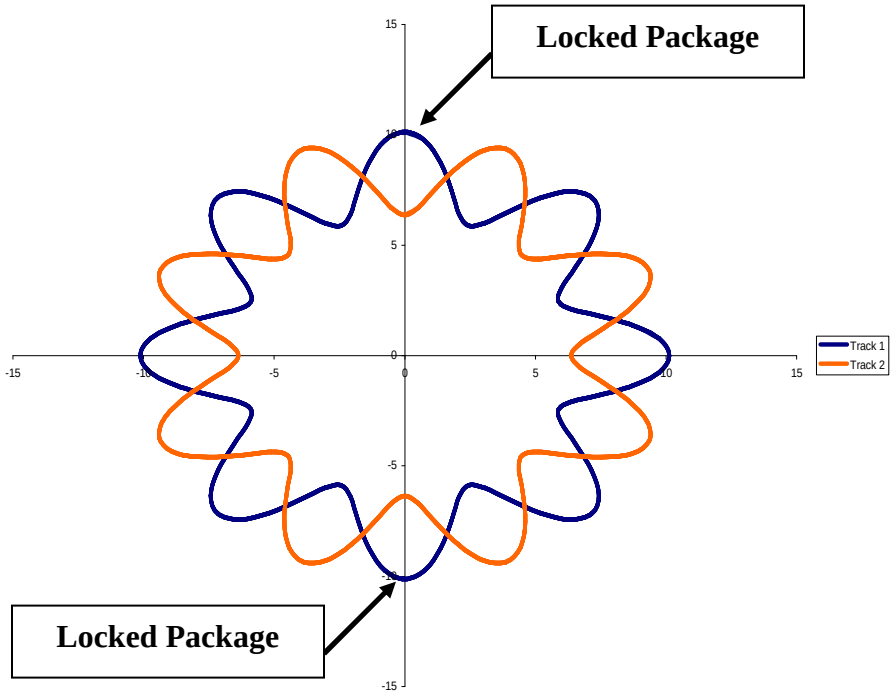


**Figure 4.20 Initial position of diametrically opposed locked packages**

Figure 4.20 shows the initial position of the packages when their release mechanism is locked. As the capstan pulls the braid, the properly functioning packages release yarn and this material contributes to the braid formation. The yarns with faulty packages do not release any new yarn. During this experiment the amount of material from the locked packages is constant and the yarns are slack when they are closest to each other and taut when furthest apart. The transition from slack to taut of the locked package yarns is investigated in more detail in Chapter 5.

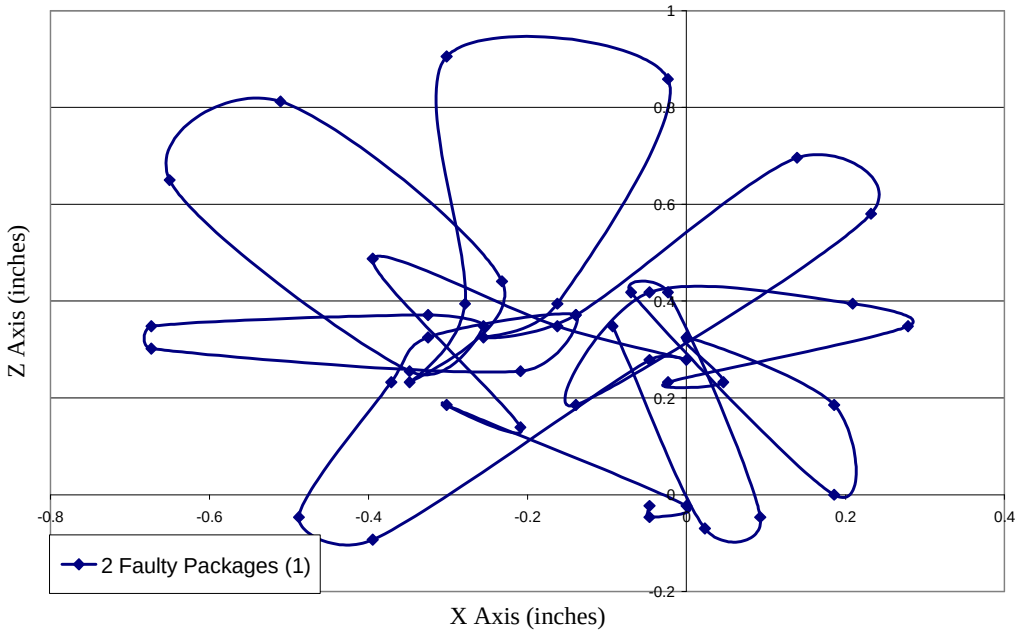


**Figure 4.21 Braid point motion with 2 diametrically opposed locked packages (First revolution)**

Figure 4.21 shows the braid point motion when 2 diametrically opposed packages are locked. The axes, x and z, are the radial displacement of the braid point given in inches. Figure 4.21 is the result of plotting the braid point motion for the first braiding machine revolution. The resulting shape is similar to the track plate paths as the high tension yarns pull the braid point along this path.

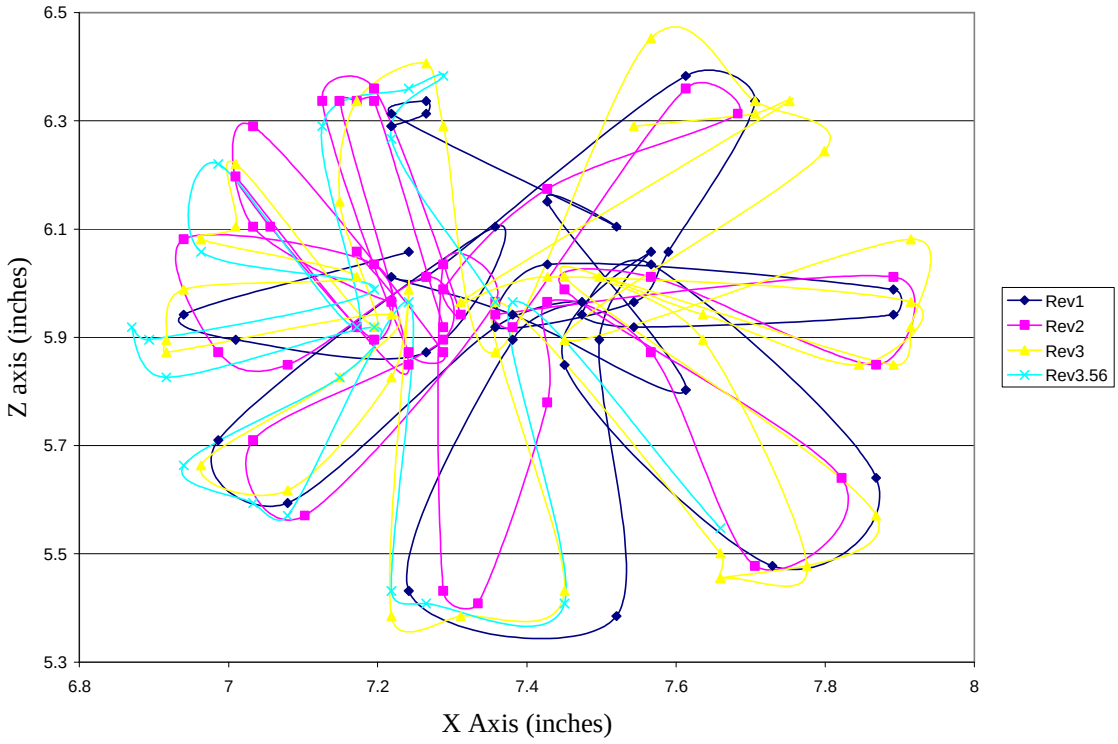


**Figure 4.22 Combined braid point motion with 2 diametrically opposed locked packages**

Figure 4.22 is the data resulting from 3.56 braiding machine revolutions to show the variation between revolutions is minimal when two diametrically opposed packages are locked and all other yarns are balanced. The axes, x and z, are the radial displacement of the braid point given in inches.

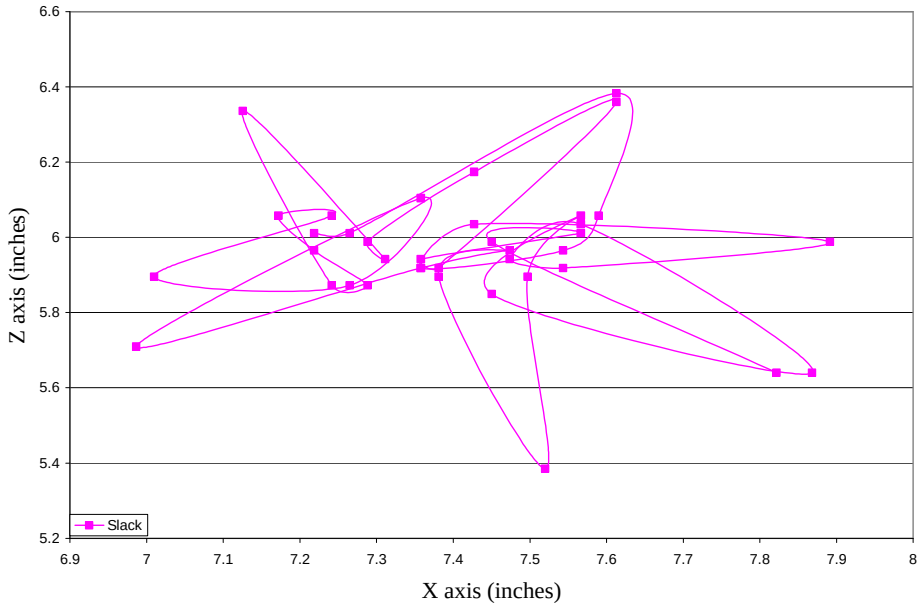


**Figure 4.23 Braid point motion while 2 yarns are slack (1 Rev).**

Figure 4.23 depicts the braid point motion when the yarns are slack; this occurs when the diametrically locked packages are on locations closest to the center. Figure 4.23 was created by plotting the data corresponding to the images when the yarns are slack. The axes, x and z, are the radial displacement of the braid point given in inches. Chapter 5 discusses how to discern when the yarns are slack and in transition to high tension.

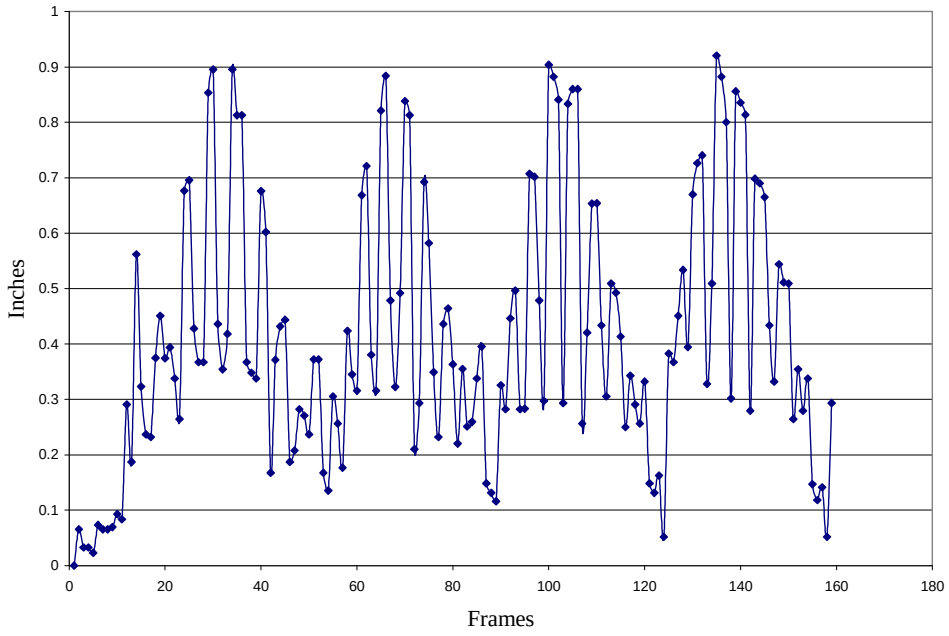


**Figure 4.24 Radial variation of 2 locked packed braid based on Figures 4.18-23**

Figure 4.24 is a plot of the distance formula applied to the x-z position of the braid point. The data in Figure 4.24 is configured from the distance formula by comparing the distance of each braid point position to the initial position. In Figure 4.24 four periodic regions are observed, they correspond to the approximately four braiding machine revolutions occurring during this experiment. The average distance from the starting braid point for two diametrically opposed locked packages is 0.42 inches.

### 4.13 Effect of two locked packages from opposite tracks on the braid point motion

Two packages on opposite tracks are locked such that the yarn does not release. The packages are arranged such that one package is in the peak while the other is in the valley of the sinuous track path. During this experiment one of the locked yarns breaks, leaving one high tension yarn and the resulting motion is similar to the results from the section 4.11.

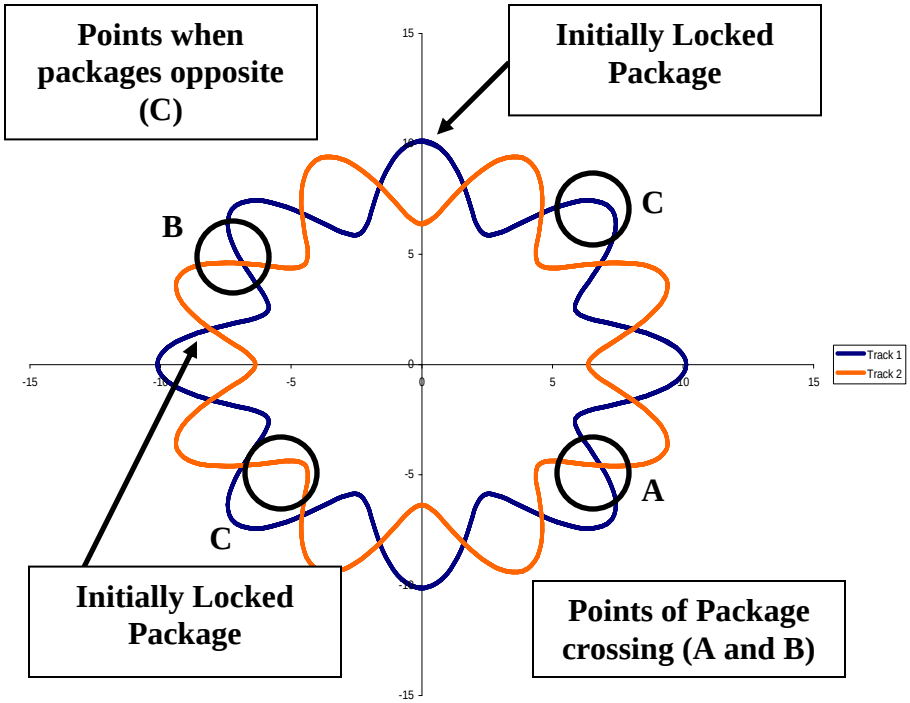


**Figure 4.25 Illustrates the initial, opposite, and crossing points of the locked packages**

Figure 4.25 shows the position of the packages when they cross (Points A and B), when the packages are opposite or furthest apart (Points C) and where they initially began. During each braiding machine revolution, the locked packages with high tension will cross each other twice and will be opposite each other (180 degrees apart) once.

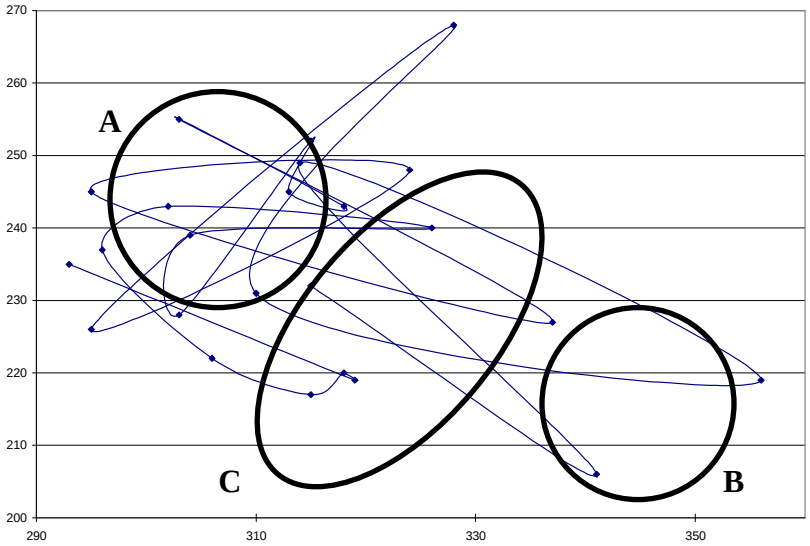


**Figure 4.26 Braid point motion with two locked packages on opposite tracks (first revolution**)

Figure 4.26 is made by plotting the braid point position for the images acquired during the first braiding machine revolution. The axes, x and z, are the radial displacement of the braid point given in inches. Point A is the first point when the locked packages, from different tracks, first encounter each other. A definite grouping of data points occur at Point A as a result of the two high tension yarns now pulling the braid from the same position. Point B is the second crossing point that occurs during the first revolution. Point C corresponds to when the yarns are furthest apart.

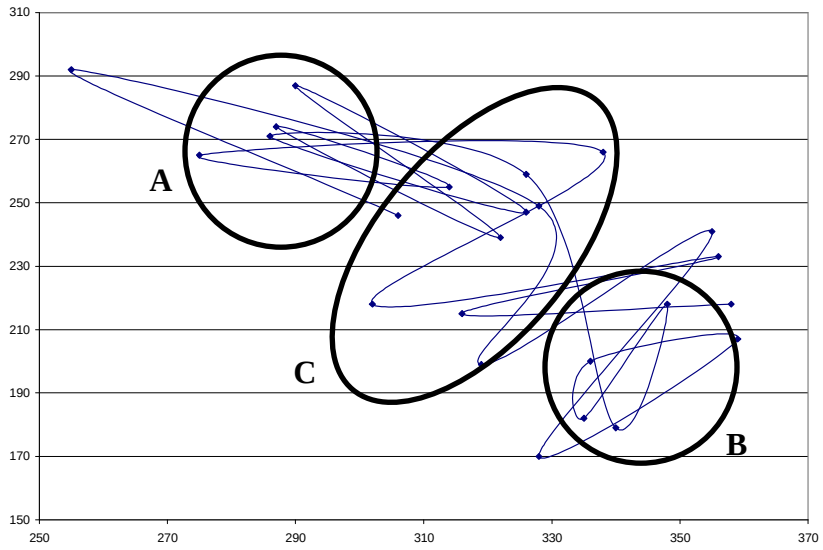


**Figure 4.27 Braid point motion with two opposite track locked packages (second revolution)**

Figure 4.27 shows the braid motion for the second braiding machine revolution. The axes, x and z, are the radial displacement of the braid point given in inches. The tension in Figure 4.27 is increasing from Figure 4.26 and the radial movement increases. Similar to Figure 4.26, Point A is the first point when the locked packages, from different tracks, first encounter each other. A definite grouping of data points occur at Point A as a result of the two high tension yarns now pulling the braid from the same position. Point B is the second crossing point that occurs and as the tension has increased from Figure 4.26, the braid point occupies more points in this region. Point C corresponds to when the yarns are furthest apart.

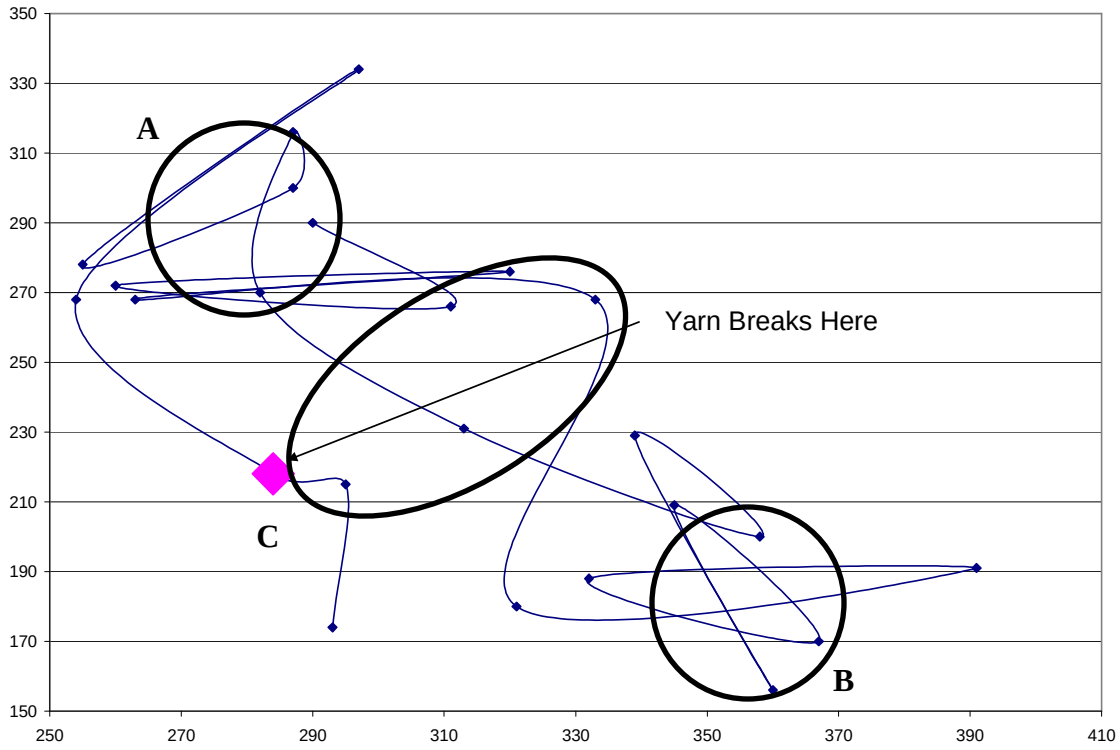


**Figure 4.28 Braid point motion with two opposite track locked packages (third revolution)**

Figure 4.28 captures the yarn break occurs toward the end of this revolution. The x and y axes of Figure 4.28, correspond to the radial (x and z) displacement of the braid point given in pixels. The tension in Figure 4.28 has increased from Figure 4.27 and the radial movement also increases as seen by the increased distance between Points A and B. Similar to Figure 4.26 and 4.27, Point A is the first point when the locked packages, from different tracks, first encounter each other. A definite grouping of data points occur at Point A as a result of the two high tension yarns now pulling the braid from the same position. Point B is the second crossing point that occurs and as the tension has increased from Figure 4.26, the braid point occupies more points in this region. Point C

corresponds to when the yarns are furthest apart. Toward the end of third revolution (Figure 4.28), the yarn with the highest tension finally breaks and the remaining braid has only one yarn with high tension.

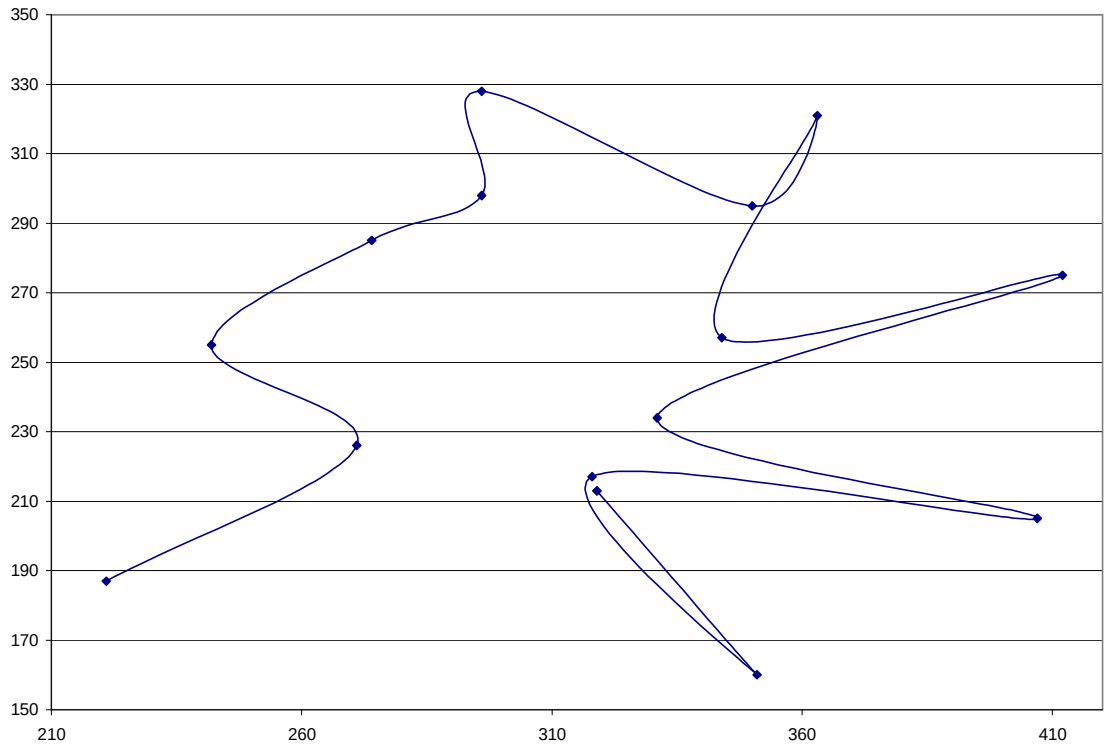


**Figure 4.29 Braid point motion with two orthogonally locked packages (.62 revolutions)**

Figure 4.29 is a plot of the braid point motion after one locked package yarn has broken. The x and y axes of Figure 4.29, correspond to the radial (x and z) displacement of the braid point given in pixels. Figure 4.29 is the result of the braid point motion with only one high tension member and is similar to the resulting motion observed in section 4.11.

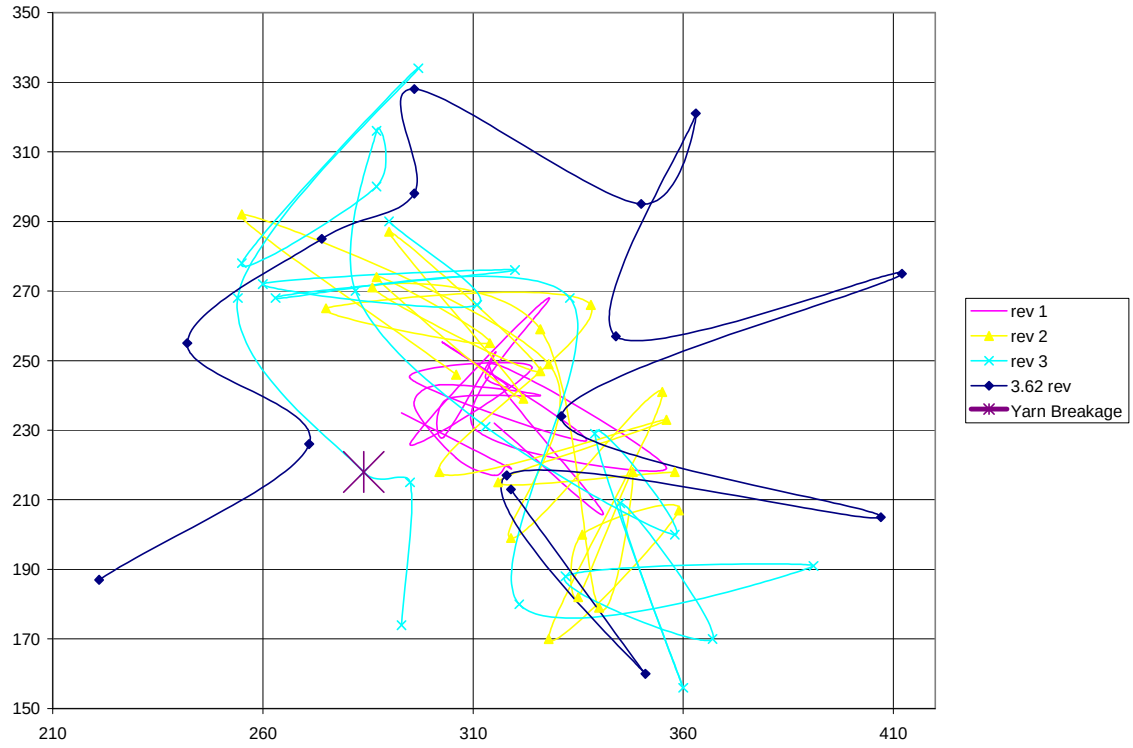


**Figure 4.30 Combined braid point motion with 2 locked packages on opposite tracks (3.62 revolutions)**

Figure 4.30 is the result of plotting data points from 3.66 braiding machine revolutions; it is a combined plot of 4.26-4.29. The x and y axes of Figure 4.30, correspond to the radial (x and z) displacement of the braid point given in pixels. Figure 4.30 shows the distinct transitions occurring in the braid point motion as the tension in a yarn increases up until it breaks. Figure 4.30 is a good example of the effects yarn tension can have on braid point motion and ultimately formation. For each revolution encountered, the yarn tension increases and ultimately the yarns will break. Figure 4.230 demonstrates the nature of high yarn tension as its influence is seen on braid point formative motion; for each revolution plotted the tension increases and the braid point formation radius increases. As a yarn increases its radial distance from the braid point,

the tension increases causing the braid point to be influenced by this increasing tension yarn. When a yarn moves into a track path valley, its radial distance decreases as well as the tension as the yarn becomes slack.

### 4.14 The effects of mechanical faults on motion data

Mechanical faults such as locked yarn require that the motors involved overcome the forces generated due to the nature of the fault. In the case of these experiments, the mechanical faults pertain to yarn tension. Kevlar® is a strong material and the loads induced throughout the braiding machine and take-up system can become significant especially when a package is locked and the braiding machine and capstan motors become engaged in what amounts to a tug of war match.

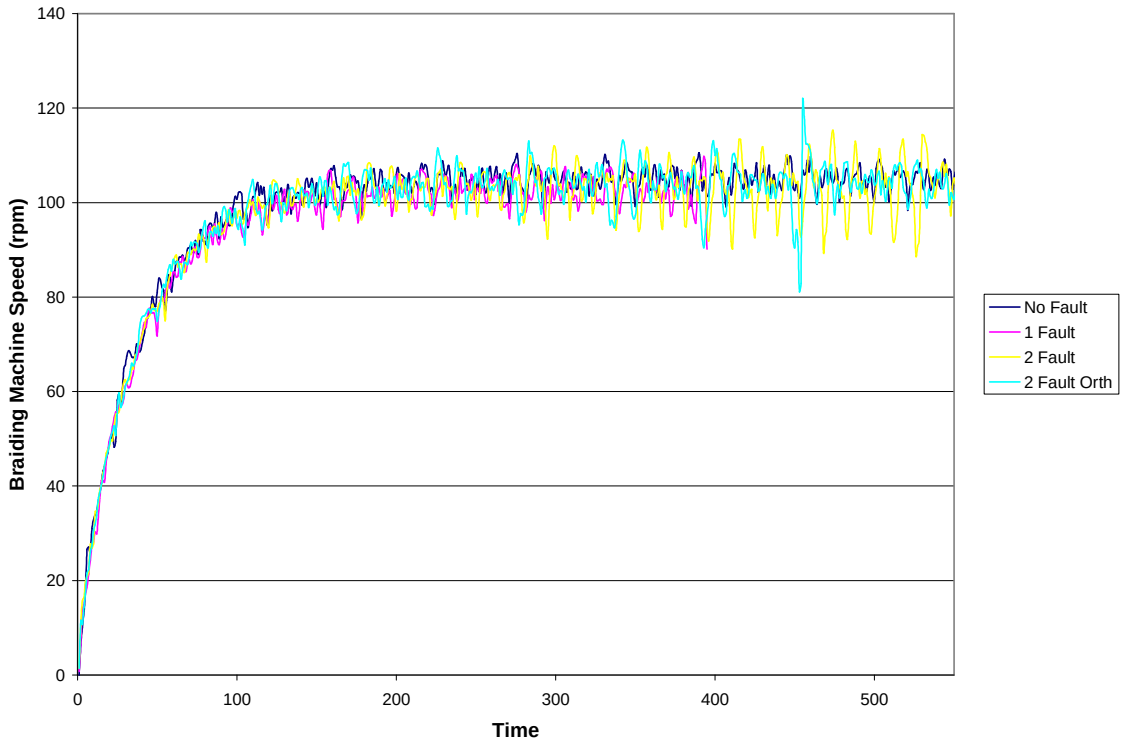


**Figure 4.31 Effects of faults on braiding machine speed**

Figure 4.31 is a comparison of the braiding machine speed for the conditions encountered in the previous experiments (section 4.13). The y axis is the braiding machine speed given in revolutions per minute (RPM). The x-axis in Figure 4.31 corresponds to the data acquisition time interval during the experiment and is given in time increments of 0.047 seconds. The DC gear-motor that is responsible for driving the braiding machine starts from zero and ramps up to the final braiding speed. Figure 4.31 is made possible by the shaft mounted encoder on the back of the braiding machine (Chapter 3) which provides information regarding the shaft position. The derivative of the shaft position with respect to time is calculated in the LabVIEW data acquisition code, written for this thesis work and the resulting data is plotted in Figure 4.31. It is interesting to note the variations in the motor speed, although difficult to see the magnitude of the motor speed variation increases with the encountering of mechanical faults.

As the capstan pulls the braid, the properly functioning packages release yarn contributing to the braid formation; however, the yarns with faulty packages do not release material and begin to distort the braid formation. Since the faulty packages do not release any new material to the braid formation, the yarn tension reaches its highest point at the furthest radial distance from the braid point. Conversely, when the yarn package reaches a low spot, i.e. a valley on track plate, the tension decreases and the yarns go slack.

### 4.15 Effect of yarn breakage on motion data

In this experiment (data from section 4.13), two packages are locked to observe the effects on the braid point motion. The packages are located on different tracks. One of the high tension yarns, resulting from the locked package, broke during the experiment.

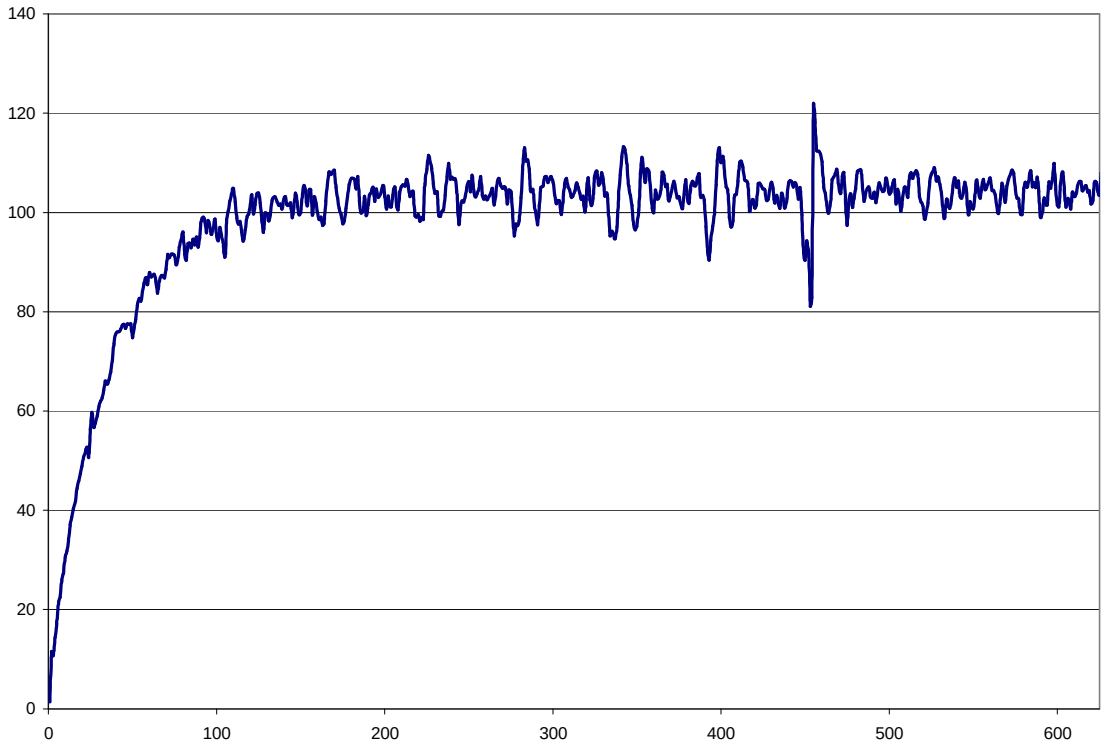


**Figure 4.32 braiding machine speed spikes from increasing yarn tension**

Figure 4.32 captures the increasing nature of variation in motor speed that the braiding machine motor experiences when encountering a locked package. Figure 4.32 is a plot of the braiding machine motor speed measured by the shaft mounted encoder and is the light blue plot from Figure 4.31. The y axis is the braiding machine speed given in revolutions per minute (RPM). The x-axis in Figure 4.32 corresponds to the data acquisition time interval during the experiment and is given in time increments of 0.047

seconds. The spikes correlate to the increase in the yarn tension required by the continuing braid formation; the motor also experiences an increase in the magnitude of the spikes until the largest spike in speed where the yarn finally breaks. Obviously, if the yarn package is locked only a fixed amount of material is available to contribute to the braid formation. Meanwhile, the properly functioning yarn packages are continuously releasing material as the capstan takes up the braid. The capstan is under closed loop control and the motion controller will attempt to maintain a constant speed by increasing the supply current and ultimately the available torque will increase until the desired speed is reached. Similar to the braiding machine speed spike observed in Figure 4.32 at the point where the yarn fails, the load required to maintain constant capstan speed also increases quite dramatically until the point of yarn failure, and the capstan quickly returns to the set speed.

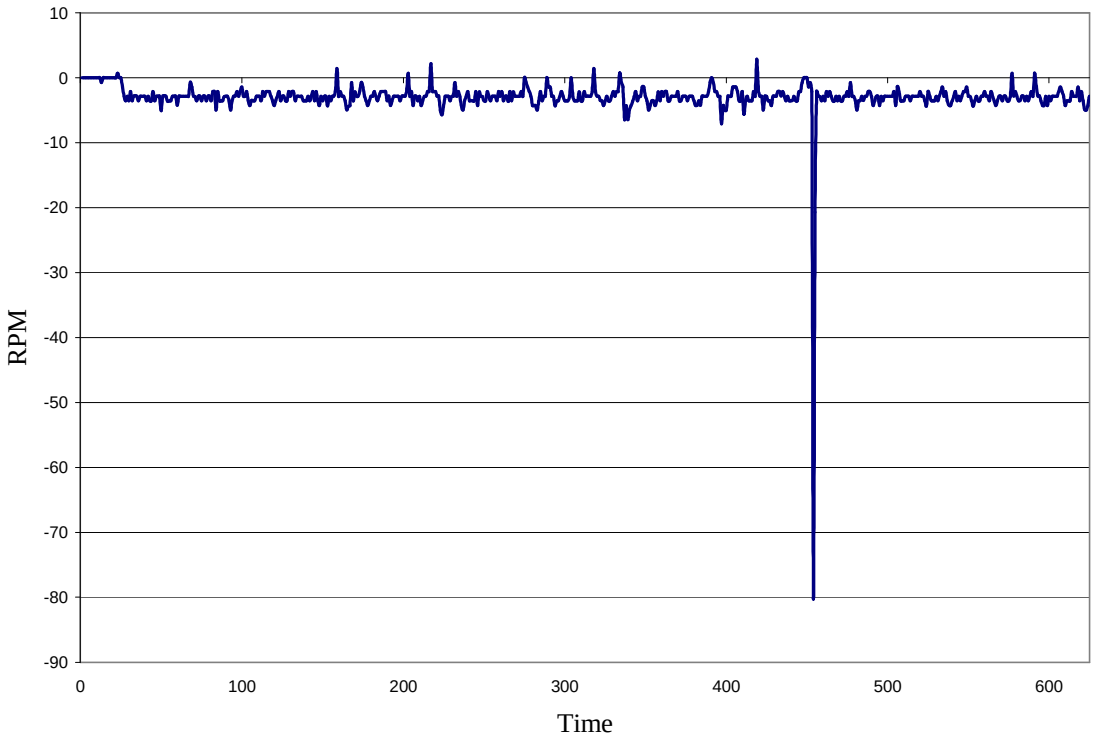

**Figure 4.33 Capstan speed spikes from increasing yarn tension.**

Figure 4.33 is a plot of the capstan motor speed in versus time when two yarns are high tension. The y axis in Figure 4.33 is RPM and the x axis is time (0.047 seconds between each data point). The large spike in speed is a result of the yarn breaking. Figures 4.32-33 show that yarn breaking affects the motor speed on both the braiding machine motor and the capstan motor. The capstan speed experiences the most dramatic speed change as expected by the compensatory nature of closed loop control.

### 4.16 Yarn breakage capture

Images from the experiment involving the two initially orthogonally locked packages on different tracks capture the yarn break as it occurs.

**Figure 4.34 Rear view before, during, and after yarn breakage**

Figure 4.34 shows the rear view of the high tension yarn one frame before, during, and after the breakage occurs. Figure 4.34 consists of three images acquired from the rear view camera during the experiment involving two orthogonally locked packages.

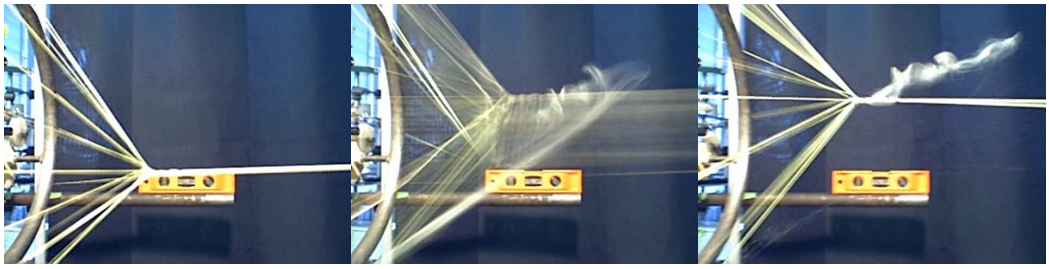

**Figure 4.35 Side view before, during, and after yarn breakage**

Figure 4.35 shows the side view of the high tension yarn one frame before, during, and after the breakage occurs. Figure 4.35 consists of three images acquired from side view camera during the experiment involving two orthogonally locked packages.

The result of the high tension break and the effect on the braid point is quite dramatic as witnessed visually in Figures 4.34-35 and in the motion data spikes from Figures 4.31-33.

**4.17 Conclusion**

The effects that mechanical faults have on braid point formation are discussed in this chapter. For the purposes of developing diagnostic measures to promote braid quality, it is important to characterize the effects of common faults and to understand the role they play in braid formation. Understanding the nature of problems encountered provides a useful foundation necessary for developing suitable control methods to mitigate the adverse effects of braiding faults. Chapter 4 first presented data that will be used in Chapter 5 as a visual approach to fault diagnostics. The braiding process is characterized by visual methodologies including both its static and dynamic components. The static test is useful to understand the force requirements of the braiding machine tension mechanisms and could be useful for prediction of disturbances in future research. The dynamic aspects of braiding or those particularly related to the initial and steady state motion are described in this chapter. The dynamic nature of braiding is categorized by three regimes. The first regime consists of an initially changing braid point position that occurs rapidly followed by an oscillation transient. The second regime is characterized as a slowly changing (migratory) and oscillating transient. The third regime is characterized as a steady state oscillating equilibrium, where the pull from each package is nearly the

same and the resulting braid is balanced. The transient motion is expected in all 3 directions of braid point motion depending on the initial position. The initial transient can be in the axial or radial direction. Radial offsets rapidly decay and axial offsets decay slowly. As the braid point transitions from initial to steady state, a slow migration may occur as the braid finds its equilibrium. The equilibrium steady state is oscillatory due to small variations in yarn tension. Finally, this chapter provides a mechanical methodology basis for fault diagnostics which is presented in Chapter 5. The effects of the various faults presented in this chapter are also seen in the mechanical performance of the braiding machine, namely from the variations observed in the motion data. As the tension in the yarn increases, so does the load imparted on the braiding machine.

# 5. FAULT DETECTION IN BRAIDING UTILIZING INEXPENSIVE USB MACHINE VISION

## 5.1 Introduction

This chapter seeks to solve the problem of detecting faults in braided structures which will improve the quality, minimize waste, and even improve operator safety. The problem of bobbin package performance is addressed from an empirical standpoint, by characterizing a properly behaving system and contrasting the performance of faulty packages. The experimental results from Chapter 4 specifically dealing with the yarn package faults are used to improve the braiding process. A diagnostic is presented that is useful for recognizing faults by comparing the radial variations of braid point formative motion to that of an optimal condition.

## 5.2 Results of tension on braided structures

The braids shown Figures 5.1 - 5.6 demonstrate the effects of packages yarn tension problems on the braid formation. The red yarn in Figure 5.1 has an irregular tension caused by increasing the effective spring constant of the release mechanism; its effects are seen by the periodic deformation occurring as the increased yarn tension dominates in the interlacing scheme.

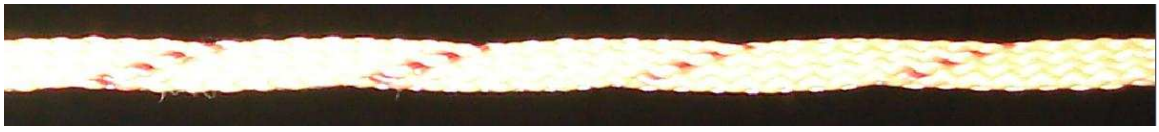

**Figure 5.1 Braid with a high tension yarn resulting from a stiff spring**

In Figure 5.1 the red yarn package has a stiff spring in the release mechanism. The effects of a higher tension yarn can be seen to distort and twist the braid.

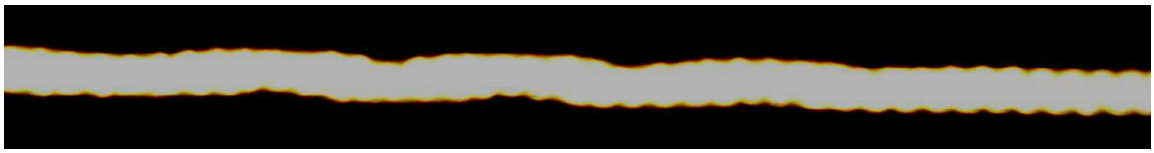

**Figure 5.2 Braid with a high tension resulting from a locked package**

In Figure 5.2 the yarn bobbins are locked such that no new material can be released and the resulting yarn increases in tension, distorting the braid as the braiding continues (left).

**Figure 5.3 Fault resulting from a locked package**

Figure 5.3 shows a serious defect in the braid resulting from high tension yarn.

**Figure 5.4 Braid with two high tension yarns resulting from 2 locked packages**

Figure 5.4 has two diametrically opposed high tension yarns that distort and twist the braid.

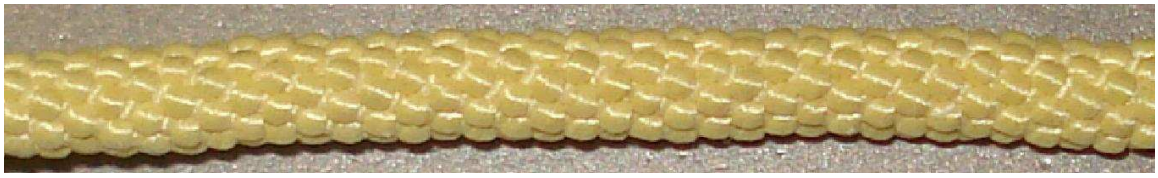

**Figure 5.5 Braid resulting from yarns beyond the jammed state**

Figure 5.5 occurs when the take-up speed is sufficiently slow that the braid point is close to the braiding machine and in this case forms a 90 degree angle with the former ring.

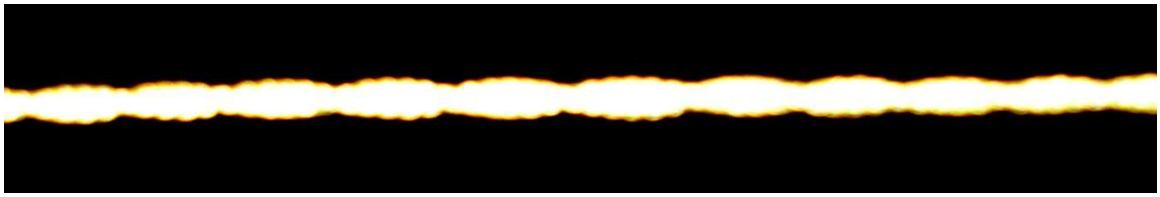

**Figure 5.6 Upstream twisting observed after braid is formed beyond jammed state**

A twisting as seen in Figure 5.6 occurs downstream of the braid point as a result of the formation seen in Figure 5.5.

### 5.3 Characteristics of a balanced braid point formation

16 packages were cleaned and wound with 30 winder traverses (of material) on the Wardwell TW-2004 Textile Winder. These efforts were in order to establish optimum braiding conditions. Clean packages, equally wound, well lubricated tend to promote even braids. Well cleaned and lubricated braiding machines, with equal package settings, are the requirements that must be met and maintained to achieve the best quality braid. Optimizing the machine mechanically provides the baseline from which other tests will be compared. Knowing braid behavior in the best case scenario is important for understanding misbehavior. The PID gains of the capstan have been tuned to achieve a constant rpm. The following error was limited to 30 encoder counts. When the constituent yarns in a braid are well balanced the braid will appear consistent as seen in Figure 5.7.

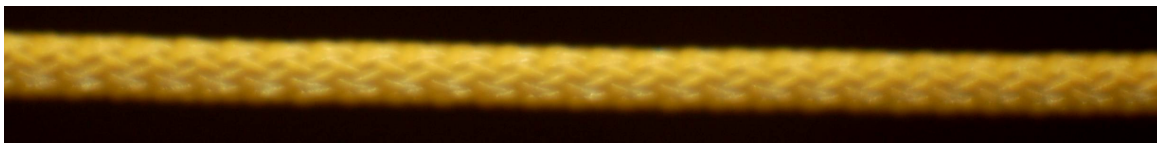

**Figure 5.7 Braid with balanced yarn tension**

The factors that influence the braiding machine mechanical performance are adjusted in order to establish what is considered optimum performance. The

manufacturer specifications regarding service are followed to promote proper operation and consistent performance. The braiding machine track plate is cleaned and lubricated. The bobbins are wound with the same amount of yarn (1420 denier Kevlar®). The bobbin packages are cleaned, lubricated, and the release springs are replaced with new Blue 10 ounce springs (Table 2.5). The take-up machine servo motors are tuned to achieve a constant capstan and spool take-up speed. The intent is to achieve the ideal operating conditions conducive to producing a consistent braided product and establish a basis for further comparison and the results are shown in Figure 5.8.

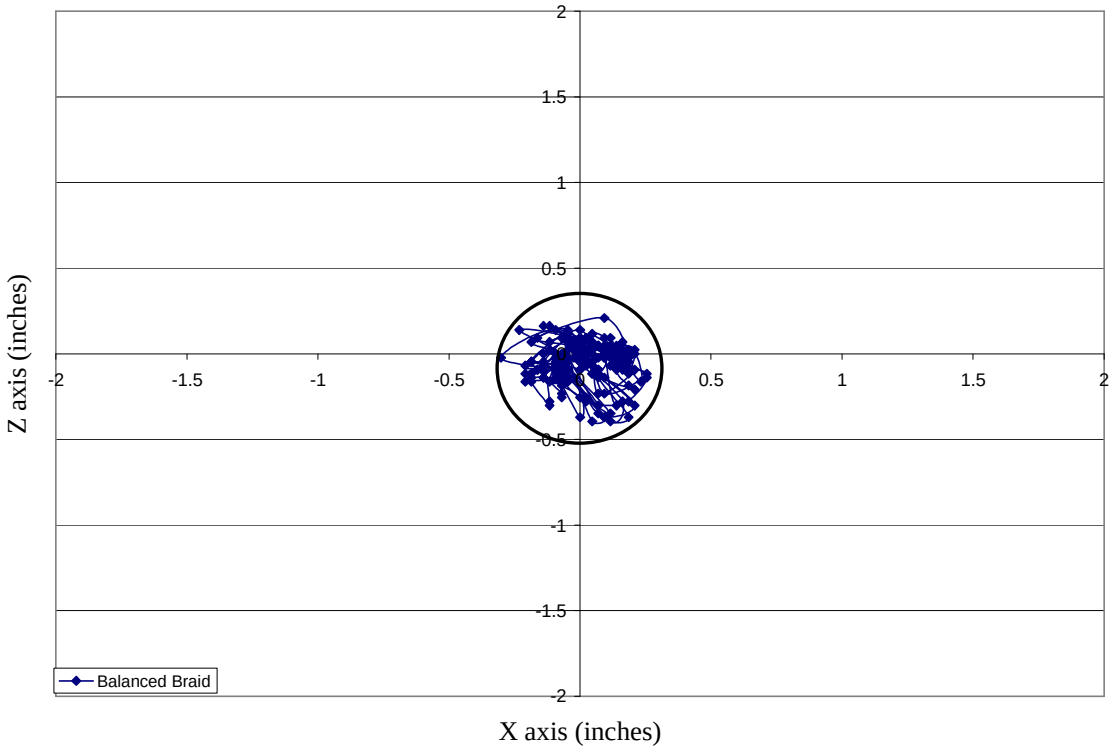


**Figure 5.8 Balanced Braid Point Motion (3.86 revolutions)**

Figure 5.8 shows the circular nature of the braid point formation motion resulting when all yarns being balanced. Each yarn has a symmetric counterpart that approximately balances the tension at the braid point. The radius of the braid point

formation when all yarns have equal contribution is the minimum among all the experiments presented in Chapter 4.

### 5.4 Comparing the effects of Faulty Package(s)

Figure 5.9 compares the braid point motion of a braid with balanced tension and that from a braid with imbalanced tension. The characteristic of a well balanced braid is reduced radial motion that appears circular in shape, as each yarn contributes equally to the formation. However, this is not the case when a yarn package is malfunctioning or sticking. As the constituent yarns begin to un-spool, material is released to form the braid, but the amount of material from the faulty package remains constant. As the capstan continues to pull at a constant rate, the tension in the yarn increases and has a dominating effect on the braid point formation. The high tension yarn in effect causes the braid to follow a path similar to the sinusoidal path of the track plate, much like a skier follows a boat.

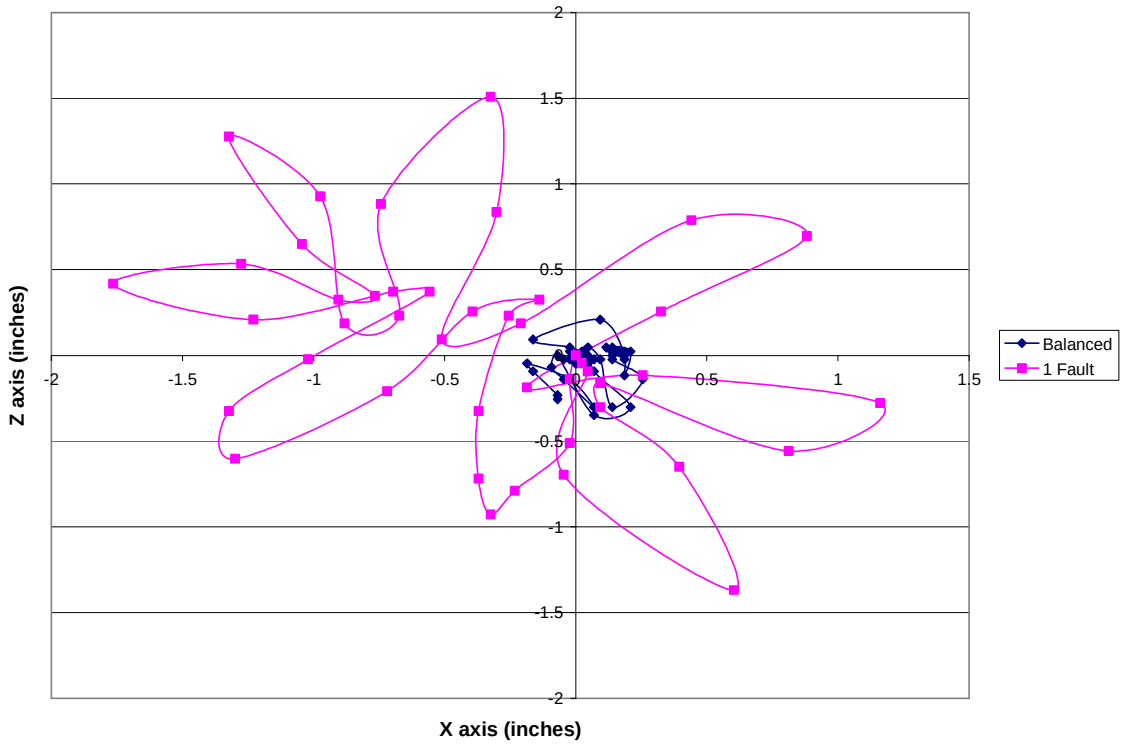


**Figure 5.9 Comparison of balanced braid and braid with 1 faulty package for 1 braiding machine revolution**

Figure 5.9 is a plot of the motion at the point of braid point formation (as acquired by the rear view camera). This figure demonstrates the nature of tension induced faults in obvious ways by comparing the apparent path and magnitude of braid point displacements for a balanced and high tension braid.

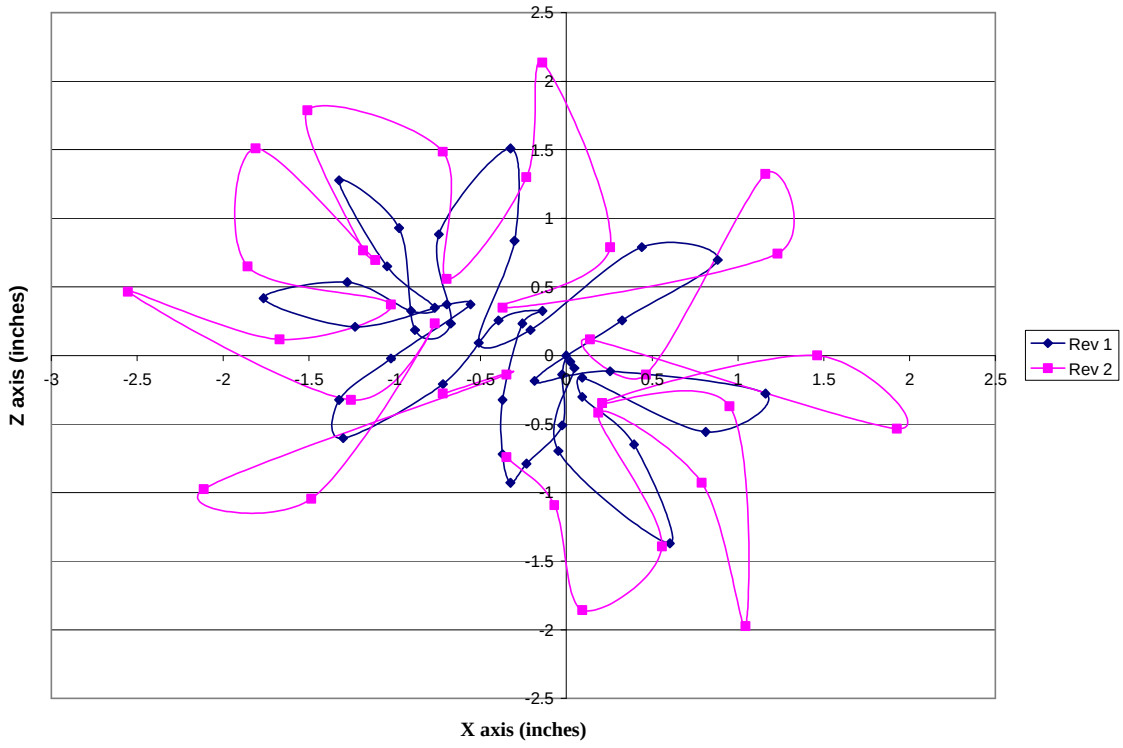


**Figure 5.10 Increasing radius of braid point movement as tension in yarn increases**

In Figure 5.10 as the braiding machine continues to produce material and the capstan takes it up, the tension in the yarn with the faulty release mechanism increases. The radius of motion increases as well as a shift of the peak occurrence position in the braid point motion. As the tension increases in the yarn with the faulty mechanism, a twisting is observed in the braid. Figures 5.1, 2, 4, and 6 provide examples of the twisting in the braid. As the twisting in the braid continues, the braided material experiences some "wind up" and the result on braid point formation is seen as the peaks shift position in Figure 5.11.

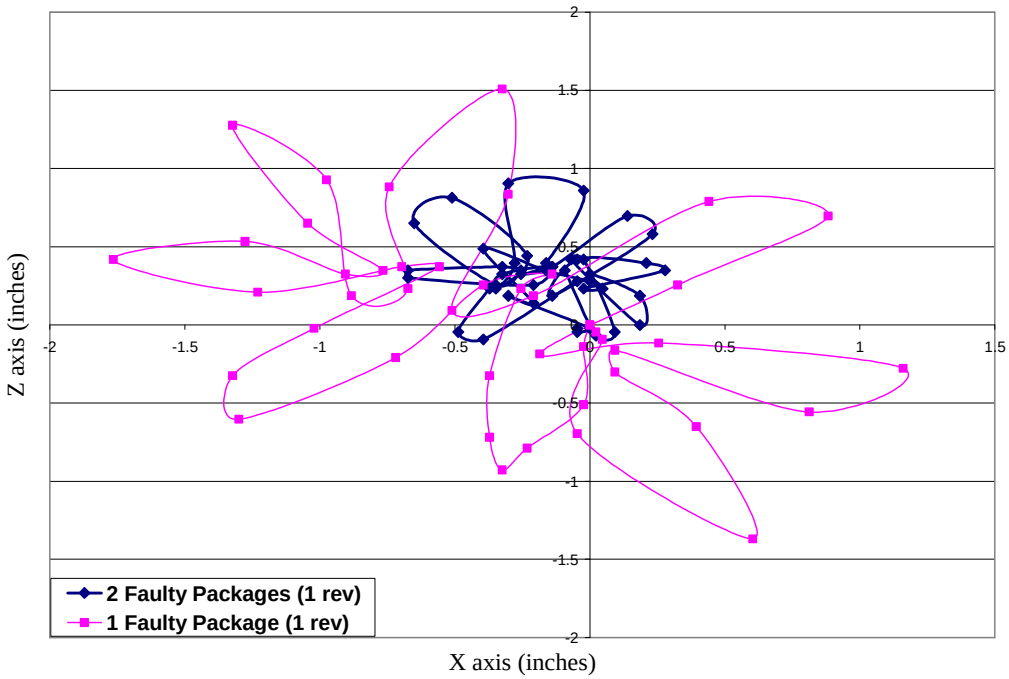


**Figure 5.11 Comparison of braid point motion between 1 and 2 locked packages**

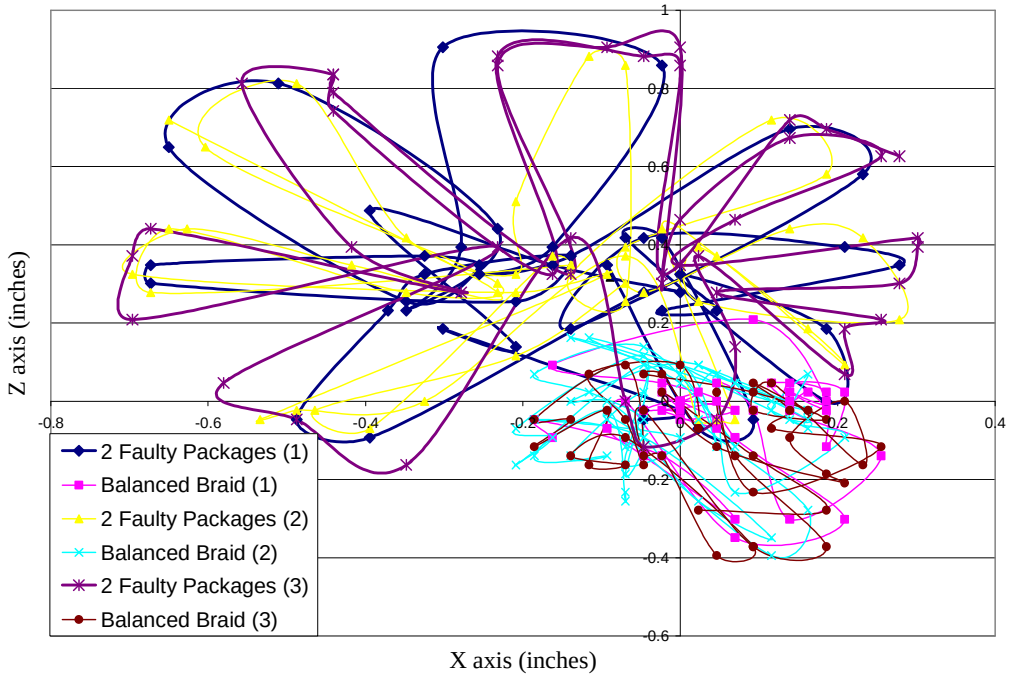


**Figure 5.12 Comparison of balanced braid and braid with 2 faulty yarn packages**

Figure 5.12 shows the increased radial variation and the track plate path shape attributed previously to tension imbalance on braid point formation. The tension

imbalance also shifts the braid point from the optimal balanced point. As soon as the high tension yarns descend into the track plate valley, the yarns lose tension and become slack. When the two yarns are slack, the braid point moves in such a way that is similar in shape to the track plate paths.

### 5.5 Investigation of Aberrant Tension: Diametrically opposed locked packages

The experiment (from section 4.11) involved locking two diametrically opposed yarn packages to study further the effects of faulty package behavior. The braid point data from the experiments in section 4.11 are reconsidered in light of the discoveries made thus far in the thesis.

The yarn packages locked in this experiment are seen in Figure 5.13. As discussed in Chapter 4, the faulty packages do not release any new material to contribute to the braid formation; and when the package position is furthest from the fell point, that is a peak on the track plate, the tension in the yarn reaches its highest point. Conversely, when the yarn package reaches a valley, i.e. a valley on track plate, the tension disappears and the yarns go slack. The transition from taut to slack in the yarns, occurs over a fraction of a second and its effects on the braid point are quite dramatic as the yarns transition to the high tension condition.

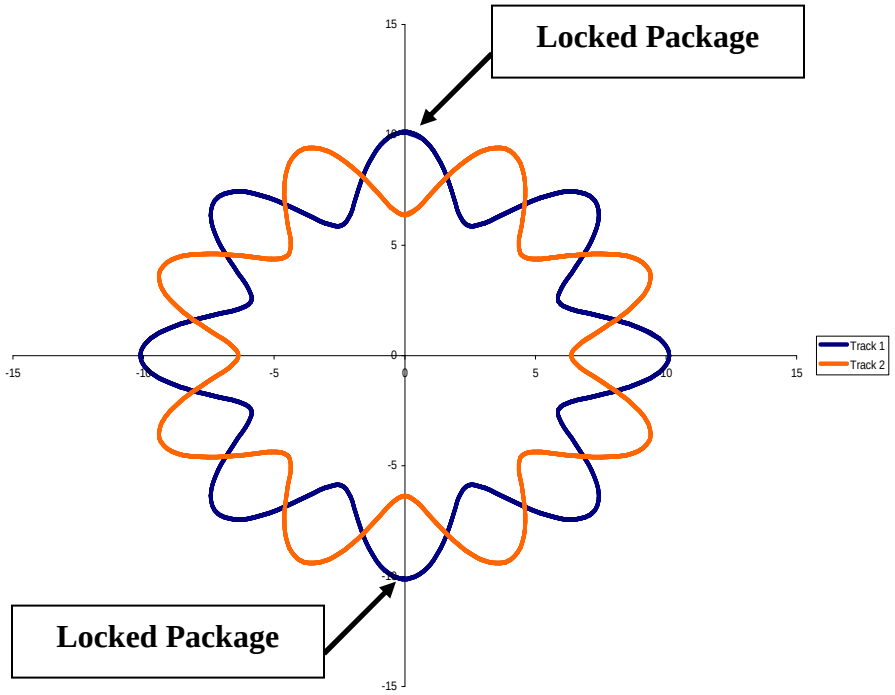


**Figure 5.13 Initial Position of diametrically opposed locked Packages**

Figure 5.13 shows the initial position of the packages when their release mechanism is locked.

A final observation (Figure 5.14) of the images reveals that the yarns undergo a dramatic change in tension while the locked packages move about the track path.

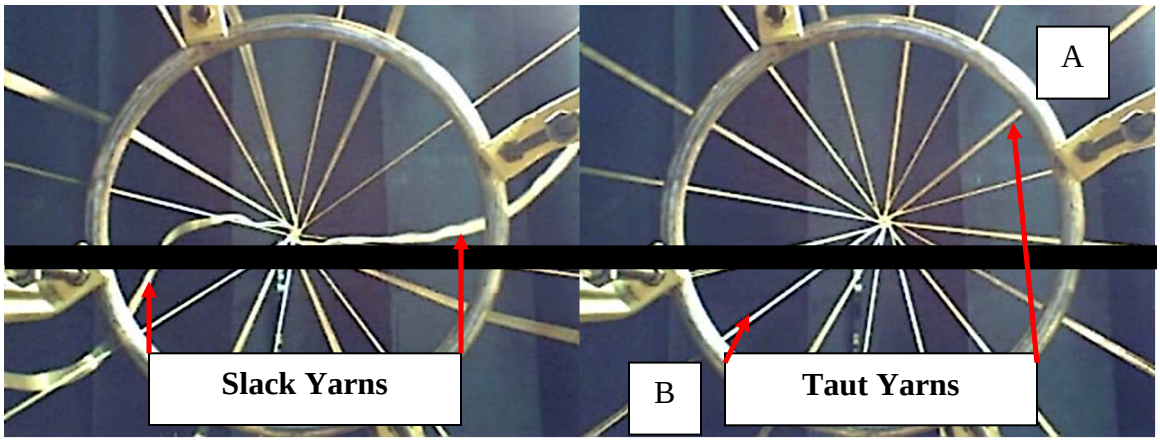


**Figure 5.14 Effects of slack and taut yarns on braid point position**

Figure 5.14 includes two images taken from the rear view camera that capture the yarns from faulty packages when they are slack and taut. Note: The yarn in position A becomes taut before yarn B and thus the braid point position is pulled in that direction. The black horizontal line is useful for observing the relative braid point motion when the yarns are slack and taut.

In light of this observation, the position data is categorized according to the condition of the yarns in the images as either slack or taut. The resulting taut and slack regions are plotted separately to show the effects of yarn tension on position.

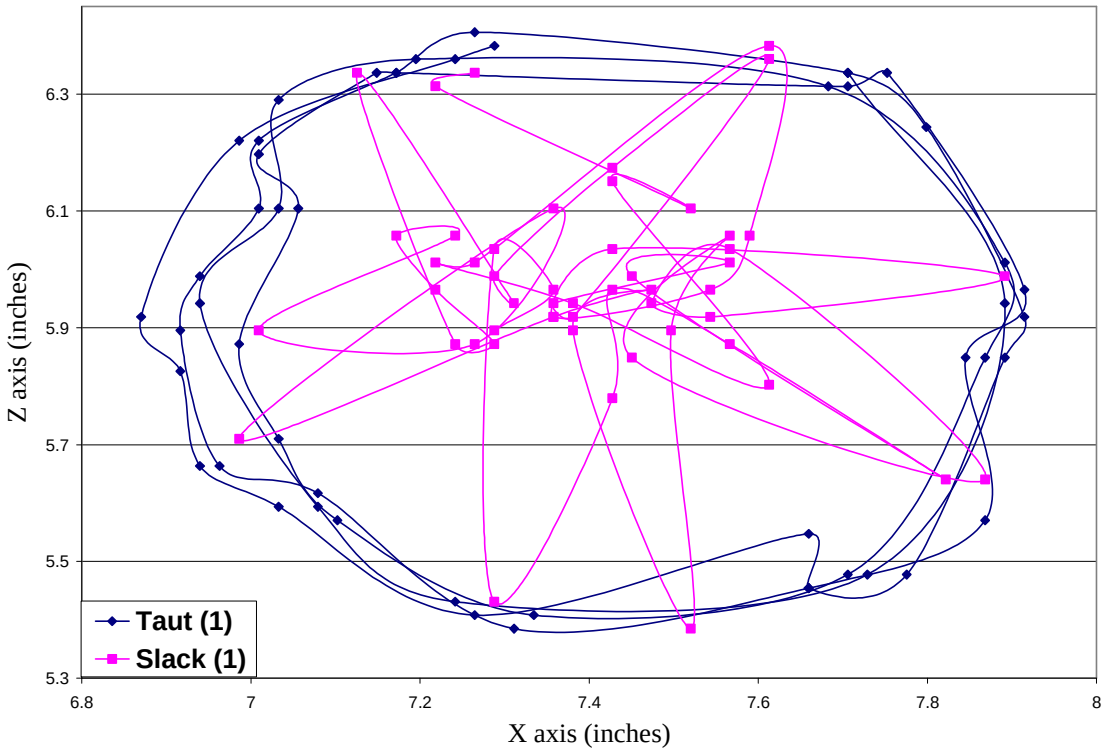


**Figure 5.15 Initial Interpretation of braid point formation for Taut and Slack conditions**

Figure 5.15 is a plot of the braid point position when the yarns are slack and taut. The outer circle is formed when two diametrically opposed yarns are in tension and the

braid point is dominated by the yarn that has the highest tension. As demonstrated previously, a high tension yarn dominates the braid point motion and so it appears that of the two high tension yarns, the one with the highest tension pulls the braid point radially outward where its position is determined when the two yarn tensions reach equilibrium. The path of the braid formation when the yarns of interest are slack is suspiciously similar to track plate path which leads to the further investigation of the following section.

### 5.6 Transition from slack to taut conditions: Final Analysis

Upon further observation of the images it is discovered that the relative braid point motion existing when both the slack and taut conditions occur is quite stable and thus Figure 5.15 is not consistent with what has been demonstrated thus far regarding tension imbalance. Tension imbalance has been shown to cause braid point motion to take a shape similar to the track plate path; however, the motion observed in Figure 5.15 by the braid point when the yarns of interest are slack is characteristic of dominant tension. Because the yarns of interest are slack and the remaining yarns are balanced the resulting braid point should be balanced.

By applying what has been learned thus far, particularly regarding the distinct nature of balanced braid formation and that of aberrant tension, a final analysis is made. When the two yarns with locked packages, although their tension mechanisms are defective, become slack, they have no effect on the braid point formation. The resulting braid becomes effectively, a braid influenced by only the 14 remaining yarns which are balanced. This balanced behavior is seen in Figure 5.16 and is comparable to the balanced braid.

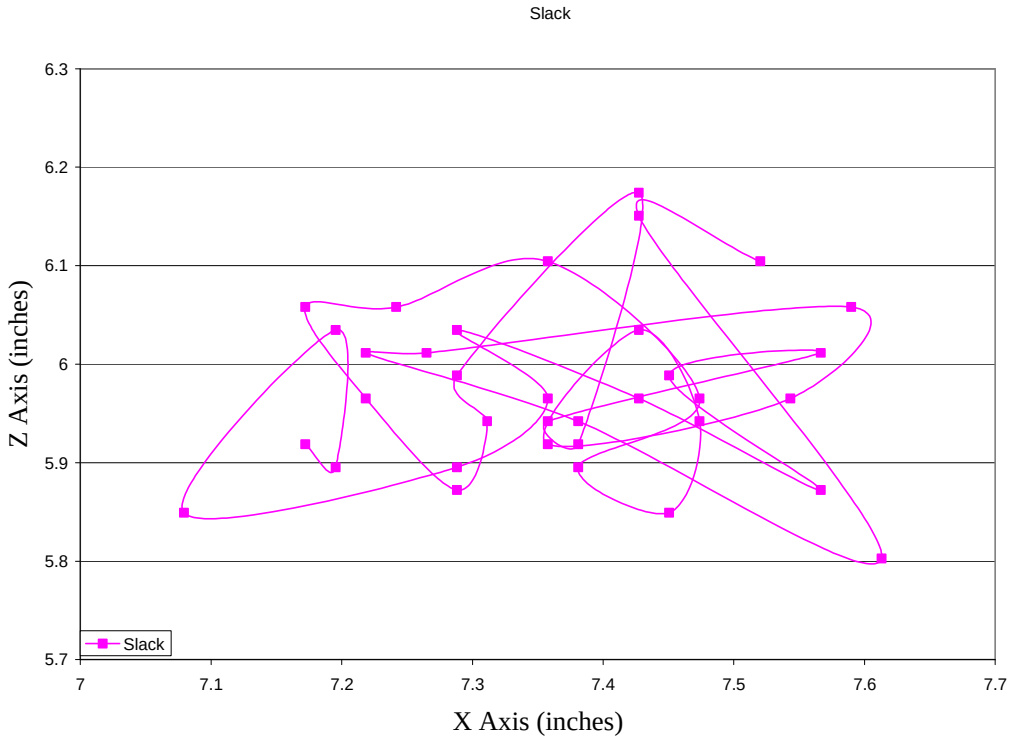


**Figure 5.16 Braid point motion of 14 balanced yarns**

Figure 5.16 is a plot of the braid formation point when 2 of the 16 yarns are slack. Observation of the braid point motion (via acquired images), when the two diametrically opposed yarns are in tension, undergoes little motion, as if the two high tension yarns are in a tug of war match and the winner determines the position of the braid point which causes a circle seen in Figure 5.17.

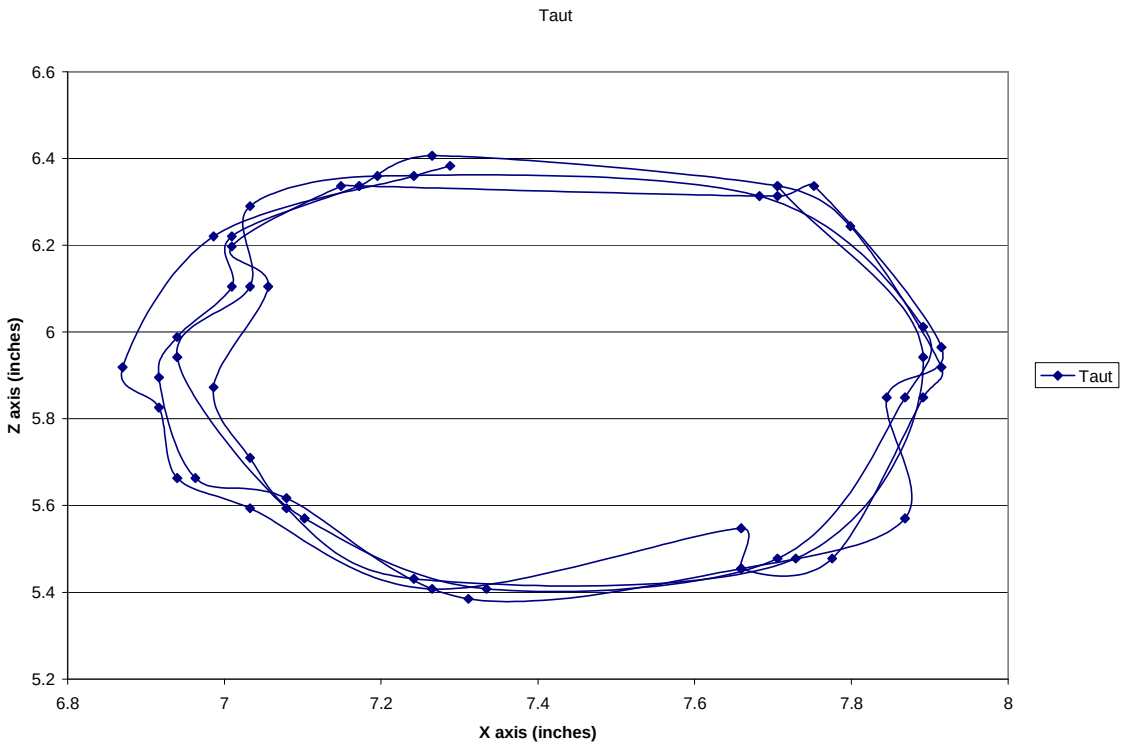


**Figure 5.17 Braid point motion while 2 yarns are in high tension**

Now by plotting the data corresponding to the slack and taut conditions, Figure 5.18 is realized.

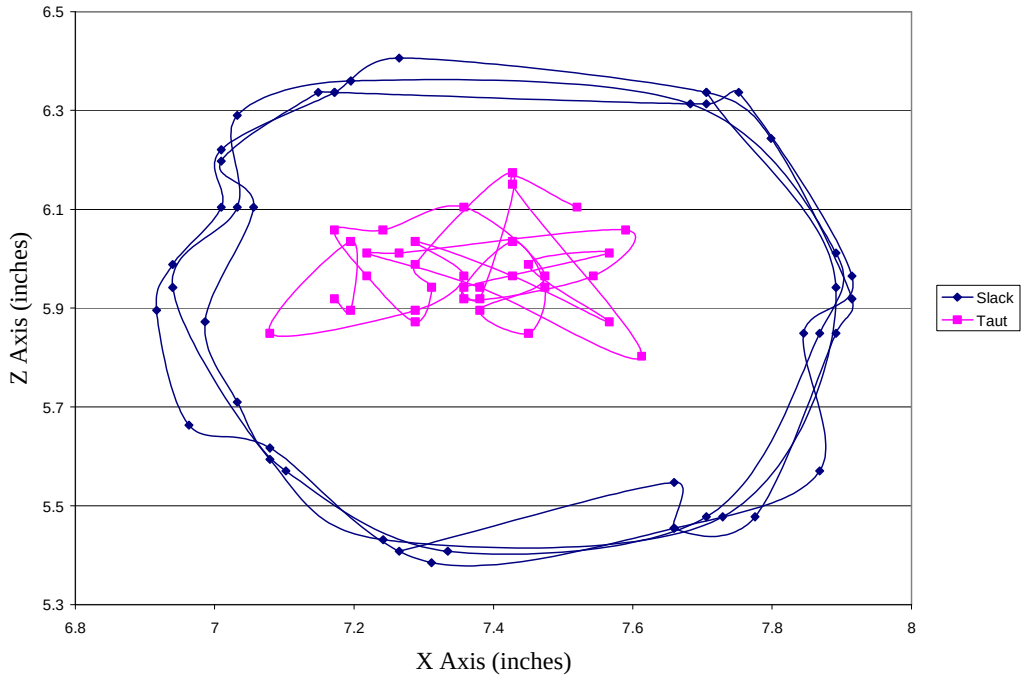


**Figure 5.18 Braid Point distinct regions corresponding to high and low yarn tension**

Figure 5.18 distinguishes the braid point formation regions when two yarns are either slack or taut.

The resulting images are further scrutinized in order to discriminate when the transition occurs and the braid point motion is unstable. From Figures 5.16 and 17, the remaining data points must be characteristic of the tension transition exerted on the yarns. These data are plotted in Figure 5.19 as transition.

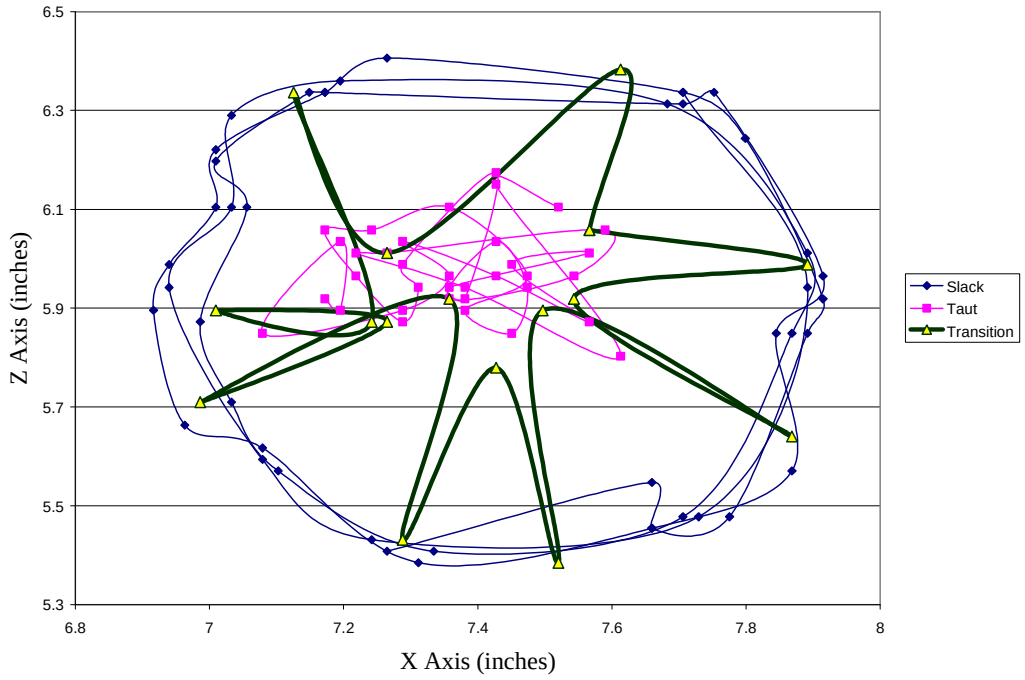


**Figure 5.19 Transition from taut (high) to slack (low) yarn tensions**

Figure 5.19 distinguishes between when the faulty yarns are slack, taut, and transitioning between those two conditions. Figure 5.19 is a more realistic account of the movement of the braid point as the yarns of interest transition from low to high tension.

From the previous experiments and the conclusions drawn about braid point formation behavior thus far, it is believed that when the yarns of interest are slack resulting from faulty packages, the remaining yarns are balanced and so the formation should be similar to that of a balanced braid formation, i.e. circular in nature.

The radial variation for the slack and taut conditions of the 2 locked package yarns is shown in 5.20.

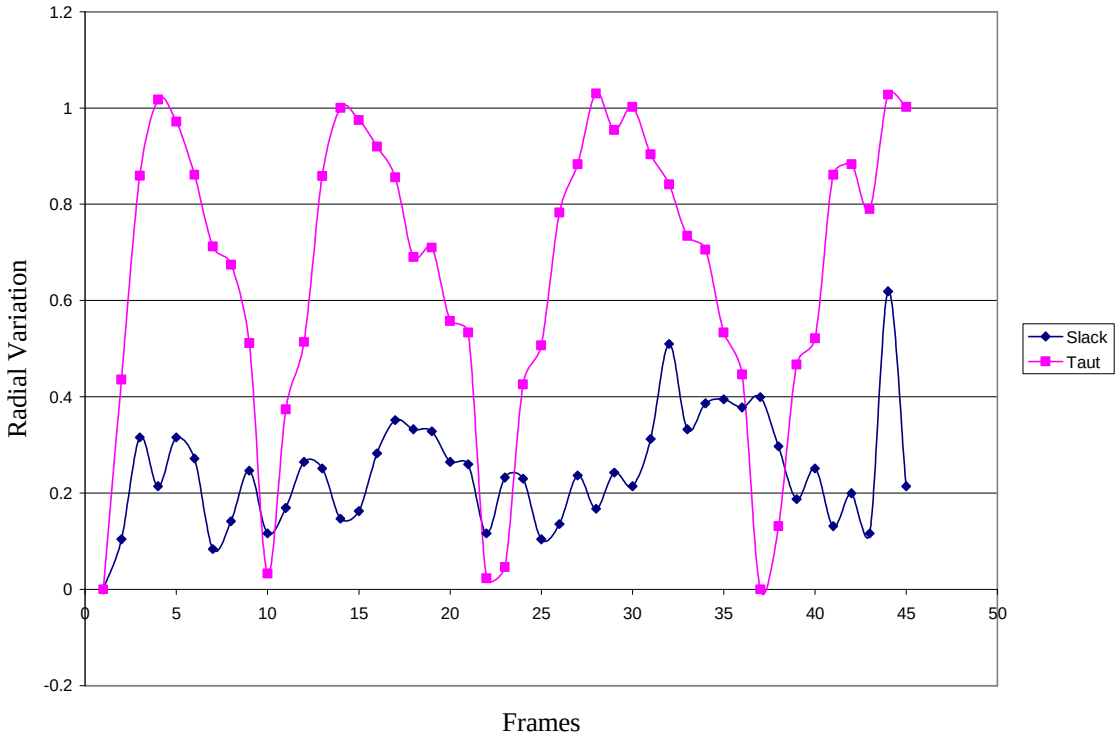


**Figure 5.20 Radial Variation of braid point when diametrically opposed yarns are taut and slack**

The average radial variation is compared to the balanced braid in Table 5.1.

| 1 Revolution | | | | |
|---|---|---|---|---|
| **Tension Condition** | **Average Radius (pixels)** | **Average Radius (inches)** | **Max. Radius** | **Percent Error** |
| Balanced | 6.84 | 0.16 | 0.42 | |
| Diametrically locked packages (Slack) | 11.83 | 0.27 | 0.78 | 73.07 |
| Diametrically locked packages (Taut) | 28.80 | 0.67 | 1.03 | 321.23 |

Table 5.1 Comparison of slack and taut conditions to balanced braid

### 5.7 Effects of increasing yarn tension on braiding machine motor speed

Several factors can affect the tension in the individual yarns including a malfunctioning package release mechanism. The braiding machine and capstan work in tandem at relatively constant speeds. Figure 5.21 exemplifies the increase in braiding machine speed variation as the motor load increases with yarn tension.

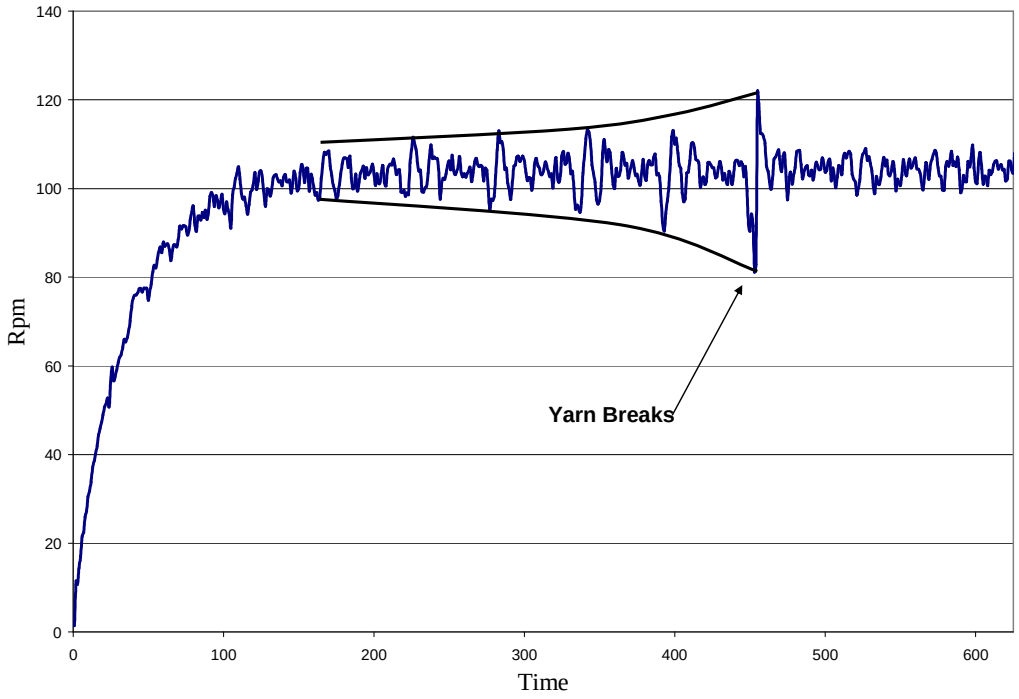


**Figure 5.21 braiding machine motor speed as yarn breaks**

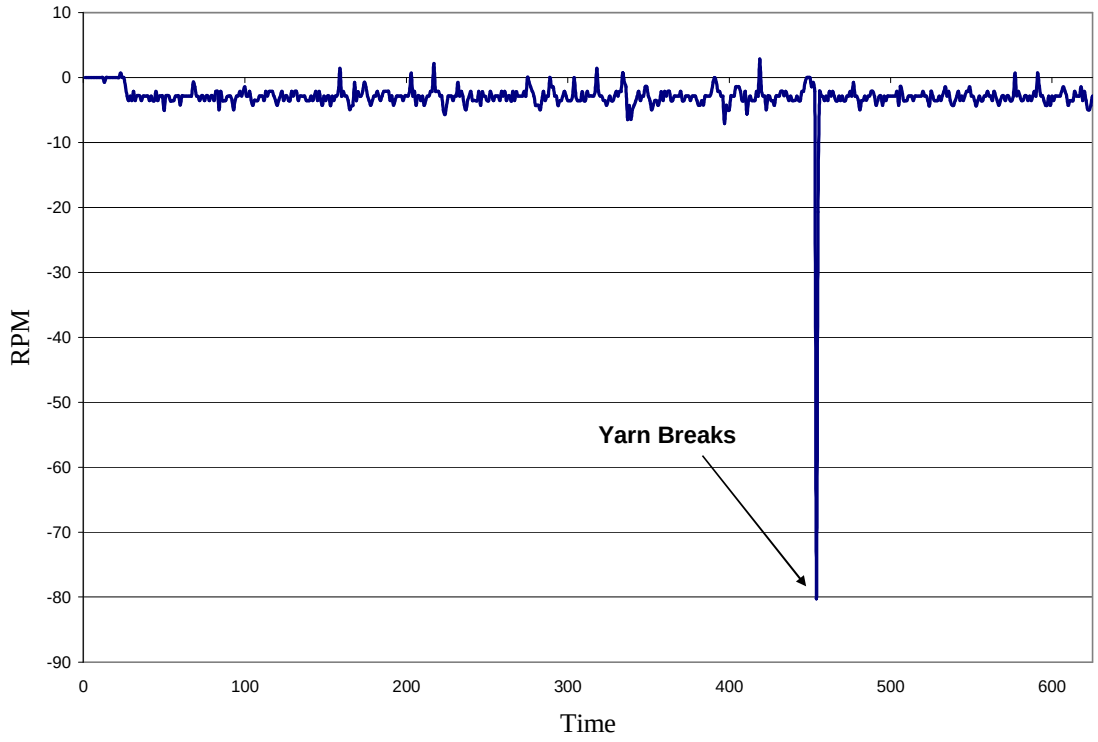


**Figure 5.22 capstan motor speed as yarn breaks**

As a servo controlled axis, the capstan will quickly accelerate in order to minimize following error. Subsequently, the yarn tension increases due to its inability to supply the braid formation with new material as it is being subjected to an increasing force of a closed loop servo axis trying to maintain a constant speed. Ultimately, the capstan take-up torque increases as the motion controller commands more motor torque in order to compensate for the increased load until the parameters are satisfied. The phenomenon of increased motor load due to yarn tension is observed as a large spike in the motor speed at which point the yarn finally breaks (Figure 5.22).

### 5.8 Visual Diagnostic Measure

If the calculated radius of braid point motion deviates by a certain amount then a tension problem may exist. The following table lists some faults and their corresponding

radius. These values can easily be incorporated into the control program and automatically shut down the machine when specified criteria is not met.

| Tension Condition | Average Radius (pixels) | Average Radius (inches) | Percent Error |
|---|---|---|---|
| Balanced | 6.84 | 0.16 | |
| 1 pink spring plus small blue section | 10.36 | 0.24 | 51.49 |
| 1.5 pink spring | 11.26 | 0.26 | 64.62 |
| max spring force | 13.16 | 0.31 | 92.53 |
| Locked package | 53.49 | 1.24 | 682.23 |
| 2 initially orthogonal locked packages | 44.95 | 1.04 | 557.36 |

Table 5.2 Fault Indication Diagnostic

### 5.9 Conclusion

Mechanical faults in the braiding process can be costly as it affects product quality. If it is possible to recognize the characteristics of a faulty package, corrections and other preventative measures can be implemented to minimize further waste and even save the product. Due to the symmetric nature of circular braids, it is important for the tension of one package with respect to its complement yarn be equal to minimize oscillating movements of the braid point. The optimal performance of a braiding machine is achieved and the subsequent braid point formation kinematics is observed. By understanding optimal braid-formation, the effects of faulty package function is introduced and discussed. Applying what has been presented thus far, particularly regarding the distinct nature of balanced braid formation and that of aberrant tension, it is possible to recognize when a locked yarn transitions from high to low tension. The take-up machine system presented in this thesis is an excellent platform for not only recognizing faults but making adjustments to counter the effects of faulty packages.

# 6. CONCLUSION

## 6.1 Introduction

A computer controlled take-up machine has been designed and manufactured to produce high quality braid. Utilizing PC technology to facilitate servo motion control as well as implement machine vision is discussed. Take-up machines used with braid over composites are typically not mechanically geared to the braiding machine, allowing the designer to choose a traverse speed. The take-up machine presented in this thesis research is independent from the braiding machine and subsequently will also work well with composite manufacturing. It can be electronically geared to the braiding machine and can also simulate the behavior of a traditional mechanically geared take-up system.

As high performance materials push the limits of conventional manufacturing technology, automation techniques become increasingly necessary. Proper tuning of the servo axes can provide the response necessary to accommodate a variety of loads due to differences in yarn properties and the spring sizes necessary for achieving a desired yarn tension. A servo axis is ideal for smoothing the braid point motion by reacting to the inherent speed variation seen by braiding machine motors. Using a non invasive machine vision based system can allow for quality assurance measurements to be made from remote location and without stopping the manufacturing process. Improving quality, minimizing, waste and detection of tension induced faults is critical for producing high quality braids suitable for space use.

### 6.2 Inexpensive PC based components

The advent of PC based hardware and software solutions is changing the paradigm of industrial automation. The components used for this take-up machine are relatively inexpensive by industrial standards and are customizable. Machine vision is realized using inexpensive USB camera and image acquisition technology. Data acquisition is accomplished using PC hardware architecture that benefits from mass production.

### 6.3 Improved manufacturing performance

Automation of the take-up process is extremely important to achieve high performance manufacturing techniques required of complicated geometric braided structures. An advantage of this system is that it uses sophisticated technology and is therefore more flexible and precise. Servo actuation is by definition a closed loop axis. Advantages of closed loop include precision control of position, and other position derived parameters such as velocity and acceleration. Closed loop control provides continuous checks and balance to the braiding process which can vary in time especially with applications such as space tethers which may require significant time to produce. Understanding the dynamic nature of braid point motion is important in order to overcome inherent latency of the braiding machine and predict required take-up motion. In effect, more complicated geometries can be manufactured with precision by using closed loop servo control. Machine vision provides the ability to integrate an image acquisition system into a control feedback loop. By incorporating the ability to utilize visual servo based control of the braid formation process, quality can be improved by maintaining braid point position and geometry.

### 6.4 Minimize waste

The ability to react quickly can mitigate the effects of mechanically induced faults and reduce braiding defects, thus reducing waste. The vision system can be used to recognize defective conditions and alert the operator or simply shut the braiding machine down. The ability to stabilize the braid point quickly will save the amount waste associated with the initial startup. Knowledge of proper and faulty braid formulation is used to diagnose common tension faults. Once a fault is determined adjustments can be made to minimize waste.

### 6.5 Ability to produce desired braid angle

Knowing the relationship between the braid angle and the capstan speed for a given braiding machine speed and the ability to produce custom braids is a must for manufacturing product according to design specifications. Using the vision system, the braid geometry can be maintained continuously by monitoring the angle and position data in real time and controlling the capstan to maintain desired braid geometry.

### 6.6 Fault Detection and Performance Monitoring

Knowledge of the optimal braid performance serves as the baseline for comparing the behavior of faults. By studying the effects of common faults a diagnostic tool is developed to recognize the onset of defects and provide some insight as to what might be causing the fault. The ability to monitor the braiding machine performance and compare operating conditions to previously established normal operating parameters is a simple method for detecting faults. Radial variation of braid point position is a good indicator of mechanical faults of the tensioning mechanisms. Observations based on mechanical and visual methods are presented as diagnostic tools. From visual observations: As the

tension in one yarn increases, with each revolution the radial variation increases until the point where one yarn breaks. From mechanical observation: The variation in motor speed increases until the point where the yarn breaks. Comparing these measures against optimal behavior can be used to shut down the machine before irreversible damage occurs.

### 6.7 Ability to electronically control tension (precise method)

Using servo technology allows for the motor torque to be changed quickly meeting any tension needs. The tension in the braid can be precisely maintained by electrically controlling the servo motor current, eliminating the need for traditional and rudimentary electro-mechanical dancer, tension based systems.

### 6.8 Speed Variability

Much like the tension control, the speed of take-up and traverse can be changed to accommodate many design requirements. Employing the braiding machine encoder and a servo axis in tandem, provides the electronic coordination necessary for an electronic gearing system that can be used to maintain any gear ratio between braiding machine and take-up. Traditional take-up systems do not typically have electronic speed variability.

### 6.9 Ideal platform for research

The computer controlled system presented in this thesis is ideal for research in braiding, servo motion, and machine vision. The system has data acquisition and image acquisition capabilities that allow for many aspects of automation to be explored. The take-up machine is capable of monitoring motor encoder data, servo motor current, and providing digital and analog outputs for controlling peripheral devices.

### 6.10 Experimental Realizations

Braiding is an inherently slow process. The yarn tension release mechanisms employed with the experimental braiding machine exhibits bi-directional tension behavior. Depending on the initial position of the braid point with respect to the equilibrium point transients, slow migrations are observed. Braid angle is a function of take-up and braiding machine speed. A migration toward the equilibrium point may take a significant amount of time. Steady state behavior of braiding is sinusoidal. Balanced braids undergo a circular motion at the braid point as all yarns have equal contribution. High tension yarns, resulting from mechanical faults, adversely affect the braid point formation causing the braid point motion to appear similar the track plate construction. Braid formation radius is a good indicator of tension induced faults. Even slight variations in tension have a detectable difference from the optimal.

## REFERENCES


1. Irene Emery, Primary Structures of Fabrics, (1966) 66-69
2. Mayer Braidtech, GmbH, http://www.mayerbraid.de/lexicon/194_201.htm
3. Pastore, C., "Opportunities and Challenges for Textile Reinforced Composites", Mechanics of Composite Materials, Vol. 36, No.2, 2000
4. Tethers Unlimited, Inc., http://www.tethers.com/TethersGeneral.html
5. Kawamoto et al, "Precise numerical simulations of electrodynamic tethers for an active debris removal system", Acta Astronautica 59 (2006) 139 – 148
6. Composites Fabrication Magazine, Bill Benjamin, Chris Red, 2004
7. Journal of Composite Materials 2007, Manufacturing of Braided Thermoplastic Composites with Carbon/Nylon Commingled Fibers, Louis Laberge-Lebel, Suong Van Hoa
8. Journal of Industrial Textiles, Braider Inflatable Tubular Structure Technology in Crash Safety, Greg Mowry and Andrew Head, 2001
9. Brunnschweiler, D., "Braids and Braiding", J. Textile Inst. 44, 666-686 (1953).
10. Brunschweiller, D.,"The Structure and Tensile Properties of Braids", J. Textile Inst. 45, T55-T77 p. 681-685 (1953)
11. G.W. Du, P. Popper, "Analysis of a Circular Braiding Process for Complex
12. Shapes", J. Textile Inst., 1994, 85, No.3, 316-337

13. C. Pastore and F. Ko, “CIM of Braided Preforms for Composites”, Computer Aided Design in Composite Material Technology, Proceedings of the International Conference, Southampton, 1988, pp 135-155
14. Ko, F.K., Pastore, C.M., and Head, A., Atkins and Pearce Handbook of Industrial of Industrial Braiding, Atkins and Pearce 1989
15. B10-64B Horizontal Composite Braiding System, Instruction and Maintenance Manual
16. Henry Cobb, P.E., Personal Communication, Department of Electrical Engineering, Auburn University (2007)
17. http://www.jamarco.com/09a_Rope/rope_glossary.htm
18. http://www.quabbin.com/tech_briefs/reelorspool.html
19. National Instruments 7340 User Manual
20. Cincinnati Arrow 750 User Manual
21. Mastercam X User Manual
22. Yaskawa Sigma II User Manual
23. BMC 12H Hardware Installation Manual
24. Sabit Adanur, Wellington Sears Handbook of Industrial Textiles, (1995)
25. Textile Research Journal, Experimental and Theoretical Characterization of the Geometry of Two-Dimensional Braided Fabrics, Lomov et al, 2002
26. Textile Structural Composites, Volume 3 Composite Material Series, R.B. Pipes
27. Journal of Advanced Materials, Design and Process Integration for Low Cost Manufacturing, Lee McKague, Slade Garner, James Campbell, 2002

28. Polymer Composites Vol 17 No 3 June 1996, Braided Thermoplastic Composites From Power-Coated Towpregs. Part II: Braiding Characteristics of Towpregs, A. Ramysamy, Youjiang Wang, and John Muzzy

## APPENDIX: TEST DATA

One initial experiment involves increasing the release mechanism tension required to un-spool material by adding springs until the maximum attainable spring force is found such that the package still function properly. The data from figure A.1 is obtained in a test of a braid made consisting of 16 yarns of various yarns and denier, as this was the configuration of the braiding machine found in the initial stages of the research.

This experiment provided insight into the bi-directional behavior of the tension release package mechanism. Similarly, the spring constant determination test is applied to one yarn and the results demonstrate the same behavior of differing forces whether pulling or resisting.

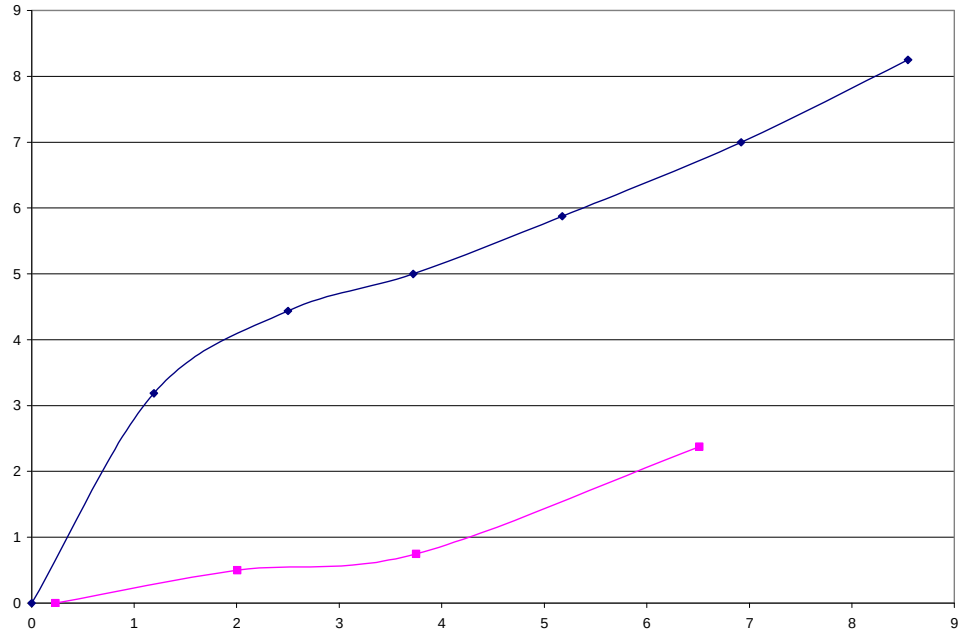


**Figure A.1 Effective spring constant typical before and after yarn un-spooling**

The pull test is performed on a single yarn and the same phenomenon exists for one yarn, suggesting that it is fundamental behavior inherent to the function of the tension mechanism.

6/13/2007

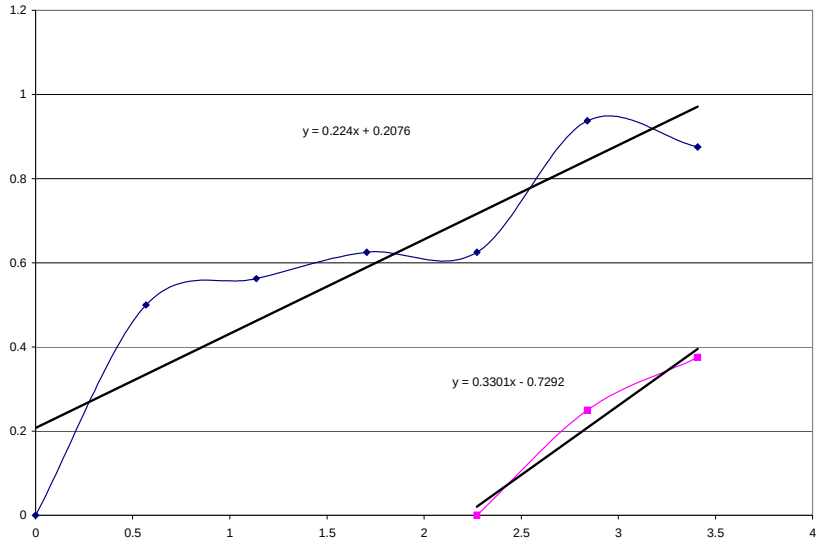


**Figure A.2 Bi-directional nature of the spring constant for one package**

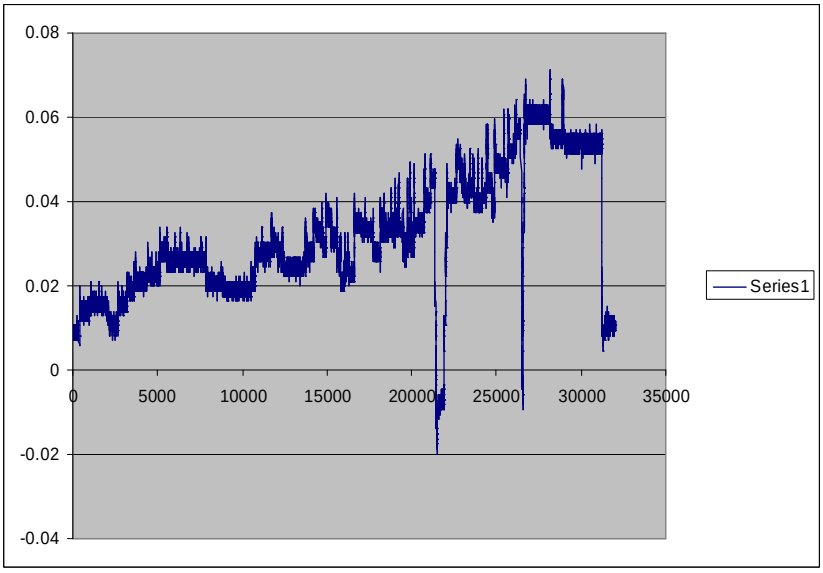


**Figure A.3 Yaskawa servo motor current monitoring**

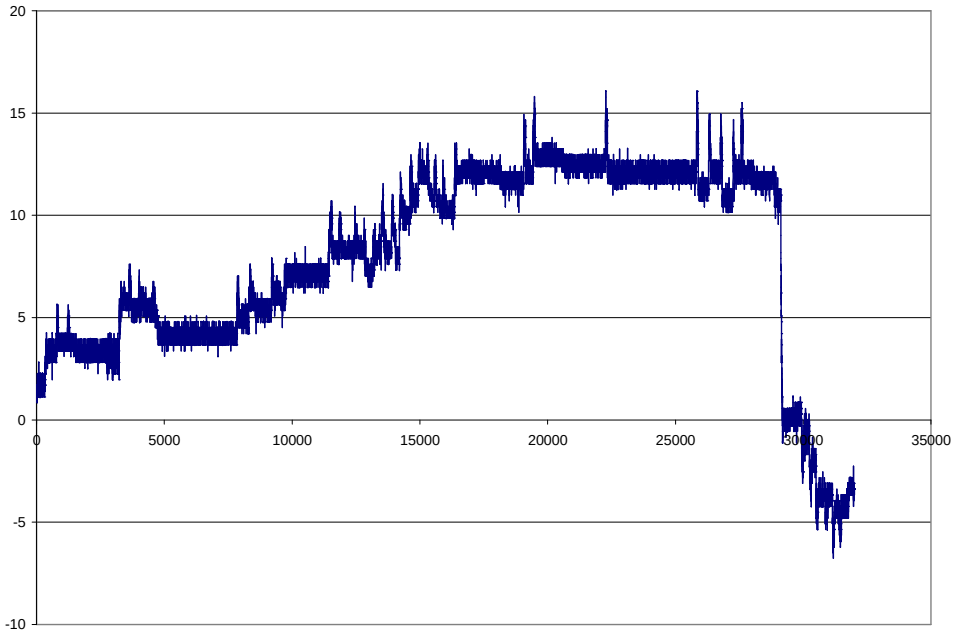


**Figure A.4 BMC servo motor torque monitoring**

**9-12-2007**

The scope of the 9-12-07 experiment will be to fine tune the measurements previously made on 9-10-07. In the previous experiment it is noticed that the braiding machine was not allowed to run until braid point migration ceases.

The encoder is initialized where the package is in the highest track position. The capstan speed is set incrementally from 1 through 5 rpm until drift is no longer observed, thus allowing the braid to reach steady state. The program will take pictures once for every complete revolution and the angles will be measured to be given as a function of take-up speed. When the yarn reaches its highest position in the braiding path (12 O'clock), the shaft mounted encoder triggers the camera to acquire an image. Initializing the braiding machine encoder provides an index to ensure that the braid angle will be calculated by using the same yarn in approximately the same position. It is observed that the braid point moves toward the

machine for capstan motor speeds less than 2 rpm, until interfering with the braiding ring. Capstan motor take-up speeds greater than 2 rpm causes the braid point to move away from the braiding machine and toward the take-up machine. The following section demonstrates that the braid point motion migrates toward or away from the braiding machine depending on where its natural point of stabilization would be; thus the angles will increase or decrease.

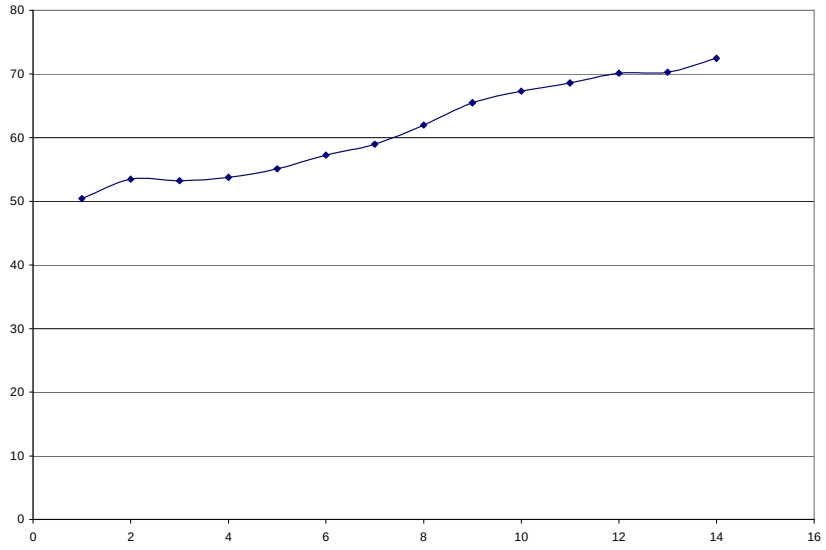


**Figure A.5 Increasing braid angle versus braiding machine revolution: 1 rpm**

Figure 4.7 shows the increasing angle for a capstan speed of 1 rpm. Figure 4.7 shows similar behavior of the angle changing despite a constant ratio between braiding machine and capstan motor speed. Figure 4.8 and Figure 4.9 demonstrate the same behavior for 2 and 3 rpm respectively.

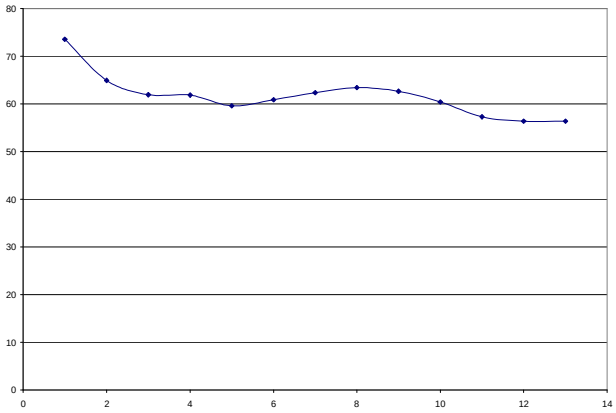


**Figure A.6 Decreasing braid angle versus braiding machine revolution: 2 rpm**

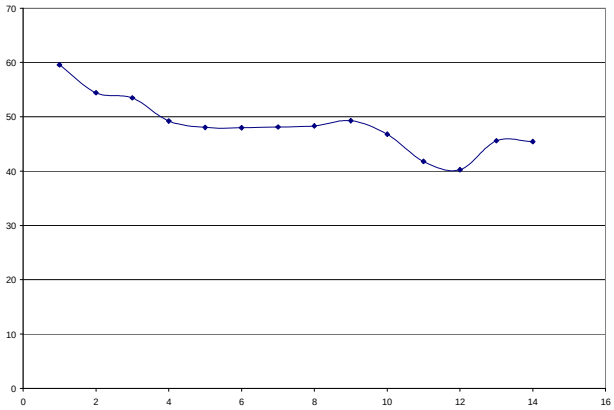


**Figure A.7 Decreasing braid angle versus braiding machine revolution: 3 rpm**

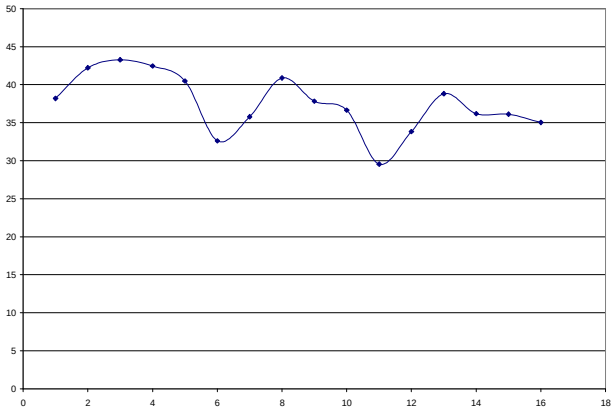


**Figure A.8 Decreasing braid angle versus braiding machine revolution: 4 rpm**

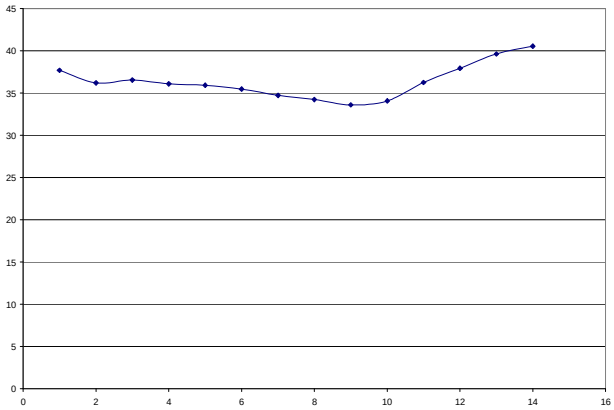


**Figure A.9 Braid angle versus braiding machine revolution: 5 rpm**

The data from this experiment is summarized in table 4.1 by calculating the average of the angles from Figures 4.7 through 4.11. Figure 4.12 displays the results of these calculations.

| RPM | Average Angle | 360-Angle |
|---|---|---|
| 1 | 298.6814 | 61.32 |
| 2 | 298.3515 | 61.65 |
| 3 | 311.5514 | 48.45 |
| 4 | 322.5106 | 37.49 |
| 5 | 323.6643 | 36.34 |

**Table A.1 Capstan speed and corresponding braid angle**

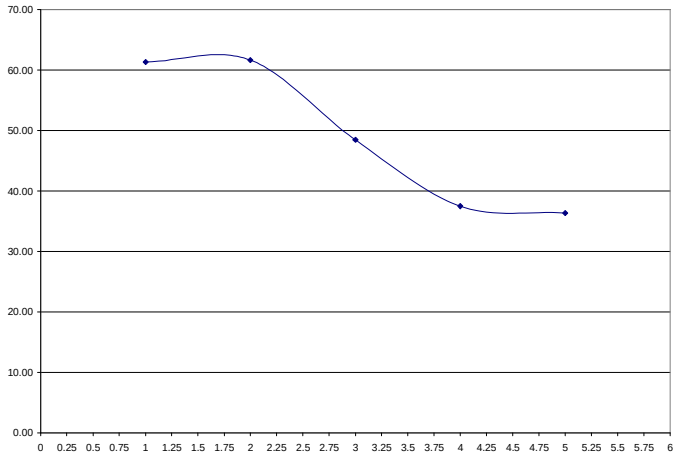


**Figure A.10 Unsettled braid point angle as function of capstan motor speed**

Considering that Table A4.1 and Figure A.10 show little difference in the angles formed (particularly 1, 2, 4, and 5 capstan motor rpm) and capstan motor speed. This evidence suggests that more time is required to allow the braid point to stabilize. Thus, one more experiment is performed with the specific objective of determining the amount of time required for the braid point migration to cease. In other words, for the given braiding parameters of braiding machine speed and capstan motor take-up speed, how many cycles are required for the braid point to stabilize?

The following plots depict the relative position of the braid point as observed by camera 1.

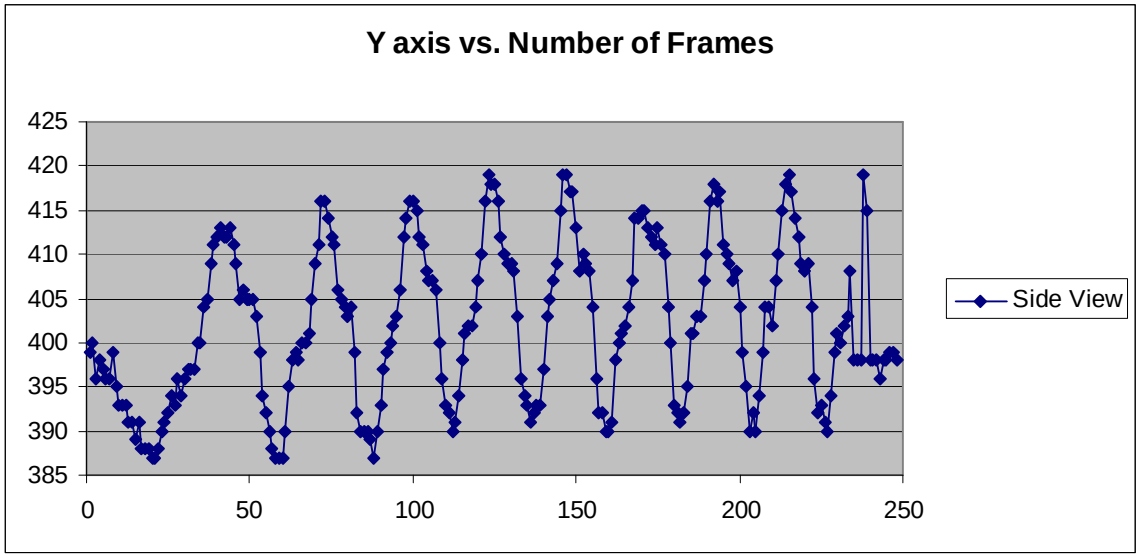


**Figure A.11 Movement of the braid point in Y (Horizontal Direction)**

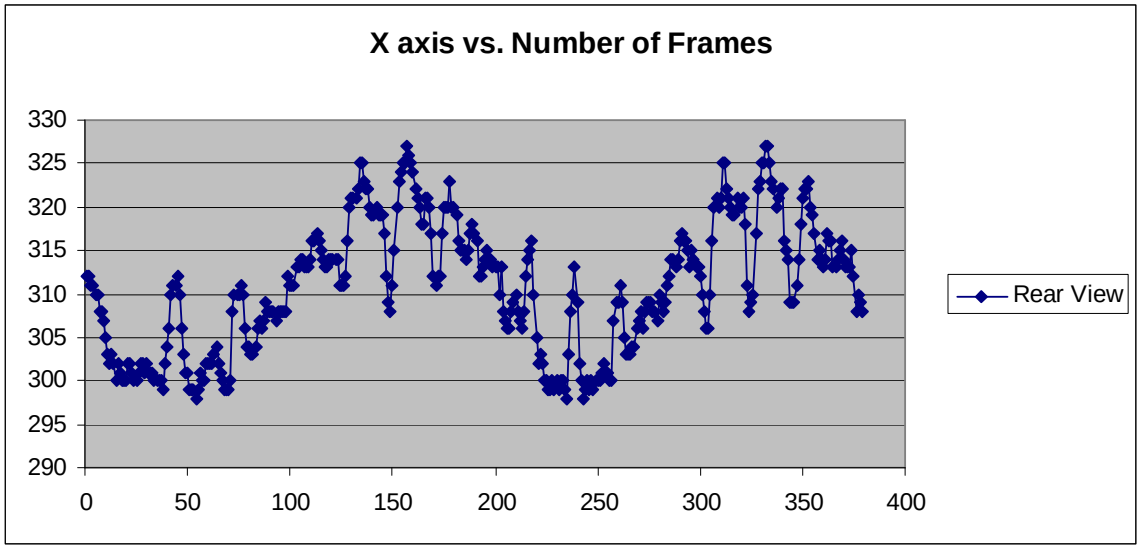


**Figure A.12 Movement of the braid point in X (Horizontal Direction)**

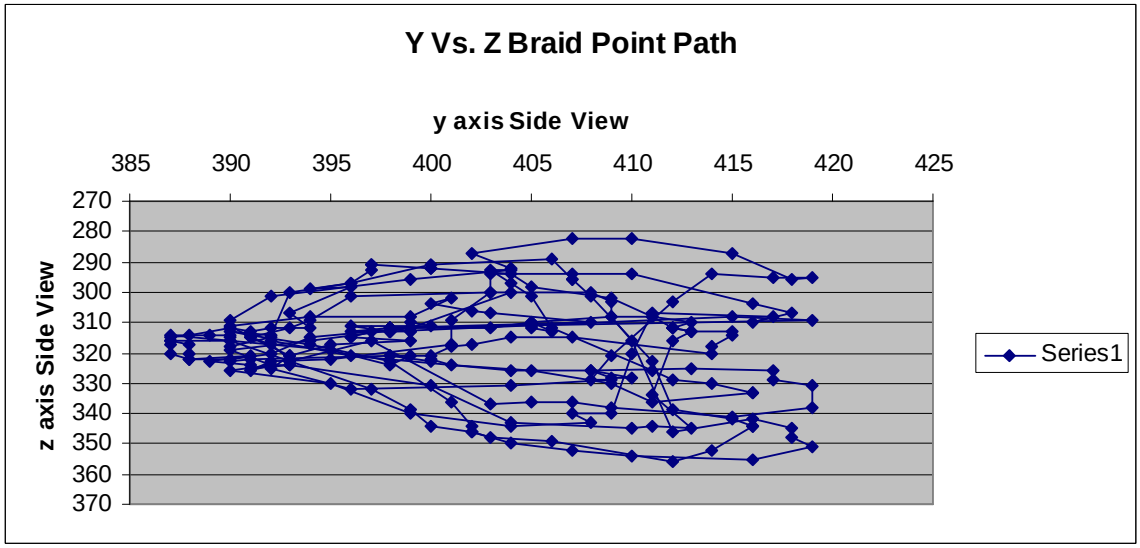


**Figure A.13 This plot outlines the braid point displacement path as viewed from camera 1**

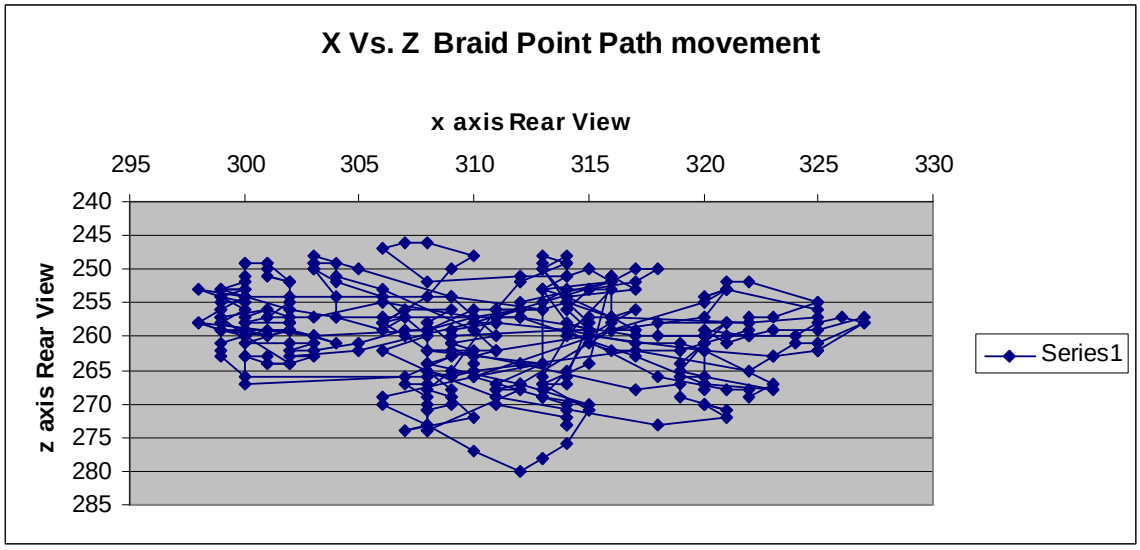


**Figure A.14 This plot illustrates the displacement path of the braid point as viewed from camera 2**

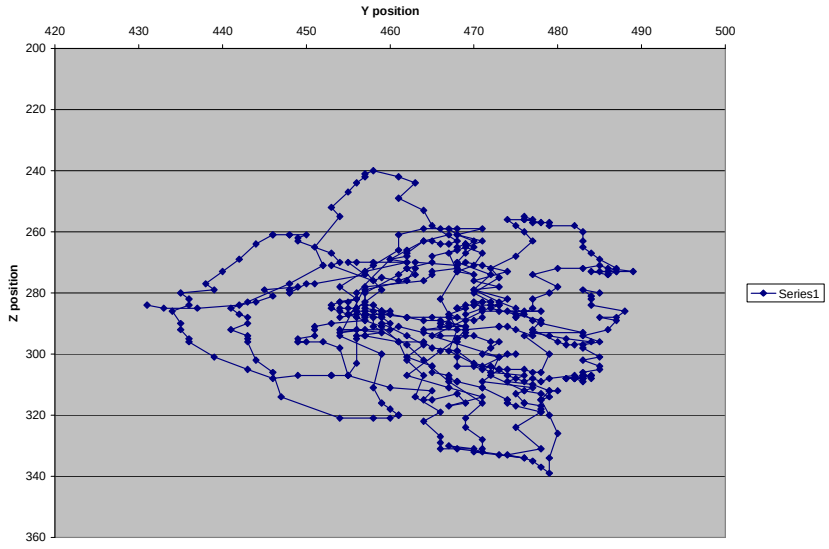


**Figure A.15 Circular nature of braid point formation**

**Characteristics of aberrant spring tension and subsequent package behavior**

After the braiding machine is performing properly, and consistent behavior is observed, the spring tension in one package is increased substantially to simulate how problems in the release mechanism (tension) of the package manifest in the formation of the

braid. The braid point movement tends to be dominated by the package with aberrant spring tension. Several plots are shown to demonstrate the characteristics of a braid that is imbalanced as a result of poor package performance.

After braiding in the best case scenario, the tension of one package is systematically altered to provide further insight. It is important for each package to contribute even tension to the braid structure. Due to the symmetric nature of circular braids, it is important that the tension of one package with respect to its complement (opponent) be equal to minimize oscillating movements of the braid point.

**Effects of Spring Tension**

**6/27-28/2007**

It is important for each package to contribute even tension to the braid structure. Due to the symmetric nature of circular braids, it is important that the tension of one package with respect to its complement (opponent) be equal to minimize oscillating movements of the braid point.

The experiment performed in this section involved changing the material on the packages and replacing them with new material. A new spool of Kevlar ™ was acquired from V2 Composites in Auburn. It is 1420 denier. 16 packages were cleaned and wound with 30 traverses on the Wardwell TW-2004 Textile Winder. These efforts were in order to establish optimum braiding conditions. Clean packages, equally wound, well lubricated tend to promote even braids. Well cleaned and lubricated braiding machines, with equal package settings, are the requirements that must be met and maintained to achieve the best quality braid. Optimizing the machine mechanically provides the baseline from which other tests will be compared. Knowing braid behavior in the best case scenario is important for

understanding misbehavior. The PID gains of the capstan have been tuned to achieve a constant rpm. The following error was limited to 30. This data is illustrated throughout this section.

After braiding in the best case scenario, the tension of one package is systematically altered to represent a sticking package and hopefully provide further insight. It is important for each package to contribute even tension to the braid structure. Due to the symmetric nature of circular braids, it is important that the tension of one package with respect to its complement (opponent) be equal to minimize oscillating movements of the braid point.

The experiment today will involve the effects of an aberrant spring tension. A yarn package's tension release mechanism is altered by increasing the spring tension to a critical point. The yarn tension is measured to be 55 grams while the remaining 15 yarns have around 14 grams. 25 seconds of data will be acquired, the resulting images analyzed to determine a trend for packages with faulty tension. The package with the aberrant spring tension is in the top most position.

**6/28a:** Tension is increased by adding a small cut section of the blue (lightest) spring to one full pink spring.

**6/28b:** Same as 6-28-a but now 1.5 pink spring.

**6/28c:** Additional pink spring added until just before package completely malfunctions.

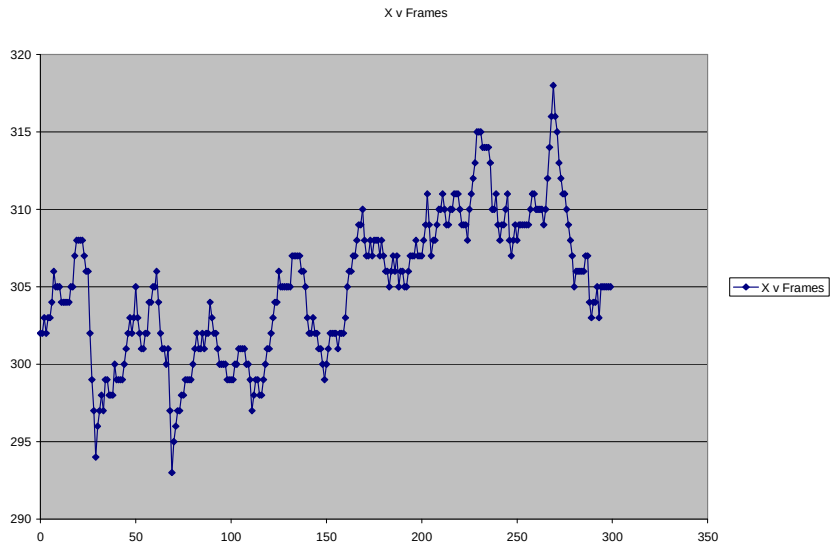


**Figure A.16 X displacement versus frames**

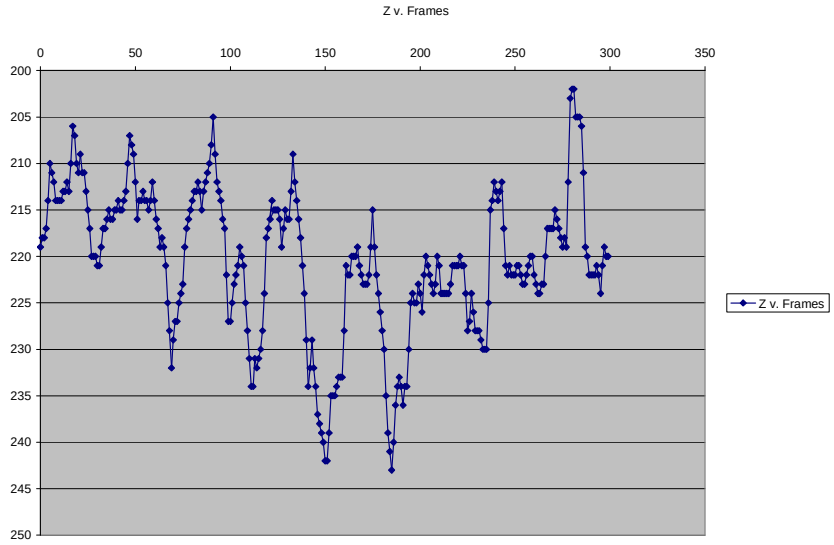


**Figure A.17 Z displacement versus frames**

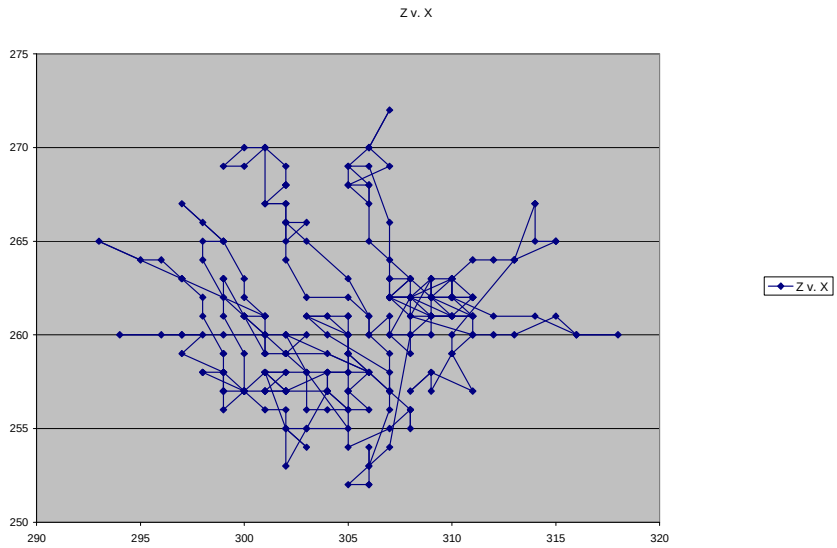


**Figure A.18 X versus Z displacement**

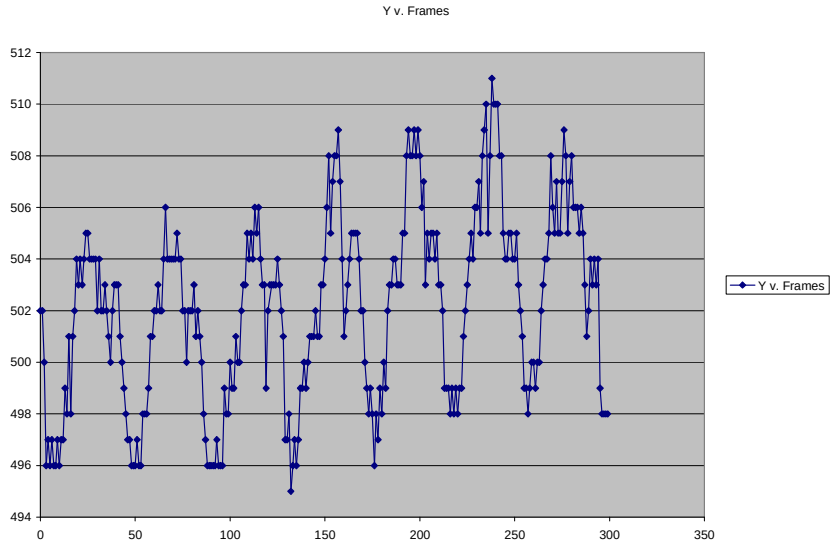


**Figure A.19 Y displacement versus frames**

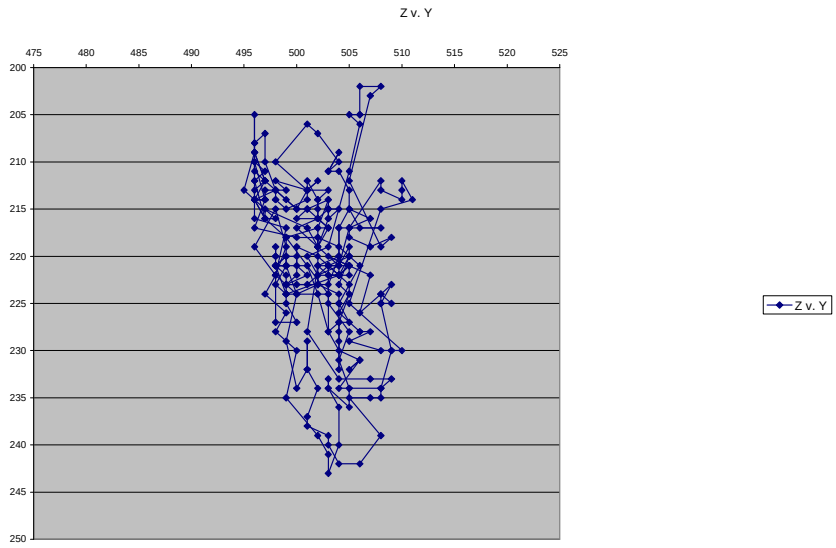


**Figure A.20 After PID tuning**

**6/27/2007 REAR VIEW**

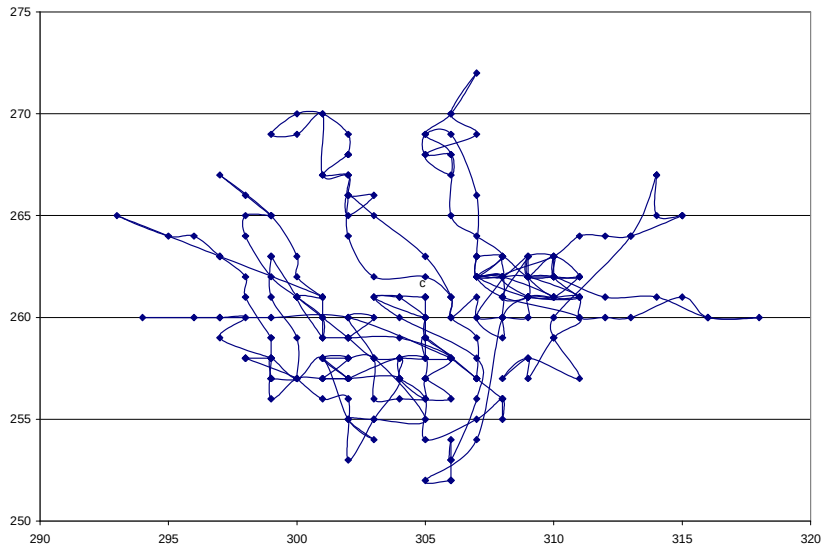


**Figure A.21 X v. Z Braid Point Motion**

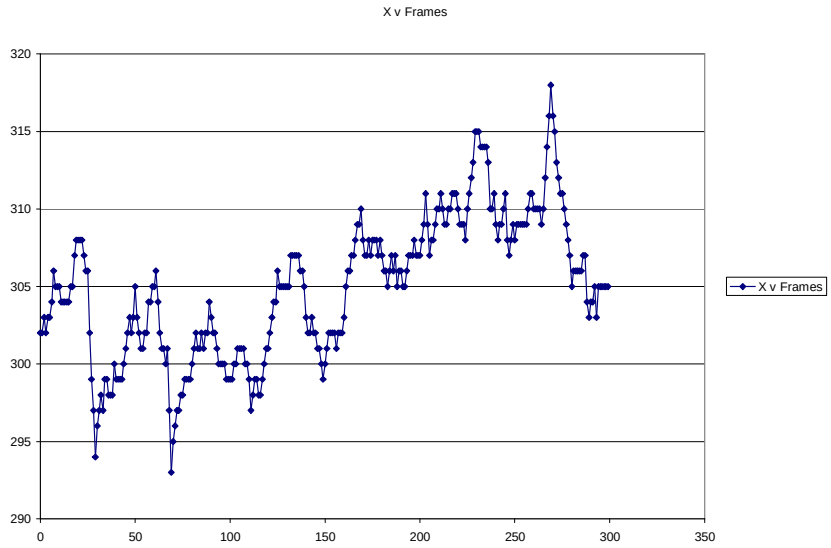


**Figure A.22 X v Frames x-y scatter plot**

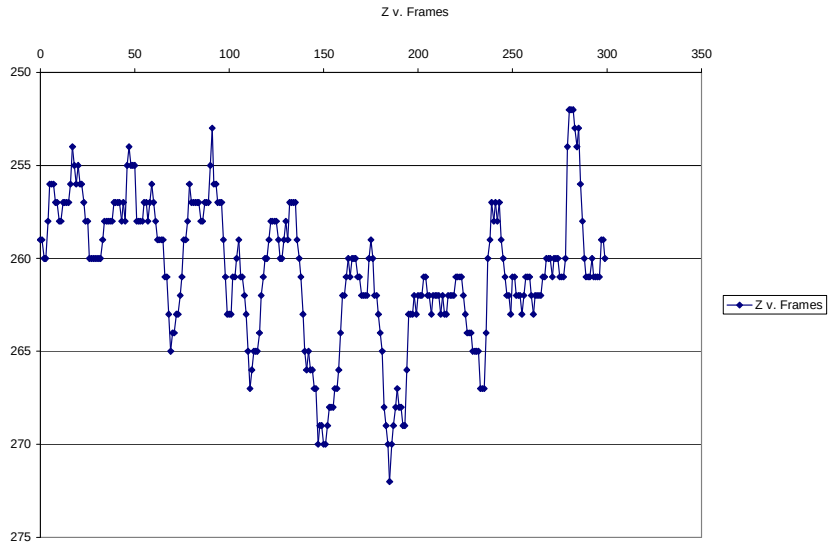


**Figure A.23 Z v frames x-y scatter plot**

## 6/27/2007 SIDE VIEW

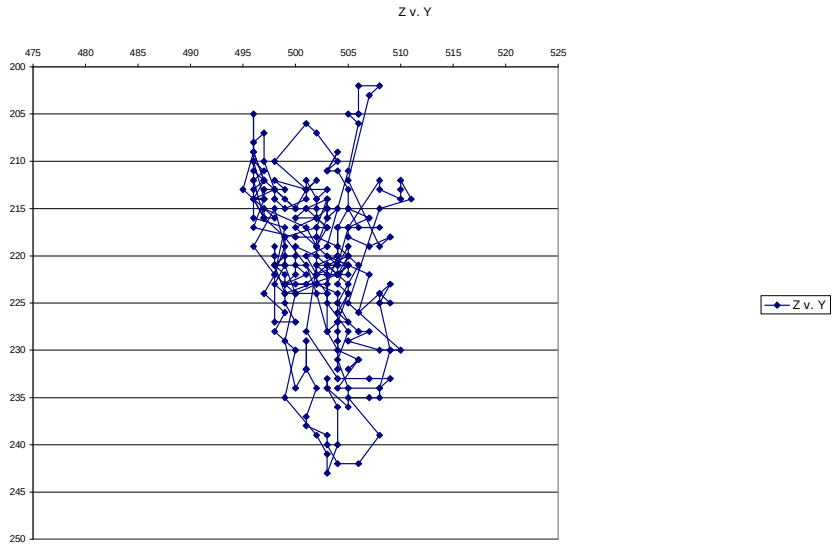


**Figure A.24 Z versus Y Side x-y scatter plot**

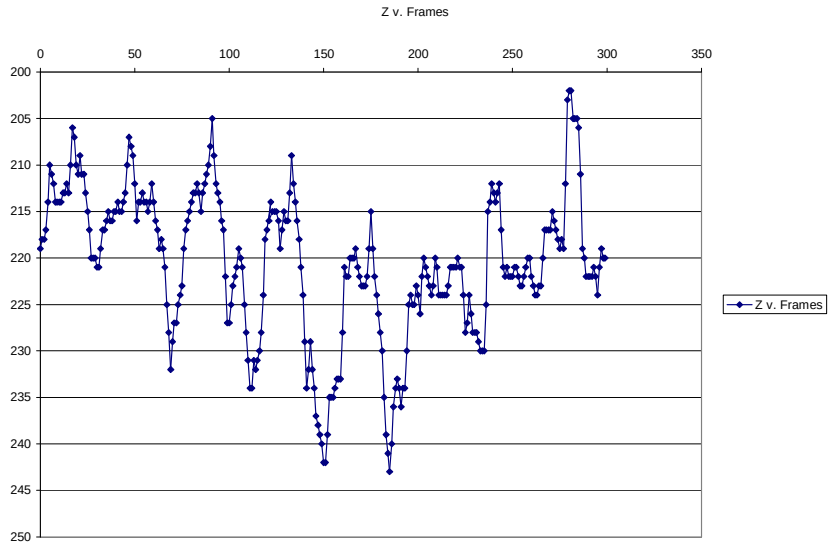


**Figure A.25 Z v. frames x-y scatter plot**

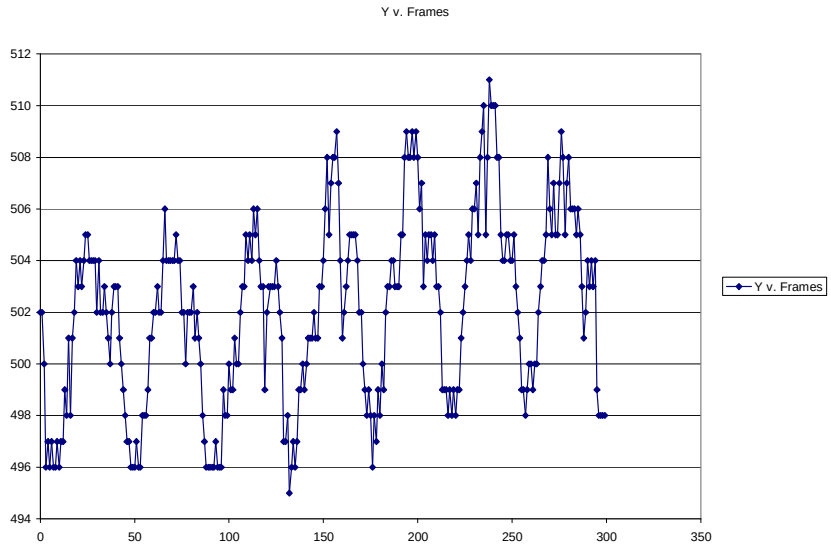


**Figure A.26 side Y v frames x-y scatter plot**

**6-28-07 SIDE VIEW Test 1 (a)**

6/28a Tension is increased by adding a small cut section of the blue (lightest) spring to one full pink spring.

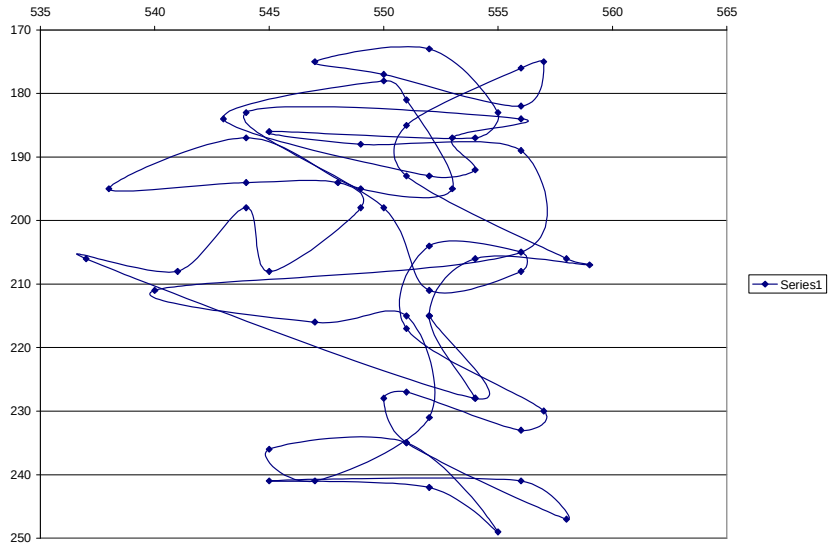


**Figure A.27 Side View braid point motion**

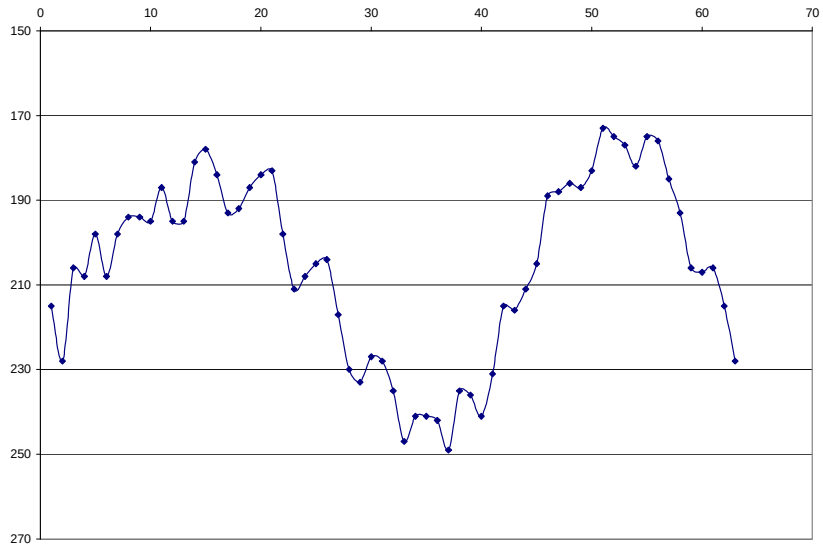


**Figure A.28 Side View Z v frames x-y scatter plot**

**Experiment 2 (b) Side View**

6/28b

Same as 6-28-a but now adding 1.5 pink spring.

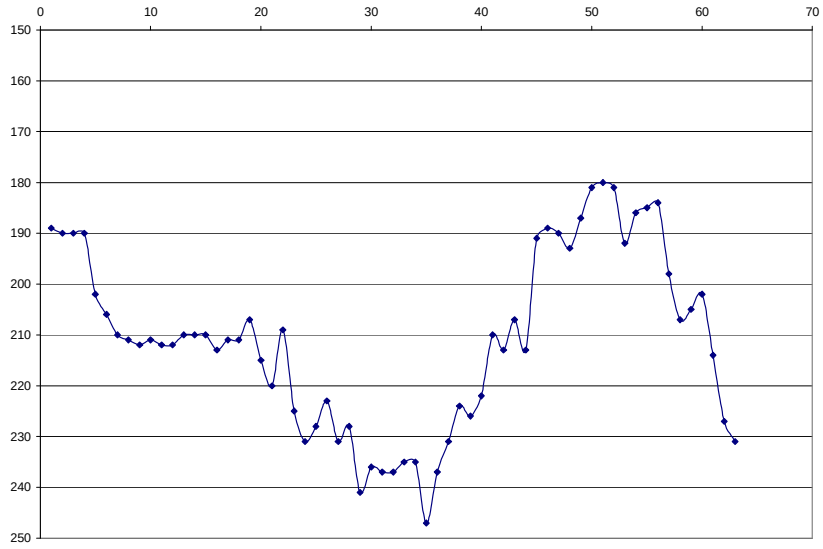


**Figure A.29 Z displacement (Side view)**

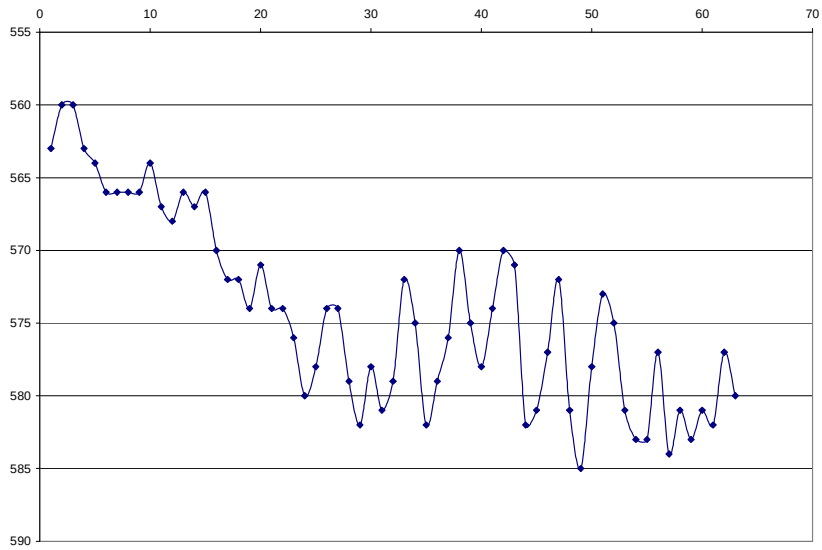


**Figure A.30 Y displacement versus frames (side view)**

**Experiment 3 (c) Side View**

6/28c

Additional pink spring is added until just before package completely malfunctions.

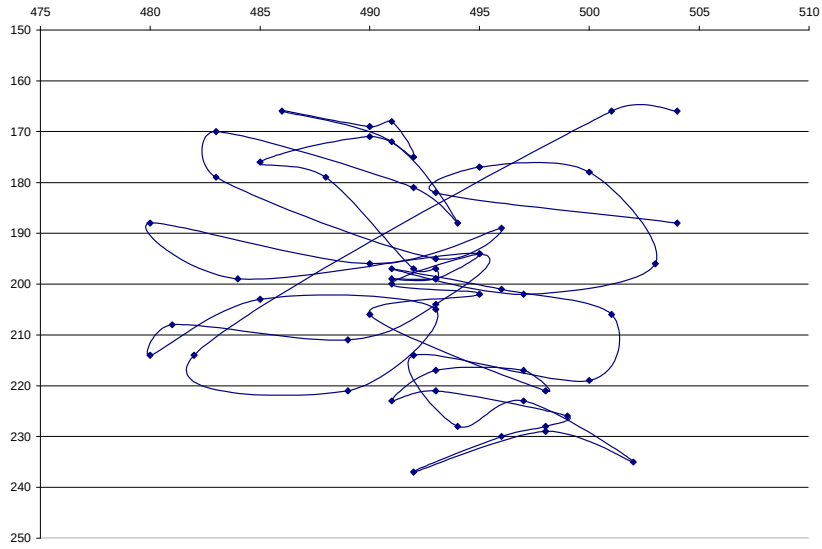


**Figure A.31 Braid point motion (rear view)**

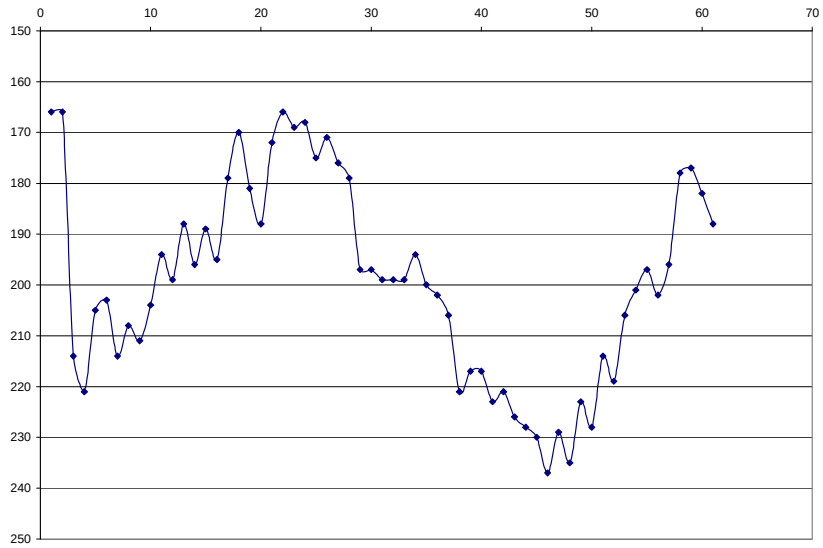


**Figure A.32 Z v frames x-y scatter plot**

**6-28-07 REAR VIEW**

**Test 1**

6/28a Tension is increased by adding a small cut section of the blue (lightest) spring to one full pink spring.

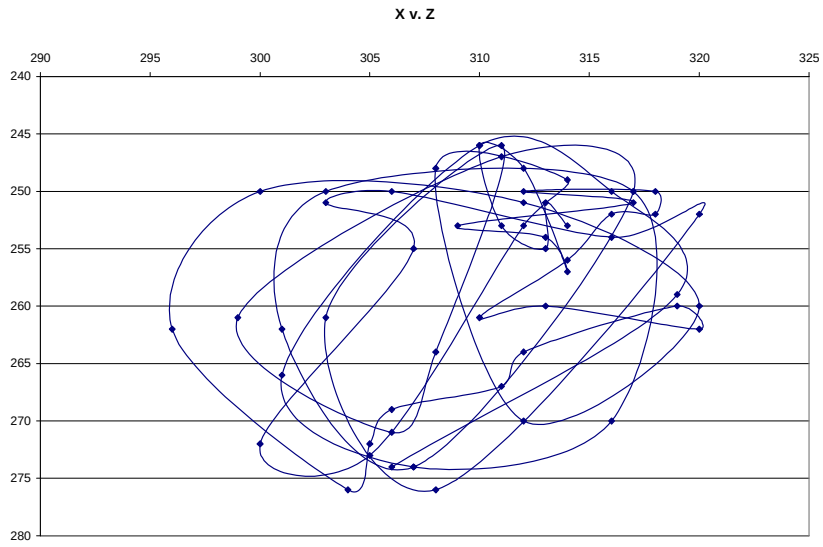


**Figure A.32 x v z braid point motion**

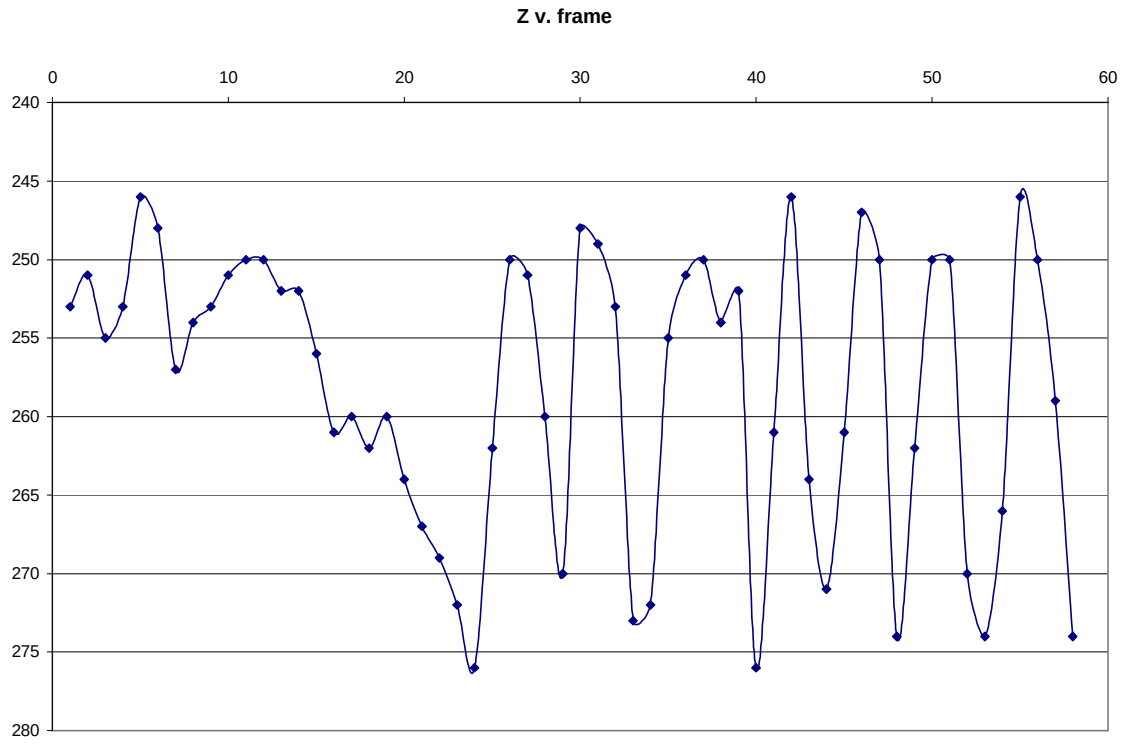


**Figure A.33 z v frame x-y scatter plot**

**Test 2 6/28b**

Same as 6-28-a but now 1.5 pink spring.

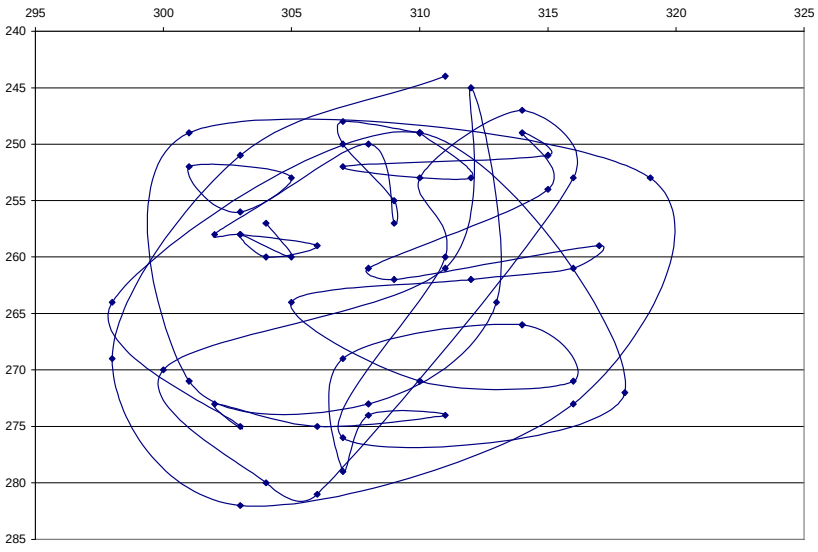


**Figure A.34 x v z Rear Braid point motion**

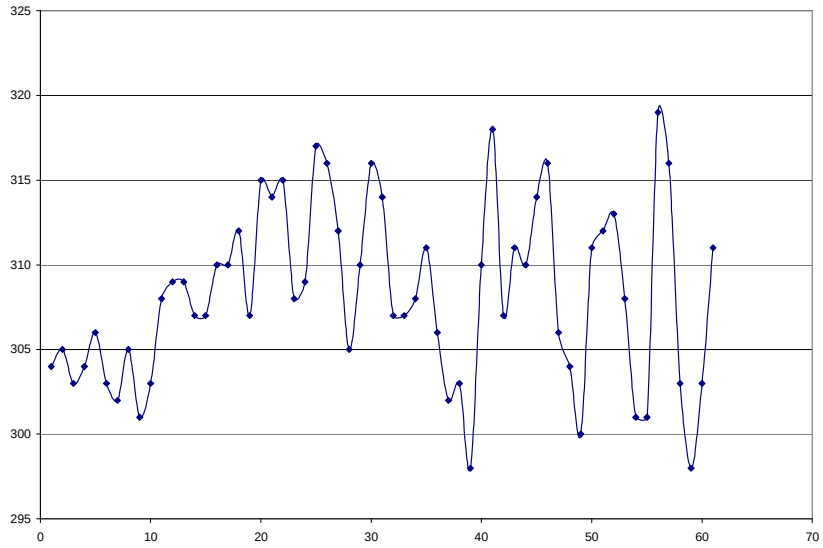


**Figure A.35 x v time x-y scatter plot**

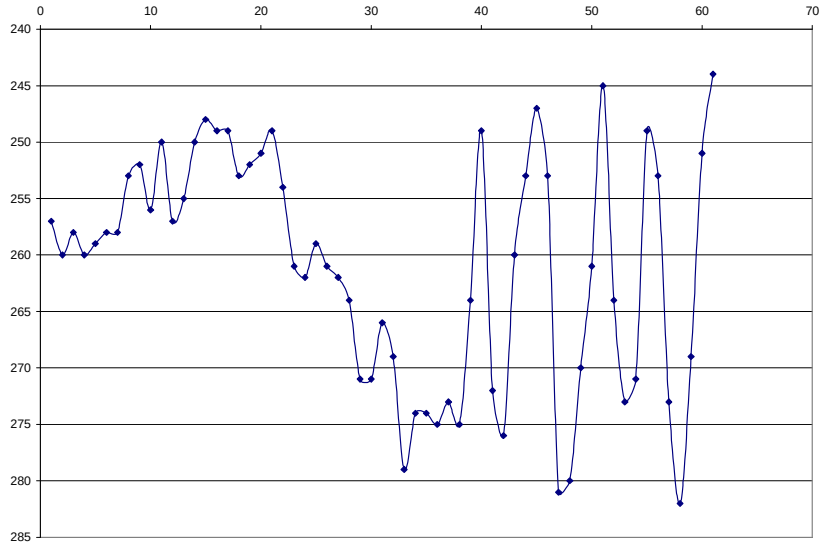


**Figure A.36 z v frames x-y scatter plot**

**Test 3**

**6/28c** More pink spring added until just before package completely malfunctions.

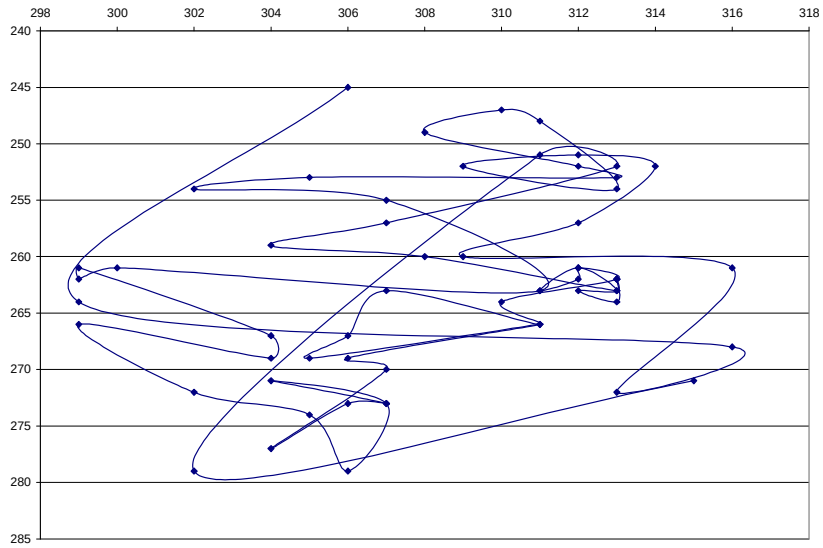


**Figure A.37 rear x v z braid point motion**

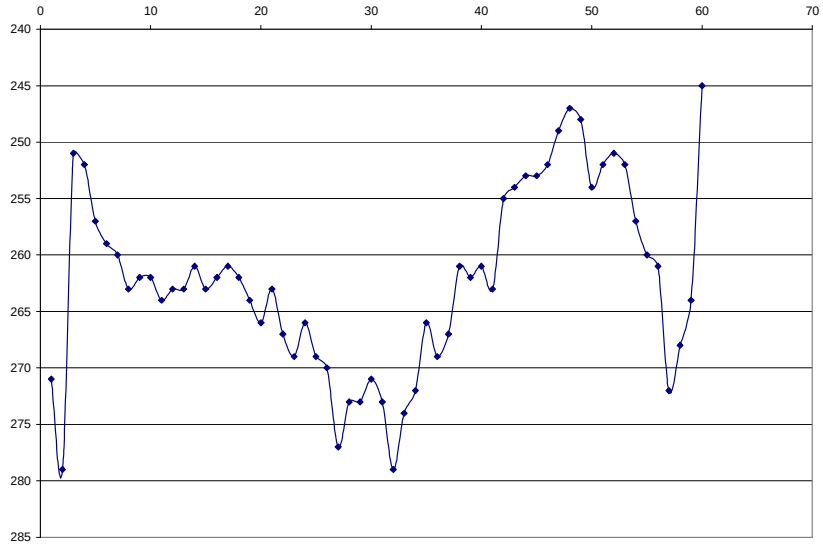


**Figure A.38 Z v frames x-y scatter plot**

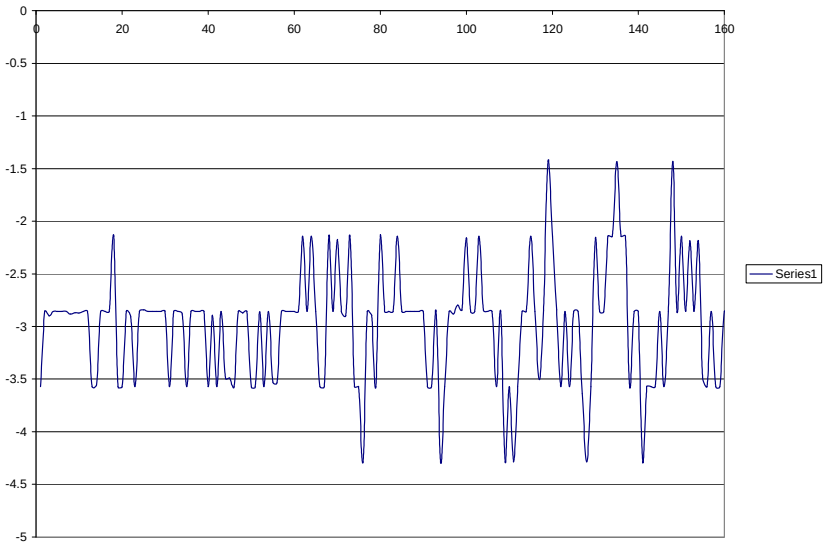


**Figure A.39 Capstan rpm**

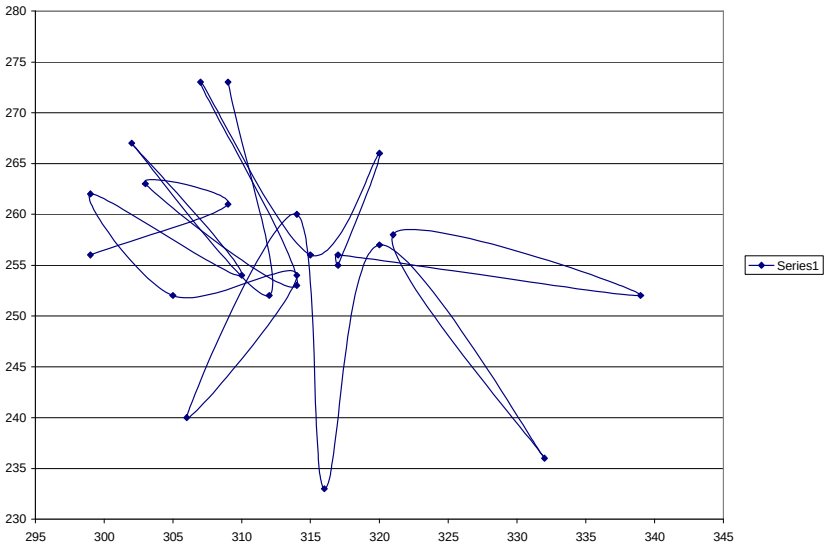


**Figure A.40 Braid point motion with 2 diametrically opposed locked packages (Second revolution)**

Figure A.40 is the result of plotting the braid point motion for the second revolution.

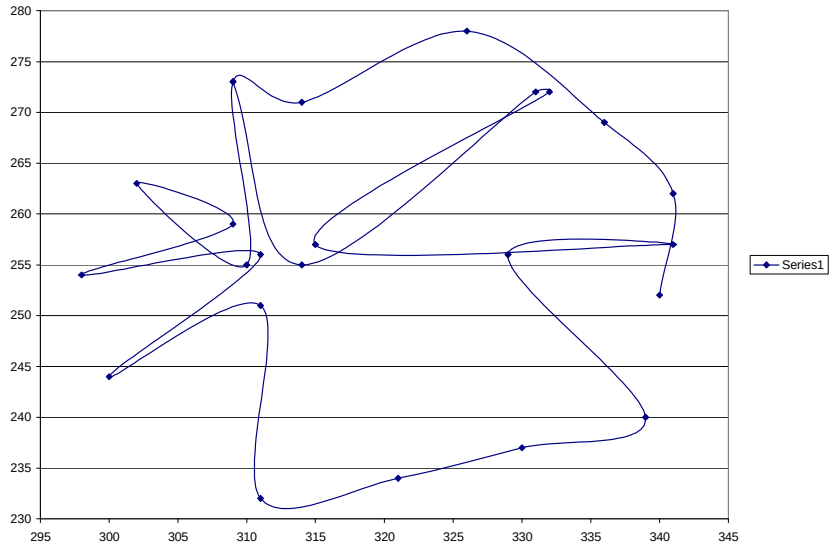


**Figure A.41 Braid point motion with 2 diametrically opposed locked packages (Third revolution)**

Figure A.41 is a plot of the braid point motion for the 3rd revolution.

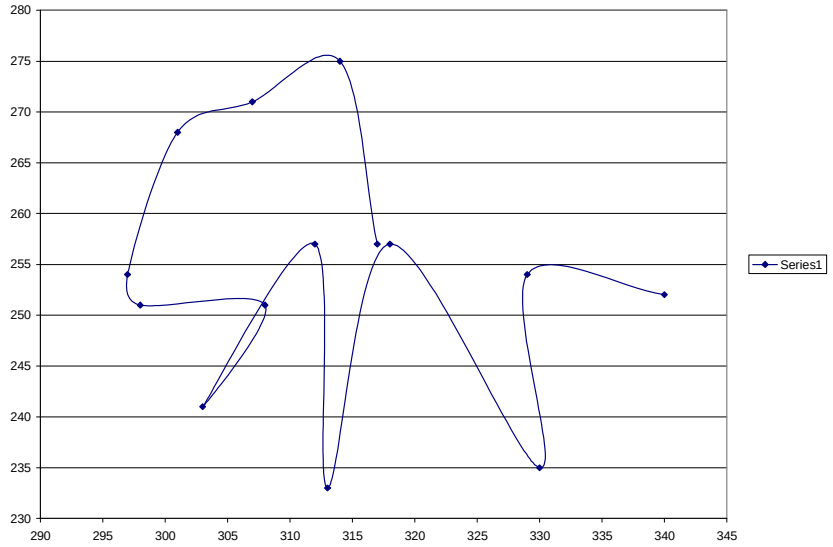


**Figure A.42 Braid point motion with 2 diametrically opposed locked packages (0.56 revolutions)**

Figure A.42 is the braid point motion plot for the remaining data of the 2 diametrically opposed locked packages experiment and is a 0.56 braiding machine revolution.

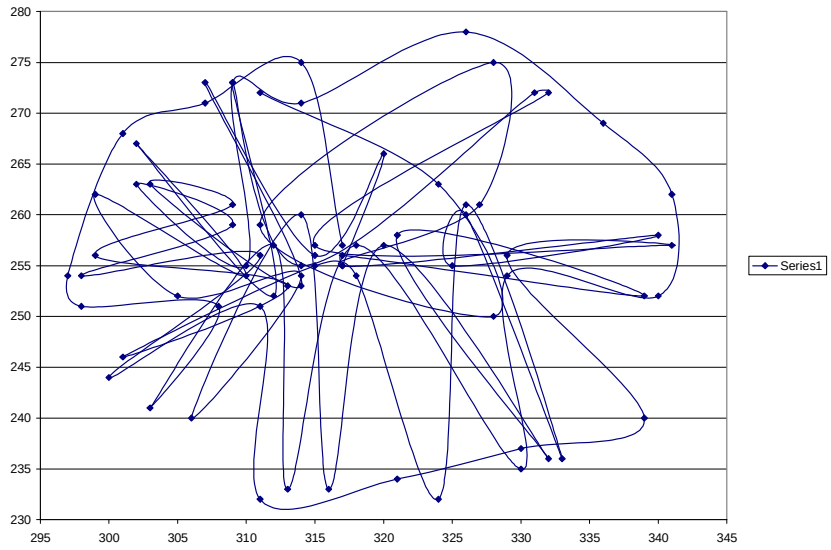


**Figure A.43 Combined braid point motion with 2 diametrically opposed locked packages (3.56 revolutions sum of data from Figures 4.40-42)**

The data from Figures 4.40-42 is combined to form the plot of Figure A.43.

**9-3-2007 Motion Data**

The DC gearmotor that is responsible for driving the braiding machine starts from zero and ramps up to the final braiding speed. This data is plotted. It is interesting to note the variations in the motor speed.

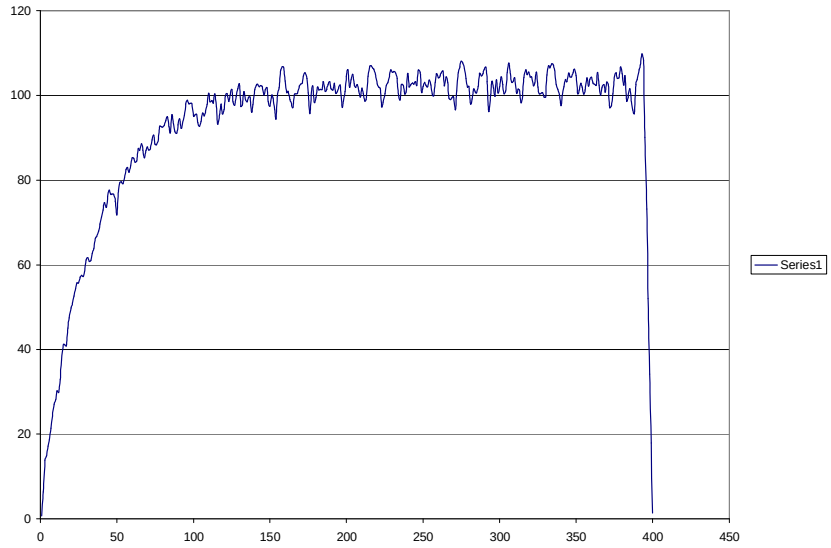


**Figure A.44 braiding machine rpm 9-3**

**9-5-2007**

This experiment involved a 16 yarn braid formation. Each package release mechanism employs the same spring stiffness. This is done to establish ideal braiding conditions to serve as a baseline from which comparison against faulty operating packages will be compared. Camera frame rate: 30 fps. The x coordinates of the braid point are plotted against time in the following figure.

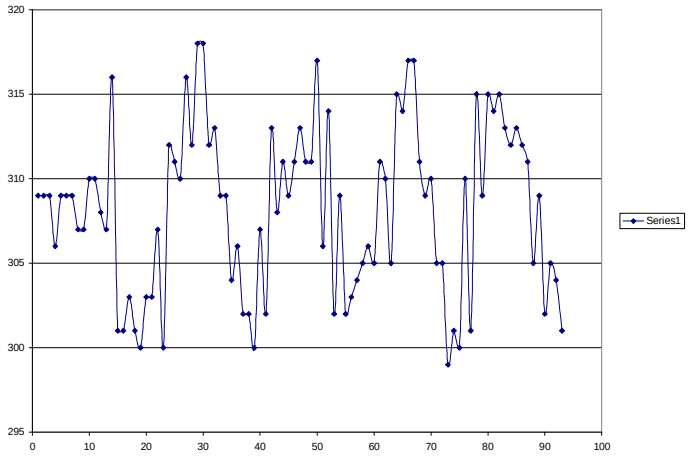


**Figure A.45 Z displacement versus frames**

The z coordinates are plotted against time in the following figure.

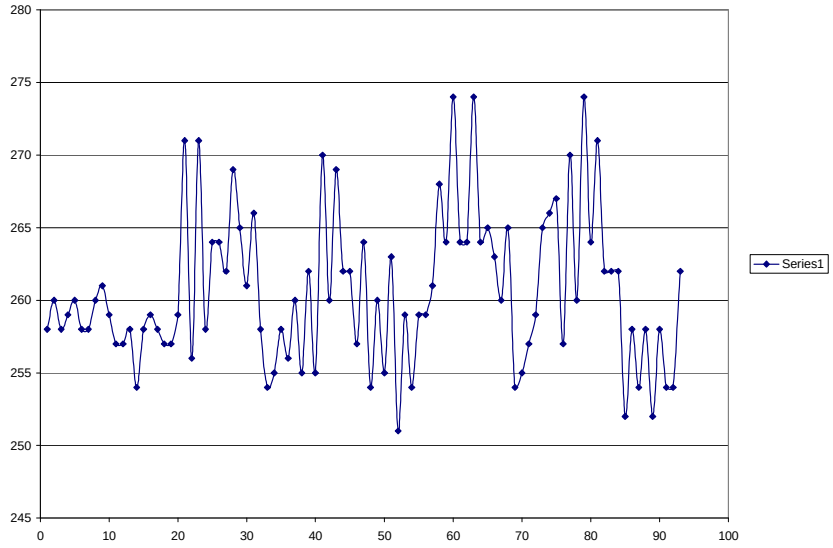


**Figure A.46 Z displacement versus frames**

The braid point motion plot for the first braiding machine revolution in the following figure is generated as an x-y scatter plot to demonstrate the apparent motion of the braid point in a Cartesian coordinate system

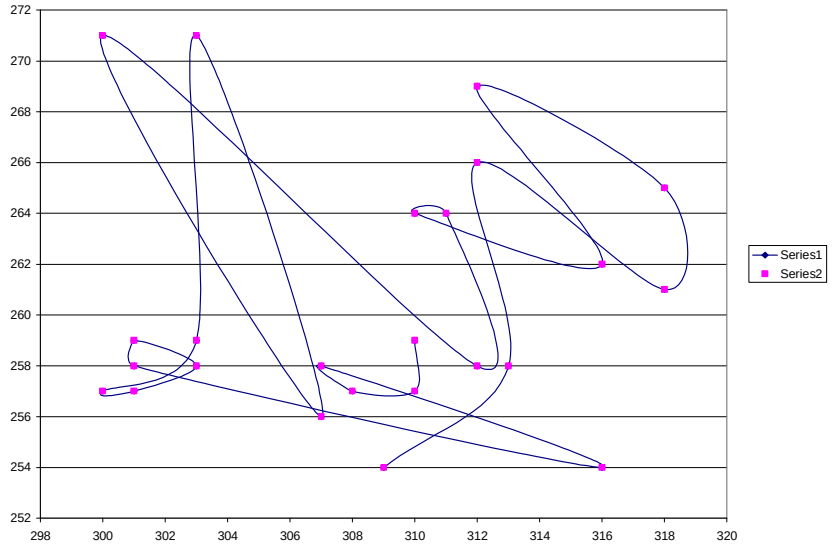


**Figure A.47 X-Z braid point motion**

The braid point motion plot for the second braiding machine revolution in the following figure is generated as an x-y scatter plot to demonstrate the apparent motion of the braid point in a Cartesian coordinate system

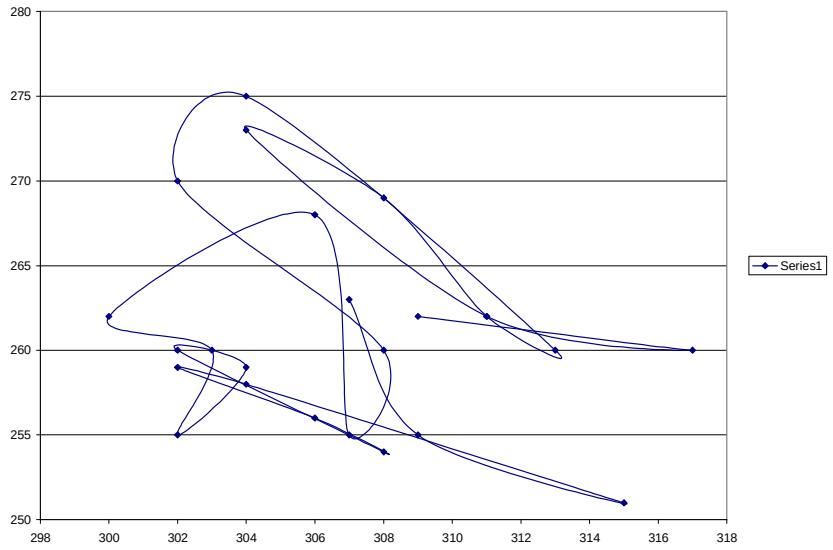


**Figure A.48 X-Z braid point motion**

The distance formula is used as a measure to determine the radial variation in the braid point from an arbitrary center.

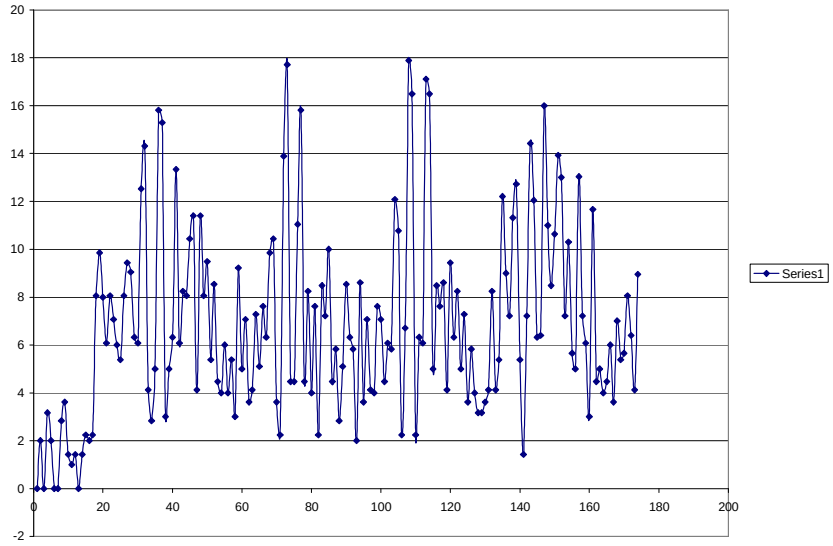


**Figure A.49 radial variation**

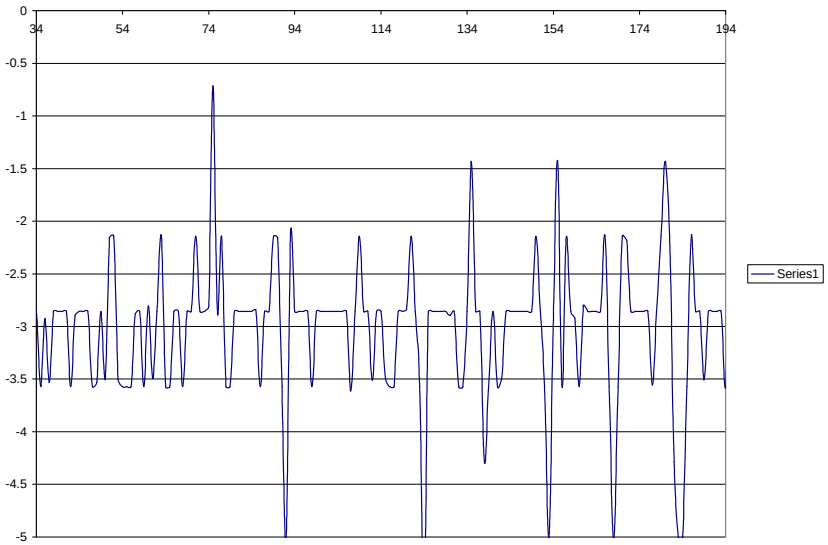


**Figure A.50 Capstan motor speed**

9-3-2007

The bottom most package is locked, causing a faulty release mechanism and producing pure tension member. That is to say, the amount of material (yarn is fixed). This effect causes a twisting of the braid as the high tension yarn twists the braid as it traverses the track plate.

The final experiment will involve 16 balanced packages, same parameters as above (9-5-07).

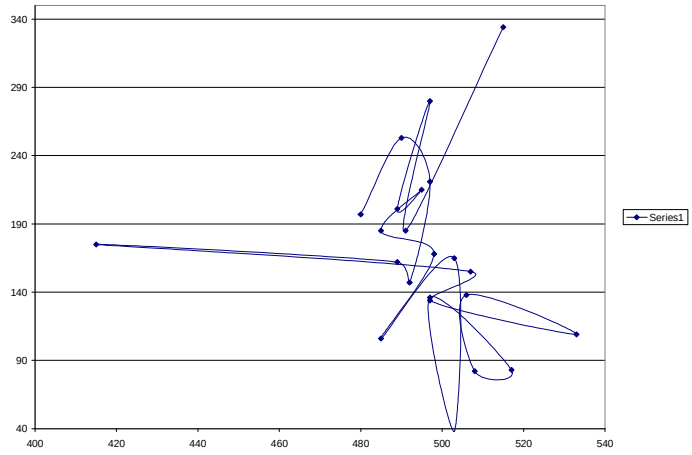


**Figure A.51 Y-Z displacement**